1. Introduction and Aims

"An expert is a man who has made all the mistakes he can in a very narrow field."

Niels Bohr

1.1. Polymers and Emulsion Polymerization

A polymer is a macromolecule that comprises of covalently linked repeat units known as monomers, typically visualized as beads on a piece of string. Polymers can span many orders of magnitude of molecular weight (from 10^3 to $10^{6\text{-}8}$ Da), and are both naturally occurring (natural rubber and polysaccharides such as starch as examples) as well as easily synthesized in the laboratory. Because of the variety of synthetic monomers with different functional groups and properties, the synthesis of polymers for industrial applications (e.g. paints, plastics, adhesives, films, barrier products, specialty medical applications and many more) has become the most widely performed chemical reaction in the world today, with polymer-based products pervading every aspect of modern society.

A typical free-radical polymerization reaction (initiated by the thermal decomposition of a molecule to form radicals) is typically robust to many different reaction conditions,[1] including a variety of different organic and aqueous solvents as well as tolerance to trace amounts of impurities. This is a massive technical advantage for industrial polymer synthesis; however the major shortcoming with bulk or solution polymerization is the relatively low percentage conversion and/or percentage solids obtainable before sample handling becomes extremely difficult (due to a significantly increased sample viscosity). As a result, emulsion polymerization (the heterogeneous polymerization of an organic monomer in an aqueous dispersed phase under constant shear, forming sub-micron scale polymer particles stabilized by surfactant) is the method of choice to synthesize polymer easily on an industrial, multi-tonne scale;[2] the aqueous phase provides excellent heat dissipation, the final sample retains a relatively low viscosity and extremely high reaction rates and molecular weights are attainable. A schematic representation of the emulsion polymerization process is given in Figure 1.1, and the resultant polymer colloid is typically known as a ‘latex.’

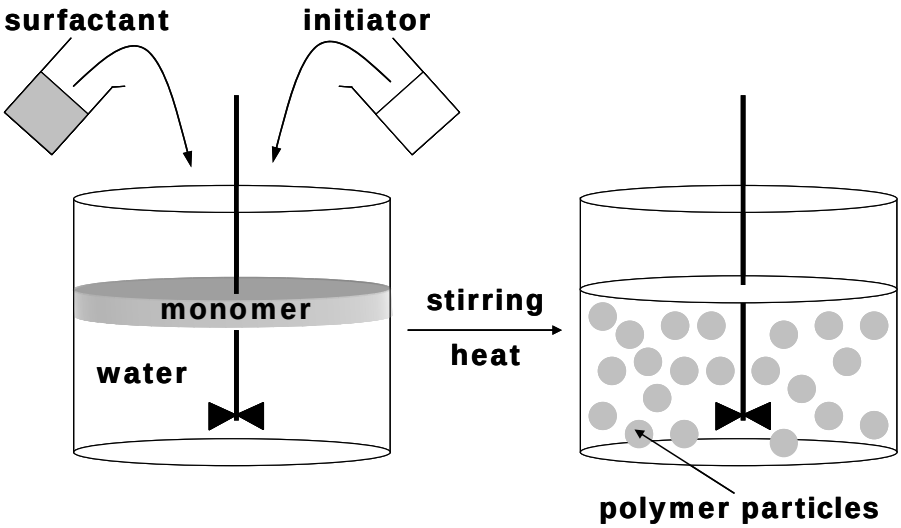

Figure 1.1. Schematic representation of the emulsion polymerization process.

Despite the ease of implementing this technique in the laboratory, the kinetics and mechanism that govern polymerization in emulsion are complicated by numerous interfacial processes, as well as the kinetics of the fundamental chemical reactions within any polymerization. As a result, the study of the many aspects of emulsion polymerization kinetics (e.g. particle formation, radical entry and exit) has become a significant academic pursuit – albeit one with important industrial implications. In order to successfully model an emulsion polymerization (with a view to improving reaction conditions and synthesizing novel and desirable polymer products), a detailed knowledge of the mechanisms governing every process taking place simultaneously is required. Naturally the synthesis of polymer on a multi-tonne scale must be modelled to prevent 'disastrous' reaction conditions (for example, an uncontrollable exotherm or substantial coagulation), and to ensure the success of these reactions the knowledge of the mechanisms that control particle formation and particle growth are of fundamental importance. Through carefully designed experiments many of these key governing mechanisms have been elucidated over the past fifty years,[3] giving the industrial chemist a solid base to work from.

One extremely significant area of study in emulsion polymerization revolves around a component that represents only a tiny fraction (by weight) of an emulsion – the stabilizing species that imparts colloidal stability for the formed polymer particles. On a small scale in the laboratory, it is common to use ionic surfactants (such as sodium dodecyl sulfate, SDS) as the stabilizer; the charge on the sulfate head group provides colloidal stability via electrostatic repulsion. The overall stability of an electrostatically stabilized latex depends on the total interaction energy profile, which is the sum of the attractive (van der Waals) and repulsive (electrostatic) terms as a function of separation distance, known as DLVO theory.[4] This in general is very good at predicting the overall stability of a polymer latex stabilized in this manner.

Much work also has been done to understand the role of the stabilizer with regards to particle formation – the 'homogeneous nucleation[3, 5, 6]' and 'micellar nucleation[7]' models for particle formation have proven extremely successful in modelling the final particle number (N_p, the number of polymer particles per litre of emulsion) as a function of stabilizer concentration under a wide range of conditions. The excellent knowledge base established for systems stabilized by conventional surfactants has meant that much research has been invested in such systems – yet commercially they are of little practical interest. Added surfactants are generally retained in any final polymeric product, increasing the water permeability of polymer films and decreasing adhesion to substrates.[8] Another mode of stabilization, (electro)steric stabilization, is often employed in industrial systems, and is discussed more in the subsequent section.

1.2. Steric and Electrosteric Stabilization

Steric stabilization of an emulsion polymer particle is when a physical barrier is placed on the particle surface to prevent coalescence of neighbouring particles and to retain colloidal stability. This physical barrier is usually in the form of hydrophilic polymer chains (either grafted or

adsorbed to the particle surface) that extend into the aqueous phase – typical examples are polymers of acrylic acid or ethylene oxide. The method of stabilization is essentially an entropic one; upon approach to one another, sterically stabilized particles begin to undergo chain entanglement and interaction between stabilizing blocks, which is thermodynamically unfavourable. This results in the particles repelling one another in order to maximise the entropic configuration of the stabilizing chains,[9] shown in Figure 1.2. If the hydrophilic monomer can be ionized (e.g. the neutralization of acrylic acid) then the particle is stabilized both sterically and electrostatically, which is often referred to as 'electrosteric stabilization.' An electrosterically stabilized polymer particle is often visualized as a particle surrounded by a corona of stabilizing hydrophilic chains, commonly referred to as a 'hairy layer.'

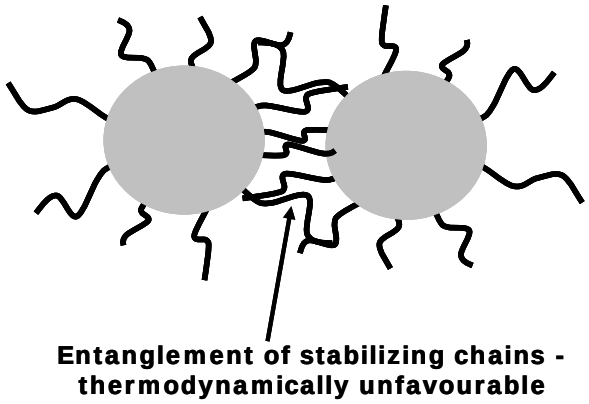

Figure 1.2. Steric stabilization of emulsion polymer particles.

The advantages of (electro)steric stabilization for industrial polymer synthesis are numerous. Firstly, the need for added surfactant is removed, as one can simply perform an emulsion copolymerization with a hydrophilic monomer to provide colloidal stability. Secondly, the stabilizer is 'built-in,' with no possibility of surfactant migration and other such problems in the final product. Finally, the new-found tools at the polymer chemist's disposal of controlled-radical polymerization via RAFT[10-14] (Reversible Addition Fragmentation Chain Transfer) and nitroxide-mediated[15-17] polymerization techniques have allowed the ability to control the length

and nature of the stabilizing block, and the synthesis of novel diblock structures that can serve as effective particle stabilizers.[8, 16, 18]

Despite the massive industrial interest in (electro)sterically stabilized systems, very little scientific endeavour has been invested in an attempt to better understand these systems. Poly(acrylic acid)[19] (polyAA) and poly(ethylene oxide)[20] stabilized latexes are plagued by secondary nucleation (the formation of new particles after the establishment of an original population of polymer particles) under conditions where new particle formation should not be possible; the rate coefficients of radical entry and radical exit (that govern the growth of polymer particles) in polyAA stabilized emulsions have demonstrated significant departures[19, 21] from the well-accepted mechanisms that govern these events in electrostatically stabilized systems. The use of amphiphilic block copolymers as 'surfactants' in *ab initio* emulsion polymerization experiments has also given strange results in the literature,[22] with unexpected dependencies on the charge on both the hydrophilic block and the initiator. It is clear that these systems are extremely poorly understood, and that the stabilizer itself plays a crucial role in the different kinetics these systems display. Nonetheless, (electro)sterically stabilized emulsions remain (to date) a poorly examined area of polymer science.

1.3. Aims and Objectives

The aim of this work is to quantitatively characterize the kinetics that govern the key processes in (electro)sterically stabilized emulsion polymerization systems – namely particle growth and particle formation. Particle growth is essentially controlled by three parameters – the relative rates of radical entry and radical exit into and out of any given particle as well as intra-particle termination, and the respective rate coefficients of entry and exit will be measured in this work. Particle formation (in particular new particle formation in seeded experiments, also known as secondary nucleation), which is extremely poorly understood in (electro)sterically stabilized

emulsion systems, will be studied by model testing and comparison to experimental data previously obtained for these systems. Through understanding and characterizing the kinetics and mechanisms that control these systems, (electro)sterically stabilized emulsions will be better understood at a molecular level, which is essentially the long-term goal of this work.

The significant technical advantage that now exists (and helps make this project possible) is the ability to develop model systems through controlled radical polymerization in emulsion.[13] This will be discussed in further detail throughout this thesis, however in essence there exists for the first time a means to synthesize an (electro)sterically stabilized emulsion where the length of the stabilizing block is known (and controllable), and of narrow molecular weight distribution. This allows the rate coefficients of interest to be studied as a function of the length of the stabilizing block and coverage of the particle surface (as well as the degree of ionization of the stabilizing block), which have previously been impossible to control. As a result new trends can be obtained (for example, the behaviour of the exit rate coefficient as a function of stabilizing block length) that allow potential optimization of reaction conditions and elucidation of the mechanisms that govern these events.

As (electro)sterically stabilized emulsions formed under RAFT control retain an active RAFT end-group that can significantly affect inter- and intra-particle kinetics,[23] the first aim of this work is to synthesize 'model' emulsions – to utilize the RAFT technique to control the nature of the stabilizing block while successfully removing /modifying the RAFT end-group at the conclusion of the synthesis, without destroying the particle structure. Upon successful removal of the RAFT agent, the rate coefficients for radical entry and exit will be measured using established techniques[3, 24-26] with a view to comparison with the accepted mechanistic models for these processes in electrostatically stabilized emulsion systems.[5, 6, 27] Upon determination of these experimental parameters, the construction of a new kinetic model (based on extensions of established kinetics) to completely describe the behaviour of these systems is viewed as a long-

term goal from this work. The final aim of this project is to provide some insight into the highly unusual behaviour regarding secondary nucleation in (electro)sterically stabilized emulsions, essentially completing the picture regarding the kinetic behaviour of these systems.

Given the wealth of experimental data in the literature regarding the polymerization of styrene, it is used as the main hydrophobic monomer in this work. Similarly as most of the prior work regarding (electro)sterically stabilized emulsions involve polyAA stabilization, acrylic acid is used as the main hydrophilic monomer for stabilization in the experiments presented in this work. The structures of these monomers are given in Figure 1.3.

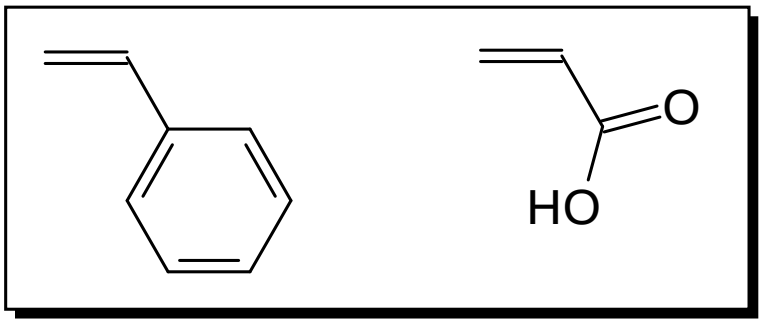

Figure 1.3. Structures of styrene (left) and acrylic acid (right).

1.4. Outline of the Thesis

This thesis is constructed in essentially 'chronological' order with regards to the aims and objectives of this work. Chapter 2 presents a comprehensive introduction to the kinetics of emulsion polymerization, and the well accepted mechanisms that govern polymerization in electrostatically stabilized systems. Chapter 3 outlines the synthesis of a model system, with the construction of well-controlled (electro)sterically stabilized emulsions with the RAFT agent removed, as well as the complexities of working with particular hydrophobic monomers for kinetic analysis. Chapter 4 presents the detailed results from radical exit experiments using these synthesized emulsions and the observed mechanistic inferences, while Chapter 5 presents the

same experimental data for radical entry experiments. Chapter 6, the product of the previous two chapters, introduces the development of a full kinetic model to describe the behaviour of (electro)sterically stabilized emulsion systems, and the supporting evidence regarding the newly postulated mechanisms in this work. Chapter 7 completes this picture with the kinetic modelling of newly proposed nucleation mechanisms that are significant in these systems, with Chapter 8 presenting the overall conclusions from this work and future directions of any subsequent research.

It should be noted that as all experimental data collected in this work was performed at pH 7, where the ionization of the stabilizing polyAA block is complete, all emulsions are electrosterically (not solely sterically) stabilized and the terms 'electrosteric' and 'electrosterically' will be used throughout this thesis without the need for distinguishing brackets – so that the reader is aware of the dual mode of stabilization present in these systems.

References

1. Moad, G.; Solomon, D. H. *Australian Journal of Chemistry* **1990,** 43, 215-39.

2. Urban, D.; Takamura, K., *Polymer Dispersions and their Industrial Applications*. Wiley-VCH: Weinheim, 2002.

3. Gilbert, R. G., *Emulsion Polymerisation: A Mechanistic Approach*. Academic Press: San Diego, 1995.

4. Verwey, E. J. W.; Overbeek, J. T. G., *Theory of the Stability of Lyophobic Colloids*. Elsevier: Amsterdam, 1948.

5. Hansen, F. K.; Ugelstad, J., Piirma book. In *Emulsion Polymerization*, Piirma, I., Ed. Academic: New York, 1982.

6. Ugelstad, J.; Hansen, F. K. *Rubber Chemistry and Technology* **1976,** 49, 536-609.

7. Smith, W. V.; Ewart, R. H. *Journal of Chemical Physics* **1948,** 16, 592-9.

8. Rager, T.; Meyer, W. H.; Wegner, G.; Mathauer, K.; Machtle, W.; Schrof, W.; Urban, D. *Macromolecular Chemistry and Physics* **1999,** 200, 1681-1691.

9. Napper, D. H., *Polymeric Stabilization of Colloidal Dispersions*. Academic: London, 1983.

10. Chiefari, J.; Chong, Y. K.; Ercole, F.; Krstina, J.; Jeffery, J.; Le, T. P. T.; Mayadunne, R. T. A.; Meijs, G. F.; Moad, C. L.; Moad, G.; Rizzardo, E.; Thang, S. H. *Macromolecules* **1998,** 31, 5559-5562.

11. Chiefari, J.; Mayadunne, R. T. A.; Moad, C. L.; Moad, G.; Rizzardo, E.; Postma, A.; Skidmore, M. A.; Thang, S. H. *Macromolecules* **2003,** 36, 2273-2283.

12. Chong, Y. K.; Krstina, J.; Le, T. P. T.; Moad, G.; Postma, A.; Rizzardo, E.; Thang, S. H. *Macromolecules* **2003,** 36, 2256-2272.

13. Ferguson, C. J.; Hughes, R. J.; Nguyen, D.; Pham, B. T. T.; Gilbert, R. G.; Serelis, A. K.; Such, C. H.; Hawkett, B. S. *Macromolecules* **2005,** 38, 2191-2204.

14. Moad, G.; Chong, Y. K.; Postma, A.; Rizzardo, E.; Thang, S. H. *Polymer* **2005,** 46, 8458-8468.

15. Delaittre, G.; Nicolas, J.; Lefay, C.; Save, M.; Charleux, B. *Chemical Communications* **2005**, 614-616.

16. Nicolas, J.; Charleux, B.; Guerret, O.; Magnet, S. *Angewandte Chemie, International Edition* **2004,** 43, 6186-6189.

17. Nicolas, J.; Charleux, B.; Guerret, O.; Magnet, S. *Macromolecules* **2004,** 37, 4453-4463.

18. Pham, B. T. T.; Nguyen, D.; Ferguson, C. J.; Hawkett, B. S.; Serelis, A. K.; Such, C. H. *Macromolecules* **2003,** 36, 8907-8909.

19. Vorwerg, L.; Gilbert, R. G. *Macromolecules* **2000,** 33, 6693-6703.

20. Hammond, M. Sterically Stabilized Emulsion Systems. Honours Thesis, Honours Thesis,The University of Sydney, Sydney, 1983.

21. Coen, E. M.; Lyons, R. A.; Gilbert, R. G. *Macromolecules* **1996,** 29, 5128-5135.

22. Leemans, L.; Jerome, R.; Teyssie, P. *Macromolecules* **1998,** 31, 5565-5571.

23. Prescott, S. W.; Ballard, M. J.; Rizzardo, E.; Gilbert, R. G. *Macromolecules* **2005,** 38, 4901-4912.

24. Gilbert, R. G.; Napper, D. H. *Journal of Macromolecular Science - Macromolecular Chemistry and Physics C* **1983,** 23, 127-186.

25. Lansdowne, S. W.; Gilbert, R. G.; Napper, D. H.; Sangster, D. F. *Journal of the Chemical Society, Faraday Transactions 1: Physical Chemistry in Condensed Phases* **1980,** 76, 1344-55.

26. Morrison, B. R.; Casey, B. S.; Lacik, I.; Leslie, G. L.; Sangster, D. F.; Gilbert, R. G.; Napper, D. H. *Journal of Polymer Science, Part A: Polymer Chemistry* **1994,** 32, 631-49.

27. Maxwell, I. A.; Morrison, B. R.; Napper, D. H.; Gilbert, R. G. *Macromolecules* **1991,** 24, 1629-40.

2. Kinetics of Emulsion Polymerization: Theory and Experiment

"The truth is incontrovertible; malice may attack it, ignorance may deride it, but in the end, there it is."

Sir Winston Churchill

2.1. Introduction

The kinetics of emulsion polymerization is a complex science, requiring well-designed experiments, the knowledge a large number of separate rate coefficients and the modelling of a number of interfacial processes. In this chapter, the foundation on which this work is based is presented – namely the well-accepted kinetics and mechanisms that govern electrostatically stabilized emulsion systems and the typical experimental techniques utilized here. Given the expected difference between the kinetics of electrostatically and the electrosterically stabilized emulsion systems of interest, mechanisms presented here are a 'reference point' for comparison to well understood systems. Any observed differences are attributed to the effect of the electrosteric stabilizer.

It should be noted that the general setting for most experiments conducted in this project involve a seeded emulsion polymerization in the presence of excess monomer. This avoids the mechanisms of particle formation complicating experimental data, while excess monomer ensures that the emulsion particle interior remains monomer saturated for the duration of the period of interest during the experiment. As a result, the rate of polymerization at the polymerization locus (the particle interior) is dependent only on the rate of introduction (entry) and the rate of removal (exit) of radicals from this location. Isolation of these events allows their respective rate coefficients to be determined and mechanisms to be studied.

2.2. Fundamental Polymerization Reactions

An emulsion polymerization reaction is a heterogeneous version of a typical free-radical polymerization, and the fundamental reactions that govern a free-radical polymerization naturally occur in emulsion systems. A discussion of the four main fundamental reactions (initiation, propagation, transfer and termination) is given below.

2.2.1. Initiation

The first fundamental reaction to be considered is initiation, the reaction that generates radical activity. An initiator molecule (typically water-soluble in the case of an emulsion system) dissociates into two radical species, usually after heating or photo-irradiation. Azo-based initiators such as azobisisobutyronitrile (AIBN, which is a hydrophobic initiator) and V-501 (a water-soluble initiator) are extremely common and involve the production of two radical moieties as well as evolution of nitrogen gas. In this project however the most widely used initiator is potassium persulfate (KPS), which thermally decomposes into two sulfate radical ions, as shown in Figure 2.1.

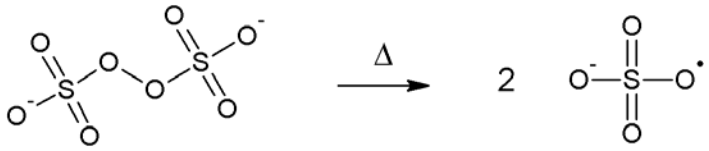

Figure 2.1. Decomposition of persulfate into initiating sulfate radical ions.

The first-order rate coefficient for initiator decomposition is denoted k_d (s^{-1}). It should be noted however that the rate of initiation is not necessarily equal to the rate of radical generation, due to geminate recombination.[1] The fraction of initiator-derived radicals that successfully initiate a polymer chain is called the initiator efficiency (denoted *f*), which can vary dramatically with conversion (due to increased viscosity in the case of bulk or solution polymerization) as well as being solvent-dependent.[2] The value of k_d for persulfate has also shown to vary in the presence of monomer[3] relative to its value in a pure solvent (such as distilled water), while under certain conditions (extremely low or high pH) the decomposition mechanism is no longer a 'clean' unimolecular dissociation[1] but is complicated by bimolecular reactions yielding different radical species.

2.2.2. Propagation

Propagation is the reaction that involves the sequential addition of monomer units onto a growing polymeric chain. Each propagation step results in the degree of polymerization (denoted DP, the number of monomeric units in the chain) increasing by one; the 'head-to-tail' propagation[1] of a poly(styrene) radical is shown in Figure 2.2.

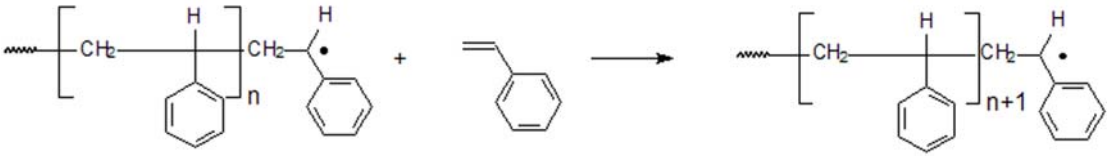

Figure 2.2. Propagation of a poly(styrene) radical with a styrene monomer unit.

The rate coefficient for propagation at the long-chain limit is denoted k_p (units M^{-1} s^{-1}); the value of this rate coefficient is typically independent of chain length. At very low degrees of polymerization the propagation rate coefficient is chain-length dependent; as an example the propagation rate coefficient of a monomeric radical (denoted k_p^1) is usually considered to be 4-10 times larger than the long-chain limit.[4-8] This result is due to the smaller rotational moment of inertia of the monomeric radical increasing the Arrhenius pre-exponential factor[7-9] that in turn increases the rate coefficient for this process. Accurate, reliable measurement of k_p values has only recently been made possible in the past twenty years through the development of the PLP-SEC[10-15] method; consequently the rate coefficients for most common organic monomers have been reported in the literature.

2.2.3. Transfer

Chain transfer (the transfer of radical activity from a growing polymeric radical to another species) is a very common reaction in free-radical polymerization. Transfer to monomer (denoted k_{tr}) is extremely common in styrene polymerization, while the addition of other 'chain

transfer agents' (denoted A-X) to the reaction medium can significantly increase the likelihood of a transfer event. A schematic chain transfer reaction is shown in Figure 2.3.

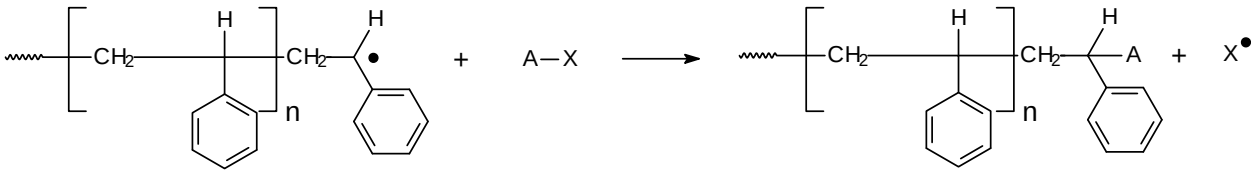

Figure 2.3. Transfer of radical activity from a growing polymer chain to a chain transfer agent.

Chain transfer results in the 'death' of a growing chain, yet there is no net loss of radical activity. As a result, addition of a chain transfer agent is a very easy means to vary the molecular weight distribution of a resultant polymer – the average degree of polymerization of any polymer will be reduced at higher chain transfer agent concentrations – without reducing the overall polymerization rate. Typically 'A' in Figure 2.3 is a hydrogen atom and most transfer reactions are simple hydrogen atom abstractions however species such as CBr_4 and CCl_4 are also extremely efficient chain transfer agents.

One very special class of chain transfer agents are known as 'Reversible Addition Fragmentation Chain Transfer' agents, more commonly known as RAFT agents.[16] These species (typically dithioesters or trithiocarbonates) allow a reversible chain transfer mechanism to take place where at any given time growing polymeric radicals are 'capped' by a RAFT end-group, minimizing bimolecular termination reactions. Addition of monomer units can only take place when the radical is not capped, affording excellent molecular weight control. Similarly the fact that at the end of the reaction all the polymer chains are still 'alive' means that novel architectures (such as di- and multi-blocks, stars and combs) can be synthesized that were not previously possible. More detail on the nature of the RAFT mechanism and 'RAFT control' will be given later in this chapter, as the advent of 'RAFT in emulsion'[17] essentially allowed this project to occur through the synthesis of well-defined electrosterically stabilized emulsions.

As well as transfer to an added chain transfer agent, transfer to polymer can be an extremely important reaction in some polymerization systems. Transfer to polymer occurs either by an intermolecular or intramolecular mechanism – the intramolecular mechanism commonly known as 'chain backbiting.' Backbiting is extremely important in alkyl acrylates[18-21] such as *n*-butyl acrylate, and the slow-to-propagate tertiary radical is known to complicate kinetic analyses of acrylate systems.[20, 22-25] The mechanism of chain backbiting (via a six-membered transition state) is shown in Figure 2.4. It will be seen through this thesis that transfer to polymer is extremely important in electrosterically stabilized emulsion systems, a mechanism never previously considered.

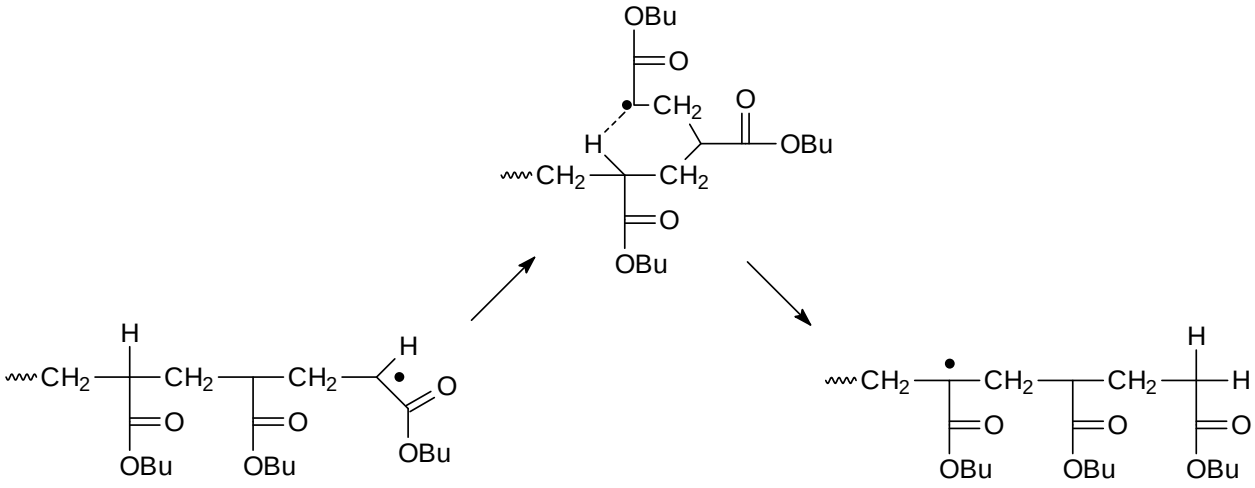

Figure 2.4. Mechanism of intramolecular transfer to polymer in alkyl acrylate systems.

2.2.4. Termination

Termination reactions occur when the radical end of growing polymeric chains approach one another, resulting in the loss of radical activity for two separate species and the formation of 'dead' polymer chains. Termination occurs by two mechanisms – combination and disproportionation – that lead to different termination products and different overall molecular weight distributions (MWDs). In the case of emulsion polymerization, it is not important to

distinguish these events kinetically – the important outcome is that the termination reaction leads to the annihilation of polymeric radical activity.

Combination (Figure 2.5) is typically the most dominant termination mechanism, and is known to occur for styrene polymerizations.[1] Two unpaired electrons form a new covalent bond linking the two polymeric radicals, resulting in a dead polymer chain where the degree of polymerization is equal to the sum of the degrees of polymerization of the component species. The actual chemical reaction itself is so fast as to be considered diffusion-controlled,[26] meaning that radical ends must simply 'encounter' one another (through centre-of-mass and segmental diffusion) for termination to take place.

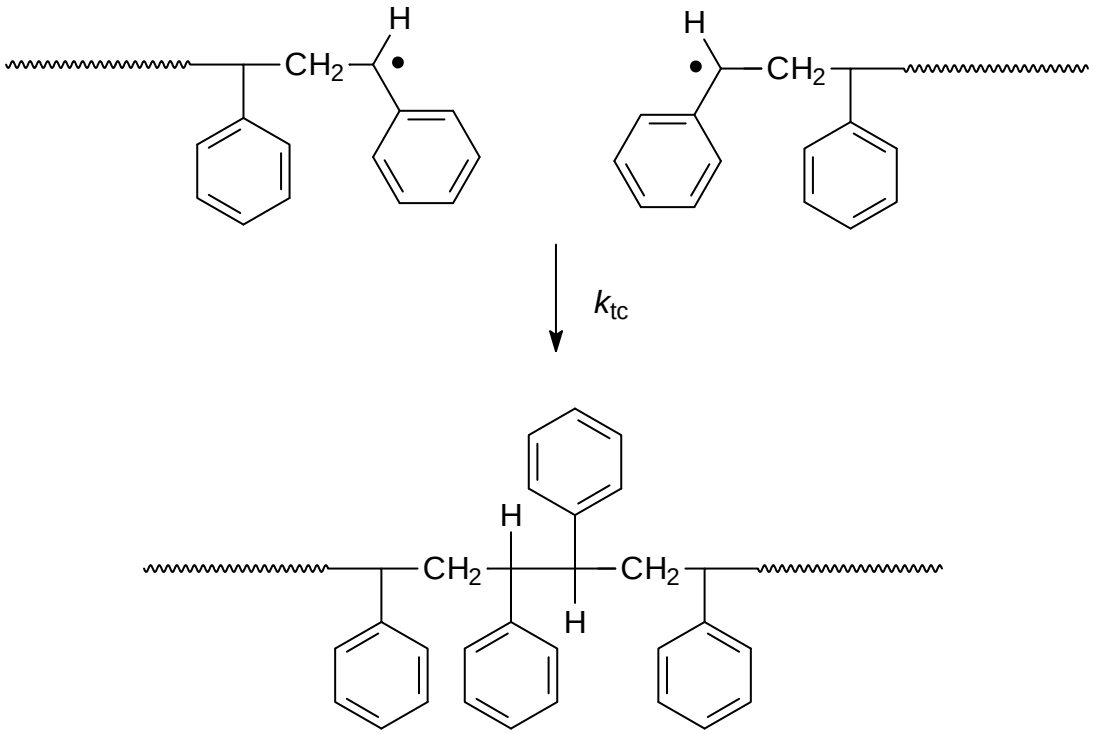

Figure 2.5. Termination by combination in the polymerization of styrene.

Disproportionation involves the formation of two dead polymer chains (rather than one in a combination reaction) through a hydrogen abstraction reaction. This yields one chain with an unsaturated end-group and one with a saturated end-group, and is typical for methyl methacrylate

(MMA) polymerizations[27] as the reaction involves two hindered species. The disproportionation reaction naturally has a higher activation energy (due to the abstraction of a hydrogen atom) compared to the combination mechanism which has an activation energy close to zero in condensed phases.

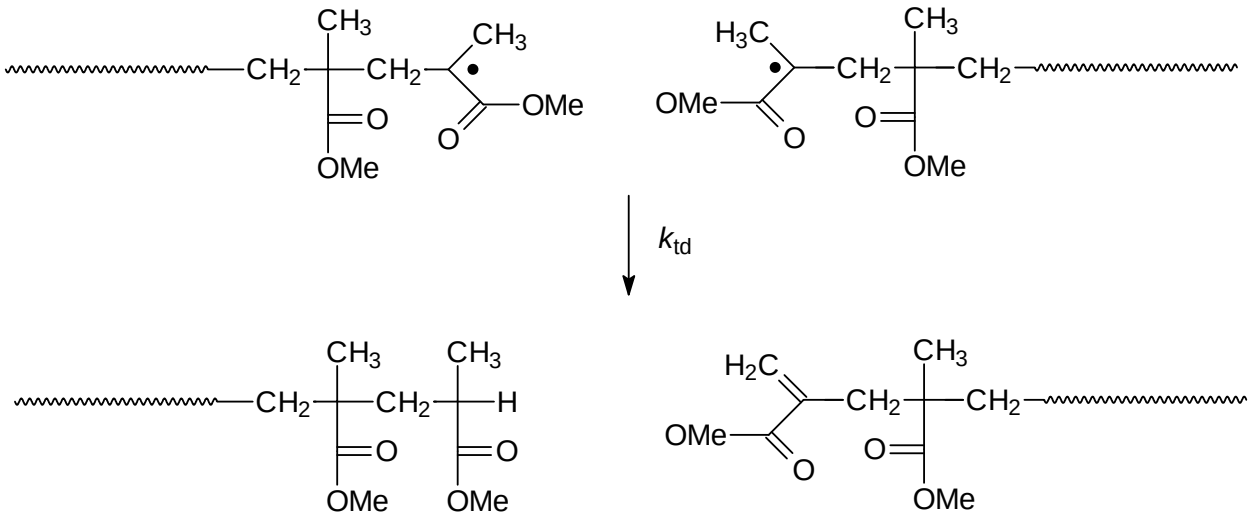

Figure 2.6. Termination by disproportionation in the polymerization of methyl methacrylate.

The dominant events in termination at low polymer concentration are still a matter of debate;[28-30] however the situation is simplified in the case of an emulsion polymerization. As the polymer concentration in a particle is always above c^{**} (the concentration at which chains are entangled), the dominant event in termination in emulsion polymerizations is expected to be the diffusion of a relatively small (mobile) radical resulting from initiator or from transfer with a much longer (relatively immobile) radical chain.

Given that the termination mechanism involves centre-of-mass as well as segmental diffusion, the process is chain-length dependent and the measurable rate coefficient for termination is an average value, denoted $\langle k_t \rangle$. Extensive work[31-36] on modelling this process has been performed. Expressions for the individual rate coefficients (denoted $k_t^{i,j}$, the termination rate coefficient between an *i*-mer and a *j*-mer) and their chain-length-dependence have been reported. The value

of $<k_t>$ is also dependent on fractional conversion, as a change in the viscosity of the reaction medium affects the ability of radicals to diffuse and encounter one another.

2.3. Emulsion Polymerization: A General Description

2.3.1. Interfacial Processes

The reactions described in Section 2.2 occur in all manner of free-radical polymerization reactions. The heterogeneous nature of an emulsion polymerization system means that additional physical and chemical processes at interfaces (as well as the generation of new phases) need to be considered. Key interfacial processes are outlined below.

2.3.1.1. Particle Formation

In the case of an *ab initio* emulsion polymerization reaction, particle formation is the process that generates new interfacial area and the creation of a new phase (on top of stabilized monomer droplets and the continuous phase). Particle formation can also take place in seeded systems (where an existing population of polymer particles is polymerized further), which is known as secondary nucleation.

Particle formation typically takes place via two dominant mechanisms – homogeneous nucleation[6, 37, 38] and micellar nucleation.[6, 39] Both mechanisms involve propagation in the aqueous phase (as initiators are typically water soluble) with the slight amount of solubilized monomer. The homogeneous nucleation mechanism involves propagation until the oligomer 'precipitates' out of solution to form a 'precursor particle.' (A precursor particle is a small, colloidally unstable particle that upon further propagational growth, coagulation and adsorption of surfactant will eventually grow to form a colloidally stable 'mature' particle). The micellar nucleation mechanism on the other hand (which only operates above the critical micelle concentration (CMC) of the added surfactant) involves an entry event into a monomer-rich

micelle when the oligomer is surface-active. These precursor particles can become swollen with more monomer, coagulate with other precursor species and grow in size until they become a true, stable latex particle. A more detailed treatment of the homogeneous nucleation mechanism will be given later in this thesis when secondary nucleation in electrosterically stabilized emulsion systems is considered (Chapter 7).

2.3.1.2. Monomer Diffusion

The interior of a formed latex particle serves as the main locus of polymerization in an emulsion system, not the emulsified monomer droplets. These droplets serve as a reservoir of monomer for the polymerization reaction, with diffusion of the monomer from the droplet into the particle interior taking place. Typical organic monomers can readily be reacted to complete conversion in an emulsion polymerization system, so monomer diffusion is not usually considered to be an important process to consider. It is rapid on the timescale of other processes and reactions taking place at the same time. It should be noted however that monomer diffusion can become rate-determining if the consumption of monomer is extremely rapid[40] or if the monomer is extremely hydrophobic (such as dodecyl methacrylate[41] and stearyl acrylate,[42] but not for others such as vinyl neodecanoate[43]).

2.3.1.3. Radical Entry and Exit

As has been mentioned previously, the main locus of polymerization in an emulsion system is the particle interior. Most initiators, however are water-soluble. As radicals are being generated in the aqueous phase, there must be a mechanism by which radical activity transfers to the particle interior, a process known as 'radical entry.' Radicals formed from direct decomposition of an initiator (such as a sulfate ion radical) are generally considered to be too hydrophilic to transport to the particle interior, and as a result it is generally considered that propagation in the aqueous phase takes place until the oligomeric species attains surface-active properties, making entry much more likely.

The controversial issue dominating the study of radical entry has been the determination of the mechanism and the rate-determining step that governs the overall entry process. Many potential mechanisms have been put forward in the literature. A detailed account of these will be given later in this Chapter. Previously, the biggest difficulty in refuting these postulated mechanisms was the limited amount of accurate experimental data, or data processing that was free of model-based assumptions. This has been overcome with carefully designed experiments[6, 44] that allow extraction of rate coefficients in a model-free way to allow for hypothesis testing. The currently accepted mechanism for radical entry will be given in Section 2.5.

As well as bimolecular termination reactions, radicals can be lost to the polymerization locus through a process known as 'radical exit.' Intuitively, this involves the movement of radicals from the particle interior to the aqueous phase, and has been shown to be a non-negligible process in the emulsion polymerization of a number of monomers.[6, 45-48] A detailed description of the exit mechanism will be given in Section 2.4 It should be noted, however, that exit is considered to be restricted to monomeric radicals (generated by chain transfer to monomer), as monomeric radicals are much more water-soluble than any other uncharged radical species.

2.3.2. The Intervals of an Emulsion Polymerization

A typical emulsion polymerization reaction can be described by three distinct intervals, labeled Intervals I, II and III.[6] These intervals correspond to different rate behaviour and different compositions of the emulsions with respect to the number of particles present as well as the presence (or absence) of monomer droplets and micelles.

Interval I is where particle formation takes place; monomer droplets, surfactant (and monomer-swollen micelles if above the critical micelle concentration, CMC) and pre-cursor particles are present. As particles are formed, the particle number (denoted N_p, the number concentration of particles per unit volume, units L^{-1}) continues to increase and throughout this interval the

reaction rate is also increasing. Particle formation (and the end of Interval I) is considered to be complete when the number of particles is high enough to capture all growing aqueous-phase oligomers before further nucleation can occur.

Interval II represents the conclusion of the particle formation period, at which the value of N_p remains constant and all aqueous-phase oligomers capable of entry into a latex particle will undergo entry. The particle interior in this Interval is saturated with monomer at a concentration C_p^{sat}, with any excess monomer residing in monomer droplets. Diffusion of monomer from droplets to the particle phase ensures a constant monomer concentration, constant polymerization rate and growth in size of the existing polymer particles. (This is in fact an approximation, but solutions to the Morton equation [49] describing monomer concentration as a function of particle size show that the saturation concentration is, to a good approximation, constant for all except very small particles. Modelling shows that the means used to infer mechanisms from appropriate data discussed in this review are quite insensitive to the small changes predicted by the Morton equation [50]).

Interval III marks the point where all monomer droplets have been depleted, with the only unreacted monomer now residing inside the particles. The monomer concentration in the particles (denoted C_p as the particle interior is no longer saturated) now decreases with conversion, resulting in a decrease in the polymerization rate. It should be pointed out, however, that above a certain weight fraction of polymer (w_p) the 'Tromsdorff-Norrish effect' or 'gel effect[51, 52]' exists where the effective termination rate is reduced due to restricted diffusion of polymeric radicals, resulting in an actual increase in polymerization rate. Naturally, as complete conversion to polymer is approached, the polymerization rate tends towards zero. A graphical representation of the three intervals described is given in Figure 2.7.

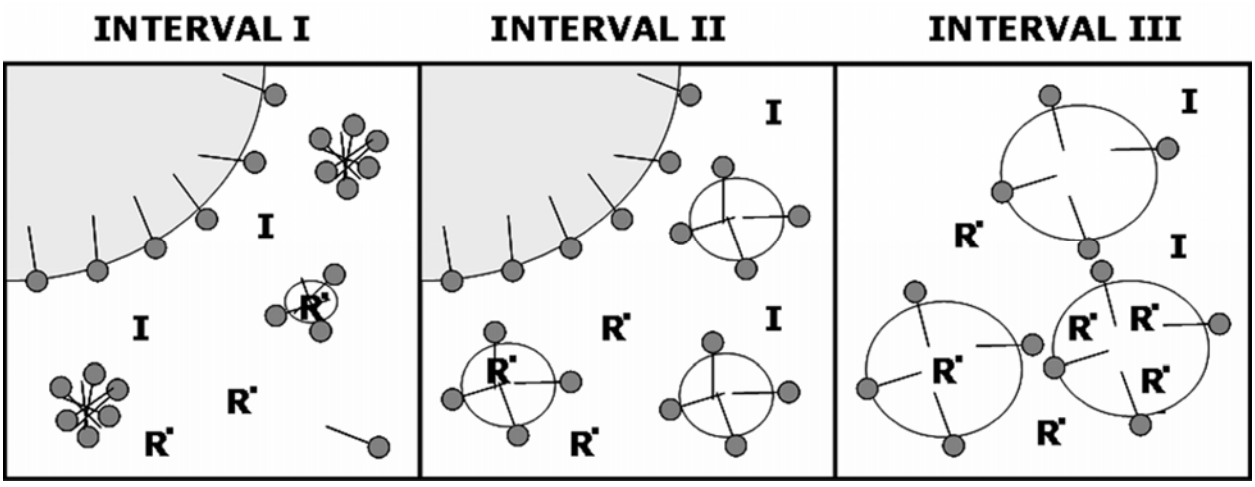

Figure 2.7. The three intervals of an emulsion polymerization reaction. Initiator molecules are denoted by I, oligomeric or polymeric radicals denoted by R. Monomer droplets and polymer particles (stabilized by surfactant) are shaded grey and white respectively.

Due to the complicated nature of the particle formation process, much research has been devoted to understanding the polymerization within Interval II, where the reaction rate is constant over a large time interval. Determination of how this steady-state polymerization rate varies as a function of particle number (N_p) and initiator concentration ([I]) gives access to the mechanisms that govern events such as radical entry and exit. However, the early attempts to explain these dependencies (such as the pioneering work of Smith and Ewart[39]) included assumptions relating to particle formation within Interval I. The complicated nature of this process means that unambiguous rate coefficients for entry and exit cannot be determined, which has made seeded experiments that begin within Interval II (by-passing particle formation) the method of choice for kinetic experiments. After the synthesis of well-defined monodisperse seed latex, further polymerization in the absence of any newly nucleated particles eliminates the complication of polymerization of new particles as well as allowing the kinetics to be followed as a function of particle size.

2.3.3. The Rate of an Emulsion Polymerization

The rate of a polymerization is normally defined as the rate of consumption of monomer. While an emulsion system has the added complication of being a heterogeneous medium where radicals and monomer are compartmentalized, the same definition still applies. This definition is:

$$\frac{\mathrm{d[M]}}{\mathrm{dt}} = -k_\mathrm{p}[\mathrm{M}][\mathrm{R}] \tag{2.1}$$

where [M] is the concentration of monomer and [R] the total radical concentration. In an emulsion where the polymerization only takes place within the particle interior [M] is replaced by C_p; the total radical concentration is given by $\bar{n}\,N_p/N_A$ where N_p is the number of latex particles per unit volume and $\bar{n}$ is the average number of radicals per particle. This quantity will be a significant focus of this work.

As the determination of fractional conversion (the fraction of monomer that has been converted to polymer) is a relatively easy quantity to measure as a function of time, the rate of change of fractional conversion (denoted x) with respect to time is considered; change of variable gives the following expression:

$$\frac{\mathrm{d}x}{\mathrm{dt}} = \frac{k_\mathrm{p}C_\mathrm{p}N_\mathrm{p}}{n_\mathrm{M}{}^0 N_\mathrm{A}}\bar{n} \tag{2.2}$$

where $n_M{}^0$ is the initial number of moles of monomer per unit volume of the reaction (all other parameters as defined previously). In Interval II, the values of N_p and C_p are known (and constant), allowing values of $\bar{n}$ to determined directly from the experimental monitoring of the polymerization rate.

2.3.4. The Smith-Ewart Equations

The first attempts to model the kinetics of emulsion polymerization systems were performed by Smith and Ewart, who developed a now-famous set of equations[39] that represent the time evolution of the number of particles containing n radicals (denoted N_n). These equations incorporated the kinetic events that involve the gain of loss of radicals within particles (i.e. radical entry, radical exit, and bimolecular termination), affecting the relative populations of each N_n. If the population of latex particles is normalized such that

$$\sum_{n=0}^{\infty} N_n = 1 \tag{2.3}$$

then the average number of radicals per particle ($\overline{n}$) is given by:

$$\overline{n} = \sum_{n=1}^{\infty} n\, N_n \tag{2.4}$$

allowing the value of $\overline{n}$ (which can be measured experimentally) to be modeled via the Smith-Ewart equations. The general form of the equations in question is:

$$\frac{dN_n}{dt} = \rho[N_{n-1} - N_n] + k[(n+1)N_{n+1} - nN_n] + c[(n+2)(n+1)N_{n+2} - n(n-1)N_n] \tag{2.5}$$

where ρ is the pseudo-first order rate coefficient for entry from the aqueous phase, k is the pseudo-first order rate coefficient for radical exit (desorption) of a single free radical from a latex particle, and c is the pseudo-first order rate coefficient for bimolecular termination (again per free radical) between two free radicals that reside within a single particle. Due to compartmentalization of radicals within latex particles, bimolecular termination between radicals in different particles need not be considered. The rate coefficients ρ, k and c are dependent on a variety of different variables such as the initiator concentration ([I]), the particle number N_p, the

particle size, the monomer concentration within the particle phase C_p, the weight fraction of polymer w_p, as well as the average number of radicals per particle itself, $\bar{n}$. These rate coefficients have detailed microscopic expressions related to their respective mechanisms, and these will be given in detail in the appropriate section.

Considering that polymerization within Interval II is marked by a period of constant polymerization rate, there is considerable interest in understanding the steady-state behaviour of the solution of Equation 2.5, and thereby determining the theoretical value for the steady-state average number of radicals per particle, $\bar{n}_{ss}$. The complete steady-state solution of these equations can be found in the work of Ugelstad and Hansen[38] as well as Gilbert and Napper,[53] however these solutions are for the case where ρ, k and c are independent of $\bar{n}$. Of particular importance for the determination of mechanistic information from kinetic experiments is the use of various limiting forms of the Smith-Ewart equation, and the knowledge of the applicability of such limits.

2.3.4.1. The 'Pseudo-Bulk' Limit

In an emulsion polymerization, radicals are compartmentalized from one another – that is, radicals in one latex particle cannot 'see' radicals contained in another particle and as a result reactions such as bimolecular termination cannot occur between radicals in different particles. The effect of compartmentalization is strongly linked to the size of the latex particles being considered, as very small particles cannot contain a large number of radicals (due to rapid termination reactions leading to a loss of radical activity).

Typically for small particles, intra-particle termination is considered to be so fast so as to not be rate-determining. This assumption can break down however under certain conditions, having the effect of lifting the assumption of compartmentalization completely, i.e. all of the N_n are non-zero, and that a number of radicals can co-exist in the same particle, undergoing all of the typical

chemical and physical fates such as propagation, transfer, desorption and termination. Because of chain-length-dependent kinetics, the complete kinetic equations describing this (the full generalization of the Smith-Ewart equations) cannot be written in closed form (although some limited solutions for this exist as in the so-called 'zero-one-two' case[54]). A limiting form of these equations however does exist. This limit is known as 'pseudo-bulk' limit as the absence of radical compartmentalization makes the system equivalent to a bulk or solution polymerization. The experimentally observable $\overline{n}$ can be modeled using the following time-dependent equation:[6, 53]

$$\frac{d\overline{n}}{dt} = \rho - k\,\overline{n} - 2\,c\,\overline{n}^2 \tag{2.6}$$

where c is the pseudo-first order rate coefficient for termination between two chains ($c = \langle k_t \rangle / N_A V_s$ where V_s is the swollen volume of the latex particle and $\langle k_t \rangle$ is the average bimolecular termination rate coefficient in the system in question). Equation 2.6 is only true when the N_n forms a Poisson distribution; this is the case for large values of $\overline{n}$.[55] Ballard and co-workers demonstrated that the pseudo-bulk equation gave excellent agreement with the full solution of the Smith-Ewart equations provided that $\rho > c$ or $k > c$,[56] ensuring that radicals rapidly exchange amongst the particle population.

2.3.4.2. The 'Zero-One' Limit

As opposed to the 'pseudo-bulk' limit, the 'zero-one' limit assumes complete compartmentalization in that any given latex particle can contain at most one radical, i.e. $N_n = 0$, $n \geq 2$. The presence of two radicals in any one particle leads to 'instantaneous' termination, which can be described mathematically as ρ, $k <<< c$. This assumption means that there are only two population equations that need to be solved, namely:

$$\frac{dN_0}{dt} = \rho (N_1 - N_0) + kN_1 \tag{2.7}$$

$$\frac{dN_1}{dt} = \rho (N_0 - N_1) - kN_1 \tag{2.8}$$

where N_0 and N_1 are the populations of latex particles with zero and one radicals respectively. In this limit $\overline{n} = N_1$, which yields the following rate equation for the time evolution of $\overline{n}$:

$$\frac{d\overline{n}}{dt} = \rho (1 - 2\,\overline{n}) - k\overline{n} \tag{2.9}$$

Equation 2.9 is readily solved in the steady-state, giving the following expression:

$$\overline{n}_{ss} = \frac{\rho}{2\rho + k} \tag{2.10}$$

It can be seen from Equation 2.10 that as the ratio ρ / k increases, $\overline{n}_{ss}$ converges towards 0.5. Within the 'zero-one' limit, this is the upper bound value for $\overline{n}$ in the steady-state region of an emulsion polymerization system – however experimental measurement of a value of $\overline{n}_{ss}$ less than 0.5 is not sufficient proof that the zero-one approximation is valid. (Originally it was often claimed that $\overline{n}_{ss}$ = 0.5 under all conditions; this however was refuted in the early work of Hawkett.[45]) It must also be shown that the 'instantaneous termination' assumption holds if a radical (be it oligomeric or monomeric) enters a particle containing a growing polymeric radical.[57] Kinetically, this is equivalent to stating that the pseudo-first-order rate coefficient for termination c is significantly larger than the rate coefficients for desorption (denoted k_{dM}, units s^{-1}) or further propagation within the particle (pseudo-first order rate coefficient $k_p{}^1C_p$ for the case of an entering species being a monomeric radical).

A detailed description of desorption and a form of the desorption rate coefficient k_{dM} will be given in the section on radical exit (Section 2.4), however it is pointed out here that k_{dM} is a

particle size dependent rate coefficient, showing an inverse square dependence on the particle radius. The pseudo-first-order termination rate coefficient *c* however is inversely proportional to the particle volume, meaning that for larger particles the 'instantaneous termination' assumption begins to break down. It is generally accepted that for poly(styrene) emulsion systems, the 'zero-one' approximation is invalid for particles larger than 100 nm unswollen diameter[47, 57] and as a result kinetic experiments are usually performed with very small latex particles to ensure the validity of this limit. Reaction conditions in this project were chosen so that the 'zero-one' limit was satisfied at all times.

In this treatment of the 'zero-one' limit, the exit of a monomeric radical assumes complete loss of this species from the reaction environment, presumably through termination in the aqueous phase. Yet while termination of an exited radical in the aqueous phase is a potential chemical fate, further re-entry of this species into another latex particle (and further subsequent reactions) must also be considered. This more detailed treatment is given in the following section.

2.4. Radical Exit

2.4.1. Accepted Model for Exit

As mentioned previously, it is generally accepted that monomeric radicals (formed by chain transfer to monomer) will be the only radical species capable of exiting[57] a latex particle due to its 'high' water solubility (similar to that of the monomer itself due to a similar structure). This was supported by the experimental data of McAuliffe,[58] who tested the water solubility of a variety of homologous series of hydrocarbons and demonstrated that the logarithm of the water solubility of a hydrocarbon decreases linearly with molecular volume – in the case of styrene, a dimeric radical is over 1000 times less soluble in water than a monomeric radical at room temperature.

The mechanism by which a monomeric radical exits a latex particle is simple diffusion from the particle interior to the aqueous phase. This first-order process (rate coefficient k_{dM}) was modeled in the work of Ugelstad and Hansen[38] and Nomura[59], and an expression for k_{dM} can be derived from considering the microscopic reversibility of desorption and adsorption by utilizing the Smoluchowski equation for diffusion-controlled adsorption of a radical into a particle. The resulting equation is:

$$k_{dM} = \frac{3\,D_w}{r_s^2}\frac{C_w}{C_p} \tag{2.11}$$

where D_w is the diffusion coefficient of the monomeric radical in water (1.3×10^{-9} m^2 s^{-1} for styrene at 323 K[6]), r_s the swollen particle radius, C_p the concentration of monomer in the particle phase and C_w the concentration of monomer in the aqueous phase. Under Interval II conditions where the aqueous phase is saturated with monomer, C_w = 4.3 mM at 323 K). It is, however important to realize that the total exit rate coefficient k is not equivalent to k_{dM}, as desorption is in competition with propagation, termination and the various fates of an exited monomeric radical. This is discussed below.

2.4.2. The Fate of an Exited Radical

Following desorption of a monomeric species, it is essential to determine the most likely fate of this radical in order to fully understand the kinetic behaviour of the emulsion system in question. The exited radical (denoted $E^{\bullet}$) can either propagate in the aqueous phase, terminate with another radical (either another uncharged monomeric radical, or an initiator-derived oligomer which will typically carry a charge) or re-enter another particle. In the pioneering work of Smith and Ewart[39] several incorrect mechanistic assumptions were made including implicit homo-termination of exited species. Other mechanistic events (in particular the process of re-entry) will

alter the 'reaction order' with respect to $\bar{n}$ of the loss term in the governing kinetic equation, as well as affecting the value of $\bar{n}_{ss}$ within Interval II and III polymerization systems.

One method of incorporating the radical flux of re-entering monomeric radicals into the rate coefficient of radical entry (ρ) is to introduce a 'fate parameter' (denoted α), representing the fraction of exited radicals that re-enter a particle. The entry rate coefficient can now be written as:

$$\rho_{total} = \rho + \alpha k \bar{n} \tag{2.12}$$

where $k\bar{n}$ is the flux of exiting radicals and the fate parameter takes a value between $\alpha = 1$ (corresponding to complete re-entry), and $\alpha = 0$ (corresponding to complete aqueous-phase homo-termination of exited radicals). Hetero-termination (with an initiator-derived radical) corresponds to a value of $\alpha = -1$. Any non-zero values of α introduce non-linearity into the Smith-Ewart equations, meaning that only numerical solutions are possible.

A major breakthrough in understanding the fate of an exited radical came in the form of the experimental work of Lansdowne *et al.*,[44] who used γ-radiation as an initiation source and then monitored reaction rate data when the sample was removed from the radiation source. This will be discussed in more detail in the Experimental section of this Chapter, however the monitoring of the decrease in reaction rate in the absence of any initiating radical flux allowed the exit rate coefficient in these systems to be monitored directly and independently. It was seen that when the 'thermal' or 'spontaneous' entry rate of radicals is considered (see Section 2.5.2), re-entry was shown to be the dominant kinetic event of an exited species in styrene emulsion systems. This was supported by the work of Morrison *et al*[47], where various techniques (such as the approach to steady-state in chemical and γ-initiated experiments) demonstrated that in 'zero-one' styrene systems the most likely fate for a styrene monomeric radical is to exit, re-enter and either

propagate or terminate in that particle (see Figure 2.8). The modeling of Casey[57] also showed that, unless the particle number (N_p) is very low (< 10^{13} L^{-1}, a number that is atypically low for an emulsion system), re-entry will be the dominant fate over termination by several orders of magnitude. The relative likelihood of these various fates are shown in Figure 2.9 for a model styrene emulsion system.

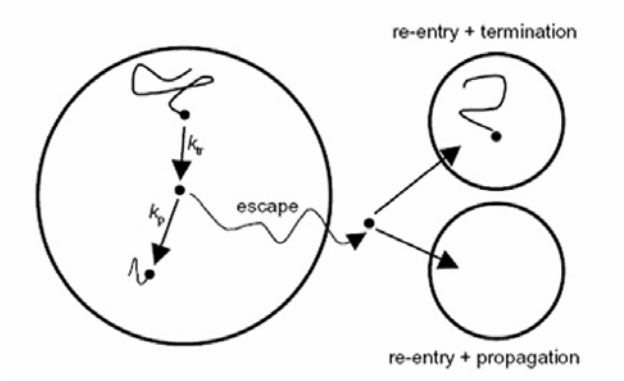

Figure 2.8. Typical exit mechanism in styrene emulsion polymerization systems.

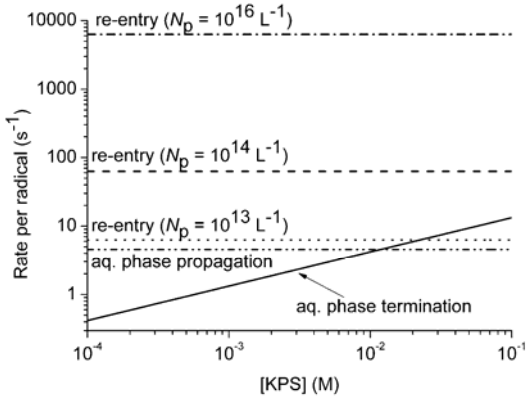

Figure 2.9. Likelihood of the various kinetic fates of an exited monomeric radical in a styrene emulsion system at 323 K as a function of initiator ([persulfate]) concentration, for particle size r_s = 50 nm.

2.4.3. The Extended Zero-One Kinetic Equations and Limits

Given the importance of accounting for the fates of monomeric radicals formed by transfer, the 'zero-one' equations are necessarily extended to differentiate between particles containing one polymeric radical (N_1^{p}) and one monomeric radical (N_1^{m}). This is done because desorption events can only take place from a particle containing a monomeric radical. Accounting for the microscopic events such as desorption, transfer, re-entry and propagation allows for a mechanistic model to be developed for the full exit rate coefficient k, based on other quantities. The following evolution equations for the three populations of interest (N_0, N_1^{m} and N_1^{p}) are as follows:

$$\frac{dN_0}{dt} = \rho\,(N_1^{p} + N_1^{m} - N_0) + k_{dM}N_1^{m} \tag{2.13}$$

$$\frac{dN_1^{m}}{dt} = \rho_{re}N_0 - \rho N_1^{m} - k_{dM}N_1^{m} + k_{tr}C_pN_1^{p} - k_p^{1}C_pN_1^{m} \tag{2.14}$$

$$\frac{dN_1^{p}}{dt} = \rho N_0 - \rho\, N_1^{p} - k_{tr}C_pN_1^{p} + k_p^{1}C_pN_1^{m} \tag{2.15}$$

where k_{tr} is the rate coefficient for radical transfer to monomer, ρ_{re} the pseudo-first order rate coefficient for re-entry of an exited radical into a particle, with all other symbols as defined previously. ρ_{re} can be written as $k_{re}[E^{\cdot}]$ where $[E^{\cdot}]$ is the population of exited radicals and k_{re} the diffusion-controlled rate coefficient for entry of a radical into a particle; if the competition between re-entry and termination is important then the population balance of $[E^{\cdot}]$ can be considered explicitly, namely:

$$\frac{d[E^{\cdot}]}{dt} = k_{dM}N_1^{m}\frac{N_p}{N_A} - k_{re}[E^{\cdot}]\frac{N_p}{N_A} - 2\,k_t[E^{\cdot}][T^{\cdot}] \tag{2.16}$$

where N_p is the number concentration of latex particles (units L^{-1}), k_t the termination rate coefficient between the two radicals being considered, $[T^{\cdot}]$ the total radical concentration within the aqueous phase and N_A Avogadro's number. Incorporation of Equation 2.16 means that only a numerical solution of Equations 2.13 – 2.15 in the steady-state is possible; an analytic steady-state solution is achieved when assuming all exited radicals re-enter, i.e. $\rho_{re} = k_{dM} N_1^{m}$.[6]

Typically the magnitude of N_1^{m} is extremely small and so to a good approximation it can be said that $N_1^{p} = \overline{n}$. Making this approximation and applying the steady-state approximation to Equation 2.14 gives the following kinetic rate equation:

$$\frac{d\overline{n}}{dt} = \rho\,(1 - 2\,\overline{n}) - 2\,k_{tr}C_p\left(\frac{k_{dM}\,\overline{n}}{k_{dM}\,\overline{n} + k_p{}^{1}C_p}\right)\overline{n} \tag{2.17}$$

Comparing the simple (Equation 2.9) and extended (Equation 2.17) versions of the evolution equation for $\overline{n}$, it can be seen that the microscopic form of the exit rate coefficient k equates to:

$$k = 2\,k_{tr}C_p\left(\frac{k_{dM}\,\overline{n}}{k_{dM}\,\overline{n} + k_p{}^{1}C_p}\right) \tag{2.18}$$

with all symbols as defined previously. Equation 2.18 itself is a function of $\overline{n}$, making direct determination of rate coefficients from experimental data extremely difficult. Two important sub-limits of the 'zero-one' approximation are made as a result. These are intuitive and allow for successful model discrimination. These limits are discussed below:

- **Limit 1 – Termination in the Aqueous Phase**

Limit 1 assumes that all exited radicals undergo either homo- or heterotermination in the aqueous phase and play no further role in the polymerization process. It is clear from this that the radical loss mechanism will be first-order with respect to $\overline{n}$ and as a result the kinetic equation governing

such systems is given by Equation 2.9, where k in this case is denoted k_{ct} (ct = complete termination) and is given by:

$$k_{ct} = k_{tr} C_p \frac{k_{dM}}{k_{dM} + k_p{}^1 C_p} \tag{2.19}$$

This expression is readily reached by considering the first-order rate of generation of monomeric radicals formed by transfer and considering the competition between desorption or further propagation.

- **Limit 2 – Complete Re-Entry**

Limit 2 is the opposite case, where all exited radicals undergo re-entry into another latex particle. Upon entry into a particle already containing a growing polymeric radical 'true' radical loss will occur through bimolecular termination; entry into a particle containing no radicals will lead to the entered species either propagating, or undergoing desorption again. The full expression to describe the exit coefficient is given by Equation 2.18, however this expression can be simplified by considering the relative magnitudes of $k_p{}^1 C_p$ and $k_{dM}\,\bar{n}$. If a re-entered monomeric radical will favour propagation (i.e. $k_p{}^1 C_p >> k_{dM}\,\bar{n}$), then Equation 2.17 can be re-written as:

$$\frac{d\bar{n}}{dt} = \rho\,(1 - 2\,\bar{n}) - 2\,\frac{k_{tr}\,k_{dM}}{k_p{}^1}\,\bar{n}^2 \tag{2.20}$$

This is known as 'Limit 2a,' and it can be seen that the loss mechanism is now second-order with respect to $\bar{n}$. The exit rate coefficient k in this case is denoted k_{cr} (cr = complete re-entry) and is given by:

$$k_{cr} = \frac{k_{tr} k_{dM}}{k_p{}^1} \tag{2.21}$$

It is well accepted[6, 47, 57] that Limit 2a is the kinetic regime that governs styrene emulsion polymerizations as the relatively large product $k_p{}^1C_p$ ensures that a re-entered radical will propagate before further desorption. Limit 2b is the converse case where desorption is more likely than propagation – this however is not widely applicable and is not discussed here.

2.5. Radical Entry

2.5.1. Previously Postulated Mechanisms for Entry

Radical entry has long been one of the most disputed areas of kinetics in emulsion polymerization systems, primarily due to the lack of accurate experimental data and potential mechanistic models containing a large number of adjustable parameters, whereby every model put forward could fit experimental data in some way or another. The development of model-free analysis of experimental data, with a minimal number of adjustable parameters has only recently made the elucidation of mechanisms in this area possible.

As has been mentioned, there must be a mechanism of radical entry from the aqueous phase to the particle interior – most initiators are water-soluble yet most polymerization takes place in the particle phase. The original supposition that all radicals formed by fragmentation of initiator eventually enter a particle[39] was proven to be incorrect by the work of Hawkett *et al*[45], Ballard *et al*[40] and Halnan *et al*[60] who demonstrated that radical entry efficiencies (the fraction of initiator derived radicals that do enter a particle) were much less than unity, indicating significant aqueous phase termination prior to entry. Many postulates have been put forward to explain the entry mechanism (all of which have been refuted in some manner.[61])

A more elaborate attempt to describe the entry mechanism was developed with the 'diffusive entry model' which assumed that the rate determining step for entry was the simple diffusion of an entering radical to the particle surface.[62] This however yielded values of k_e (the second-order

rate coefficient for entry, different to the pseudo-first-order rate coefficient for entry ρ) that were orders of magnitude too large than those determined by experiment. Yesileeva[63] suggested that the rate-determining step in the radical entry process may be the required desorption of a surfactant molecule off the particle surface to allow an entering radical into the particle interior. This mechanism however would suggest that the entry rate coefficient would be a function of surface coverage on the particle surface, a result that was refuted experimentally.[61] This was in fact the first time a postulated entry mechanism had been successfully refuted by experimental data anywhere in the literature.

The work of Penboss[64] suggested that the entry process is either a diffusion-controlled event dependent on surfactant displacement (later disproven), or that the entering species is of 'colloidal' dimensions (with a degree of polymerization of the order of 50 monomer units). However such a species would be completely insoluble in the aqueous phase, while the work of Adams[61] demonstrated the activation energy of the entry process did not agree with any of the mechanisms presented at the time.

2.5.2. The 'Control by Aqueous Phase Growth' Entry Mechanism

In light of this body of experimental data as well as the extensive evidence that far less than 100% of initiating radicals successfully entering a latex particle, the now well-accepted mechanism of Maxwell *et al*[65] was developed by considering persulfate-initiated styrene emulsion systems. The premise of this mechanism was based on the previously suggested idea[66] that a radical derived directly from an initiator molecule was far too hydrophilic to directly undergo entry; aqueous phase propagation (and termination) would have to be considered. The crucial step in the model is the addition of a sufficient number (denoted z) of monomer units to an initiator-derived radical so that the oligomer becomes surface active; the entry process at this stage is assumed to be so fast as to be diffusion-controlled (entry into a particle being their only

possible chemical fate). This was a significant departure from previous models for entry that focused on the interactions between a radical and a particle.

The approach developed by Maxwell *et al* allowed the rate of entry to be found directly from the rate of formation of *z*-mers, which was achieved by considering the following chemical equations that govern polymerization in the aqueous phase prior to entry:

$$\text{initiator} \xrightarrow{fk_d} 2\,I^{\bullet} \tag{2.22}$$

$$I^{\bullet} + M \xrightarrow{k_{pi}} IM^{\bullet} \tag{2.23}$$

$$IM_{i-1}^{\bullet} + M \xrightarrow{k_{pw}} IM_{i}^{\bullet}\,,\ i < z \tag{2.24}$$

$$IM_{i}^{\bullet} + T^{\bullet} \xrightarrow{k_{tw}} \text{dead product},\ i < z \tag{2.25}$$

$$IM_{z}^{\bullet} + \text{particle} \xrightarrow{\rho_{init}} \text{entry} \tag{2.26}$$

where $I^{\bullet}$ is a radical derived from thermal decomposition of the initiator (rate coefficient fk_d), M a monomer unit, $T^{\bullet}$ any aqueous phase radical, $IM_i^{\bullet}$ an aqueous-phase oligomer containing *i* monomer units and $IM_z^{\bullet}$ a surface-active oligomer. The rate coefficients for propagation, termination and entry (all in the aqueous phase) are given by k_{pw}, k_{tw} and ρ_{init} respectively. It should be noted that Equation 2.26 does not imply that every encounter between a '*z*-mer' and a latex particle results in a true entry event (entry is normally considered to have been successful when the oligomer begins to propagate in the interior of a particle), as adsorption and desorption may occur numerous times; rather the only chemical fate that a *z*-mer undergoes will be an entry event. It should also be noted that in this model, Equation 2.23 (the addition of a monomer unit

to an initiator fragment, rate coefficient k_{pi}) is considered to be so rapid as to not be rate-determining, a result based on pulse radiolysis experiments[67, 68] involving styrene.

By making the steady-state approximation in the evolution equations that govern Equations 2.22 – 2.26, one obtains the following expressions:

$$[IM_1^\bullet] = \frac{2 f k_d [I]}{k_{pw} [M]_w + 2 k_{tw} [T_w^\bullet]} \tag{2.27}$$

$$[IM_i^\bullet] = \frac{k_{pw} C_w [IM_{i-1}^\bullet]}{k_{pw} C_w + 2 k_{tw} [T_w^\bullet]}, \; 1 < i < z \tag{2.28}$$

$$\rho_{init} = k_{pw} C_w [IM_{z-1}^\bullet] \frac{N_A}{N_p} \tag{2.29}$$

where $[T_w^\bullet]$ is the total aqueous-phase radical concentration (i.e. the sum of all the oligomer concentrations) and C_w is the concentration of monomer in the aqueous phase. Equations 2.27 – 2.29 are readily solved in an iterative routine until convergence, however an analytic expression for ρ_{init} can be found by making the following approximation:

$$[T_w^\bullet] = \left(\frac{f k_d [I]}{k_{tw}} \right)^{0.5} \tag{2.30}$$

This approximation gives the following analytic expression for ρ_{init}:

$$\rho_{init} \approx \frac{2 f k_d [I] N_A}{N_p} \left\{ \frac{2\sqrt{f k_d [I] k_{tw}}}{k_{pw} C_w} + 1 \right\}^{1-z} \tag{2.31}$$

For a seed latex with known N_p, the only unknown parameter within this model is the value of z. While this model is an over-simplification of reality (as there will be oligomers that propagate beyond the length z), it helps to provide physical understanding to the kinetics as an 'average' degree of polymerization in the aqueous phase before surface-activity is attained. It was initially

shown[65] that excellent agreement with experimentally obtained entry rate coefficients for styrene/persulfate systems was obtained with a value z = 2-3, and to date this model has provided excellent agreement to all studies involving electrostatically stabilized latex systems[43, 48, 65, 69, 70] and is yet to be refuted. Indirect experimental evidence (such as isotachophoresis of aqueous-phase oligomers from a styrene/persulfate emulsion system,[71] infra-red spectroscopy and molecular weight analysis of trapped oligomers in MMA emulsion systems[72] and MALDI-TOF mass spectroscopy of oligomers from surfactant-free MMA/persulfate emulsion systems[73]) has also provided good agreement with model predictions as to the length of the entering oligomeric species.

Analysis of Equation 2.31 demonstrates that if z = 1, entry occurs just after the initial (rapid) first propagation step and that every initiator derived radical will undergo entry (and as a result $\rho_{init} \propto$ [I]). For any other values of z, the fraction of initiator-derived radicals that eventually undergo entry (known as the entry efficiency, denoted f_{entry}) is significantly less than unity. According to the 'control by aqueous phase growth' mechanism, the expression to calculate f_{entry} is given by:

$$f_{entry} = \left\{ \frac{2\sqrt{f k_d [I]\, k_{tw}}}{k_{pw} C_w} + 1 \right\}^{1-z} \tag{2.32}$$

It can be seen from Equation 2.32 that f_{entry} is independent of N_p, so the fraction of initiator-derived radicals should be equal for all emulsion systems at any given initiator concentration and reaction conditions. This is generally valid except at extremely low values of N_p, where aqueous-phase termination and propagation become competitive processes. However this result provides an excellent means to compare experimental data from different seed latex conditions.

The 'Maxwell-Morrison' entry model predicts the entry rate coefficient made due to initiator-derived radicals; the overall entry rate coefficient however is actually the sum of the initiator (ρ_{init}) and 'spontaneous' entry rate (ρ_{spont}) coefficients. It is well known that many monomers,

such as styrene and chlorobutadiene[74], undergo non-negligible amounts of polymerization in the absence of any added chemical initiator. The exact origin of this spontaneous polymerization is unclear – it is often thought that residual peroxides that are formed on the particle surface during seed latex synthesis may break down when the latex is polymerized further, leading to the generation of additional radical species. It has also been shown that in the case of styrene, a Diels-Alder rearrangement reaction[27] can generate a radical that can initiate polymerization. At very low initiator concentrations the contribution of ρ_{spont} to the total entry rate coefficient can be extremely significant and must be accounted for during hypothesis testing.

2.5.3. The Thermodynamics of Entry

The concept of 'z' in the Maxwell-Morrison entry model can be understood on thermodynamic grounds – it is the number of units required to impart surface activity to an aqueous phase radical. All radicals will encounter a latex particle at some time – however the criterion of surface activity ensures that the radical is less likely to desorb and more likely to enter. The larger the equilibrium constant is with respect to adsorption (i.e. the greater the hydrophobic free energy $|\Delta G^{hyd}|$), the more likely a true entry event will take place.

For a hydrophobic monomer such as styrene with a low water solubility (C_w^{sat} = 4.3 mM at 323 K[6]), the hydrophobic free energy of a monomeric unit is given by:

$$\Delta G^{hyd} \approx RT \ln C_w^{sat} \tag{2.33}$$

(where the argument of the logarithmic term is the activity, a dimensionless quantity which for dilute solutions such as this is numerically equal to the concentration in M). This quantity is –15 kJ mol^{-1} in the case of styrene. A sulfate ion radical however is very water-soluble, so the key question is how many styrene units would have to be added to such a radical to create a radical that is surface active. Using aliphatic alkyl sulfates as model compounds,[75] it was seen that

$|\Delta G^{hyd}| \approx 23$ kJ mol^{-1} is the minimum value of the hydrophobic free energy to impart surface activity. It can be seen simply that for styrene in this case the addition of two styrene units will satisfy this criteria, i.e. $z = 2$. For persulfate-initiated systems, the value of z can be calculated from the following formula:

$$z = 1 + \text{int}\left(\frac{-23 \text{ kJ mol}^{-1}}{RT \ln C_w^{sat}}\right) \tag{2.34}$$

where 'int' rounds the quantity in the brackets down to the nearest integer. Using this equation, z values for other monomers can be estimated on the basis of solubility; MMA gives z = 4-5 (i.e. a more water-soluble monomer will have to add more units in the aqueous phase before it becomes surface-active). Marestin *et al*[72] added a radical trap onto the surface of a poly(MMA) latex particle in order to determine the DP of an entering oligomer; the maximum degree of polymerization of the trapped oligomers was found to be 5 which was in agreement with the thermodynamic result. The nature of the initiator (chemical structure and charge) will affect the hydrophobic free energy required to impart surface activity as was shown by van Berkel and co-workers.[48] An estimate of this energy is possible from functional group contribution tables[76] for initiators that have not been studied.

Radical entry has remained an often studied event since the development of the 'control by aqueous-phase growth' mechanism and the associated supporting experimental evidence. Asua and co-workers[77] carried out extensive modeling of styrene emulsion polymerizations to determine the behaviour of the rate coefficients of entry and exit as a function of particle size. Their results demonstrated that the rate coefficient of entry was essentially independent of particle size, in line with a propagational mechanism governing the process (as opposed to diffusional, collisional or colloidal.)

Kim and co-workers[78] considered one of the key assumptions of the Maxwell-Morrison mechanism – that upon reaching the critical length *z*, the radical is instantaneously and irreversibly captured by a particle regardless of what occurs in the particle interior. By stating that the rate of radical entry is a function of what occurs in the particle interior (be it propagation or termination), the rate of entry is related to the flux at the particle surface and a 'transient' entry rate can be calculated. It was shown through this modeling that besides the first few seconds of the overall reaction, the magnitude of the steady-state entry rate is unchanged and the assumptions of the Maxwell-Morrison approach are, in general, robust and correct.

Radical entry involving other monomers has also been studied. Kshirsagar *et al.*[79] studied radical entry in seeded emulsion polymerization experiments involving vinyl acetate (with a poly(styrene) seed. The seed latex was doped with a water-insoluble inhibitor to capture and form stable oligomers of poly(vinyl acetate), in order to determine the critical DP for entry in this system. Fast atom-bombardment mass spectrometry was used to determine the size of the formed oligomers; results showed that the critical length for entry in this system was 5-6 monomer units, in line with the predicted value from the Maxwell-Morrison entry mechanism on thermodynamic grounds. De Bruyn *et al.* studied the kinetics of vinyl neodecanoate,[43] an extremely water-insoluble monomer. The combination of chemically initiated and γ-initiated seeded dilatometry experiments provided experimental data in support of the developed entry mechanism. Due to the extremely low monomer solubility in water, the critical length *z* was only 1-2 units in this case.

Dong and Sundberg[80] developed a lattice model to estimate the change in free energy of oligomers of differing lengths as adsorption onto a latex interface took place. The variation of this free energy term allowed for estimation of the critical length *z* where entry (and adsorption) is spontaneous. Theoretically derived values of *z* were in excellent agreement with experiment. The developed model also allowed for estimating critical lengths for entry in co-monomer

systems, revealing that the sequence distribution within the oligomer itself had little effect on the value of *z*. Further modelling[81] took into account the propagation step at the water/latex interface in the overall entry mechanism; this is of particular importance in monomer-starved experimental conditions where propagation may be rate determining. Results again supported the Maxwell-Morrison assumptions.

The concept of propagation to a critical length *z* has recently been challenged by the group of Tauer,[82] who claimed that primary initiator-derived radicals (such as the sulfate ion radical) can directly enter latex particles without addition of any monomer units. This was claimed on the basis of experiments where latexes containing RAFT agents had the RAFT agent destroyed/modified by the introduction of potassium persulfate to the system, in the absence of any monomer. The work of Goicoechea[83] however proved that this result was most likely due to the complicated decomposition mechanism of persulfate ions, that can regularly lead to the generation of the more hydrophobic hydroxyl radical. Experiments where hydroxyl radical generation was suppressed demonstrated that this effect was no longer observed. While persulfate-initiated emulsion polymerization experiments can lead to the formation of radicals that can directly enter latex particles, this most likely represents a small contribution to the overall entry process that is governed by aqueous-phase propagation.

2.6. Experimental Measurement of Kinetic Parameters

Accurate experimental data is the crucial requirement for the determination of rate coefficients of interest in an emulsion polymerization system (or any chemical system for that matter). Once a seed latex has been synthesized it must be characterized accurately (to determine a precise average particle size), and the reaction rate for seeded experiments must be determined with precision and in real time. Commonly used techniques and methods for both are discussed below.

2.6.1. Seed Particle Size Measurement

Several different techniques exist to obtain either the average particle size or particle size distribution (PSD) of a latex. These techniques (outlined below) vary in their method of measurement as well as their precision, however all are used with a view to obtain consistency between the methods and be confident of the determined size.

- **Dynamic Light Scattering**

The technique of Dynamic Light Scattering (DLS) is based on Brownian motion, whereby large particles (or molecules) move more slowly than small particles (or molecules) in a medium due to a difference in diffusion coefficients. Upon illumination with a laser beam, the particles scatter the incident light at a variety of angles, which is measured by a detector. A 'correlation' function is generated that relates the intensity of scattered light at time t=0 to a certain delay time t (in the range of 1 μs to 1 s); smaller particles that move more quickly will have a rapidly decaying correlation function than larger particles. An average size is thus back-calculated from the obtained correlation function. Size distributions from DLS are generally meaningless as the technique is heavily biased towards larger particles (as intensity scales as the sixth power of the particle size[84]) and the relation between the auto-correlation function and the PSD cannot be exactly inverted as it is an ill-conditioned problem.

Two separate DLS techniques were used in this work to determine an average particle size. The first, Photon Correlation Spectroscopy (PCS), measures scattered light at 90° relative to the incident laser beam. Measurements were taken on a Brookhaven instrument consisting of a BI-200SM Version 2 goniometer with a 633 nm 35 mW He-Ne laser; samples were kept at a constant temperature (298 K) by a continually circulating water bath. Samples (consisting of one drop of latex in a scintillation vial full of de-ionized water (Milli-Q) were filtered through a 0.45 μm membrane to ensure the minimization of dust and other particulates. The other light

scattering technique used was a backscattering technique employed on a Malvern High Performance Particle Sizer (HPPS) instrument.

- **Separation Techniques**

Two separation techniques to determine particle size were used in this work. Unlike light scattering, where the particle size is determined from the behaviour of the (diluted) sample in the presence of a light source, the separation techniques (Capillary Hydrodynamic Fractionation (CHDF) and Hydrodynamic Chromatography (HDC)) separate particles on the basis of size, allowing a full particle size distribution (PSD) to be determined.

Both CHDF and HDC operate on similar principles – the latex sample is injected into a narrow tube and larger particles elute more quickly than smaller particles. In CHDF (where the tube is a thin capillary), smaller particles are more likely to be near the walls of the capillary and due to the curvature of the front of the mobile phase, they will elute more slowly. HDC involves a column packed with a cross-linked gel; smaller particles will be able to traverse a larger number of pores and as a result take a more torturous path through the column, leading to longer elution times. Both techniques require monodisperse standards to correlate elution time with particle size.

CHDF analyses were carried out using a MATEC Applied Sciences CHDF-1100 fitted with a C570 high sensitivity column and employing GR500™ eluent at a flow rate of 1.4 mL min^{-1}. HDC analyses were carried out using a Particle Size Distribution Analyzer (Polymer Laboratories) with a PSDA-Type 2 column, employing a PL-PSDA proprietary eluent at a flow rate of 1.7 mL min^{-1}. Latex standards (ranging from 50 nm to 3 μm diameter) were obtained from Polymer Laboratories.

- **Transmission Electron Microscopy**

Transmission Electron Microscopy (TEM) is in essence the 'ideal' sizing technique (especially for very small latex particles) as a direct image of the particles is obtained, and as a result their size (and PSD) can be determined. For hard polymers, such as poly(styrene), TEM is ideal as the polymer does not deform under the electron beam (as can happen with acrylates). However, sample preparation time does make it laborious compared to the ease of a light scattering or separation technique. Typically the sizes of (at least) 1000 particles are determined in order to develop a PSD and obtain a value of the latex polydispersity (the ratio of the weight-average particle size to number-average particle size).

TEM samples were prepared by depositing a dilute sample of the latex onto a carbon-coated Cu grid, and dried at ambient temperature. Images were acquired using the Philips CM120 Biofilter (120 kV) at the Electron Microscope Unit at The University of Sydney.

Once the particle size of the seed latex has been determined and the solids content is known, the particle number (N_p) can be easily calculated. The value of N_p (units L^{-1}) is given by:

$$N_p = \frac{m_p^0}{\frac{4}{3}\pi r_u^3 d_p} \tag{2.35}$$

where m_p^0 is the mass of polymer per unit volume of the latex, r_u the unswollen radius (weight-average) of the seed latex and d_p the density of the polymer.

2.6.2. Determination of the Intra-Particle Monomer Concentration

The value of the monomer concentration within the particle interior (denoted C_p), is of extreme importance in emulsion polymerization, as it is directly related to the polymerization rate (Equation 2.2). In the case of a seeded experiment, monomer is added to a pre-established latex and with further emulsification (and time) the monomer will migrate to the particle interior

leading to swelling of the latex. The extent of the swelling of a particle is related to the balance between several thermodynamic concepts; the surface free energy of the particles (which increases with particle size) and the free energy of mixing of monomer and polymer (which decreases with particle size).[49] At equilibrium, the particles will be at maximum swelling and will be saturated with monomer; any more monomer present will reside in monomer droplets stabilized by surfactant (Interval II starting conditions). As a result, knowing the saturation concentration (C_p^{sat}) within the particles is of great importance.

Two common techniques exist to measure the value of C_p^{sat}, and they are discussed below.

- **Static Swelling**

Static swelling[6, 40, 60] is a conceptually easy method to understand; excess monomer is added to a seed latex (to ensure saturation), along with surfactant and inhibitor (to prevent thermal polymerization) within a dilatometer vessel (the technique of dilatometry is described in Section 2.6.3.1). The emulsion is stirred overnight at reaction temperature (323 K) to allow for the monomer to migrate into the particle phase and the particles to reach their maximum swollen size. Upon the cessation of stirring, the excess monomer (that is residing in monomer droplets) will separate into an immiscible phase on top of the monomer-swollen emulsion, which is displaced into the capillary of the dilatometer apparatus to determine the amount of excess monomer m_M^{excess}. Through simple mass balance, the mass of monomer within the particle phase (m_M^P) can be determined and as a result C_p^{sat} obtained through the following equations:

$$m_M^P = m_M^{total} - m_M^{excess} - C_w^{sat} V_w M_0 \tag{2.36}$$

$$C_p^{sat} = \frac{m_M^P / M_0}{\frac{m_M^P}{d_M} + \frac{m_P^{seed}}{d_p}} \tag{2.37}$$

where m_M^{total} is the total mass of monomer used in the experiment, C_w^{sat} is the saturation concentration of the monomer in the aqueous phase, V_w is the volume of the aqueous phase, M_0 the molecular weight of the monomer, m_P^{seed} the mass of the polymer within the seed latex, and d_M and d_p the densities of monomer and polymer respectively.

- **Kinetic Method**

The kinetic method involves using the rate behaviour of a seeded emulsion polymerization experiment to calculate the value of C_p^{sat}. As can be seen in Equation 2.2, the polymerization rate is a function of C_p, and under Interval II conditions (where $C_p = C_p^{sat}$) this rate is constant. When the particle phase is no longer saturated with monomer and C_p begins to decrease, the reaction rate will also change from its previously constant value. By identifying the fractional conversion (x_{change}) where this deviation from constant polymerization rate begins, the value of C_p^{sat} can be determined from the following equation:[6]

$$C_p^{sat} = (1 - x_{change}) \frac{m_M^{total}/M_0}{\frac{m_M^P}{d_M} + \frac{m_P^{seed}}{d_p} + x_{change}\, m_M^{total}\left(\frac{1}{d_M} - \frac{1}{d_p}\right)} \tag{2.38}$$

In the experiments conducted in this project the values of C_p^{sat} determined by the kinetic method were found to be in variation from the value obtained by the static swelling method by no more than 3 %, suggesting the reliability of the values obtained and both methods described here.

2.6.3. Reaction Rate Measurements

Determination of accurate rate coefficients requires extremely accurate data for the fractional conversion of monomer into polymer as a function of time. Techniques such as gravimetry (which is generally not accurate enough for these purposes) and calorimetry[85] exist however the method regularly employed in this work is dilatometry, which is discussed in detail below.

2.6.3.1. Dilatometry

Dilatometry works on the premise that the density of a polymer is slightly larger than the density of its component monomer and as a result the polymerization medium shrinks as a function of time. While this technique is sensitive to any outside factors that can influence the measurement of this contraction, dilatometry can be used to monitor the conversion to polymer as a function of time without the need for taking regular samples. Using a polymerization vessel with a narrow capillary in the top (see Figure 2.10) this contraction can be monitored accurately by measuring the change in meniscus height as a function of time by an automated tracking device. The contraction factor (CF) of the emulsion can be determined assuming perfect mixing of monomer and polymer, which is:

$$\mathrm{CF} = (d_\mathrm{M})^{-1} - (d_\mathrm{p})^{-1} \tag{2.39}$$

where d_M and d_p are the densities of the monomer and polymer respectively. Knowledge of the change of height as a function of time $h(t)$ can then be related to the fractional conversion $x(t)$ via the following equation:

$$x(t) = \frac{\pi r^2 h(t)}{m_\mathrm{M}^{\,0} V_\mathrm{W} \mathrm{CF}} \tag{2.40}$$

where r is the radius of the capillary, $m_\mathrm{M}^{\,0}$ the initial mass of monomer per unit volume of the aqueous phase, V_w the volume of water in the dilatometer and CF the contraction factor.

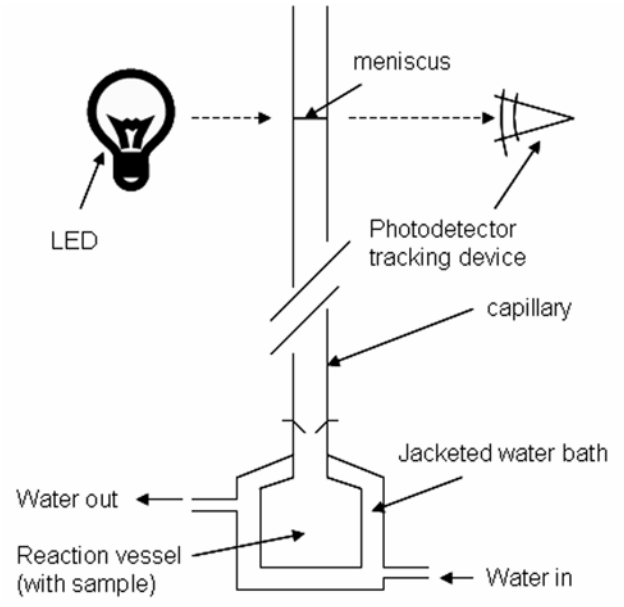

Figure 2.10. A typical setup for a dilatometry experiment.

A temperature-controlled water bath to regulate the temperature of the emulsion is used in a dilatometry experiment as slight changes in the temperature will affect the expansion/contraction of the medium and subsequently affect the results. Similarly the addition of the initiator solution (normally the last step) requires a finite time period to mix and thermally equilibrate with the rest of the emulsion; as a result there is often a brief period of expansion at the start of a dilatometry experiment as this solution reaches reaction temperature. It is normally assumed that time '$t = 0$' is when contraction first begins; location of the true starting time is of high importance for data analysis.

The height of the meniscus within the capillary is tracked by a light-emitting diode (LED) and a phototransistor. The light emitted from the LED will be refracted to differing degrees (and as a result the intensity of light reaching the phototransistor will be different) depending on whether the light is passing through glass and air (i.e. above the meniscus) or through dodecane (below the meniscus; a small amount of dodecane is typically placed on top of the water in the capillary to ensure a good meniscus).The tracker is moved up or down a series of 'steps' (2.35 μm

increments in the case of the setup at The University of Sydney) by a motor connected to the sensor until the meniscus is found; this process is repeated at fixed time intervals (typically 20 s) and the height of the meniscus as a function of time is logged by a computer.

A detailed description of the experimental setup of a dilatometry experiment is given in the relevant chapters. Where such work is presented, however, it should be pointed out that great care was taken to ensure the degassing of all the reaction components; the seed latex, water and monomer were all degassed under vacuum separately and then the reaction mixture was degassed as a whole before and after the temperature of the water bath was raised to that of the required reaction conditions. This was done to ensure that no oxygen (a polymerization inhibitor) was present in the reaction medium and that no dissolved gas could form bubbles over the course of the polymerization, a phenomenon that disrupts the accurate measurement of volume that is crucial to the success of the dilatometry technique.

2.6.4. The Slope-and-Intercept Method

The objective of accurately monitoring the fractional conversion as a function of time is naturally to extract important kinetic parameters from the obtained rate data; in our case it is the average number of radicals per particle, $\bar{n}$. It can be seen from Equation 2.2 that the polymerization rate is directly proportional to $\bar{n}$, assuming that N_p (the particle number) remains constant (i.e. no secondary nucleation.) Once it has been shown that no new particles have been formed (via TEM or a chromatographic technique), it is safe to say that

$$\frac{dx}{dt} = A\,\bar{n} \tag{2.41}$$

where A is the collection of constants in Equation 2.2. Within Interval II the polymerization rate is constant (the conversion-time curve x(t) is essentially linear), and Equation 2.41 allows the value of $\bar{n}_{ss}$ to be calculated directly. As the magnitude of the rate coefficients for radical entry

(ρ) and radical exit (k) are of primary interest, it is possible to extract values for these parameters from rate data by considering the appropriate evolution equation for $\bar{n}$. In the case of 'Limit 1' zero-one kinetics (Equation 2.9), integration yields the following expression:

$$\bar{n} = \frac{\rho}{2\rho + k} + \left(\bar{n}_0 - \frac{\rho}{2\rho + k}\right) e^{-(2\rho + k)t} \tag{2.42}$$

where $\bar{n}_0$ is the initial value of $\bar{n}$ at $t = 0$. Combining Equations 2.41 and 2.42 gives an expression for the fractional conversion as a function of time, namely:

$$x(t) - x_0 = \frac{A}{2\rho + k}\left\{\rho\, t + \left(\bar{n}_0 - \frac{\rho}{2\rho + k}\right)\left(1 - e^{-(2\rho + k)t}\right)\right\} \tag{2.43}$$

where x_0 is the fractional conversion at $t = 0$. In the long-time limit, Equation 2.43 reduces to a linear function (i.e. $x(t) - x_0 = a + b\, t$ where a and b are the intercept and slope of the linear region of the conversion-time plot). Therefore by fitting a linear function to the Interval II region of the conversion-time curve obtained by a dilatometry experiment, the slope and intercept allow direct determination of both ρ and k. This technique is known as the 'slope and intercept' method. The expressions to calculate the two rate coefficients of interest are:

$$\rho = \frac{b}{a}\left(\bar{n}_0 - \frac{b}{A}\right) \tag{2.44}$$

$$k = \left(\frac{A}{a} - 2\,\frac{b}{a}\right)\left(\bar{n}_0 - \frac{b}{A}\right) \tag{2.45}$$

with all parameters as defined previously. The equations presented here correspond to the kinetics of an emulsion system where re-entry of an exited radical is considered not to occur Allowing for re-entry (Limit 2a, Equation 2.20) does complicate the mathematics somewhat,

however both rate coefficients can still be extracted (see the text of Gilbert[6] for full derivations) from the slope and intercept of the linear region of the conversion-time curve.

2.6.5. Gamma-Relaxation Dilatometry

While the slope-and-intercept method is a simple and easily implemented technique to determine the entry and exit rate coefficients in an emulsion system, it can be prone to significant error. The problem is that an accurate value of the intercept is not easy to find, as small perturbations in the early stages of the polymerization (i.e. residual oxygen acting as an inhibitor, difficulty in determining the true starting time) can greatly affect the value of the intercept. The long-term slope however can be easily (and accurately found), so ideally a second, independent technique should be employed to determine one of the rate coefficients in question.

The technique that was finally successful in achieving such an aim was γ-relaxation dilatometry, pioneered by Lansdowne[44] and co-workers. γ radiation (from a ^{60}Co source) is able to initiate polymerization through the formation of •OH radicals and high energy electrons that soon become protonated,[68] with the powerful nature of the radiation ensuring uniform initiation in an opaque latex (a feat that is not achievable with UV radiation). The key to the technique however is that the radical flux provided by the initiating radiation can be 'switched off' by removing the sample from the radiation source. When the sample is 'out-of-source' the polymerization rate decreases due to the events of radical loss (exit in a 'zero-one' system). By monitoring the change in rate as a function of time upon removal from the radiation source, one has direct access to the value of the exit rate coefficient k via an independent experiment. This value then allows entry rate coefficients to be calculated from the value of $\overline{n}_{ss}$, namely:

$$\rho = \frac{k_{ct}\,\overline{n}_{ss}}{1 - 2\,\overline{n}_{ss}}\ \text{(Limit 1)};\ = \frac{2\,k_{cr}\,\overline{n}_{ss}^{\,2}}{1 - 2\,\overline{n}_{ss}}\ \text{(Limit 2a)} \tag{2.46}$$

where k_{ct} and k_{cr} are as defined previously.

γ-relaxation dilatometry works on the same principles as conventional dilatometry, however the apparatus is located inside substantial lead casing containing ^{60}Co rods, with the dilatometer vessel on top of a moveable platform inside the casing (see Figure 2.11). The platform can be raised and lowered electronically, allowing the sample to be placed into the radiation source and subsequently removed from it. The steady-state rate reached when the sample is outside of the radiation source is typically non-zero, due to the effects of thermal or spontaneous polymerization discussed previously. Upon re-insertion into the γ source, the original polymerization should once again be obtained; the kinetics of re-insertion can also be used to obtain entry and exit rate coefficients. A typical conversion-time curve from a γ-relaxation experiment is shown in Figure 2.12.

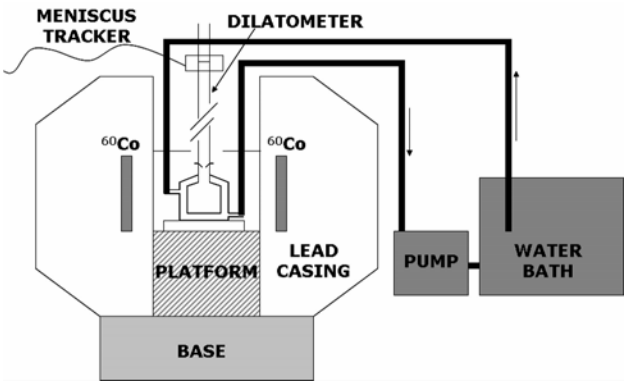

Figure 2.11. Experimental setup for a γ-relaxation dilatometry experiment.

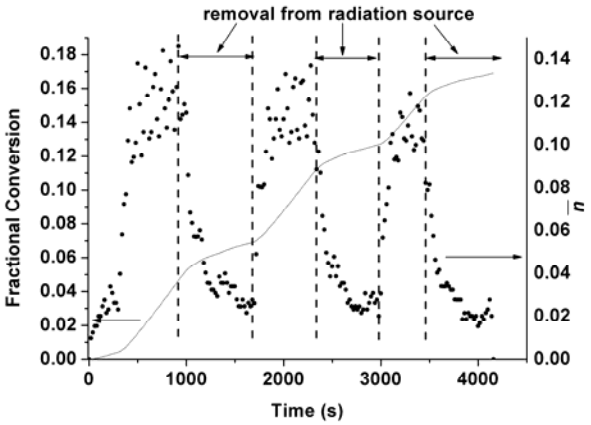

Figure 2.12. Typical conversion-time curve from a γ-relaxation dilatometry experiment.

2.6.6. Chemically Initiated Dilatometry

Chemically initiated dilatometry, as the name suggests, involves the use of a water-soluble initiator (such as potassium persulfate, KPS) to initiate polymerization. The initiator solution is typically prepared separately to allow the emulsion (the seed latex, monomer and surfactant) to emulsify at the desired reaction temperature and allow the seed particles to swell, without any polymerization taking place. The initiator is introduced to the emulsion via a syringe after thorough degassing, after which collection of conversion data as a function of time is commenced.

The sole purpose of these experiments is to determine the value of $\bar{n}_{ss}$ for a wide range of initiator concentrations (typically spanning two orders of magnitude), in order to then calculate the variation of ρ with respect to initiator concentration and to allow for mechanistic testing and model comparison.

2.6.6.1. Presentation of Kinetic Data

As seen in Equation 2.31, the entry rate coefficient ρ is inversely proportional to N_p. As a result, a variation in N_p from different seed latexes ensures that the presentation of entry rate coefficient

data is difficult (and at times misleading). The radical entry efficiency (f_{entry}) however is independent of N_p and allows for comparison between results obtained from different seed latexes In the current work it allows for the presentation of entry data from latexes with 'hairy layers' of different lengths to be presented on the one graph.

Similarly, results obtained from different chemical initiators are complicated by the fact that initiators possess different values of the decomposition rate coefficient k_d, making data obtained at the same initiator *concentration* meaningless. As a result, the total radical flux ($2\ k_d\ [I]$) should be compared between different initiators, as it is a measure of the rate of generation of initiating radicals and accounts for differing rates of decomposition. Because of these two factors, data from chemically initiated dilatometry experiments will be presented as entry efficiency as a function of radical flux to ensure meaningful comparison of data.

2.6.7. Size Exclusion Chromatography (SEC)

Size Exclusion Chromatography (SEC) is a method of determining molecular weight distributions (MWDs) of polymers. While not a technique that delivers kinetic information instantaneously (such as dilatometric techniques that measure the fractional conversion as a function of time), SEC is a powerful tool for obtaining important kinetic rate coefficients that are inferred from the MWD itself. Transfer and termination rate coefficients are often determined in this manner; similarly mechanisms can be determined (such as combination or disproportionation as the dominant termination mechanism) from MWD data.

A commonly used form of SEC is Gel Permeation Chromatography (GPC), in which individual polymer chains are separated on the basis of hydrodynamic volume (the volume the polymer coil occupies in three-dimensional space). With a stationary phase consisting of a highly porous material such as a heavily cross-linked polymer or hydrogel, the path that the polymer chain is forced to take through this phase is dictated by its size. Smaller, shorter chains are able to enter

smaller pores and thus will have a longer elution time than longer chains, leading to a distribution based on size.[86] The signal from a GPC distribution is proportional to the mass of the polymer chain (M) and the elution volume is proportional to the logarithm of molecular weight. (It should be pointed out however that this relation is only valid for linear polymers; for branched polymers or polymers with other architectures this relationship breaks down.[87]) From this it can be shown[6] that

$$w(\log \mathrm{M}) = \mathrm{M}^2 P(\mathrm{M}) \tag{2.47}$$

where $P(\mathrm{M})$ is the number distribution of polymer chains of degree of polymerization M. (For polymers that are governed by random growth and stoppage mechanisms, $P(\mathrm{M})$ will be a single exponential[88]). Absolute molecular weight distributions can be found through a combination of light scattering and differential refractometry measurements, however it is common (as is the case at the Key Centre for Polymer Colloids) that only a single mass-sensitive detector is used (such as a refractive index detector) and a distribution is determined relative to a series of known polymeric standards. A series of standards of different molecular weight and low polydispersity (typically poly(styrene)) are used to build a calibration curve that relates the molecular weight to the elution volume, allowing the MWD of the unknown sample to be determined.

One problem that SEC and related techniques suffer from is that of band broadening,[89] a phenomenon that means polymer chains with the same molecular weight will in fact elute over a range of elution times. This broadening is due to axial dispersion, caused by molecular diffusion and multiple flow paths within the column. This can have quite a pronounced effect on the overall MWD, especially at the low and high molecular weight 'tails' of the distribution. From a kinetic perspective, techniques such as the '$\ln P$' method[88] (a method of obtaining transfer rate coefficients by plotting the logarithm of the number distribution as a function of molecular

weight) can be strongly affected by band broadening and techniques to correct data[48, 90] for this phenomenon are recommended.

In this work the use of SEC experiments is restricted to ln*P* measurements for the determination of transfer coefficients, as well as the use of the on-line UV spectrophotometer in order to determine whether UV-active species (such as particular polymeric end-groups of interest) are present or not within a given sample.

2.7. Kinetics of Electrosteric Stabilization

2.7.1. Prior Work and Interpretation of Results

Despite being a widely used method of emulsion stabilization in industrial polymer formulations, very little work has been devoted to understanding the kinetics of electrosterically stabilized emulsion systems. There are some inherent difficulties in the characterization of these systems (to be discussed below), making determination of accurate rate coefficients and the testing of mechanisms ambiguous at best. Nonetheless, the limited work that has been reported in the literature on this topic has revealed at times significant departures from the expected mechanisms of particle growth and formation for electrostatically stabilized systems.

One of the earliest attempts to study the mechanisms of entry and exit (using the techniques outlined in this chapter) for sterically stabilized systems was performed by Hammond,[91] who studied poly(styrene) latexes stabilized by poly(ethylene oxide). Meaningful rate coefficients were unobtainable due to extensive secondary nucleation, meaning a constant N_p for kinetic calculations was not possible. This was however a spectacular result given that under such conditions ($N_p = 5 \times 10^{16}$ L^{-1}), secondary nucleation via the homogeneous nucleation mechanism should not be possible.

Shoaf and Poehlein[92] investigated the kinetics of emulsion copolymerizations of styrene with acid comonomers, namely acrylic acid (AA) and methacrylic acid (MAA). An electrostatically stabilized poly(styrene) latex was used as a seed. The kinetics of emulsion copolymerizations are sufficiently complex to prevent unambiguous rate coefficients being obtained via conversion-time data (for example, the 'slope and intercept' method), however the results revealed a decrease in the overall polymerization rate relative to seeded styrene homopolymerization under the same conditions. Monomer partitioning was shown to be important, with MAA-styrene polymerizations proceeding faster than AA-styrene polymerizations, as the more hydrophobic MAA partitions more extensively into the particle phase (which is a monomer-rich environment, allowing for faster consumption). An 'Interval IV' was also postulated in the case of AA-styrene systems – the reaction rate was shown to decrease in these systems if the particle surface was initially decorated with a polyAA stabilizing layer, suggesting radical trapping by a densely covered surface. It was thought that in such systems if the 'hairy layer' is sufficiently dense and entry cannot occur, the locus of polymerization will shift back to the aqueous phase where the remaining AA will be consumed. No evidence however was presented for the existence of such an interval.

The work of Leemans *et al*[93] involved the use of amphiphilic block copolymers (poly(MMA)-*block*-poly(sulfonated glycidyl methacrylate) and poly(MMA)-*block*-poly(quaternized dimethylaminoethyl methacrylate)) as 'surfactants' in *ab initio* emulsion polymerization experiments of MMA. A variety of different initiators bearing different charges were used in combination with these copolymers in order to test the effect of the charges on both the initiating radical and the stabilizing hydrophilic block. The results showed that when the charges on the initiator and stabilizing layer were of opposite sign, significant rate reductions were observed, suggesting that diffusion of the entering species through this stabilizing layer was a rate determining step under various conditions. For some initiator/stabilizer charge combinations, an increase in 'surfactant' concentration led to a decrease in the polymerization rate, the opposite of

what is predicted by Smith-Ewart kinetics for electrostatically stabilized systems.[39] Unfortunately this work did not quantify the behaviour of $\overline{n}$ or any key rate coefficients that control particle growth. Similarly no quantification of final N_p values was presented.

The work of Coen *et al*[70] was the first experimental work reported that looked at the entry and exit rate coefficients in poly(styrene) latexes stabilized by polyAA, a very common industrial system. Seed latexes were made by first synthesizing a monodisperse electrostatically stabilized poly(styrene) latex, and then building a 'hairy layer' onto the surface of the particle by further polymerization of AA and styrene. At pH 7 (full ionization of the acid groups), there was significant reductions in the value of ρ and k relative to the expected mechanisms for a styrene emulsion system. There were also reported variations in both rate coefficients with respect to particle size, pH and the ionic strength of the emulsion. However the data obtained from γ-relaxation dilatometry was subject to significant uncertainty. Vorwerg[94] and co-workers performed equivalent experiments and reported a reduction in both ρ and k, however not to the extent as seen in Coen's work. The reduction seen was a function of acrylic acid surface coverage, leading to the conclusion that the diffusion of radicals into and out of the latex particle was restricted by the density of the hairy layer on the particle surface. Some results were compromised by the appearance of secondary nucleation (again under conditions where new particle formation should not be possible) with the interesting result that secondary nucleation only occurred at neutral and high pH.

The biggest difficulty in making meaningful mechanistic inferences from the data of Coen and Vorwerg was that the 'hairy layer' was synthesized by the free-radical polymerization of acrylic acid. With no means to control the molecular weight of the stabilizing chains (and the poorly understood and variable rate coefficients of acrylic acid propagation[95-97]), the 'hairy layer' was likely to have an uncontrolled morphology (with no guarantees of uniformity) with a broad molecular weight distribution – making it impossible to relate the variation in the rate

coefficients of interest to the width or density of the stabilizing area. De Bruyn *et al*[98] used Small Angle Neutron Scattering (SANS) to characterize the 'hairy layer' of polyAA-stabilized poly(styrene) latexes, which allowed the shell thickness around the particle core to be determined. It was shown that the shell thickness was dependent on the initial AA concentration in the synthesis, further complicating analysis. The results however were somewhat ambiguous (and model dependent with respect to data processing). In general SANS is a complex technique and not a convenient method to regularly characterize the stabilizing layer of a latex particle.

2.7.2. Model Systems and Controlled-Radical Polymerization

A new route to the synthesis of well-defined electrosterically stabilized latexes has recently been developed through the advent of successful controlled-radical polymerization in emulsion, in particular the reversible addition-fragmentation chain transfer (RAFT) technique.

RAFT polymerization[16] is one of several newly developed techniques (other such techniques include nitroxide-mediated polymerization[99-104] and atom transfer radical polymerization[105-107] (ATRP)) to form polymers of controlled molecular weight and low polydispersity. RAFT agents are typically dithioesters or trithiocarbonates, with the thiocarbonyl (C=S) bond acting as a site that a growing polymeric radical can add to. Many reviews on the finer details of RAFT polymerization[108-110] exist; however the key reaction that governs the success of the RAFT process is the reversible equilibrium between addition of a growing radical to a RAFT agent and its subsequent fragmentation (see Figure 2.13). The rates of addition and fragmentation are governed by the leaving group of the RAFT agent (denoted the 'R group') and the stabilizing group (denoted the 'Z group'), and as a result the quality of the RAFT agent itself. Typically addition to a RAFT agent is so fast that at any given time, nearly all growing radicals in the reaction medium are 'capped' by a RAFT end-group, minimizing bimolecular termination and allowing the molecular weight to increase with conversion. This technique also affords block

structures and other novel morphologies to be synthesized, given that polymer chains are still 'living' at the end of polymerization and can subsequently be reacted further.

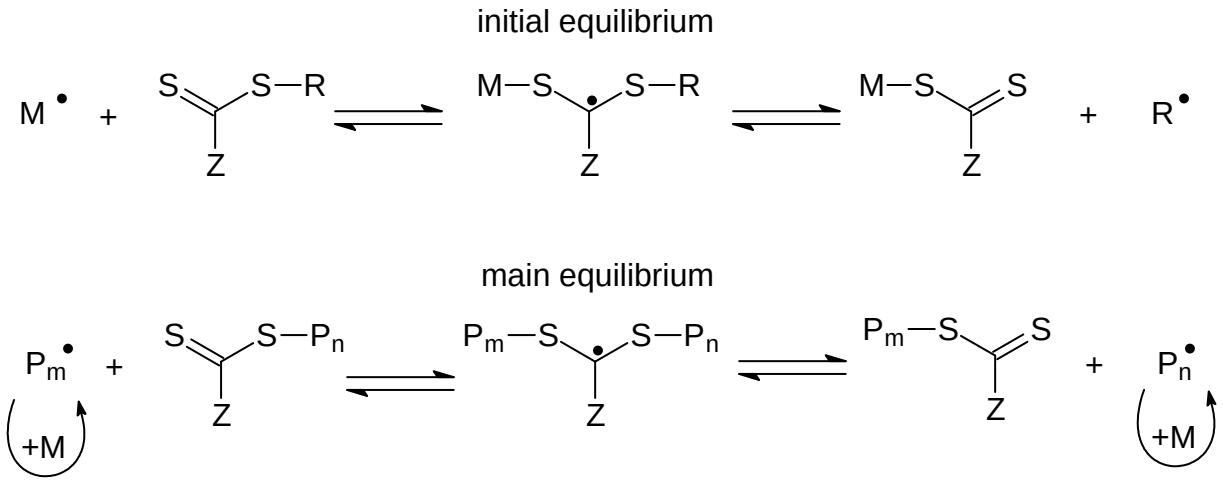

Figure 2.13. The equilibrium reaction central to the RAFT polymerization mechanism.

RAFT polymerization is particularly robust to trace impurities, can be used with a wide variety of monomers and extreme reaction conditions are not required and as a result it is an extremely versatile method to synthesize well-defined polymeric structures. However for a long period the use of RAFT in emulsion polymerization was completely unsuccessful; the RAFT agent would phase-separate from the emulsion, extensive coagulation would be seen and no molecular weight control was evident. It was believed that the RAFT agent was solubilizing in the droplet phase, leading to the rare 'droplet nucleation.' Prescott[111] was the first to successfully obtain molecular weight control in emulsion using RAFT by transporting the RAFT agent into the interior of a pre-formed seed latex via a co-solvent (acetone). However the polymer from the seed latex itself is formed in an uncontrolled manner which is undesirable for many purposes.

The revolution in this area came about when Ferguson and co-workers[17, 112] used an amphiphilic RAFT agent of moderate water solubility to build *in situ* surfactant-like polymers. The RAFT agent was first polymerized with AA in water to form short oligomers (of DP 5-10) that were water soluble; the molecular weight distribution of this species was estimated via Electrospray

Mass Spectrometry (ESI-MS). A second, more hydrophobic monomer (such as styrene or *n*-butyl acrylate) was then fed into the reaction vessel very slowly (to ensure that the monomer concentration was below saturation level in the aqueous phase), allowing amphiphilic diblock copolymers to form. Beyond a certain degree of polymerization of the second monomer, the polymer chains become 'surface active' and begin to self-assemble, forming dynamic micellar-like structures (see Figure 2.14) that is essentially the beginning of particle nucleation. Further addition of the hydrophobic monomer allows these particles to grow to a desired size, leading to fairly monodisperse latex particles stabilized by anchored hydrophilic chains on the particle surface, of known and controllable length.

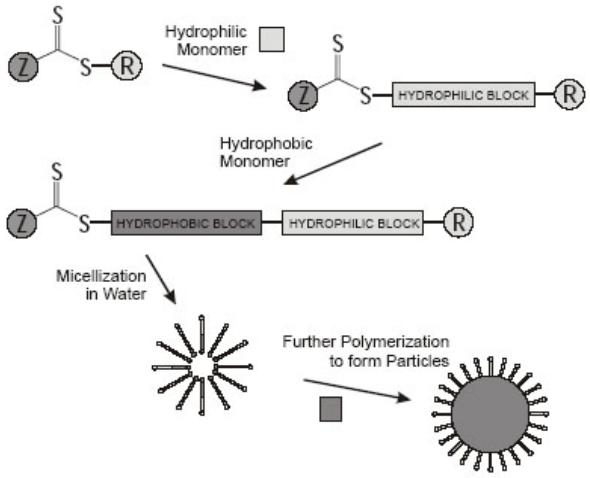

Figure 2.14. The 'RAFT-in-emulsion' to synthesize well-defined electrosterically stabilized latex particles.

The work presented in this thesis takes advantage of this recently developed technique to synthesize latexes with stabilizing moieties of known and controllable length, with the global aim of testing the well-accepted mechanisms for radical entry and exit in emulsion systems for electrosterically stabilized latexes as a function of experimentally adjustable parameters (length of the stabilizing block, particle size, pH, etc.) Importantly, the latex formed from this technique cannot be used 'as is' for kinetic studies, as it is well known that the presence of active RAFT

end-groups within the particle interior can have a massive effect on the intra-particle kinetics[113] in emulsion polymerization systems. Because of this, to develop a model system for kinetic analysis a means to remove the RAFT functionality without compromising the particle morphology must be found, a topic that is the main subject of the next chapter of this thesis.

References

1. Moad, G.; Solomon, D. H., *The Chemistry of Free Radical Polymerization 2nd Edn.* Elsevier: Amsterdam, 2006.

2. Moad, G.; Solomon, D. H. *Australian Journal of Chemistry* **1990,** 43, 215-39.

3. van Berkel, K. Y.; Russell, G. T.; Gilbert, R. G. *Polymer* **2006,** 47, 4667-75.

4. Fischer, H.; Radom, L. *Angewandte Chemie, International Edition* **2001,** 40, 1340-1371.

5. Fischer, H.; Radom, L. *Macromolecular Symposia* **2002,** 182, (3rd IUPAC-Sponsored International Symposium on Free-Radical Polymerization: Kinetics and Mechanism, 2001), 1-14.

6. Gilbert, R. G., *Emulsion Polymerisation: A Mechanistic Approach*. Academic Press: San Diego, 1995.

7. Heuts, J. P. A.; Gilbert, R. G.; Radom, L. *Macromolecules* **1995,** 28, 8771-8781.

8. Heuts, J. P. A.; Gilbert, R. G.; Radom, L. *Journal of Physical Chemistry* **1996,** 100, 18997-19006.

9. Huang, D. M.; Monteiro, M. J.; Gilbert, R. G. *Macromolecules* **1998,** 31, 5175-5187.

10. Beuermann, S.; Buback, M.; Schmaltz, C.; Kuchta, F.-D. *Macromolecular Chemistry and Physics* **1998,** 199, 1209-1216.

11. Beuermann, S.; Paquet, D. A.; McMinn, J. H.; Hutchinson, R. A. *Macromolecules* **1996,** 29, 4206-4215.

12. Kornherr, A.; Zifferer, G.; Olaj, O. F. *Macromolecular Theory and Simulations* **1999,** 8, 260-271.

13. Olaj, O. F.; Bitai, I.; Gleixner, G. *Makromolekulare Chemie* **1985,** 186, 2569-2580.

14. Olaj, O. F.; Schnöll-Bitai, I. *European Polymer Journal* **1989,** 25, 635.

15. Santos, A. M. *Entropie* **1998,** 34, 31-35.

16. Chiefari, J.; Chong, Y. K.; Ercole, F.; Krstina, J.; Jeffery, J.; Le, T. P. T.; Mayadunne, R. T. A.; Meijs, G. F.; Moad, C. L.; Moad, G.; Rizzardo, E.; Thang, S. H. *Macromolecules* **1998,** 31, 5559-5562.

17. Ferguson, C. J.; Hughes, R. J.; Nguyen, D.; Pham, B. T. T.; Gilbert, R. G.; Serelis, A. K.; Such, C. H.; Hawkett, B. S. *Macromolecules* **2005,** 38, 2191-2204.

18. Ahmad, N. M.; Heatley, F.; Lovell, P. A. *Macromolecules* **1998,** 31, 2822-2827.

19. Chiefari, J.; Jeffery, J.; Mayadunne, R. T. A.; Moad, G.; Rizzardo, E.; Thang, S. H. *Macromolecules* **1999,** 32, 7700-7702.

20. Nikitin, A. N.; Hutchinson, R. A. *Macromolecules* **2005,** 38, 1581-1590.

21. Loiseau, J.; Doërr, N.; Suau, J. M.; Egraz, J. B.; Llauro, M. F.; Ladavière, C. *Macromolecules* **2003,** 36, 3066-77.

22. Arzamendi, G.; Plessis, C.; Leiza, J. R.; Asua, J. M. *Macromolecular Theory and Simulations* **2003,** 12, 315-324.

23. Couvreur, L.; Piteau, G.; Castignolles, P.; Tonge, M.; Coutin, B.; Charleux, B.; Vairon, J.-P. *Macromolecular Symposia* **2001,** 174, (Polymerization Processes and Polymer Materials I), 197-207.

24. Nikitin, A. N.; Castignolles, P.; Charleux, B.; Vairon, J.-P. *Macromolecular Theory and Simulations* **2003,** 12, 440-448.

25. van Herk, A. M. *Macromolecular Rapid Communications* **2001,** 22, 687-689.

26. Benson, S. W.; North, A. M. *Journal of the American Chemical Society* **1962,** 84, 935-40.

27. Zammit, M. D.; Davis, T. P.; Haddleton, D. M.; Suddaby, K. G. *Macromolecules* **1997,** 30, 1915-1920.

28. Barner-Kowollik, C.; Buback, M.; Egorov, M.; Fukuda, T.; Goto, A.; Olaj, O. F.; Russell, G. T.; Vana, P.; Yamada, B.; Zetterlund, P. B. *Progress in Polymer Science* **2005,** 30, 605-643.

29. Buback, M.; Egorov, M.; Gilbert, R. G.; Kaminsky, V.; Olaj, O. F.; Russell, G. T.; Vana, P.; Zifferer, G. *Macromolecular Chemistry and Physics* **2002,** 203, 2570-2582.

30. Russell, G. T. *Australian Journal of Chemistry* **2002,** 55, 399-414.

31. Russell, G. T. *Macromolecular Theory and Simulations* **1994,** 3, 439-68.

32. Russell, G. T. *Macromolecular Theory and Simulations* **1995,** 4, 497-517.

33. Russell, G. T. *Macromolecular Theory and Simulations* **1995,** 4, 519-48.

34. Russell, G. T. *Macromolecular Theory and Simulations* **1995,** 4, 549-76.

35. Russell, G. T.; Gilbert, R. G.; Napper, D. H. *Macromolecules* **1992,** 25, 2459-69.

36. Russell, G. T.; Gilbert, R. G.; Napper, D. H. *Macromolecules* **1993,** 26, 3538-52.

37. Hansen, F. K.; Ugelstad, J., Piirma book. In *Emulsion Polymerization*, Piirma, I., Ed. Academic: New York, 1982.

38. Ugelstad, J.; Hansen, F. K. *Rubber Chemistry and Technology* **1976,** 49, 536-609.

39. Smith, W. V.; Ewart, R. H. *Journal of Chemical Physics* **1948,** 16, 592-9.

40. Ballard, M. J.; Napper, D. H.; Gilbert, R. G. *Journal of Polymer Science, Polymer Chemistry Edition* **1984,** 22, 3225.

41. Rimmer, S.; Tattersall, P. *Polymer* **1999,** 40, 5729-5731.

42. Leyrer, R. J.; Machtle, W. *Macromolecular Chemistry and Physics* **2000,** 201, 1235-1243.

43. De Bruyn, H.; Miller, C. M.; Bassett, D. R.; Gilbert, R. G. *Macromolecules* **2002,** 35, 8371-8377.

44. Lansdowne, S. W.; Gilbert, R. G.; Napper, D. H.; Sangster, D. F. *Journal of the Chemical Society, Faraday Transactions 1: Physical Chemistry in Condensed Phases* **1980,** 76, 1344-55.

45. Hawkett, B. S.; Napper, D. H.; Gilbert, R. G. *Journal of the Chemical Society, Faraday Transactions 1: Physical Chemistry in Condensed Phases* **1980,** 76, 1323-43.

46. Lacík, I.; Casey, B. S.; Sangster, D. F.; Gilbert, R. G.; Napper, D. H. *Macromolecules* **1992,** 25, 4065-4072.

47. Morrison, B. R.; Casey, B. S.; Lacik, I.; Leslie, G. L.; Sangster, D. F.; Gilbert, R. G.; Napper, D. H. *Journal of Polymer Science, Part A: Polymer Chemistry* **1994,** 32, 631-49.

48. van Berkel, K. Y.; Russell, G. T.; Gilbert, R. G. *Macromolecules* **2003,** 36, 3921-3931.

49. Morton, M.; Kaizerman, S.; Altier, M. W. *Journal of Colloid Science* **1954,** 9, 300-12.

50. Hawkett, B. S.; Napper, D. H.; Gilbert, R. G. *Journal of the Chemical Society, Faraday Transactions 1: Physical Chemistry in Condensed Phases* **1981,** 77, 2395-2404.

51. Norrish, R. G. W.; Smith, R. R. *Nature* **1942,** 150, 336-7.

52. Trommsdorff, E.; Kohle, H.; Lagally, P. *Makromolekulare Chemie* **1948,** 1, 169-98.

53. Gilbert, R. G.; Napper, D. H. *Journal of Macromolecular Science - Macromolecular Chemistry and Physics C* **1983,** 23, 127-186.

54. Prescott, S. W.; Ballard, M. J.; Gilbert, R. G. *Journal of Polymer Science, Part A: Polymer Chemistry* **2005,** 43, 1076-1089.

55. Lukacs, E., *Probability and Mathematical Statistics*. Academic Press: New York, 1972.

56. Ballard, M. J.; Gilbert, R. G.; Napper, D. H. *Journal of Polymer Science, Polymer Letters Edition* **1981,** 19, 533-7.

57. Casey, B. S.; Morrison, B. R.; Maxwell, I. A.; Gilbert, R. G.; Napper, D. H. *Journal of Polymer Science, Part A: Polymer Chemistry* **1994,** 32, 605-630.

58. McAuliffe, C. *Journal of Physical Chemistry* **1966,** 70, 1267-75.

59. Nomura, M., Piirma book. In *Emulsion Polymerization*, Piirma, I., Ed. Academic: New York, 1982; pp 191-219.

60. Halnan, L. F.; Napper, D. H.; Gilbert, R. G. *Journal of the Chemical Society, Faraday Transactions 1: Physical Chemistry in Condensed Phases* **1984,** 80, 2851-65.

61. Adams, M. E.; Trau, M.; Gilbert, R. G.; Napper, D. H.; Sangster, D. F. *Australian Journal of Chemistry* **1988,** 41, 1799-813.

62. Fitch, R. M.; Shih, L.-B. *Progress in Colloid & Polymer Science* **1975,** 56, 1-11.

63. Yeliseeva, V. I., Polymerization of polar monomers. In *Emulsion Polymerization*, Piirma, I., Ed. Academic: New York, 1982; pp 247-88.

64. Penboss, I. A.; Gilbert, R. G.; Napper, D. H. *Journal of the Chemical Society, Faraday Transactions 1: Physical Chemistry in Condensed Phases* **1986,** 82, 2247-68.

65. Maxwell, I. A.; Morrison, B. R.; Napper, D. H.; Gilbert, R. G. *Macromolecules* **1991,** 24, 1629-40.

66. Priest, W. J. *Journal of Physical Chemistry* **1952,** 56, 1077.

67. McAskill, N. A.; Sangster, D. F. *Australian Journal of Chemistry* **1979,** 32, 2611-15.

68. McAskill, N. A.; Sangster, D. F. *Australian Journal of Chemistry* **1984,** 37, 2137-43.

69. Maxwell, I. A.; Morrison, B. R.; Napper, D. H.; Gilbert, R. G. *Makromol. Chem.* **1992,** 193, 303-13.

70. Coen, E. M.; Lyons, R. A.; Gilbert, R. G. *Macromolecules* **1996,** 29, 5128-5135.

71. Morrison, B. R.; Maxwell, I. A.; Napper, D. H.; Gilbert, R. G.; Ammerdorffer, J. L.; German, A. L. *Journal of Polymer Science, Part A: Polymer Chemistry* **1993,** 31, 467-483.

72. Marestin, C.; Guyot, A.; Claverie, J. *Macromolecules* **1998,** 31, 1686-1689.

73. Thomson, B.; Wang, Z.; Paine, A.; Lajoie, G.; Rudin, A. *Journal of Polymer Science, Part A: Polymer Chemistry* **1995,** 33, 2297-304.

74. Christie, D. I.; Gilbert, R. G.; Congalidis, J. P.; Richards, J. R.; McMinn, J. H. *Macromolecules* **2001,** 34, 5158-5168.

75. Davies, J. T.; Rideal, E. K., *Interfacial Phenomena*. Academic Press: New York, 1961.

76. Plyasunov, A. V.; Shock, E. L. *Journal of Supercritical Fluids* **2001,** 20, 91-103.

77. Asua, J. M.; De la Cal, J. C. *Journal of Applied Polymer Science* **1991,** 42, 1869-77.

78. Kim, J. U.; Lee, H. H. *Macromolecules* **1994,** 27, 3337-40.

79. Kshirsagar, R. S.; Poehlein, G. W. *Journal of Applied Polymer Science* **1994,** 54, 909-21.

80. Dong, Y.; Sundberg, D. C. *Macromolecules* **2002,** 35, 8185-8190.

81. Dong, Y. *Journal of Colloid and Interface Science* **2005,** 288, 390-395.

82. Tauer, K.; Nozari, S.; Ali, A. M. I. *Macromolecules* **2005,** 38, 8611-8613.

83. Goicoechea, M.; Barandiaran, M. J.; Asua, J. M. *Macromolecules* **2006,** 39, 5165-5166.

84. Berne, B. J.; Pecora, R., *Dynamic Light Scattering: With Applications to Chemistr, Biology and Physics*. Dover Publications: 2000.

85. Lamb, D. J.; Fellows, C. M.; Morrison, B. R.; Gilbert, R. G. *Polymer* **2005,** 46, 285-294.

86. Mori, S.; Barth, H. G., *Size Exclusion Chromatography*. First ed.; Springer Verlag: New York, 1999.

87. Flory, P. J., *Principles of Polymer Chemistry*. Cornell University Press: Ithaca, 1953.

88. Clay, P. A.; Gilbert, R. G. *Macromolecules* **1995,** 28, 552-69.

89. Baumgarten, J. L.; Busnel, J. P.; Meira, G. R. *Journal of Liquid Chromatography & Related Technologies* **2002,** 25, 1967-2001.

90. Castro, J. V.; van Berkel, K. Y.; Russell, G. T.; Gilbert, R. G. *Australian Journal of Chemistry* **2005,** 58, 178-181.

91. Hammond, M. Sterically Stabilized Emulsion Systems. Honours Thesis, Honours Thesis,The University of Sydney, Sydney, 1983.

92. Shoaf, G. L.; Poehlein, G. W. *Journal of Applied Polymer Science* **1991,** 42, 1213-37.

93. Leemans, L.; Jerome, R.; Teyssie, P. *Macromolecules* **1998,** 31, 5565-5571.

94. Vorwerg, L.; Gilbert, R. G. *Macromolecules* **2000,** 33, 6693-6703.

95. Lacik, I.; Beuermann, S.; Buback, M. *Macromolecules* **2001,** 34, 6224-6228.

96. Lacik, I.; Beuermann, S.; Buback, M. *Macromolecules* **2003,** 36, 9355-9363.

97. Lacik, I.; Beuermann, S.; Buback, M. *Macromolecular Chemistry and Physics* **2004,** 205, 1080-1087.

98. De Bruyn, H.; Gilbert, R. G.; White, J. W.; Schulz, J. C. *Polymer* **2003,** 44, 4411-4420.

99. Hawker, C. J.; Barclay, G. G.; Orellana, A.; Dao, J.; Devonport, W. *Macromolecules* **1996,** 29, 5245-5254.

100. Moad, G.; Anderson, A. G.; Ercole, F.; Johnson, C. H. J.; Krstina, J.; Moad, C. L.; Rizzardo, E.; Spurling, T. H.; Thang, S. H. *ACS Symposium Series* **1998,** 685, (Controlled Radical Polymerization), 332-360.

101. Benoit, D.; Chaplinski, V.; Braslau, R.; Hawker, C. J. *Journal of the American Chemical Society* **1999,** 121, 3904-20.

102. Ohno, K.; Izu, Y.; Yamamoto, S.; Miyamoto, T.; Fukuda, T. *Macromolecular Chemistry and Physics* **1999,** 200, 1619-1625.

103. Benoit, D.; Grimaldi, S.; Robin, S.; Finet, J. P.; Tordo, P.; Gnanou, Y. *Journal of the American Chemical Society* **2000,** 122, 5929-5939.

104. Prodpran, T.; Dimonie, V. L.; Sudol, E. D.; El-Aasser, M. S. *Macromolecular Symposia* **2000,** 155, 1-14.

105. Wang, J.-S.; Matyjaszewski, K. *Journal of the American Chemical Society* **1995,** 117, 5614-5.

106. Xia, J. H.; Matyjaszewski, K. *Macromolecules* **1997,** 30, 7697-7700.

107. Matyjaszewski, K. *Macromolecules* **1998,** 31, 4710-4717.

108. Chiefari, J.; Mayadunne, R. T. A.; Moad, C. L.; Moad, G.; Rizzardo, E.; Postma, A.; Skidmore, M. A.; Thang, S. H. *Macromolecules* **2003,** 36, 2273-2283.

109. Chong, Y. K.; Krstina, J.; Le, T. P. T.; Moad, G.; Postma, A.; Rizzardo, E.; Thang, S. H. *Macromolecules* **2003,** 36, 2256-2272.

110. Moad, G.; Chong, Y. K.; Postma, A.; Rizzardo, E.; Thang, S. H. *Polymer* **2005,** 46, 8458-8468.

111. Prescott, S. W.; Ballard, M. J.; Rizzardo, E.; Gilbert, R. G. *Macromolecules* **2002,** 35, 5417-5425.

112. Ferguson, C. J.; Hughes, R. J.; Pham, B. T. T.; Hawkett, B. S.; Gilbert, R. G.; Serelis, A. K.; Such, C. H. *Macromolecules* **2002,** 35, 9243-9245.

113. Prescott, S. W.; Ballard, M. J.; Rizzardo, E.; Gilbert, R. G. *Macromolecules* **2005,** 38, 4901-4912.

3. Synthesis of a Model Seed Latex

Sections of the work presented in this Chapter have previously been published as:

Thickett, S.C and Gilbert, R.G. *Midchain Transfer to Polymer in Styrene-Poly(butyl acrylate) Systems: Direct Evidence of Retardative Effects,* Macromolecules, **2005**, 38, 9894-9896.

"Minds are like parachutes. They only function when they are open."

Sir James Dewar

3.1. Introduction

In this Chapter, work is presented that resulted in the development of a methodology to design and synthesize model electrosterically stabilized latexes for kinetic experiments. As was outlined in Chapter 2, the 'RAFT in emulsion[1]' technique is ideal for controlling the molecular weight of the stabilizing moiety on the particle surfaces in such latexes; however the procedure results in a latex still under RAFT control at the conclusion of polymerization. This situation is unacceptable for kinetic experiments designed to obtain information on conventional (not controlled) emulsion polymerizations, as the active RAFT agent and its ability to influence polymerization kinetics will potentially result in the study of the rate coefficients of interest (those of radical entry and exit) being unnecessarily complicated.

As a consequence, the aim of the work presented here is to develop a method to successfully remove or chemically modify the RAFT end-group after latex formation (in order to remove the 'living' nature of the polymerization system) while not destroying the particle morphology through coagulation or harsh reaction conditions. Some of the various techniques to remove or modify RAFT agents are described below.

3.1.1. RAFT Removal Techniques

While RAFT polymerization has numerous advantages in terms of molecular weight control and chain architecture, for many industrial applications there are significant negatives such as the colour of the polymer or latex (typically bright yellow or red) and the smell. As a result, removal of the RAFT agent through some means is an important process and one that has received significant attention in the literature in recent times.

Base-catalyzed hydrolysis[2] has proven successful for dithiocarbamate RAFT agents; however this technique is essentially only applicable for solution polymerizations, due to the very high pH

reaction conditions. If this technique were transferred to an emulsion system the latex would most likely lose its colloidal stability as a result of the process. Thermolysis[3] has also proven a successful method of eliminating trithiocarbonate end-groups; however this is clearly not a suitable technique for an emulsion system. Aminolysis[4, 5] with primary or secondary amines has also proven successful in converting a RAFT end-group into a resultant thiol and thioamide; however it is an approach that is not suitable for use with all monomer systems, especially carboxylic acid monomers. For this system this approach is not valid, as the particles being synthesized are stabilized by a corona of poly(acrylic acid) (polyAA).

Due to the minimal number of disadvantages, the approach that was chosen in this work was the oxidation of the RAFT agent through the use of peroxides or hydroperoxides. Charmot *et al.*[6] demonstrated that under reflux conditions in an organic solvent, peroxides such as lauroyl peroxide were successful in converting the thiocarbonyl group to a carbonyl group, removing the living nature of the RAFT end-group. This technique was shown to be applicable for a wide variety of different monomers, including carboxylic acid monomers. Given that for an emulsion polymerization system the use of organic solvents and reflux conditions is undesirable, this technique was modified. A lower reaction temperature (to ensure that the aqueous phase does not boil) and a more hydrophilic peroxide (in this case, *tert*-butylhydroperoxide, TBHP) were used. The only drawback in the use of peroxides and hydroperoxides is that they can act as chain transfer agents[7, 8] themselves, so they too must be removed from the reaction medium before the latex is used as a chain transfer agent. The success in the application of this technique is described later in this Chapter.

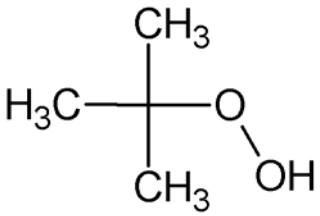

Figure 3.1. *Tert*-butylhydroperoxide (TBHP)

3.2. Experimental

Reagents. Acrylic acid (AA, Sumika) was purified by vacuum distillation to remove dimeric structures and polymerization inhibitors. *n*-Butyl acrylate (*n*-BA) (Sigma Aldrich) was purified by passing the monomer through an inhibitor removal column (Sigma Aldrich) to remove the Methyl Ethyl Hydroquinone (MEHQ) inhibitor. Granular NaOH (Sigma Aldrich) and the initiator 4,4′-azobis(4-cyanopentanoic acid) (commonly known as V-501, Wako Industries) were used as received. The RAFT agent, 2-([(butylsulfanyl)carbonothioyl]sulfanyl)propanoic acid (commonly known as RAFT V) was received in recrystallized form from Dulux Australia. *Tert*-butylhydroperoxide (TBHP, 70% aqueous solution, Sigma Aldrich), sodium dodecyl sulfate (SDS, Aldrich) and potassium persulfate (KPS, Merck) were used as received. All water used in this work was high-purity deionised water (Milli-Q).

Synthesis of macro-RAFT Agent. The experimental procedure described here relates to the synthesis of a macro-RAFT agent with a target degree of polymerization of five (5) monomer units. As is the case in RAFT polymerization, this target can be changed through the modification of the molar ratio between the monomer and the RAFT agent. Latexes were made from macro-RAFT agents of average degrees of polymerization of 5, 10 and 20 units.

AA (2.51 g, 35 mmol), NaOH (0.28 g, 7 mmol), V-501 (0.19 g, 0.6 mmol) and RAFT V (1.65 g, 7mmol) were added to water (3.39 g) and stirred magnetically until all solids had dissolved. The reaction vessel was sealed with a rubber septum and nitrogen was bubbled through the reaction

mixture for 30 minutes at room temperature to remove any inhibitory oxygen. The reaction vessel was placed in a temperature-calibrated oil bath set at 333 K and polymerization was allowed to take place for two hours with constant stirring. Conversion to polymer was checked by gravimetry and was shown to be approximately 100 %. A sample of this polymeric species was analyzed by ESI-MS to determine if the polymerization target was reached. ESI-MS analyses were performed on a Finnigan Mat LCQ MS detector with Finnigan LCQ Data Processing and Instrument Control Software at The University of Sydney. Polymeric samples were dissolved in a methanol/water 50:50 w/w mixture, with a feed rate into the ionization unit of 0.2 mL min^{-1}. The applied voltage was 5 kV, with 7 kPa nitrogen acting as the aspirating gas. The heating element was at 473 K.

Synthesis of Electrosterically Stabilized Latex Using *n*-butyl acrylate. NaOH (0.09 g, 2.3 mmol), V-501 (0.07 g, 0.25 mmol) and macro-RAFT (0.31 g) were added to deionized water (80.3 g) and stirred magnetically at room temperature until complete dissolution of all solids. The reaction vessel was sparged with high-purity N_2 for 15 minutes to remove dissolved oxygen.

Uninhibited *n*-BA (20 g, 0.16 mol) was sparged with N_2 separately and placed in a gas-tight glass syringe. Under constant shear and at 333 K, the *n*-BA was fed into the reaction vessel by a syringe pump under the following addition rate: 0.1 g initially, 1 g/h for two hours, followed by 5.97 g/h for the next three hours. Another hour of polymerization was followed after complete addition of the *n*-BA.

Upon completion of the reaction, a milky yellow latex was formed. Conversion to polymer was checked via gravimetry, and the latex dialyzed for one week with daily changes of water.

Removal of the RAFT Agent. To a sample of the poly(*n*-BA)-RAFT latex (20 g), TBHP was added to a concentration of 5% w/w. The emulsion was stirred magnetically to help disperse the added peroxide, with high purity N_2 bubbled through the mixture for 15 minutes. The latex was

then heated at 353 K for five hours with constant stirring. Small amounts of coagulum were removed by passing the resultant latex through glass wool. To help determine the mechanism of oxidation involved in the removal of the RAFT agent, the same treatment was applied purely to RAFT V dissolved in excess toluene, with the resultant solution analyzed by ESI-MS.

As the RAFT agent (specifically the thiocarbonyl group) is a UV chromophore, the success of the removal/chemical modification of the RAFT endgroup was determined by size exclusion chromatography (SEC) with an online UV-visible spectrometer. Dried polymer samples from the latex before and after treatment with TBHP were analyzed, with particular interest in the UV absorption at 290 nm where the RAFT agent in question was shown to absorb.

SEC analyses of the resultant polymer samples was performed on an Organic SEC (Shimadzu), consisting of in-line solvent de-gasser with a 0.1 μm solvent filter, guard column (Waters) and an HR-2, HR-3 and HR-4 Styragel SEC Column (Waters) in series with one another. Columns were stored in a GPC Column Oven (Shimadzu) set at 303 K. Samples were injected by an auto-injector (Shimadzu). 50 μL of sample was injected into the column, with the mobile phase consisting of a 95:5 v/v % Tetrahydrofuran/Acetic acid (THF/AcA) mixture. Flow rate was set at 1 mL min^{-1}, with the signal response recorded by a RID-10A refractive index detector (Shimadzu). The UV signal as a function of elution time was recorded on an SPD-10A-VP in-line UV detector. All data was collected and processed using Cirrus™ GPC software. For 'universal calibration,' the Mark-Houwink-Sakaruda parameters used in this work were $K = 1.14 \times 10^{-4}$ dL g^{-1}, α=0.716 for styrene and $K= 1.22 \times 10^{-4}$ dL g^{-1}, $\alpha = 0.7$ for *n*-BA.

Synthesis of an Electrostatically Stabilized Poly(*n*-butyl acrylate) Latex. SDS (1.74 g, 3.67 mmol) was dissolved in Milli-Q grade water (409 g). BA (44.06 g, 0.35 mol) was added and stirred vigorously to effect emulsification, the mixture then heated (353 K), while high-purity nitrogen was bubbled through the mixture. KPS (0.38 g, 1.46 mmol) dissolved in 5 mL of water

was added via syringe. Polymerization took place for 3 h, the resultant latex filtered through glass wool then dialyzed against distilled water for a week with daily changes of water.

Latex Characterization. Both latexes were characterized in terms of particle size through the use of Photon Correlation Spectroscopy (PCS, Brookhaven), HPPS and Capillary Hydrodynamic Fractionation (CHDF, Matec), as described in Chapter 2.

Chemically Initiated Dilatometry. Styrene (5 g, 48 mmol), Milli-Q water (17 g) and seed latex (10 g) were separately degassed under vacuum then loaded into a dilatometer. SDS (0.005 g, 3.5 μmol) was added, the dilatometer sealed with a rubber septum and the headspace evacuated via syringe at room temperature. Magnetic stirring of the solution took place overnight to allow transfer of monomer to the particle interior and the mixture then heated to 323 K. Stirring was ceased and the reaction vessel evacuated again to remove dissolved oxygen.

A KPS solution (1 mL) was added via syringe; following this a glass capillary (1.51 mm radius) was inserted into the top of the vessel. Water was added until the solution was 10-12 cm up the capillary; stirring then recommenced. Dodecane (1 mL) was added to the top to prevent evaporation. The meniscus height was tracked automatically to provide conversion/time data. Duplicate experiments at five different initiator concentrations (spanning two orders of magnitude) were performed.

Gamma-Initiated Dilatometry. Polymerization was initiated using a ^{60}Co γ source (dose rate = 105 Gy h^{-1}). The automated dilatometer was lowered into the radiation source until the polymerization rate reached a steady state, then removed from the source, allowing the rate decrease to be monitored. Successive insertions and removals from the radiation source were performed to provide extensive data for analysis.

3.3. Results

As the approach taken in the synthesis of an electrosterically stabilized latex in this work mirrors the approach taken in the pioneering work of Ferguson *et al.*,[1, 9] the resultant latex has quite similar properties – a reasonably small average particle size (62 nm diameter as confirmed by CHDF) and as a result a high particle number N_p. The particle size distribution (PSD) is not very narrow (PDI = 1.08 as confirmed by CHDF) as the particle formation period in this 'self-assembly' approach is quite long[10] and as a result the latex adopts a broader than normal distribution. The distribution of hydrophilic chains on the particle surface was confirmed by ESI-MS to be at the target degree of polymerization and narrow particle size distribution (see Figure 3.2) although it should be noted that the obtained distribution by this method is not quantitative. As the obtained particle size through this approach is ideal for 'zero-one' kinetic analyses,[11] the aim of the RAFT removal work is to retain the same (or similar) particle size and morphology while removing the capacity for the polymer chains present in the system to no longer undergo controlled polymerization.

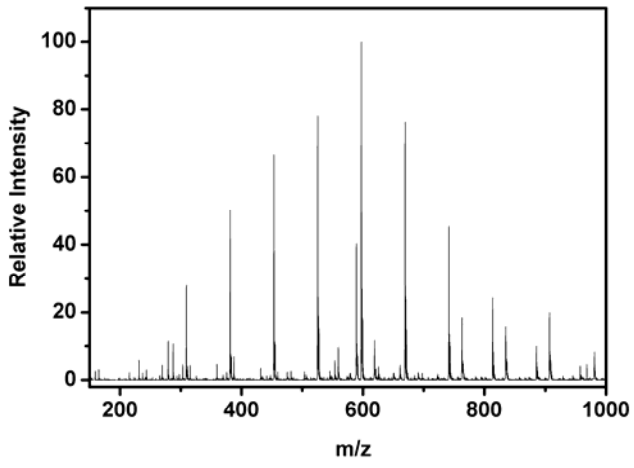

Figure 3.2. Distribution of polyAA as confirmed by Electrospray Ionization Mass Spectrometry (ESI-MS).

3.3.1. Success of the RAFT Agent Removal Method

The RAFT 'removal' method (through chemical modification by reaction with TBHP) was shown to be a successful method of removing the RAFT functionality on the ends of the polymer chains within the latex. As TBHP is moderately water-soluble (over 10 g / 100 mL H_2O) it is able to transport through the aqueous phase, while the *tert*-butyl group ensures that it is able to migrate into the particle interior (where the active RAFT end-groups are located). Visual confirmation of the success of the method was demonstrated by the fairly rapid removal of the yellow colour of the emulsion; by the end of the reaction the latex had a classic white appearance. Minimal coagulation was also noted by using this technique, and no appreciable change in the particle size was observed (see Table 3.1).

Table 3.1. Particle Size, PDI and MW Data of Latexes Before and After TBHP Treatment.

Sample	$\bar{M}_n$ (kDa)	PDI	r_{PCS} (nm)	PDI (PCS)	N_p (L^{-1})
RAFT latex	40.3	1.37	43.1	1.08	4.91×10^{17}
Oxidised latex	40.4	1.53	44.5	1.17	4.04×10^{17}

A more quantitative approach to determine the extent of the success of modification of the RAFT agent was taken by considering the change in the UV absorbance due to the thiocarbonyl group at 290 nm due to the RAFT end-group. SEC equipped with an on-line UV spectrophotometer allowed for the UV signal due to these polymers to be determined as a function of elution time, with the area under the signal-time curve considered to be equivalent to the total concentration of thiocarbonyl moieties. As seen in Figure 3.3, treatment with TBHP has little to no effect on the DRI (differential refractive index) signal, indicating no change to the molecular weight distribution (MWD) of the polymer, while the UV signal is essentially reduced to zero.

Comparison of peak areas gives a figure of 99.5 % success in the removal of thiocarbonyl groups, leading to essentially complete loss of the ability to control and maintain a 'livingness' of polymerization in these systems. Seeded experiments after the reaction with TBHP confirmed that the polymer was no longer under RAFT control due to the fact that two clear distributions within the SEC distribution are evident – the seed polymer and the polymer from the second stage polymerization (see Figure 3.4).

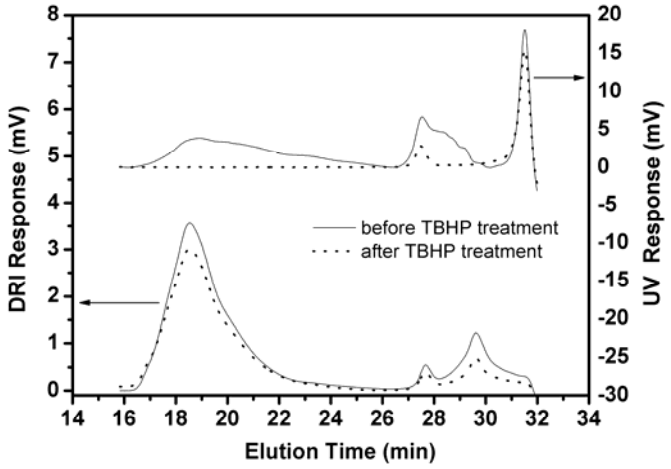

Figure 3.3. UV and DRI Signal via SEC of Polymers from Latex – Before and After Treatment with TBHP

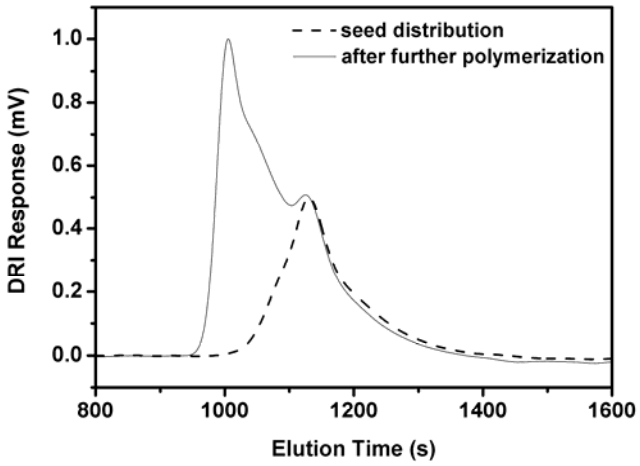

Figure 3.4. SEC Distribution from Seeded Experiment to Prove Loss of Living Character After TBHP Treatment.

Work by Vana *et al.*[12] has shown that for short-chain oligomers made by RAFT, oxidation by TBHP converts the thiocarbonyl group to a carbonyl group (C=O), as indicated by ESI-MS of these treated oligomers. The mechanism of this oxidation is somewhat unclear; however it is believed that the process involves a reactive sulfine intermediate.[13-15] Under the same conditions employed in the latex treatment, the RAFT agent (dissolved in toluene) was oxidized by TBHP at an elevated temperature to help confirm the nature of the conversion of the C=S group. ESI-MS analysis of the resultant mixture (Figure 3.5) supports the mechanism postulated by Vana – a decrease in m/z of 16 amu of the main peak is seen, indicating conversion of the C=S group into the C=O functionality. Other peaks present in the spectrum correspond to recombination products; however it is seen that this oxidation is not entirely 'clean.'

In the work of Alper,[13] the oxidation from a thiocarbonyl group to a carbonyl group only took place under basic conditions, and given the extremely high activation energy of TBHP decomposition (186 kJ mol^{-1}), the oxidation reaction is highly unlikely to involve radicals formed by decomposition of the peroxide bond ($t_{1/2} >> 10^4$ hrs at 353 K). Le Nocher *et al.*[16]

reported the conversion of the thiocarbonyl group into a stable sulfine through the use of *meta*-chloroperoxybenzoic acid (mCPBA) as an oxidizing agent; the proposed mechanism (see Figure 3.6a) of oxidation involved a 'whole molecule' rearrangement to form a benzoic acid and the resultant sulfine. Given the reported success of TBHP as an oxidizing agent both elsewhere and in this work, it is likely that the mechanism of oxidation similarly involves the hydroperoxide functionality and a molecular rearrangement of the reactants. A similar mechanism is presented (whereby *tert*-butyl alcohol is liberated as a by-product) in Figure 3.6b. The sulfine then ultimately undergoes a intramolecular rearrangement mechanism to liberate elemental sulfur and form the carbonyl moiety;[13] this mechanism involves a 3-membered ring as an intermediate which would most likely only proceed at elevated temperatures due to the high degree of bond angle strain.

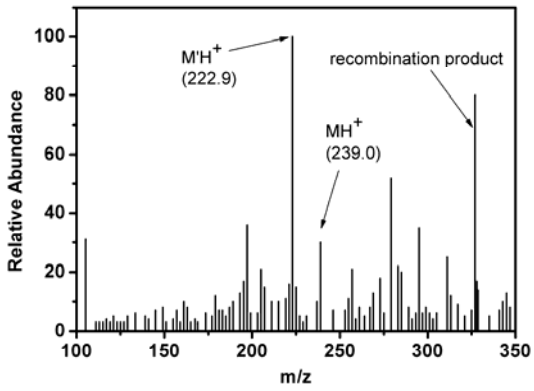

Figure 3.5. ESI-MS signal for oxidised RAFT agent. Original RAFT peak = MH^+ = 239, Oxidised peak = $M'H^+$ = 222.9.

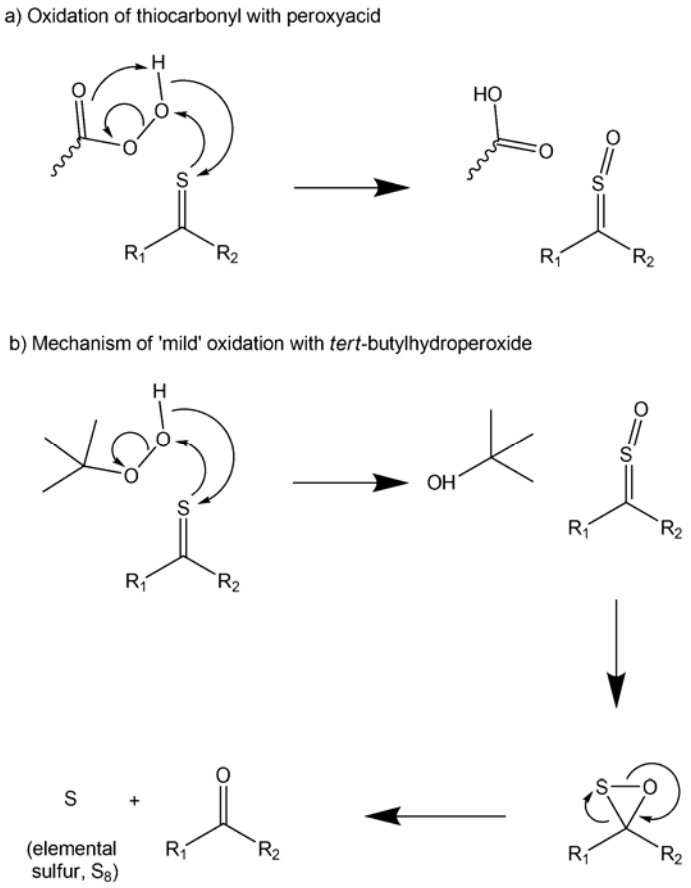

Figure 3.6. a) Mechanism of oxidation of thiocarbonyls by peroxyacids as postulated by Le Nocher *et al.*[16]; b) Proposed mechanism of thiocarbonyl oxidation through the use of TBHP.

While it seems that this oxidative process yields an 'ideal' seed (an electrosterically stabilized seed no longer under RAFT control), two problems remain: the oxidation liberates sulfur, which could potentially form thiols (that can act as chain transfer agents) or inhibit polymerization itself, as has been reported in the literature.[17, 18] Secondly, the presence of residual TBHP will be a problem in that it is a potential source of primary radicals and that the seeded experiments (which make up the bulk of this project) will be affected by the presence of another radical source besides the added initiator. Similarly the presence of a labile hydrogen means TBHP can act as a chain transfer agent,[19] which again poses a problem for this work.

Given the relative amounts of TBHP added to the system compared to the number of RAFT end-groups (and potential sulfur-based inhibitory by-products from the reaction with TBHP), any inhibition or retardation seen in these systems would be due to TBHP acting as a chain transfer agent (a value of $C_{tr} = 0.066$ has been reported[8] for TBHP at 333 K). It has also been postulated[20] that after hydrogen abstraction, the tert-butylperoxy radical is a poor chain re-initiator and so some radical activity is lost. As TBHP is moderately water-soluble, its presence in the aqueous phase of the emulsions of interest is certain to 'disrupt' the mechanism of radical entry, complicating any performed kinetic experiments. Extensive dialysis became an essential part of the methodology of the seed latex synthesis, performed for two weeks with daily changes of water. The residual peroxide concentration was shown by two separate methods (the spectrophotometric 'iodine test' where 1 mL of the centrifuged aqueous phase of the latex is added to 1 mL of a 10% w/w NaI/KI in glacial acetic acid solution, and the intensity of the yellow colour is spectrophotometrically related to the peroxide concentration, as well as Quantofix™ peroxide testing strips) was shown to be of the order of 1 ppm (approximately 10^{-5} M), a concentration that is kinetically insignificant for such a chain transfer agent.

3.3.2. The Kinetics of Seeded Styrene – Poly(*n*-Butyl Acrylate) Systems

While the seed latexes synthesized by the 'RAFT-in-Emulsion' method comprise a poly(*n*-butyl acrylate) core, it is the kinetics of styrene in these electrosterically stabilized latexes that is of interest, due to the wealth of existing data concerning styrene polymerization for comparison. Solubility parameters and cohesive energy terms[21, 22] indicate that there is no compatibility or solubility issues with regards to swelling a poly(*n*-BA) latex with styrene monomer, and as a result it was anticipated that such systems would return results typical for the kinetics of styrene emulsion polymerization systems. To provide a system to act as a 'reference' latex, an electrostatically stabilized poly(*n*-BA) latex (i.e. a latex with no stabilizing 'hairs' on the surface)

was synthesized and the kinetics of styrene emulsion polymerization in such a system was studied by chemically initiated and gamma-initiated dilatometry.

Of particular surprise was the fact that rate data using chemical initiation gave steady-state $\bar{n}$ values ($\bar{n}_{ss}$, see Figure 3.7) significantly lower than predicted by theory (i.e. Limit 2a kinetics[11, 23, 24] within the 'zero-one' limit) (Note also that the Limit 1 values for $\bar{n}_{ss}$ are much closer to the experimentally determined values). This would mean that ρ is far lower, and/or that k is far higher, than predicted for styrene in a poly(styrene) seed, for which the models are reliable. As radical entry depends only on aqueous-phase kinetics, ρ should not be dependent on the particle interior – leaving the radical loss process as the parameter most likely to be affected by the presence of poly(*n*-BA) as the seed polymer.

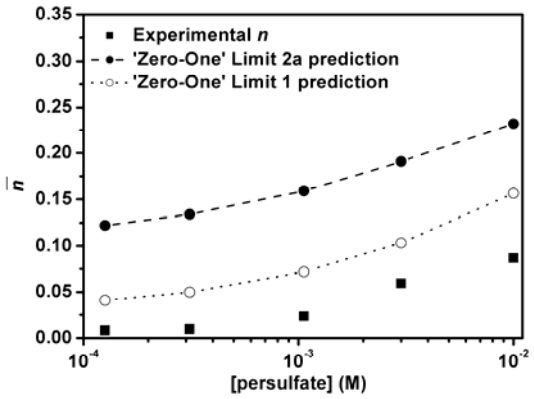

Figure 3.7. Variation of steady-state average number of radicals per particle ($\bar{n}_{ss}$, black squares) as a function of initiator (KPS) concentration, as well as comparison with predicted values (Limit 2a values = filled circles with dashed lines, Limit 1 values = open circles with dotted lines).

Using γ-relaxation dilatometry, data analysis of the out-of-source polymerization periods (Figure 3.8) allowed a value of the exit rate coefficient k to be determined. The equations that govern first- and second-order loss kinetics were fitted to the data; it should be noted however that it is essentially impossible to *visually* distinguish first- and second-order loss kinetics from rate data

due to experimental scatter.[24] The first- and second-order loss rate coefficients were $k = (2.2 \pm 1.3) \times 10^{-2}$ and $(4.2 \pm 1.1) \times 10^{-2}$ s^{-1} respectively. These values are both significantly higher than the predicted values for this system ($k = 9 \times 10^{-3}$ s^{-1} using first-order loss, 1×10^{-2} s^{-1} for second-order loss for particles of this size (27 nm unswollen radius, PDI = 1.04)), and partially explain the significantly reduced steady-state rate.

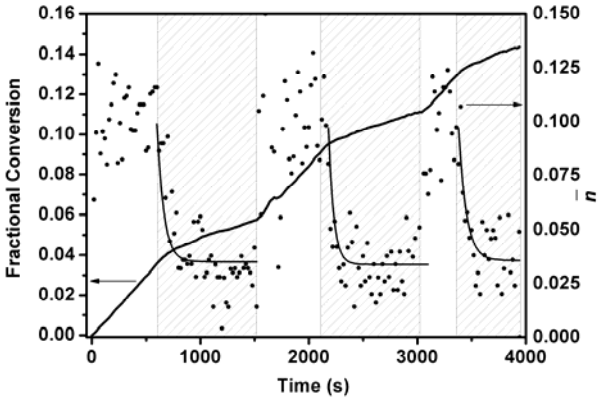

Figure 3.8. Conversion/time data (line) and $\bar{n}$ -time (points) data for the γ-radiation initiated polymerization of styrene in a poly(*n*-BA) seed latex Shaded regions represent the 'out-of-source' polymerization periods, where the $\bar{n}$ -time data is fitted by the appropriate equation (solid curved lines) to obtain an exit rate coefficient *k*.

Using the obtained values of k and $\bar{n}_{ss}$, values of the entry rate coefficient ρ (and as a result the radical entry efficiency f_{entry}) were calculated. First-order loss kinetics (Limit 1) gives f_{entry} values in accordance with the Maxwell-Morrison 'aqueous phase growth' model[25] that predicts the entering species are oligomers of length 2-3 (Figure 3.9). Similar calculations assuming second-order loss kinetics (Limit 2a) give f_{entry} values that are substantially lower than predicted by the model, which seems implausible as a different particle interior should not affect polymerization in the aqueous phase. From these sets of results, it seems apparent that styrene-poly(*n*-BA) latexes obey the somewhat unexpected Limit 1 kinetic profile – an explanation of which is put forward in the following section.

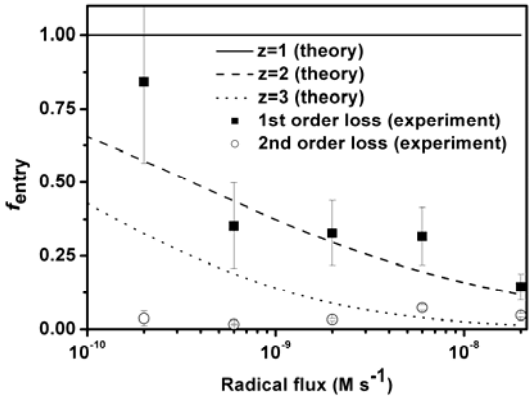

Figure 3.9. f_{entry} versus radical flux for chemically initiated experiments, with the data processed assuming first order loss (black squares) and second order loss (open circles). Lines: predicted entry efficiency from the Maxwell-Morrison model, for *z* (critical degree of polymerization for entry) = 1 (solid line), 2 (dashes) and 3 (dots).

3.3.3. Chain Transfer to Polymer

An explanation for the apparent first-order loss mechanism exhibited in these systems is that transfer to poly(*n*-BA) is the dominant chain-stopping mechanism for growing styrene radicals, with the formed mid-chain radical (MCR) unable to desorb from a particle (it is generally considered that only monomeric radicals can desorb into the aqueous phase due to their moderately high water solubility[23]). If propagation from the backbone site is slow, the next entry event will terminate this radical and lead to radical loss (Figure 3.10). This explanation seems feasible, given that there is evidence from simulations that propagation off this backbone site is dramatically slower than 'conventional' propagation.[26]

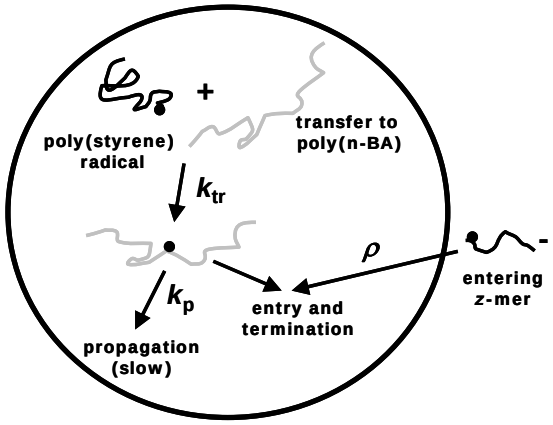

Figure 3.10. Transfer of radical activity from growing poly(styrene) radical to polyBA backbone as a means to explain low $\bar{n}$ values.

The significance of intermolecular chain transfer is shown in the molecular weight distribution (MWD) of formed polymer (performed on a Shimadzu SEC system with 3 × HT6E Waters columns, THF eluent with a flow rate of 1 mL min[1], polystyrene standards ranging from 5×10^3 to 1.2×10^7 Da). After considering the elution-time profile of the poly(*n*-BA) seed with second-stage poly(styrene), the signal due solely to the formed poly(styrene) can be obtained by subtracting the suitably normalized[27] MWD of the seed. It is apparent that the formed polystyrene has significantly lower molecular weight than predicted from the well tested theory for this quantity in a styrene zero-one system[28] (Figure 3.11). Using the 'ln*P*' method[29] (plotting the logarithm of the number MWD as a function of molecular weight), including correcting for SEC band broadening,[30-32] the slope of the ln*P* plot at the maximum in the SEC distribution (Figure 3.12) is $k_{tr,pol}$[poly(*n*-BA)]/k_p[styrene]M_0, where [poly(*n*-BA)] and [styrene] = polymer and monomer concentrations within the particle respectively, $k_{tr,pol}$ = rate coefficient for transfer to polymer, M_0 = styrene molecular weight. This yields $k_{tr,pol} = 0.101$ M^{-1} s^{-1}, a value that is 10 times higher than that for transfer to monomer.[33] This is a significant effect that is consistent with first-order radical loss by retardative transfer. This value is also over 20 times higher than the estimated value of $k_{tr,pol}$ found by Plessis *et al.* by model fitting,[34] and may provide further insight into modeling styrene - *n*-butyl acrylate copolymerization reactions.

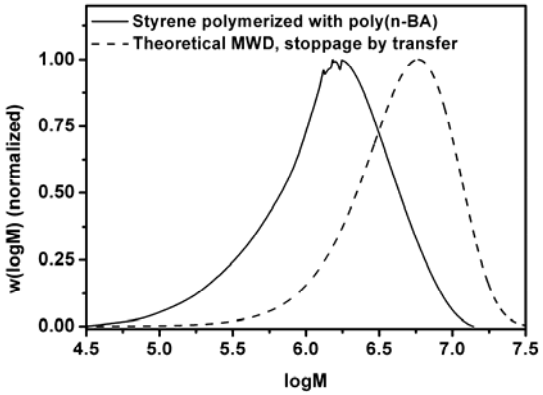

Figure 3.11. SEC distribution of formed poly(styrene) (solid line) from a chemically initiated experiment ([persulfate] = 3 mM) and the predicted GPC distribution (broken line) assuming transfer to monomer is the dominant chain stopping mechanism.

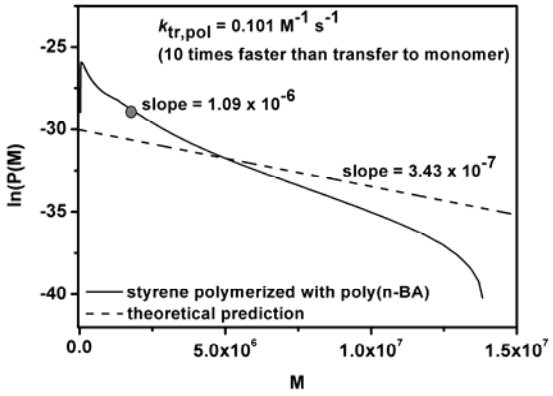

Figure 3.12. Observed and predicted ln*P*(M) for the formed polystyrene (solid line) MWD. The grey circle is at the peak maximum in the original SEC distribution (where the slope of the line is measured), which corrects for band broadening.

3.3.4. Synthesis of Electrosterically Stabilized Latexes Using Styrene

Given the added complication of intermolecular chain transfer to poly(*n*-BA) in the emulsions described previously in this Chapter, the decision to switch to latexes with a poly(styrene) core was made due to the knowledge that no compatibility issues exist with poly(styrene) and its

monomer. The use of the 'RAFT-in-Emulsion' technique for styrene however requires some modifications due to the lower water solubility and propagation rate of styrene relative to *n*-BA; it is more difficult to reach the particle formation stage whilst avoiding droplet nucleation.

To compensate for this, the macro-RAFT agents used in the syntheses of these latexes were poly(styrene-*block*-acrylic acid) diblocks rather than polyAA monoblocks. The presence of a pre-formed poly(styrene) block on this initial polymers ensures that self-assembly takes place at an earlier stage and that particle formation (and hence growth) can be achieved in a controlled manner. Diblocks were synthesized in butanone with equimolar amounts of acrylic acid and styrene, e.g. RAFT-$(styrene)_{10}$-$(AA)_{10}$, with all other facets of the latex synthesis as reported earlier. Three latexes were synthesized with stabilizing blocks of average DP 5, 10 and 20 – the latexes were hence denoted ST5, ST10 and ST20. The 'RAFT removal' technique with TBHP was also proven to be as successful in poly(styrene) based systems.

Particle sizing techniques indicated that the use of pre-formed diblocks ensures nucleation of very small, fairly monodisperse latex particles. The average particle diameter (unswollen) determined by most techniques was shown to be a little over 20 nm; a TEM image of the resultant ST5 latex is shown in Figure 3.13. Tabulated particle size results by a variety of techniques are presented in Table 3.2. The result of such small latexes is an excellent one as these latexes are certain to fall within the 'zero-one' kinetic limit,[11] ensuring an ease of comparison of kinetic data with traditional electrostatically stabilized emulsion systems.

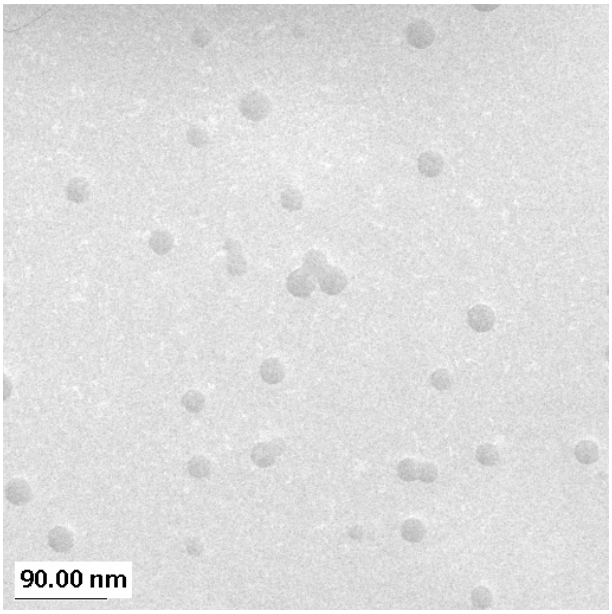

Figure 3.13. TEM Image of ST5 Latex.

Table 3.2. Particle Size Measurements for Electrosterically Stabilized Poly(styrene) Latexes. Polydispersity Indices are given in brackets. All sizes are particle diameters (nm).

	Light Scattering		Separation		Direct Count
LATEX	HPPS	PCS	CHDF	HDC	TEM
ST5	30.5 (1.15)	27.4 (1.02)	36.8 (1.19)	22.8 (1.07)	23.6 (1.03)
ST10	30.4 (1.12)	25.8 (1.05)	33.5 (1.12)	22.9 (1.07)	23.5 (1.04)
ST20	28.2 (1.11)	25.4 (1.11)	31.6 (1.18)	23.0 (1.13)	23.2 (1.03)

3.4. Conclusions

Using the 'RAFT-in-Emulsion' technique as a template, a methodology was developed to create model electrosterically stabilized latexes for kinetic analysis. The technique provides latexes where the stabilizing hydrophilic block on the particle surface is of known average degree of polymerization with a narrow molecular weight distribution. The use of TBHP at elevated temperatures was shown to be very efficient in destroying the RAFT end-group without upsetting the particle morphology, removing the complications associated with the kinetics of RAFT polymerization. Extensive dialysis was then shown to be sufficient in removing TBHP and any trace impurities that may affect subsequent polymerization.

Kinetic experiments involving electrostatically stabilized poly(*n*-BA) latexes polymerized with styrene gave highly unusual results, with reduced reaction rates and average number of radicals per particle ($\bar{n}$) compared to predicted theoretical values. γ-relaxation dilatometry experiments demonstrated an increased value of the exit rate coefficient k, and agreement with the 'Maxwell-Morrison' entry model for this latex was only possible when first-order loss kinetics was assumed. It was postulated that a growing poly(styrene) radical would undergo intermolecular chain transfer to poly(*n*-BA), yielding a mid-chain radical that is unable to desorb. The eventual termination of this radical would give the observed first-order loss mechanism; SEC measurements indicated that the MWD of the formed poly(styrene) was of much lower molecular weight than expected, in agreement with the developed postulate. A switch then was made to latexes with poly(styrene) cores, ensuring no compatibility issues with styrene monomer. It is these latexes that were to be used in further kinetic experiments to study the entry and exit mechanisms in such systems.

References

1. Ferguson, C. J.; Hughes, R. J.; Nguyen, D.; Pham, B. T. T.; Gilbert, R. G.; Serelis, A. K.; Such, C. H.; Hawkett, B. S. *Macromolecules* **2005,** 38, 2191-2204.

2. Schilli, C.; Lanzendoerfer, M. G.; Mueller, A. H. E. *Macromolecules* **2002,** 35, 6819-6827.

3. Postma, A.; Davis, T. P.; Moad, G.; O'Shea, M. S. *Macromolecules* **2005,** 38, 5371-5374.

4. Wang, Z.; He, J.; Tao, Y.; Yang, L.; Jiang, H.; Yang, Y. *Macromolecules* **2003,** 36, 7446-7452.

5. Thomas, D. B.; Convertine, A. J.; Hester, R. D.; Lowe, A. B.; McCormick, C. L. *Macromolecules* **2004,** 37, 1735-1741.

6. Charmot, D.; Chang, H. T.; Wang, W.; Piotti, M. Cleaving and replacing thio control agent moieties from polymers made by living-type free radical polymerization. 2003-407405

2003232938, 2003.

7. Moad, G.; Solomon, D. H., *The Chemistry of Free Radical Polymerization 2nd Edn.* Elsevier: Amsterdam, 2006.

8. Odian, G., *Principles of Polymerization*. 4th ed.; Wiley Interscience: 2004.

9. Ferguson, C. J.; Hughes, R. J.; Pham, B. T. T.; Hawkett, B. S.; Gilbert, R. G.; Serelis, A. K.; Such, C. H. *Macromolecules* **2002,** 35, 9243-9245.

10. Sprong, E.; Leswin, J. S.; Lamb, D. J.; Ferguson, C. J.; Hawkett, B. S.; Pham, B. T.; Nguyen, D.; Such, C. H.; Serelis, A. K.; Gilbert, R. G. *Macromolecular Symposia* **2006,** 231, 84-93.

11. Gilbert, R. G., *Emulsion Polymerisation: A Mechanistic Approach*. Academic Press: San Diego, 1995.

12. Vana, P.; Albertin, L.; Barner, L.; Davis, T. P.; Barner-Kowollik, C. *Journal of Polymer Science, Part A: Polymer Chemistry* **2002,** 40, 4032-4037.

13. Alper, H.; Kwiatkowska, C.; Petrignani, J. F.; Sibtain, F. *Tetrahedron Letters* **1986,** 27, 5449-50.

14. Buggle, K.; Fallon, B. *Monatshefte fuer Chemie* **1987,** 118, 1197-9.

15. Cerreta, F.; me Nocher, A.-M.; Leriverend, C.; Metzner, P.; Pham, T. N. *Bulletin de la Societe Chimique de France* **1995,** 132, 67-74.

16. Le Nocher, A. M.; Metzner, P. *Tetrahedron Letters* **1991,** 32, 747-50.

17. Tomita, K.; Nakagawa, T. Polymerization inhibition of vinyl compounds using phenothiazine and strong acids. 99-362125

2001172224, 19991221., 2001.

18. Bartlett, P. D.; Trifan, D. S. *Journal of Polymer Science* **1956,** 20, 457-76.

19. Abuin, E.; Avaria, L.; Lissi, E. *Boletin de la Sociedad Chilena de Quimica* **1987,** 32, 215-20.

20. Rizzardo, E., Personal communication. In 2004.

21. Bicerano, J., *Prediction of polymer properties*. 2nd ed.; Marcel Dekker: New York, 1996.

22. van Krevelen, D. W., *Properties of Polymers*. 3rd ed.; Elsevier: Amsterdam, 1997.

23. Casey, B. S.; Morrison, B. R.; Maxwell, I. A.; Gilbert, R. G.; Napper, D. H. *Journal of Polymer Science, Part A: Polymer Chemistry* **1994,** 32, 605-630.

24. Morrison, B. R.; Casey, B. S.; Lacik, I.; Leslie, G. L.; Sangster, D. F.; Gilbert, R. G.; Napper, D. H. *Journal of Polymer Science, Part A: Polymer Chemistry* **1994,** 32, 631-49.

25. Maxwell, I. A.; Morrison, B. R.; Napper, D. H.; Gilbert, R. G. *Macromolecules* **1991,** 24, 1629-40.

26. Nikitin, A. N.; Hutchinson, R. A. *Macromolecules* **2005,** 38, (5), 1581-90.

27. Clay, P. A.; Gilbert, R. G.; Russell, G. T. *Macromolecules* **1997,** 30, 1935-46.

28. Clay, P. A.; Christie, D. I.; Gilbert, R. G., Termination rate coefficients from molecular weight distributions. In *Advances in Free-Radical Polymerization*, Matyjaszewski, K., Ed. A.C.S.: Washington D.C., 1998; Vol. 685, pp 104-19.

29. Clay, P. A.; Gilbert, R. G. *Macromolecules* **1995,** 28, 552-69.

30. Castro, J. V.; van Berkel, K. Y.; Russell, G. T.; Gilbert, R. G. *Australian Journal of Chemistry* **2005,** 58, 178-181.

31. Konkolewicz, D.; Taylor, J. W., II; Castignolles, P.; Gray-Weale, A.; Gilbert, R. G. *Macromolecules* **2007,** 40, 3477-3487.

32. van Berkel, K. Y.; Russell, G. T.; Gilbert, R. G. *Macromolecules* **2003,** 36, 3921-3931.

33. Tobolsky, A. V.; Offenbach, J. *Journal of Polymer Science* **1955,** 16, 311-14.

34. Plessis, C.; Arzamendi, G.; Leiza, J. R.; Schoonbrood, H. A. S.; Charmot, D.; Asua, J. M. *Macromolecules* **2001,** 34, 5147-5157.

4. Kinetics of Radical Exit in Electrosterically Stabilized Systems

Sections of the work presented in this Chapter have previously been published as:

Thickett, S.C and Gilbert, R.G. *Rate Controlling Events for Radical Exit in Electrosterically Stabilized Emulsion Polymerization Systems,* Macromolecules, **2006**, 39, 2081-2091.

"Science does not know its debt to imagination."

Ralph Waldo Emerson

4.1. Introduction

In this Chapter, the results of kinetic experiments involving model electrosterically stabilized latexes (the synthesis of which was described in detail in the preceding Chapter) with known (and differing) degrees of polymerization of the stabilizing block are presented, with the specific aim of using well defined procedures in order to measure the exit rate coefficient k. As was described in Chapter 2, experimental rate parameters of interest (such as the entry and exit rate coefficients) are typically coupled within experimental observables such as the reaction rate and average number of radicals per particle ($\overline{n}$) and thus explicit values for each parameter are often not achievable without a number of model-based assumptions. The development of γ-relaxation dilatometry[1] however provided a means to *independently* obtain the value of k explicitly (with the proviso of needing to determine whether the loss is best described as first or second order) and in a reliable fashion, and it is the results of these experiments that are presented in this Chapter.

The results for the measurement of the exit rate coefficient in these systems are presented prior to the results for radical entry, as knowledge of the value of k is required to then indirectly calculate the value of ρ from steady-state rate data. Consequently the results are presented in this order and conclusions drawn in a similar fashion. Results obtained for the values of k in these 'hairy' systems are compared to the well-understood exit kinetics of electrostatically stabilized poly(styrene) latexes, with a view to determining any differences in the exit mechanism.

In order to demonstrate a consistency between approaches (and as a result, the reliability of the measured rate coefficients), values of k were obtained through several different means and subsequently compared. All involve the approach or departure from the steady-state rate in a variety of different experiments that are described in more detail below.

4.1.1. Data Treatment

Exit rate coefficient (k) values can be found using a variety of different means using the data obtained from kinetic experiments. Brief descriptions of the approaches are given here.

- **Direct Fitting to Relaxation Data**

This is the most widely-used approach in this work due to its reliability providing the means to directly access a value of k with a minimum number of other complications. Using γ-radiation to initiate seeded dilatometric experiments (as outlined in Chapter 2 (Section 2.6.5)), removal of the sample from the radiation source leads to a subsequent decrease in the polymerization rate (known as 'relaxation mode') due to radical loss (exit) events and no initiating radical flux present. By collecting kinetic data until the sample reaches its new steady state (often with a non-zero rate due to 'spontaneous' or thermally initiated polymerization[2, 3] in some monomer systems) the $\overline{n}\,(t)$ curve can be fitted to the appropriate equation to yield k (and ρ_{spont}) values. Those equations are:

$$\overline{n} = \frac{p - \lambda\,\delta\exp(-\gamma t)}{1 - \delta\exp(-\gamma t)} \tag{4.1}$$

where:

$$p = \frac{-g - \gamma}{2\,\omega};\quad \lambda = \frac{-g + \gamma}{2\,\omega};\quad \gamma^2 = g^2 - 4\,\omega\,\boldsymbol{\rho}_{\mathbf{spont}};$$

$$\delta = \frac{p - \overline{n}_0}{\lambda - \overline{n}_0};\quad \omega = -2\,\alpha\,\boldsymbol{k};\; g = -2\,\boldsymbol{\rho}_{\mathbf{spont}} - (1 - \alpha)\,\boldsymbol{k}$$

where $\overline{n}_0$ is the value of $\overline{n}$ at $t = 0$ (where $t = 0$ in this case is when the sample is removed from the radiation source). In the case of Limit 2a kinetics (re-entry of an exited radical, well accepted[4, 5] in the case of styrene polymerization systems in electrostatically stabilized particles)

$\alpha = 1$. These equations are only correct when α is assumed to be an integer.While the equations look complex the problem merely reduces to one of data fitting (through non-linear least squares regression for example) to obtain the 'best fit' values of ρ_{spont} and k. For Limit 1 kinetics $\alpha = 0$ and an even simpler set of equations can be used. An example of data-fitting is given in Figure 4.1.

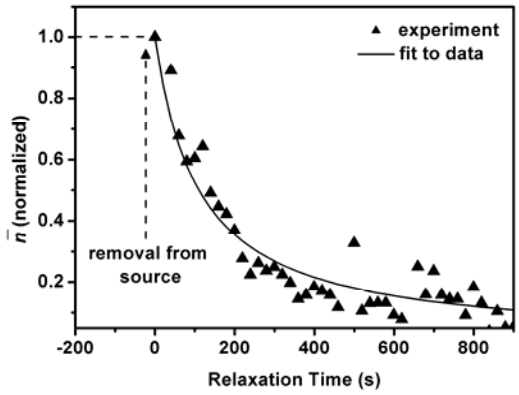

Figure 4.1. Example of Data-Fitting to Out-of-Source Polymerization Period in γ-Relaxation Experiment.

- **Slope-And-Intercept Method (Chemical Initiation)**

This method is generally not considered as robust a means to obtain k values in seeded dilatometric experiments compared to γ-relaxation experiments, as both the entry and exit rate coefficients are coupled within the experimental data and one cannot access one parameter directly. In this approach the conversion-time data is fitted (see Figure 4.2) by a linear function (as the polymerization rate within Interval II is essentially constant) with a view to obtaining the value of the intercept (a) and the slope (b) of this straight line; from these parameters and the collection of constants known as A (see Equation 2.41), the values of both rate coefficients can be found from the following expressions:

$$k = A\,\frac{\ln F}{2a}\,,\ \rho = G\,k \tag{4.2}$$

where:

$$G = \frac{2b^2}{A\,(A-2b)}\ ,\ F = \frac{1}{2} + \frac{G + 2\,\bar{n}_0}{4G(G+\ 2)^{0.5}}$$

(Note once more that these are the expressions for assuming Limit 2a kinetics; simpler equations exist if the system is in the Limit 1 regime.) While the value of *b* can be found quite accurately due to the large interval over which the polymerization rate is constant, this approach suffers because of the difficulty in accurately measuring the intercept *a*. Experimental difficulties (such as residual inhibitors, dissolved oxygen etc.) mean that the intercept from a linear fit in these systems can be difficult to obtain accurately. In this work, values of *k* found using this approach are only used for comparative purposes with those values obtained from γ-initiated experiments.

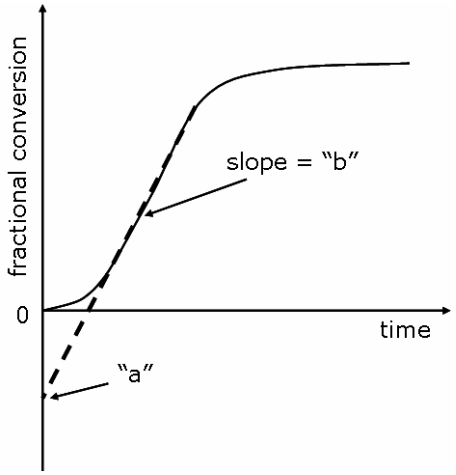

Figure 4.2. The 'Slope and Intercept' Method for Chemically Initiated Systems

- **Slope-And-Intercept Method (γ-Initiation)**

Data fitting to the conversion-time curve from γ-initiated experiments to obtain entry and exit rate coefficients is also possible using the same equations outlined previously (Equation 4.2).

One advantage in these systems is that after multiple insertions and removals from the radiation source, any inhibitor or dissolved oxygen should be 'burnt up' and more reliable values of the slope and intercept are achievable. The approach can be used to consider 'relaxation' data (that is, removal from the radiation source until a new, reduced steady-state is reached) or 'approach' data (returning the sample to the radiation source and monitoring the increase in rate until the steady-state value is again obtained). These are illustrated in Figure 4.3. The only difference between approaches is that the value of $\overline{n}_0$ will be different depending on when $t = 0$ is taken from (i.e. removing or re-inserting the sample).

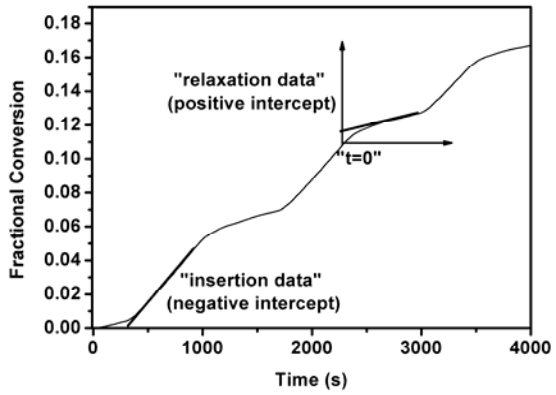

Figure 4.3. The Slope-And-Intercept Approach in γ-Initiated Experiments.

For comparative purposes, an electrostatically stabilized polystyrene latex (denoted ST0, as the 'hairs' on the surface are of DP = 0) was synthesized and the exit rate coefficient for this latex was compared to the values obtained for ST5, ST10 and ST20. Details of the latex synthesis are given in the Experimental section.

4.2. Experimental

Reagents. Styrene (Sigma Aldrich) was purified by passing the monomer through an inhibitor removal column (Sigma Aldrich) twice to remove inhibitor and other artefacts. Granular NaOH

(Sigma Aldrich) and potassium persulfate (KPS, Merck) were used as received. Sodium hydrogencarbonate (Sigma Aldrich) and the surfactants AMA-80 (Cytec Industries) and sodium dodecyl sulfate (SDS, Sigma Aldrich) were used as received. All water used in this work was high-purity deionized water (MilliQ).

Synthesis of Electrosterically Stabilized Latexes. The method used was as described previously in Chapter 3, using a variant of the 'RAFT-In-Emulsion[6, 7]' technique. This variation involved the synthesis of AA-*block*-styrene copolymers as macro-RAFT agents for the latex synthesis, where the AA (and styrene) block lengths were 5, 10 and 20 monomer units. These diblocks were synthesized in butanone (Sigma Aldrich) using the RAFT agent described in Chapter 3; synthesis took place using the V-501 initiator at 343 K.

The diblock solution (6.09 g, containing 1.79 g of diblock) was dried down in a vacuum oven overnight to remove butanone. Sodium hydroxide (0.39 g, 9.8 mmol) was dissolved in water (403 g), with the solution added to the vessel containing the dried diblock. Equimolar amounts of sodium hydroxide and carboxylic acid groups were used to partially ionize the diblock to assist dissolution.

V-501 (0.19 g, 0.6 mmol) was added to the solution and the mixture stirred magnetically while high-purity nitrogen was bubbled through the vessel. A temperature-controlled oil bath was preheated to 353 K and the vessel lowered into it with continual stirring, after which a small amount of deoxygenated styrene (0.55 g, 5.2 mmol) was introduced to the vessel by syringe. Using an electronically controlled feed pump, styrene (46.05 g, 0.44 mol) was added to the mixture via gas-tight syringe using the following feed profile: 1.13 g/h for the first two hours, followed by the remainder added at 10.58 g/h for the next four hours. After all the styrene had been added, further V-501 (0.19 g dissolved in 9.04 g water) was added to the latex and the polymerization left overnight in order to polymerize any remaining monomer. The resultant latex was filtered through glass wool to remove any residual coagulum.

Using the methodology described in Chapter 3, *tert*-butylhydroperoxide (TBHP) was used at elevated temperature to remove the RAFT functionality, after which extensive dialysis for two weeks took place.

Synthesis of Conventional Seed Latex (ST0). Sodium hydrogencarbonate (0.85 g, 10 mmol) and AMA-80 (8.48 g, 22 mmol) were added to water (405 g) and the resultant mixture was stirred magnetically to ensure complete dissolution. Deoxygenated styrene (49.8 g, 0.48 mol) was added to the reaction vessel and stirred vigorously to effect emulsification. High-purity nitrogen was bubbled through the emulsion to remove any dissolved oxygen for thirty minutes while the reaction vessel was brought to 363 K. KPS (0.88 g, 3.2 mmol) dissolved in water (5 mL) was introduced via syringe and polymerization took place for five hours. The resultant latex was filtered through glass wool and dialyzed for one week to remove any residual surfactant.

Gamma Relaxation Dilatometry. For each seed latex, the following methodology was employed for seeded kinetic studies:

Styrene (5 g, 48 mmol), Milli-Q water (17 g) and seed latex (10 g) were separately degassed under vacuum then loaded into a jacketed dilatometer vessel. SDS (0.005 g, 3.5 μmol) was added in order to stabilize monomer droplets, the dilatometer vessel sealed with a rubber septum and the headspace evacuated via syringe at room temperature. Magnetic stirring of the solution took place overnight to allow transfer of monomer to the particle interior and the mixture then heated to 323 K. Stirring was ceased and the reaction vessel evacuated again to remove dissolved oxygen.

A glass capillary (1.189 mm radius) was inserted into the top of the vessel, with water added until the solution was 10–12 cm up the capillary; stirring then recommenced. Dodecane (1 mL) was added to the top to prevent evaporation. Polymerization was initiated using a ^{60}Co γ source (dose rate = 105 Gy h^{-1}), available at the Australian Nuclear Science and Technology

Organization (ANSTO). The automated dilatometer was lowered into the radiation source until the polymerization rate reached a steady state, then removed from the source, allowing the rate decrease to be monitored. The meniscus height was tracked automatically to provide conversion/time data. Multiple insertions and relaxations took place per sample in order to obtain a large number of experimental values.

4.3. Results

4.3.1. Comparison of Rate Coefficient Values with Established Theory

A typical conversion-time plot from a γ-relaxation experiment involving multiple insertions into the radiation source is shown in Figure 4.4, with average rate coefficients (measured by a variety of different methods as described in the introduction; data from chemically initiated experiments however are omitted here) for the four different latexes in question listed in Table 4.1. Full details of the measured rate coefficients can be found in Appendix A2. The reliability of the approaches in arriving at similar values of the exit rate coefficient is shown graphically in Figure 4.5. Besides the ST20 latex and the extremely large error bar in the 'Slope-and-Intercept: Re-Insertion' method, the values are essentially consistent across the techniques used.

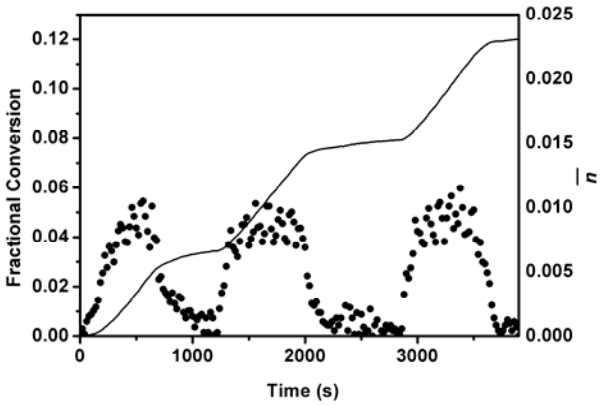

Figure 4.4. Example conversion-time (solid line) and $\bar{n}$ -time (dots) from a γ-relaxation experiment involving the ST5 latex, involving multiple insertions to maximize the amount of experimental data.

Table 4.1. Exit Rate Coefficients (*k*, Limit 2a kinetics) and Spontaneous Entry Rate Coefficients (ρ_{spont}) Measured By A Variety of Different Techniques (Units s^{-1})

Latex	Direct Data Fitting		Slope-Intercept (Relaxation)	Slope-Intercept (Re-Insertion)
	k	ρ_{spont}	k	k
ST0	$3.87 (\pm 0.52) \times 10^{-2}$	$2.2 (\pm 1.9) \times 10^{-5}$	$3.68 (\pm 0.41) \times 10^{-2}$	$3.49 (\pm 0.32) \times 10^{-2}$
ST5	$1.51 (\pm 0.58) \times 10^{-2}$	-	$2.06 (\pm 0.82) \times 10^{-2}$	$2.83 (\pm 0.38) \times 10^{-2}$
ST10	$5.14 (\pm 1.90) \times 10^{-3}$	-	$7.85 (\pm 2.66) \times 10^{-3}$	$1.45 (\pm 0.44) \times 10^{-3}$
ST20	$4.32 (\pm 2.07) \times 10^{-3}$	-	$6.64 (\pm 2.90) \times 10^{-3}$	$3.26 (\pm 2.03) \times 10^{-2}$

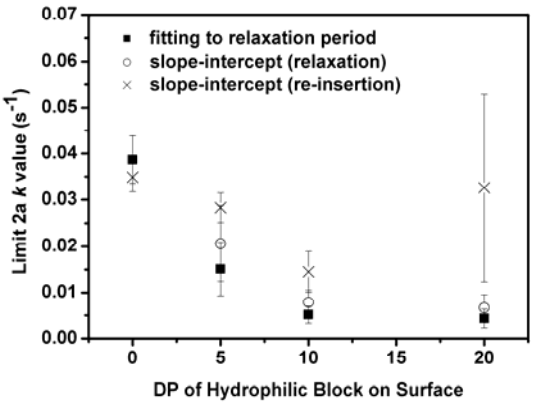

Figure 4.5. Graphical Comparison of Exit Rate Coefficient Values Obtained by Different Methods.

The first variation between the conventionally stabilized ST0 latex and the three electrosterically stabilized latexes in this study is that there was essentially no spontaneous ('thermal') entry measured when electrosteric stabilization was present. It is well known that there is a small, but measurable rate of polymerization in emulsion polymerizations in the absence of any added chemical initiator;[2] however the origins of this polymerization are unclear. As spontaneously generated radicals from the reaction involving the Diels-Alder dimer of two styrene molecules are unlikely to form[8] at the relatively low temperature of 323 K, the only likely source of spontaneously initiated polymerization is surface-generated peroxides formed during the seed latex synthesis.[2] While the spontaneous polymerization phenomenon is often dependent on latex preparation, it does seem striking that all three electrosterically stabilized latexes had no out-of-source polymerization rate in the relaxation experiments performed. This may be due to a number of reasons, one of which is that the presence of the polymeric layer grafted to the surface of the particle could prevent peroxides from forming on the surface, or that any oxy-centered radicals generated react with the polyAA chains on the surface, restricting entry of thermally generated radicals. However in order to have a more complete understanding of the thermal entry

mechanism, specifically designed experiments involving radical traps[2] must be employed. This was beyond the scope of this project.

The most important result from the γ-initiated experiments however is that there is a significant variation in the exit rate coefficient *k* between electrostatically and electrosterically stabilized latexes. Even with an extremely short hairy layer (of average length 5 AA units), a substantial decrease in the exit rate coefficient is observed, as seen in the much longer relaxation time for the ST5 latex (Figure 4.6). The experimentally determined value of *k* decreases with increasing hydrophilic block length, although the values for ST10 and ST20 differ only slightly (Figure 4.7). This decrease however is consistent with the postulate that the exit mechanism is restricted by the monomeric radical having to diffuse through a viscous polymeric layer on the surface of the particle. The fact that the *k* values for the three electrosterically stabilized latexes are substantially lower than that for ST0 also acts as another validation of the RAFT removal technique. It has been shown that for particles with RAFT concentrations as low as 1 mM that a ten-fold increase in the exit rate coefficient can occur,[9] so the decrease in *k* observed in this work indicates that the removal of the active RAFT end-groups was extremely successful.

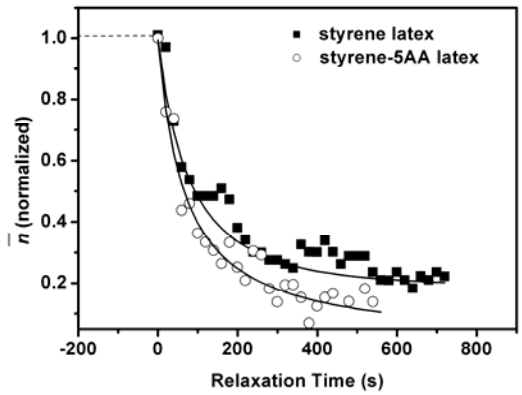

Figure 4.6. Normalized relaxation data (i.e. $\bar{n}/\bar{n}_0$ so that the relaxation data begins at a value of 1 for all latexes) comparing ST0 (solid squares) and ST5 (open circles) latexes. Solid lines shown are the least-squares fit, allowing k and $\rho_{thermal}$ to be calculated.

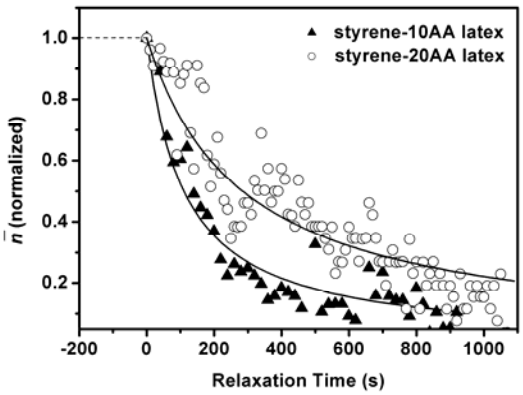

Figure 4.7. Normalized relaxation data (i.e. $\bar{n}/\bar{n}_0$ so that the relaxation data begins at a value of 1 for all latexes) comparing ST10 (solid triangles) and ST20 (open circles) latexes with least-squares fit.

One difficulty in comparing rate coefficients between latexes is that they are all of different average particle size (Figure 4.8). While it is easy to grow small, relatively monodisperse particle with polyAA stabilization using RAFT, there are currently no means to grow electrostatically

stabilized latexes of the same small size with low polydispersity due to long particle nucleation times. It is well known (see Chapter 2) that *k* possesses an inverse square dependence on swollen particle radius.[3] Thus, a means to take the particle size dependence into account is to divide the experimental *k* values by the Limit 2a predicted *k* value for that particle size. The results are given in Table 4.2. One sees that the same trend is observed with both the exit rate coefficient ratio and the exit rate coefficient – a significant decrease from ST0 to ST5, with only a slight decrease thereafter when the average hydrophilic block length is extended up to 10 and 20 units. The decrease by a factor of 10 is very large and indicative of the extent of the restriction of the exiting radical in electrosterically stabilized systems.

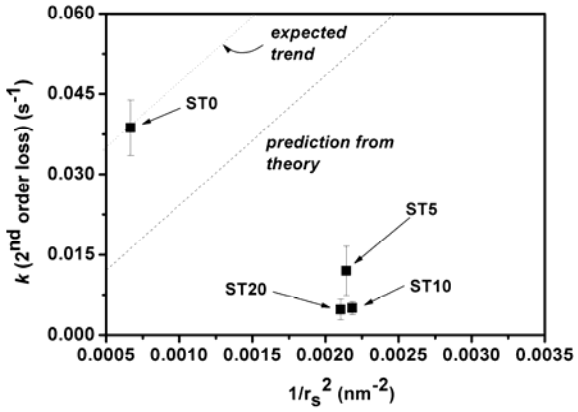

Figure 4.8. Experimental *k* values as a function of inverse square of the particle radius. Also shown is the predicted Limit 2a *k* values from accepted theory (dashed line) as well as the expected trend (dotted line) from the ST0 latex.

Table 4.2. Ratio of Experimental and Theoretical Limit 2a *k* Values.

Latex Type	k_{actual} / k_{theory}
ST0	2.3 ± 0.3
ST5	0.28 ± 0.11
ST10	0.11 ± 0.03
ST20	0.11 ± 0.04

As the behavior of these electrosterically stabilized latexes is so different to what is predicted for electrosterically stabilized latexes of the same size, it is pertinent to consider the use of other kinetic limits in the processing of γ-relaxation data for calculating *k*. In 'zero-one' systems, Limit 1 kinetics (complete termination of desorbed radicals in the aqueous phase) gives only a first-order dependence on $\overline{n}$ with respect to the radical loss mechanism. This is not implausible in these systems, as the re-entry rate may conceivably also be slowed significantly, to the point where termination of these radicals in the aqueous phase would be their most likely fate. The results for the calculated Limit 1 *k* values are shown in Table 4.3 as well as the theoretically expected values for these latexes.

Table 4.3. Experimentally Determined *k* Values Assuming Limit 1 Kinetics and Comparison With Predicted Values From Theory.

Latex	Experimental k (Limit 1) (s^{-1})	Theoretical k (Limit 1) (s^{-1})	k_{exp}: k_{theory}	Theoretical ratio
ST5	$(6.8 \pm 1.6) \times 10^{-3}$	2.7×10^{-2}	0.25 ± 0.06	0.38
ST10	$(5.1 \pm 1.7) \times 10^{-3}$	2.7×10^{-2}	0.19 ± 0.06	0.31
ST20	$(5.1 \pm 1.4) \times 10^{-3}$	2.7×10^{-2}	0.19 ± 0.05	0.24

As also seen in the Limit 2a regime, the values of k obtained by treating the data with Limit 1 kinetics are substantially lower than predicted by theory, with only a slow decrease at longer hydrophilic block lengths. While the actual values themselves differ, the same qualitative trend can be seen from the data.

4.3.2. The Origin of the Observed Effect

While extreme care was taken to prevent impurities and other external factors influencing the observed results, there are two obvious possibilities for sources of experimental contamination: residual TBHP (which can function as a chain transfer agent[10]) and RAFT oxidation by-products, both of which could potentially alter the measured k values. In order to confirm that the reduced k values for the three electrosterically stabilized latexes was due to the 'hairy layer' and not contaminants, two separate experiments were performed with ST0 – an electrostatically stabilized latex. If any change in the behaviour of this 'normal' latex (i.e., without a hairy layer) was seen after contaminating the latex with either TBHP or RAFT oxidation by-products, it could be claimed that the effect seen was not due to the stabilizing 'hairs.'

To determine the impact of residual TBHP, a sample of ST0 was doped with a small amount of TBHP until a concentration of approximately 2 ppm was reached (the same concentration of hydroperoxide measured in the three electrosterically stabilized latexes after two weeks of dialysis following the oxidation reaction). The exit rate coefficient k and ρ_{spont} were measured for this latex using the γ-relaxation technique described previously, with multiple insertions into the radiation source to provide a set of experimental values. As seen in Figure 4.9, essentially the same values for k and ρ_{spont} were measured (within experimental error) for ST0 in the presence of 2 ppm TBHP, clearly indicating that residual TBHP is not the cause of the reduced k values in the three electrosterically stabilized systems. Significantly, the presence of TBHP (which is moderately water-soluble) did not lead to the absence of a spontaneous out-of-source polymerization rate.

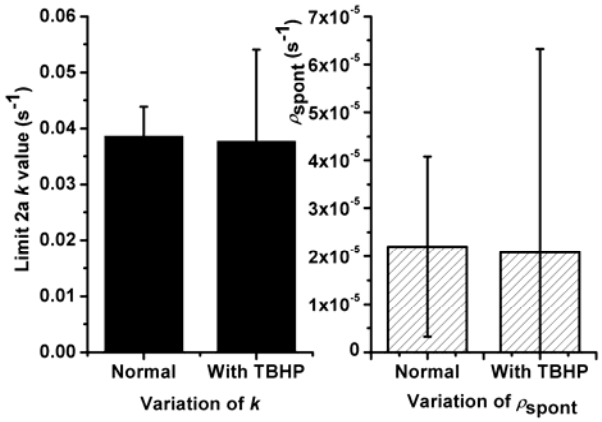

Figure 4.9. Comparison of experimental k and ρ_{spont} values for ST0 latex with no added TBHP (solid columns) vs 2ppm TBHP (shaded columns).

In order to determine the significance of by-products formed during the RAFT removal process, the 'acetone transport' technique developed by Prescott *et al.*[11] was utilized to transport the dodecyl analog of the RAFT agent (where a dodecyl group is present rather than the more water-soluble butyl group, used so that no RAFT agent will reside in the aqueous phase) into the interior of the particle. 30 mg of the dodecyl RAFT agent was added to a 2:1 mixture of

acetone:ST0 and was stirred at room temperature for 72 h with the organic co-solvent allowing the transfer of the RAFT agent into the particle. The acetone was subsequently removed by a rotary evaporator (308 K for 1 h) and the remaining latex was subjected to an identical RAFT removal treatment (2 % w/w TBHP added with heating and stirring for 24 h at 353 K) to that employed for the electrosteric latexes. After two weeks of dialysis, both k and ρ_{spont} were measured via a series of γ-relaxation experiments. In an unexpected result, the stability of ST0 during the RAFT removal procedure was poor, unlike the three electrosterically stabilized latexes studied which demonstrated no coagulation during this process. A significant increase in particle size (the swollen radius measured by HDC increased from 39.7 nm to 79.3 nm) was seen and this was most likely due to coalescence of particles under an extended period at elevated temperature in the absence of added surfactant. Not only does the value of the exit rate coefficient k vary with particle size[3] making comparisons difficult, but the applicability of the appropriate kinetic limit is brought into question,[5] as the kinetic behavior may no longer be able to be classified as 'zero-one.'

Assuming that Limit 2a 'zero-one' kinetics is still applicable for these larger latex particles, the average experimental k value obtained follows the expected $1/r_s^2$ proportionality relative to the untreated ST0 latex (Figure 4.10). Although the choice of kinetic limit is debatable in this case, the fact that while working within the same limit there is not a dramatic increase or decrease in k allows us to safely say that the observed experimental variation is due to the hairs on the particle surface and not to any by-products formed during the RAFT removal. There was a clearly measurable 'spontaneous' polymerization rate for this latex (with $\rho_{spont} \approx 10^{-4}$ s^{-1}), which also suggests that the absence of ρ_{spont} in the electrosteric latexes is due to the presence of the hairs on the surface.

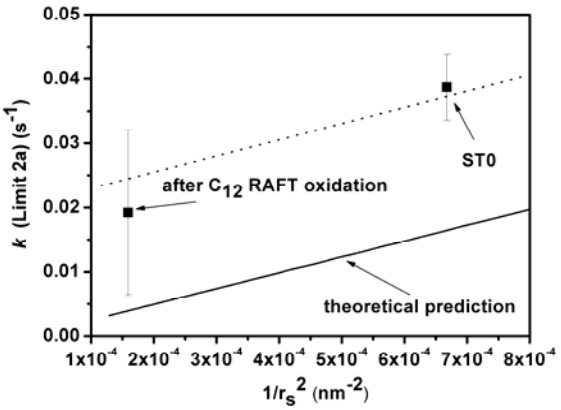

Figure 4.10. Experimental *k* values for ST0 latex before and after RAFT oxidation treatment as a function of r_s^{-2} (nm^{-2}); also shown are theoretical values (solid line) and expected trend (dashes).

4.3.3. Restricted Diffusion: A Model to Explain Observed Behaviour

Both *ab initio*[12] and seeded[13, 14] kinetic studies on electrosterically stabilized latexes have suggested that diffusion through the polymeric layer on the surface has a significant impact on the interfacial mechanistic events that control the rate of an emulsion polymerization. While the importance of charge effects is well accepted when the polymeric hairs can be ionized and interact with a charged molecule, this work has shown that there is a significant restriction for an uncharged monomeric radical exiting a particle. This is in agreement with the modeling work of Asua,[15] whose calculations suggested that if the diffusion of an exiting species is slowed, the value of the exit rate coefficient can decrease significantly: a significant 'steric' or diffusion effect imparted by the stabilizing layer.

The currently accepted model for exit is transfer of radical activity to monomer, followed by diffusion of the radical out into the aqueous phase with rate coefficient k_{dM}. For conventional emulsion systems, the mathematical modeling for k_{dM} is achieved by assuming the microscopic reversibility of the diffusion controlled adsorption reaction (rate coefficient k_{ads}) onto a particle.[3]

For diffusion-controlled reactions such as this, the rate coefficient is given by the Smoluchowski equation:

$$k_{ads} = 4\,\pi\,D_w\,r_s\,N_A \tag{4.3}$$

The reversibility of adsorption and desorption allows a mathematical description for k_{dM} to be obtained, which is repeated here for convenience:

$$k_{dM} = \frac{3\,D_w}{r_s^2}\frac{C_w}{C_p} \tag{4.4}$$

For particles with electrosteric stabilization, a modified version of the Smoluchowski equation is required to account for the fact that a given species has a different diffusion coefficient in the polymeric layer to that in the aqueous phase. The following simple treatment has similarities to the much more complex description derived by Asua.[15] A pictorial representation is given in Figure 4.11; a particle of swollen radius r_s with polymeric layer of fixed width δ, with differing diffusion coefficients for a monomeric species through both the aqueous phase (D_w) and the polymeric hairy layer (D_h). Assuming appropriate boundary conditions (with the derivation given in Appendix A3), the expression for k_{ads} in this case is given by

$$k_{ads} = 4\pi\left(\frac{r_s\,(r_s+\delta)}{\delta + r_s(D_h/D_w)}\right)D_h\,N_A \tag{4.5}$$

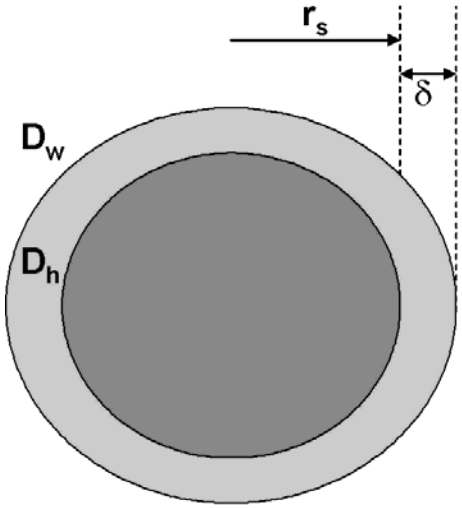

Figure 4.11. Model for adsorption/desorption of a monomeric radical onto electrosterically stabilized particles. Surrounding the particle of swollen radius r_s is a 'hairy layer' of fixed width δ, with two separate diffusion coefficients: through the aqueous phase (D_w) as well as through the hairy layer (D_h)

Assuming the reversibility of adsorption and desorption, we have a new expression for k_{dM}, which is:

$$k_{dM} = 3D_h \frac{C_w}{C_p}\left(\frac{r_s + \delta}{r_s^2\,(\delta + r_s(D_h/D_w))}\right) \tag{4.6}$$

This is subsequently used in the Limit 2a expression for the overall exit rate coefficient k. Equation 4.6 reduces to Equation 4.5 when $\delta = 0$.

To compare the 'restricted diffusion' model to experimental results, appropriate, realistic values for the parameters present in Equation 4.6 must be determined. Values such as $C_w = 4.3 \times 10^{-3}$ M (the saturation concentration of styrene in water at 323 K) and $D_w = 1.3 \times 10^{-9}$ m^2 s^{-1} (the diffusion coefficient of a styrene monomer unit in water) are well accepted;[4] estimation of δ and D_h are both non-trivial yet crucial to the accuracy of the exit model.

The estimation of δ (the width of the hairy layer) is complex. No reliable data exists for this property for such short chains and theory (especially for a system such as this where the chain concentration is not in the dilute region) is not yet sufficiently reliable (as presented in the review by Dobrynin and Rubenstein[16]). In this work a number of assumptions are made to estimate this width. Firstly, it is assumed that every chain in the hairy layer is of identical length of 5, 10 or 20 units. This is obviously not true given that a narrow distribution exists around the target average chain length from the RAFT polymerization technique and that chain burial within the particle can occur.[6] However, it will serve as an effective approximation in this work. Using an appropriate chain extension factor (C_∞) for water-soluble polymer chains of 6.7[17] and assuming that the chain dimensions of tethered chains are 15-30% larger than free chains,[18] the radius of gyration of the polyAA chains and hence the hairy layer width can be easily calculated. The values of δ are reported in Table 4.4.

Table 4.4. Parameters Used in 'Restricted Diffusion' Exit Model

Parameter	Value
D_w	1.3×10^{-9} m^2 s^{-1}
D_h	2.4×10^{-11} m^2 s^{-1}
C_w	4.3×10^{-3} M
C_p	6 M
k_{tr}	9.3×10^{-3} M^{-1} s^{-1}
k_p	260 M^{-1} s^{-1}
k_p^1	4 k_p^1
δ (ST5)	1.18 nm
δ (ST10)	1.67 nm
δ (ST20)	2.37 nm

The estimation of D_h (the diffusion coefficient of a styrene radical/monomer unit through the polymeric layer) is complicated as no experimental data exist in this area. Diffusion coefficients of monomeric and oligomeric species in polymer solutions, however, can be determined using

Pulsed-Field Gradient NMR (PFG-NMR).[19] The PFG-NMR experiments of Strauch *et al.*[20] involved diffusion of a strongly hydrogen-bonded, water-soluble monomer (hydroxyethyl methacrylate (HEMA)) in an aqueous solution of its polymer. However, the diffusion coefficient values from this work are not entirely appropriate in the present work, as the hydrophobicities of our monomer (styrene) and polymer (polyAA) are totally different and this is likely to impact on the rate of diffusion.

The most applicable data for these systems comes from the work of Yamane *et al.*[21] where spatial inhomogeneities in polyAA gels were detected by measuring the diffusion coefficient of probe molecules (poly(ethylene glycol) (PEG) standards) by PFG-NMR. The lightly cross-linked gels in this work are of similar weight fraction polymer (w_p) (30%) to the surface coverage of our electrosterically stabilized latexes (approximately 40 ± 10 % of the particle surface covered, calculated by surfactant titration). However, the average w_p value within the whole hairy layer is significantly lower than the amount of surface that is covered due to the presence of water around the hydrophilic polymer chains. The average w_p in the whole hairy layer was estimated as ~5% for all three latexes. This was found by calculating the mass of polyAA on each particle surface (i.e. the number (moles) of AA units per chain multiplied by the average number of chains per particle (Table 4.5), converted into mass) as well as the volume of the hairy layer shell around the particle. This is calculated by the following relation:

$$w_p = \frac{\overline{X}_n(\mathrm{AA})\, n_{chains} \frac{m_{AA}}{N_{av}}}{\frac{4}{3}\pi \left((r_s + \delta)^3 - r_s^3 \right) d_{water}} \qquad (4.7)$$

where $\overline{X}_n(\mathrm{AA})$ = number-average degree of polymerization of the AA units per chain, n_{chains} = number of chains per particle, m_{AA} = molar mass of acrylic acid and d_{water} = density of water.

Table 4.5. Average Number of RAFT-Capped Chains Per Particle.

Latex	RAFT Chains/Particle
ST5	220
ST10	232
ST20	288

Using the conditions most similar to within the 'hairy layer' as a reference point, a value of $D = 4.4 \times 10^{-13}$ m^2 s^{-1} was reported[21] for the PEG probe molecule, which was a short chain polymer with $\bar{M}_n = 1500$ Da. The corresponding degree of polymerization is 25, and this species will diffuse far slower than a monomeric unit. Using the well-tested empirical diffusion scaling law,[22] namely

$$D_i = \frac{D_{mon}}{i^{0.66+ 2w_p}} \tag{4.8}$$

where i is the degree of polymerization of the oligomer in question. This yields a value of $D_{mon} = 2.5 \times 10^{-11}$ m^2 s^{-1}, approximately 50 times lower than D_w. This is the value applicable at the w_p of the systems used in the work of Yamane *et al.*,[21] approximately 0.3. This quantity must be converted to a value applicable for the wp estimated for the hairy layer, viz., 0.05. For this purpose, the diffusion coefficient was scaled by the ratio of diffusion coefficients predicted for the same values of w_p using the free-volume fitting of HEMA diffusion data by Strauch *et al.,*[20] which yields $D_{mon} = 7.3 \times 10^{-11}$ m^2 s^{-1}. Using this value of D_{mon} to represent D_h in our model, the comparison between the model and experimental data points is given in Figure 4.12. It can be seen that the observed trend with $\bar{X}_n$(AA) is reproduced acceptably, but not the absolute values.

Given the many uncertainties involved in this estimation of D_h, it was deemed acceptable to adjust its value somewhat and it was found (see Figure 4.12) that decreasing this by a factor of 3 (considered to be reasonable given the experimental uncertainty in the parameters in question) gives good absolute agreement with the data. Using the same value of D_h, Limit 1 k values (Table 4.3) can also be predicted via this model. Once again the same excellent agreement between experiment and theory is seen, and while the actual fate of exited radicals (i.e., whether the system obeys Limit 1 or Limit 2a kinetics) cannot yet be elucidated, the same effect on both approaches is seen.

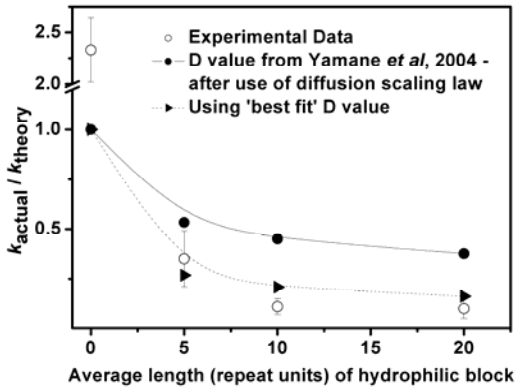

Figure 4.12. Comparison of experimental *k* ratio data (open circles) with new diffusion model (filled circles, using diffusion coefficients from Yamane *et al.*, 2004) and filled triangles ('best fit' diffusion coefficient value).

As can be seen in Figure 4.12, increasing the estimated value of D_h naturally increases the experimental k value for our electrosterically stabilized latexes (as the diffusion through the polymeric layer is faster). While the agreement with experimental results is not as good with this new D_h value, the same trend is seen between both the experimental and the theoretical approach. Taking into consideration that there is significant uncertainty in estimating D_h, it is felt that the mathematical model developed in this work is able to rationalize and semi-quantitatively predict exit rate coefficient values for electrosterically stabilized latex particles. Quantitative

prediction must await better experimental data and theory for both the spatial extent (and inhomogeneity therein) of the hairy layer, and of diffusion coefficients of appropriate species in this semi-dilute aqueous polymer solution.

The results presented here suggest that, even for a monomeric species, diffusion through a polymeric 'hairy layer' is strongly restricted and a major influence on exit kinetics is seen as a result. With the information available at the time, it is anticipated that these electrosterically stabilized latexes exhibit 'expected' kinetics for styrene-based systems, albeit with the added consideration of a restricted diffusion step at the particle surface.

4.3.4. Comparison with Other Exit Models

A first-principles model for radical desorption kinetics has been developed by Asua[15] that incorporates the effect due to the presence of a layer of steric surfactant on the surface of the particle. Similar to the model presented in this Chapter, the model presented by Asua requires parameters such as the width of the hairy layer and the diffusion coefficient of the desorbed monomeric radical through this layer, making comparison between the two models of high interest. Asua's treatment yields an expression for the rate coefficient for radical desorption. The use of a zero-one system enables such a rate coefficient to be related to the experimental observable; that is, the rate of radical loss with a minimum of model-based assumptions. The model developed by Asua is essentially 'assumption free' – there is no assumption of 'zero-one' kinetics or that the rate determining step for radical loss is exit (i.e. Limit 2a within the zero-one regime). As the model developed in this work is constructed using the definition for k assuming Limit 2a kinetics (i.e. assuming that radical loss is second order with respect to $\overline{n}$ as a desorbed radical enters another particle and either propagates or is terminated, Equation 2.20), the k values obtained from the two approaches are likely to be significantly different. While it is impossible to refute or support proposed mechanisms using this purely theoretical approach as there are more adjustable parameters than unambiguous pieces of experimental data (unlike the use of the

simple kinetic limits, 'zero-one' in the present case, that can be fitted to experiment), it is nonetheless an interesting exercise to compare the two approaches.

The rate coefficient expression for radical desorption presented by Asua is:

$$k = \lambda \frac{\gamma N_A}{\eta m}\left(1 - \frac{\lambda N_p}{\lambda N_p + k_p C_w + 2\, k_t [R]_w}\right) \tag{4.9}$$

where

$$\eta = \frac{k_p C_p}{D_p} \tag{4.10}$$

$$\gamma = \frac{\frac{k_{tr} C_p}{V_s N_A}}{D_p} \tag{4.11}$$

$$\lambda = \frac{4\,\pi\, D_w r_s}{1 + \frac{D_w}{D_h}\frac{\delta}{r_s} + \frac{D_w}{D_p m}\frac{1}{r_s\sqrt{\eta}\coth(r_s\sqrt{\eta}) - 1}} \tag{4.12}$$

where D_p is the diffusion coefficient of a monomeric radical inside a latex particle, V_s the swollen volume of a latex particle, k_t the bimolecular termination rate coefficient in the aqueous phase, $[R]_w$ the concentration of radicals in the aqueous phase and m the partition coefficient relating the concentration of monomeric radicals at either side of the particle/hairy layer interface.[15] All other parameters are the same as identified previously.

As pointed out by a number of authors (e.g. Gilbert *et al.*[3, 23] and Asua[15]), the definition of an exit (or desorption) rate coefficient is often ambiguous because this definition depends on the fate of exited free radicals (especially in the aqueous phase) and whether or not the definition counts as

'true' exit when an exited monomeric radical re-enters another particle and continues polymerization without loss of radical activity. The great advantage of the treatment of emulsion polymerization kinetics as two limiting cases (zero-one and pseudo-bulk and the subdivision of the former into various limits, i.e. Limit 1 and Limit 2a) is that this definition is quite unambiguous and that the exit rate coefficient can be obtained uniquely from experiment without any model assumptions except as to which limit is involved This in turn can usually be deduced from simple order-of-magnitude estimates of various rate coefficients.[4, 5] This is quite a different point of view from that of Asua, whose approach gives a very detailed quantitative mechanistic description for radical exit. On the other hand, this description does not permit direct comparison between model and experiment, because the model contains many parameters whose values are hard to determine with sufficient precision.

This model predicts a significant decrease in k is seen when D_h is decreased, all other parameters being constant. This is consistent with the experimental trend seen in this work (as a densely covered particle surface restricts the diffusion of the monomeric radical). Because (as just stated) it is impossible to make an unambiguous direct comparison with experiment without choosing values of rate parameters that cannot be accurately determined by independent experiment, this comparison was carried out by choosing what was felt to be the best available values.

Using the parameters quoted in Table 4.46.1 as well as $D_p = 2 \times 10^{-10}$ m^2 s^{-1},[15] $m = 70$ [15] and $k_t = 1.75 \times 10^9$ M^{-1} s^{-1},[5] the variation of k from Equation 4.9 as a function of D_h is shown in Figure 4.13 for the three electrosterically stabilized latexes in question. In choosing the various parameter values, a value of $[R]_w = 3 \times 10^{-9}$ M was chosen so that the k values from Equation 2.21 (the Limit 2a exit rate coefficient expression) and Equation 4.9 were in agreement for latexes of this size with no hairy layer. It is noted that $[R]_w$ will vary with each system and indeed with the time evolution of the radiolysis system as it is removed from the source but decreasing this quantity by an order of magnitude only changes the calculated value of k by 30

%. As expected, there is a slight (calculated) decrease in k as the width of the hairy layer is increased (although this decrease does not hold for all values of D_h due to the slightly different N_p values). The experimentally determined k values for ST5, ST10 and ST20 are also shown in Figure 4.13 at the 'best' value for D_h used in the modeling work discussed earlier ($D_h = 2.42 \times 10^{-11}$ m^2 s^{-1}). The experimental values show the same decrease in k as the width of the hairy layer increases; however the k values are far lower than predicted by Asua's model. The reason for the discrepancy cannot be ascertained at present because, as stated, the model contains parameters whose values have not been determined independently. One means of comparison would be to analyze latexes with different surface coverages (and hence different D_h values) to see the predictive behavior of both models. One can conclude, however, that the diffusion coefficient of a monomeric radical within this hairy layer is greatly reduced relative to the aqueous phase and this is reflected in both theoretical exit models.

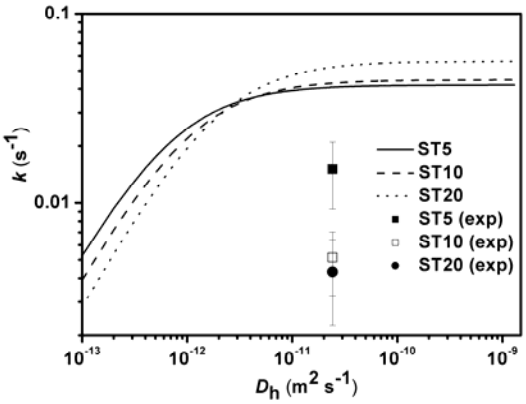

Figure 4.13. Experimental *k* values for electrosterically stabilized latexes with comparison to theoretical desorption model developed by Asua, *Macromolecules*, 2003. Solid line, filled square = ST5 ($N_p = 3.22 \times 10^{18}$ L^{-1}), dashed line and open square = ST10 ($N_p = 3.2 \times 10^{18}$ L^{-1}), dotted line and filled circle = ST20 ($N_p = 2.4 \times 10^{18}$ L^{-1}).

4.4. Conclusions

In this Chapter, the results from kinetic experiments specifically designed to measure the exit rate coefficient were presented for model electrosterically stabilized poly(styrene) latexes with known and well-characterized hydrophilic blocks of polyAA on the particle surface. The aim of this was to study (for the first time) the effect of the stabilizing block length on the behaviour of the exit rate coefficient. The results from an electrostatically stabilized poly(styrene) latex were also presented for comparative purposes and to test the well accepted 'transfer-diffusion' exit mechanism.

It was shown that even short 'hairs' (e.g. of degree of polymerization = 5) led to a substantial decrease in the exit rate coefficient relative to an electrostatically stabilized system, with k decreasing as a function of hairy layer width. This decrease is consistent with the occurrence of a diffusion-controlled process whereby the exiting monomeric radical is strongly restricted from exiting a particle. The value of the 'spontaneous' entry rate coefficient was found to be negligible for these electrosterically stabilized systems, which may be attributable to 'spontaneously' formed radicals (perhaps from peroxides formed during the seed latex preparation process) being trapped by or reacting with the polyAA hairs on the surface of the particle.

Through a modification of the Smoluchowski equation for diffusion-controlled reactions in solution (with some of the same starting points as the more complex work of Asua), a quantitative description for the rate coefficient for desorption (k_{dM}) of a monomeric radical in this system was deduced, giving the quantitative dependences of the loss rate coefficient on both the width of the hairy layer and the diffusion coefficient of a radical within the hairy layer. Based on estimates from data where diffusion coefficients of probe molecules within lightly cross-linked polyAA gels were measured, the diffusion coefficient of a monomeric radical within our polymeric layer was estimated to be approximately 50 times lower than in water. This value gave

semi-quantitative agreement with experimentally obtained values, and a good reproduction of the observed trend with the degree of polymerization in the hairs, consistent with the postulate that the exit of a monomeric radical from a particle in these systems is restricted by the dense polymeric layer on the particle surface.

It is emphasized that consistency with the 'restricted diffusion' mechanism does not prove this mechanism is dominant, and indeed the observations of the present chapter will be later seen to be similarly consistent with changes brought about by another effect, the occurrence of rapid chain transfer and the presence of mid-chain radicals.

References

1. Lansdowne, S. W.; Gilbert, R. G.; Napper, D. H.; Sangster, D. F. *Journal of the Chemical Society, Faraday Transactions 1: Physical Chemistry in Condensed Phases* **1980,** 76, 1344-55.

2. Christie, D. I.; Gilbert, R. G.; Congalidis, J. P.; Richards, J. R.; McMinn, J. H. *Macromolecules* **2001,** 34, 5158-5168.

3. Gilbert, R. G., *Emulsion Polymerisation: A Mechanistic Approach*. Academic Press: San Diego, 1995.

4. Casey, B. S.; Morrison, B. R.; Maxwell, I. A.; Gilbert, R. G.; Napper, D. H. *Journal of Polymer Science, Part A: Polymer Chemistry* **1994,** 32, 605-630.

5. Morrison, B. R.; Casey, B. S.; Lacik, I.; Leslie, G. L.; Sangster, D. F.; Gilbert, R. G.; Napper, D. H. *Journal of Polymer Science, Part A: Polymer Chemistry* **1994,** 32, 631-49.

6. Ferguson, C. J.; Hughes, R. J.; Nguyen, D.; Pham, B. T. T.; Gilbert, R. G.; Serelis, A. K.; Such, C. H.; Hawkett, B. S. *Macromolecules* **2005,** 38, 2191-2204.

7. Ferguson, C. J.; Hughes, R. J.; Pham, B. T. T.; Hawkett, B. S.; Gilbert, R. G.; Serelis, A. K.; Such, C. H. *Macromolecules* **2002,** 35, 9243-9245.

8. Olaj, O. F.; Kauffmann, H. F.; Breitenbach, J. W. *Makromolekulare Chemie* **1977,** 178, 2707-17.

9. Prescott, S. W.; Ballard, M. J.; Rizzardo, E.; Gilbert, R. G. *Macromolecules* **2005,** 38, 4901-4912.

10. Odian, G., *Principles of Polymerization*. 4th ed.; Wiley Interscience: 2004.

11. Prescott, S. W.; Ballard, M. J.; Rizzardo, E.; Gilbert, R. G. *Macromolecules* **2002,** 35, 5417-5425.

12. Leemans, L.; Jerome, R.; Teyssie, P. *Macromolecules* **1998,** 31, 5565-5571.

13. Vorwerg, L.; Gilbert, R. G. *Macromolecules* **2000,** 33, 6693-6703.

14. Coen, E. M.; Lyons, R. A.; Gilbert, R. G. *Macromolecules* **1996,** 29, 5128-5135.

15. Asua, J. M. *Macromolecules* **2003,** 36, 6245-6251.

16. Dobrynin, A. V.; Rubinstein, M. *Progress in Polymer Science* **2005,** 30, 1049-1118.

17. De Bruyn, H.; Gilbert, R. G.; White, J. W.; Schulz, J. C. *Polymer* **2003,** 44, 4411-4420.

18. Feigin, R. I.; Napper, D. H. *Colloid and Polymer Science* **1980,** 258, 1153-8.

19. Callaghan, P. T. *Australian Journal of Physics* **1984,** 37, 359-87.

20. Strauch, J.; McDonald, J.; Chapman, B. E.; Kuchel, P. W.; Hawkett, B. S.; Roberts, G. E.; Tonge, M. P.; Gilbert, R. G. *Journal of Polymer Science, Part A: Polymer Chemistry* **2003,** 41, 2491-2501.

21. Yamane, Y.; Ando, I.; Buchholz, F. L.; Reinhardt, A. R.; Schlick, S. *Macromolecules* **2004,** 37, 9841-9849.

22. Griffiths, M. C.; Strauch, J.; Monteiro, M. J.; Gilbert, R. G. *Macromolecules* **1998,** 31, 7835-7844.

23. Whang, B. C. Y.; Napper, D. H.; Ballard, M. J.; Gilbert, R. G.; Lichti, G. *Journal of the Chemical Society, Faraday Transactions 1: Physical Chemistry in Condensed Phases* **1982,** 78, 1117.

5. Radical Entry in Electrosterically Stabilized Systems

Sections of the work presented in this Chapter have previously been published as:

Thickett, S.C and Gilbert, R.G. *Mechanism of Radical Entry in Electrosterically Stabilized Emulsion Polymerization Systems,* Macromolecules, **2006**, 39, 6495-6504.

Thickett, S.C., Gaborieau, M. and Gilbert, R.G. *Extended Mechanistic Description of Particle Growth in Electrosterically Stabilized Emulsion Polymerization Systems,* Macromolecules, **2007**, 40, 4710-4720.

"If something comes to life in others because of you, then you have made an approach to immortality."

Norman Cousins

5.1. Introduction

In this Chapter, the results from chemically initiated dilatometric experiments are presented, with a view to determining the entry rate coefficient (ρ) and the entry efficiency (f_{entry}) for the model electrosterically stabilized latexes synthesized previously. Entry rate coefficients in this work are examined as a function of the length of the stabilizing block on the particle surface (the average DP of the stabilizing blocks were 5, 10 and 20 units of AA respectively) as well as the charge on the initiating radical; three different chemical initiators were used in this work, bearing a positive, negative and neutral charge. It was anticipated that charge effects may be significant, especially as the poly(acrylic acid) (polyAA) blocks on the particle surface are completely ionized.

Given the wealth of knowledge and supporting evidence developed since the 'control by aqueous phase growth' mechanism[1] was first presented, the results of these experiments are viewed to be the first rigorous test of this mechanism with respect to electrosterically stabilized latexes. As the results for the radical exit process were shown to be significantly different to 'predicted' kinetics in the previous Chapter, one would anticipate that the results for radical entry would demonstrate a similar variation.

5.1.5. Determination of Entry Rate Coefficients in This Work

This work on radical entry follows the work on radical exit because the value of the exit rate coefficient k is required to determine an accurate value of the entry rate coefficient ρ. As outlined in Chapter 2, use of the steady-state rate from chemically initiated dilatometric experiments alone means that both rate coefficients must be obtained from 'slope-and-intercept' data, which is susceptible to large errors.[2, 3] Through γ-relaxation experiments[4] an independent k value can be determined, allowing more accurate determination of entry rate coefficient values

(as the steady-state rate (and consequently the steady-state average number of radicals per particle, $\bar{n}_{ss}$) can be determined extremely accurately) from the following expressions:

$$\rho = \frac{k_{ct}\,\bar{n}_{ss}}{(1 - 2\,\bar{n}_{ss})}\ \text{(Limit 1 kinetics)};\quad \rho = \frac{2\,k_{cr}\,\bar{n}_{ss}^{\,2}}{(1 - 2\,\bar{n}_{ss})}\ \text{(Limit 2a kinetics)} \tag{5.1}$$

where once again it is assumed that these systems obey 'zero-one' kinetics (i.e. that the particles are below a critical size whereby two radicals in one particle will result in 'instantaneous' termination[5]). The value of f_{entry} is then simply determined by considering the ratio of ρ to $\rho_{100\,\%}$ (i.e. the entry rate coefficient assuming that all initiator-derived radicals lead to an entry event), which is given by:

$$f_{entry} = \frac{\rho}{2\,k_d\,[I]\,\dfrac{N_A}{N_p}} \tag{5.2}$$

where k_d is the decomposition rate coefficient of the initiator (units s^{-1}), N_p is the particle number of the seed latex (L^{-1}), [I] the initiator concentration (M) and N_A is Avogadro's constant. Presentation of data as f_{entry} vs. radical flux removes the complication of latexes with different N_p values and initiators with different decomposition rates.

5.2. Experimental

Reagents. Acrylic acid (AA) (Sumika), toluene (Sigma Aldrich) and dodecanethiol (Sigma Aldrich) were purified by vacuum distillation to remove any polymerization inhibitors. Styrene (Sigma Aldrich) was purified by passing the monomer through an inhibitor removal column (Sigma Aldrich) twice to remove inhibitor and other extraneous species. The initiators 4,4′-azobis(4-cyanopentanoic acid) (V-501, Wako Industries), 2,2'-Azobis(2-methylpropionamide) dihydrochloride (V50, Wako Industries), 2,2'-Azobis[2-methyl-N-(2-hydroxyethyl)propionamide] (VA-086, Wako Industries) and potassium persulfate (KPS, Merck)

were used as received. Azobisisobutylonitrile (AIBN, Sigma Aldrich) was recrystallized in hexane prior to use. Sodium dodecyl sulfate (SDS, Sigma Aldrich) and sodium hydroxide (NaOH, Sigma Aldrich) were used as received. Deuterium oxide D_2O (99.9 %) was purchased from Cambridge Isotope Laboratories Inc. All water used in this work was high-purity deionized water (MilliQ). Latexes ST0, ST5, ST10 and ST20 were synthesized as reported in previous Chapters.

Chemically Initiated Dilatometry. For each seed latex, the following methodology was employed for seeded kinetic studies:

Styrene (5 g, 48 mmol), Milli-Q water (17 g) and seed latex (10 g) were separately degassed under vacuum then loaded into a jacketed dilatometer vessel. SDS (0.005 g, 3.5 μmol) was added in order to stabilize monomer droplets. The dilatometer vessel sealed with a rubber septum and the headspace evacuated via syringe at room temperature. Magnetic stirring of the solution took place overnight to allow transfer of monomer to the particle interior and the mixture then heated to 323 K. Stirring was ceased and the reaction vessel evacuated again to remove dissolved oxygen.

In a separate vessel an aqueous initiator solution was prepared – the three initiators used here being KPS (negatively charged radical), VA-086 (neutral radical) and V-50 (positive radical). The initiator solution was de-gassed under vacuum and heated to reaction temperature; 2 mL of the solution was then added to the dilatometry vessel via a syringe. Typical initiator concentrations ranged from 0.1 to 10 mM, with the aim to keep the same radical flux between initiators.

Upon addition of the initiator solution a glass capillary (1.51 mm radius) was inserted into the top of the vessel. The capillary was filled with water; stirring was then recommenced. Dodecane (1 mL) was added to the top of the water to provide a smooth meniscus and to prevent

evaporation. The meniscus height was monitored automatically using a LED 'tracker' to provide conversion/time data. The resultant latex was checked for secondary nucleation via HDC to ensure the validity of the kinetic analysis. Results from these chemically initiated experiments are given in full in Appendix A4.

Synthesis of Acrylic Acid Oligomers. Oligomers of AA were synthesized using a variation of the precipitation polymerization procedure reported by Doherty *et al*.[6] AA (1.13 g, 15.6 mmol) was polymerized in the presence of dodecanethiol (3.64 g, 18 mmol) in toluene (15.3 g) for 24 hours at 323 K. The initiator was azobisisobutylonitrile (AIBN, 0.062 g, 0.4 mmol), chosen specifically as it has a low initiator transfer constant.[7] The target molecular weight was approximately 1000 Da, i.e. short chains to model the oligomeric 'hairs' on the particle surface. Conversion was measured by gravimetry and was ≈ 100%. The solvent was removed and the polymer washed twice with hexane to remove any impurities. A variation of this above recipe was also performed to synthesize a polyAA sample of much higher molecular weight, with more AA (2 g, 28 mmol) used in the presence of less chain transfer agent (0.22 g dodecanethiol, 1 mmol).

Bulk Chain-Transfer Experiments. Experiments to determine the extent of chain transfer of styrene with polyAA as the 'chain transfer agent' was achieved by polymerizing bulk styrene in the presence of different amounts of the synthesized oligoAA; the molar ratios of pAA to styrene used were 0, 0.01, 0.05 and 0.48. An identical experiment was performed using the longer chain polyAA at a [polyAA]:[styrene] ratio of 0.1. AIBN was once again the initiator; 0.01 g was used for every 2 g of styrene. Polymerization took place at 323 K under continuous magnetic stirring for 1 h; the fractional conversion was low (less than 3% in all experiments), with the samples quenched after 1 h with a 0.05% hydroquinone solution to prevent any subsequent polymerization. The MWD of the formed polystyrene, as well as any modifications to the MWD of the original pAA, was measured using SEC.

Nuclear Magnetic Resonance. The samples produced for the 'chain transfer' experiments were analyzed by NMR; all NMR work was performed by Dr Marianne Gaborieau. The oligo(acrylic acid) sample before styrene polymerization is denoted CT1 and the sample after styrene polymerization is denoted CT2. Quantitative solution-state NMR spectra were recorded on a Bruker Avance 300 spectrometer at Larmor frequencies of 300.13 MHz for ^{1}H and 75 MHz for ^{13}C. The samples were left to evaporate at room temperature then dissolved in D_2O (10 % w/w for CT1, lower for CT2) and measured at 60 °C. For ^{1}H spectra, 4 transients were recorded with 7.9 μs 90° pulse and a relaxation delay of 5 s. The spectra were calibrated with respect to the residual water signal at 4.79 ppm. ^{13}C spectra were recorded using a 6μs 90° pulse and a relaxation delay of 10 s, with 192 transients for CT1 (31 min) and 5585 transients for CT2 (15 h 30 min).

Solid-state NMR spectra of CT1 and CT2 were recorded on a Bruker Avance 300 spectrometer at Larmor frequencies of 300.13 MHz for ^{1}H and 75 MHz for ^{13}C. The samples were packed in a 4 mm o.d. ZrO_2 rotor and spun at 4.5 MHz MAS. Spectra were recorded at room temperature. For ^{1}H spectra, 16 transients were recorded with a 5.6 μs 90° pulse and a relaxation delay of 20 s. ^{13}C single-pulse excitation (SPE-MAS) spectra were recorded using a 5.5 μs 90° pulse and a relaxation delay of 20 s, with 1220 transients for CT1 (6 h 50 min) and 3048 transients for CT2 (17 h 06 min). A ^{13}C cross-polarization (CP-MAS) spectrum of CT1 was recorded using a contact time of 10 ms and a relaxation delay of 5 s with 1024 transients (1 h 30 min).

Seeded Dilatometric Experiments: Conventional Latex with Added polyAA. 0.032 g of the synthesized polyAA was added to 30 g of the ST0 latex (conventional stabilization through ionic surfactant). NaOH was added to ensure a high level of ionization of all AA groups. The amount of polyAA was added to mimic the total weight fraction of AA in the electrosterically stabilized polystyrene latexes synthesized by the RAFT-in-emulsion method (ST5, ST10 and ST20). This latex was used as a seed latex in seeded dilatometric studies using the same dilatometry

methodology as described earlier in this section. KPS was used as initiator, with the concentration range spanning two orders of magnitude.

5.3. Results

5.3.1. Chemically Initiated Dilatometry Experiments

It is well established through prior work that for electrostatically stabilized styrene emulsion polymerization systems, the critical z value is approximately 2–3 for KPS[1, 8] and 1 for V-50.[8] This can be rationalized on the basis of the number of styrene units required to add on to the initiator-derived radical before the oligomer becomes surface active. Because the radical from the thermal decomposition of V-50 is not as water-soluble as the persulfate radical (due to functional groups in the radical (see Figure 5.1)), it takes less styrene units to impart surface activity. As the value of z is the critical parameter in the Maxwell-Morrison entry model, the z values for the initiators considered in this work for electrostatically stabilized emulsion systems will act as the reference point for comparison to our electrosterically stabilized systems. As no experimental z value has been reported for the VA-086 radical, it was measured via seeded kinetic studies using the ST0 latex (parameters used for data processing such as the decomposition rate coefficient of initiator k_d are given in Appendix A5). Using the value of the exit coefficient k found from independent γ-relaxation experiments (see Chapter 4) and the C_p value found via the 'static swelling' method[5, 9] (results reported in Table 5.1; C_p values from the 'kinetic method' only differ by ~ 10 %, a difference that has little impact on obtained $\overline{n}_{ss}$ and f_{entry} values), the entry efficiency as a function of radical flux was found for the ST0/VA-086 system (as shown in Figure 5.2). It can be seen that the f_{entry} values are in excellent agreement with the Maxwell-Morrison entry model assuming $z \approx 3$. Using group contribution values to the free energy of hydration (ΔG^{hyd}) for the VA-086 radical,[10] a good estimate for this species is ΔG^{hyd} =

– 33 kJ mol^{-1}. An approximate value for ΔG^{hyd} is given by $RT\ln C_w$, which is approximately –15 kJ mol^{-1} for styrene at 323 K. Using the equation[1]

$$z = 1 + \text{int}\left(\frac{-33\ \text{kJ mol}^{-1}}{RT \ln C_w}\right) \tag{5.3}$$

we obtain a theoretical z value of 3, in agreement with experiment. This value is our reference value for the neutral VA-086 initiator.

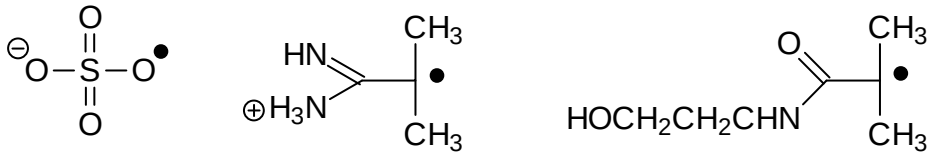

Figure 5.1. Chemical structure of initiating radicals from potassium persulfate (KPS), V-50 and VA-086.

Table 5.1. Values of C_p measured by the 'static swelling' method as well as exit rate coefficient and spontaneous entry rate coefficient values (from Chapter 4).

Latex	C_p (M)	k (Limit 2a) (s^{-1})	k (Limit 1) (s^{-1})	ρ_{spont} (s^{-1})
ST0	6.09	3.87×10^{-2}	n/a	2.18×10^{-5}
ST5	6.91	1.51×10^{-2}	6.76×10^{-3}	≈ 0
ST10	7.09	5.14×10^{-3}	5.12×10^{-3}	≈ 0
ST20	6.95	4.32×10^{-3}	5.05×10^{-3}	≈ 0

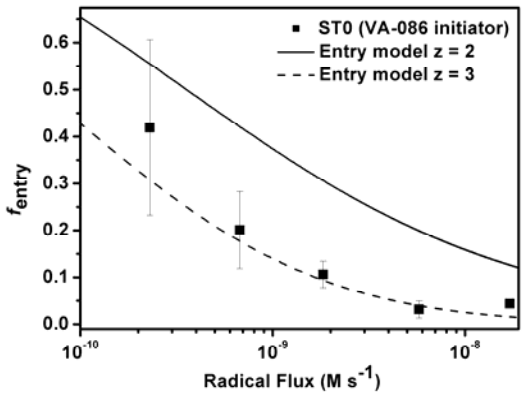

Figure 5.2. Entry efficiency (f_{entry}) as a function of radical flux for the ST0 latex, VA-086 as initiator; predicted entry efficiency from the Maxwell-Morrison model shown for z = 2 (solid line) and z = 3 (dashed line).

The first comparison made between a conventionally stabilized latex and an electrosterically stabilized system was the comparison between the ST0 and ST5 latexes using KPS as initiator.

Five different initiator concentrations were used spanning two orders of magnitude, with $\bar{n}_{ss}$ values determined from the steady-state rate. As seen in Figure 5.3, a significant reduction in $\bar{n}_{ss}$ was seen in the ST5 seeded experiments. While smaller $\bar{n}_{ss}$ values are predicted by theory for smaller particles,[5] the reduction seen here is substantially lower than the expected 'zero-one' value.

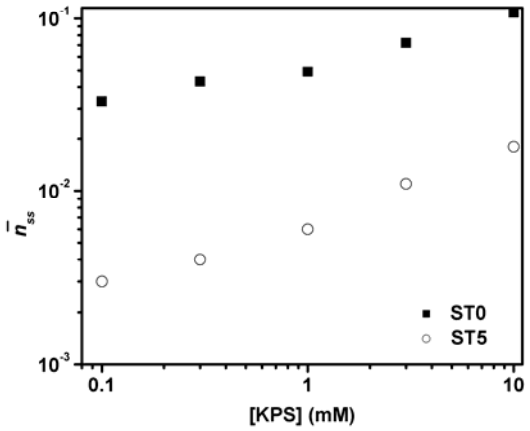

Figure 5.3. Variation of $\bar{n}_{ss}$ for the ST0 (black squares) and ST5 (open circles) latexes, initiated with KPS.

Calculation of ρ_{init} and f_{entry} (via Equations 5.1 and 5.2 (second-order loss kinetics) for these two latexes) yields excellent agreement with the Maxwell-Morrison model for ST0 (z = 2, as demonstrated in previous work), but an extremely low and approximately constant entry efficiency for the ST5 latex (Figure 5.4, left panel). A constant entry efficiency suggests z = 1. However the values measured here are orders of magnitude lower than the expected 100% entry of initiator-derived radicals. Moreover, the calculated values of ρ_{init} for the ST5/KPS system are two orders of magnitude lower than 'normal' values of the entry rate coefficient in typical emulsion polymerization systems (ρ_{init} = 10^{-7} – 10^{-6} s^{-1}; see Figure 5.4, right panel); rate coefficients this small are smaller than an expected thermal or 'spontaneous' polymerization entry rate coefficient[11] and so not physically reasonable. It should be pointed out that other

latex/initiator combinations yield even lower values of ρ_{init}, adding weight to the inference that they are not physically reasonable values for this rate coefficient.

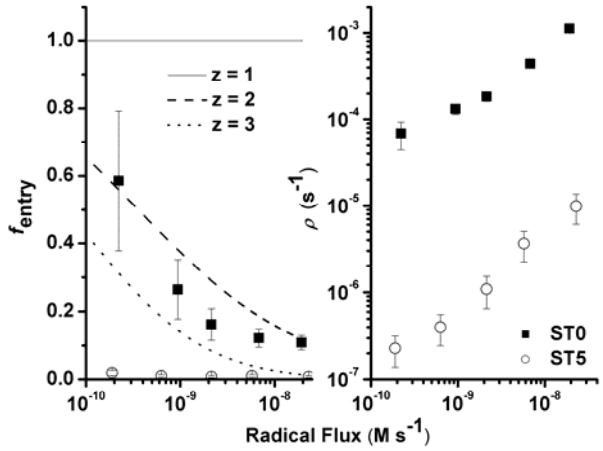

Figure 5.4. Comparison of f_{entry} (left panel) and ρ (right panel) the ST0 (black squares) and ST5 (open circles) latexes (initiated with KPS), assuming Limit 2a kinetics. Predicted f_{entry} values for z = 1 (solid line), z = 2 (dashes) and z = 3 (dots) are also shown.

The preceding physically unreasonable values were obtained assuming Limit 2a kinetics, which is the accepted kinetic limit for styrene emulsion polymerizations in electrostatically stabilized particles.[2, 3, 5] However, using first-order loss kinetics (Equation 5.1) to calculate ρ_{init} and f_{entry} values from the experimental $\overline{n}_{ss}$ for ST5 (using the Limit 1 value of k for this latex) gives both physically reasonable values of ρ_{init} and f_{entry} values that are also in excellent agreement with the Maxwell-Morrison entry model (well approximated with $z \approx 2$–3; see Figure 5.5). (It should be noted that a different value of k_d (the decomposition rate coefficient of the initiator), 4×10^{-6} s^{-1}, was used for KPS in this system, as the presence of acrylic acid accelerates the decomposition of KPS,[12] due to its complicated decomposition mechanism that can involve pathways that incorporate water). This suggests that the impact that electrosteric stabilization has on the emulsion kinetics is not a reduction in f_{entry} or increase in z (as suggested previously[13]) but

instead the kinetic limit changes from a second-order loss mechanism to a first-order one. This is an important and unexpected result from this work.

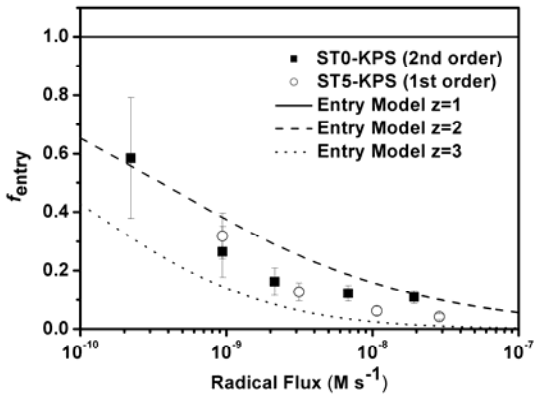

Figure 5.5. Comparison of f_{entry} for the ST0 (black squares) and ST5 (open circles) latexes (initiated with KPS), assuming Limit 1 kinetics for the ST5 system. Predicted f_{entry} values for z =1 (solid line), z = 2 (dashes) and z = 3 (dots) are also shown.

Processing all data obtained from the three electrosterically stabilized latexes in question (ST5, ST10 and ST20) assuming first order loss kinetics, it was found that the value of f_{entry} was independent of the length of the stabilizing unit on the surface of the particle (see Figure 5.6). This is a different result than that obtained for the radical exit presented in Chapter 4, which saw a monotonic decrease in the exit rate coefficient k as a function of AA chain length. One may conclude that as the rate of adsorption of an entering oligomer onto a particle surface is so fast (diffusion-controlled) compared to the magnitude of the desorption rate coefficient k_{dM}, the timescale is insufficient for the decreased diffusion coefficient within the 'hairy layer' to affect the entry process.

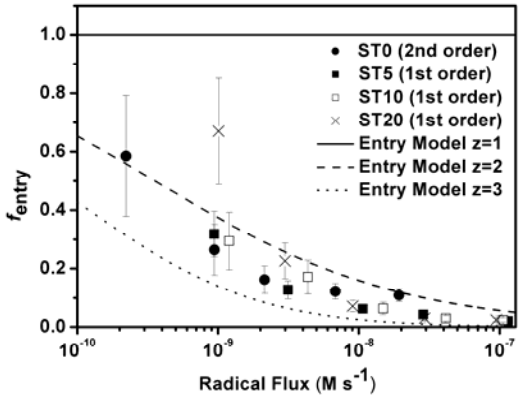

Figure 5.6. Comparison of f_{entry} for the ST0 (black circles) with the three electrosterically stabilized latexes assuming Limit 1 kinetics: ST5 (black squares), ST10 (open circles) and ST20 (crosses). Systems initiated by KPS. Predicted f_{entry} values for z = 1 (solid line), z = 2 (dashes) and z = 3 (dots) are also shown.

The neutral entering radical generated via decomposition of the VA-086 initiator (expected value of z = 3) also demonstrated no difference in entry efficiency in electrosterically stabilized systems (see Figure 5.7), apart from the necessity of processing the data using Limit 1 kinetics. The positively charged radical from V-50 decomposition (z = 1), however, showed a significant reduction in f_{entry} (Figure 5.8) when compared to an electrostatically stabilized polystyrene system.[8] This may be rationalized as being due to the opposite charges on the polyAA hairs and the entering oligomer; electrostatic attraction between the two may lead to greater residence times of the entering species in the aqueous phase, increasing the likelihood of termination before entry. The major conclusion from this work however is (besides the case where the stabilizing unit and the entering oligomer of opposite charge) that emulsion particles stabilized by polyAA in this manner obeys a first order loss mechanism, with no impediment to the entry process due to the stabilizing blocks on the surface.

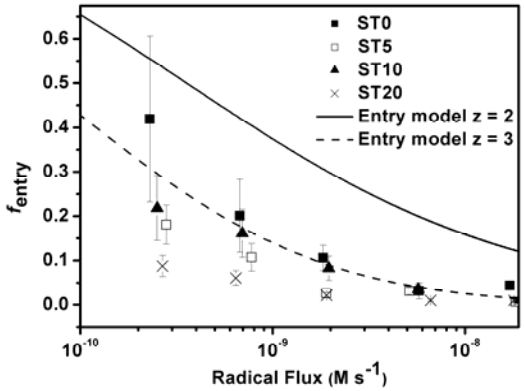

Figure 5.7. Variation of f_{entry} as a function of stabilizing block length for the ST5 (open squares), ST10 (black triangles) and ST20 (crosses) latexes using VA-086 as initiator, assuming Limit 1 kinetics. Results for the ST0 latex (filled squares, Limit 2a kinetics) shown for comparative purposes. Predicted f_{entry} values for z = 2 (solid line) and z = 3 (dashes) are also shown.

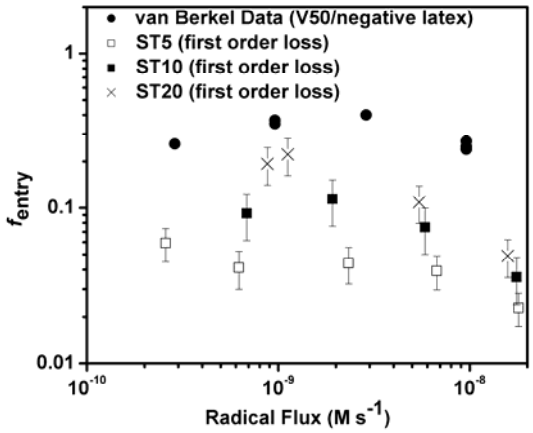

Figure 5.8. Variation of f_{entry} as a function of stabilizing block length for V-50 initiated systems. ST5 (open squares), ST10 (black squares) and ST20 (crosses) are assumed Limit 1 kinetics; comparison is made to the data of van Berkel *et al.* (black circles). Note that the y-axis is logarithmic.

It is essential to note that this first-order mechanism in this electrosterically stabilized (polyAA) system results in a much lower rate compared to that in an electrostatically stabilized one which obeys second-order radical loss.

5.3.2. Rationalizing the First-Order Loss Mechanism

The experimental results presented in the previous section would suggest that the kinetics that govern these systems obey a first-order loss mechanism. This is on the basis that excellent agreement with the accepted 'control by aqueous phase growth' entry model is obtained, as well as the calculation of unfeasibly small entry rate coefficients when second-order loss kinetics are assumed.

The postulate that a styrene emulsion polymerization system, electrosterically stabilized or otherwise, obeys first-order loss kinetics is difficult to rationalize. It has been well established both experimentally and theoretically[2, 5] that in this type of electrostatically stabilized systems, styrene emulsion systems obey a second-order loss mechanism. An exited monomeric radical will re-enter another particle and either propagate or terminate. This can be rationalized by considering that the rate of re-entry is orders of magnitude higher than the rate of aqueous-phase termination, namely

$$k_{re}\frac{N_p}{N_A} >> k_{t,aq}[T^{\cdot}] \tag{5.4}$$

where k_{re} is the second-order radical re-entry rate coefficient (given by the Smoluchowski equation for diffusion-controlled reactions), N_p the particle number, $k_{t,aq}$ the aqueous-phase termination rate coefficient and $[T^{\cdot}]$ the total radical concentration in the aqueous phase. Even with the reduced re-entry rate coefficient due to diffusion through a two-phase (water plus polyAA layer) regime,[14] the value of N_p in all but the most unusual emulsion systems is so high as to cause the re-entry rate to significantly outweigh the rate of termination. Considering that it

would appear that the electrosterically stabilized systems in question are obeying first-order kinetics, it would seem that some other mechanistic event is taking place to modify the overall kinetics.

One validation of the postulate that using first-order loss kinetics is appropriate to model the ST5, ST10 and ST20 latexes is the use of the 'slope and intercept' method[5] to calculate the overall rate of entry ($\rho\ N_p/N_A$) assuming first-order loss and compare this to the value for the electrostatically stabilized ST0 system assuming second-order loss. The 'slope and intercept' method calculates ρ from the gradient and y-intercept of the linear fit to the steady-state region of the conversion-time ($x(t)$) curve without the use of an independent k value calculated from separate experiments. While this method is more prone to error than the indirect calculation used in this work (due to oxygen inhibition/retardation that may affect the approach to steady-state) it makes use of additional data within a single experiment to obtain ρ rather than combining data from two experiments (γ relaxation plus chemical steady state) used previously. It can be seen (Figure 5.9) that when using this approach, the same overall entry rate (within experimental error) is seen across all four latexes in question. (The overall entry rate was the parameter examined due to the fact that the entry rate coefficient is dependent on the particle number which differs from latex to latex). This would support the supposition that the entry efficiency in electrosterically stabilized latexes stabilized in this manner is as predicted by the Maxwell-Morrison entry model (which predicts independence of charge on the entering z-mer, as verified experimentally for electrostatically stabilized systems[8]), but unexpectedly, the overall reaction process obeys first-order loss kinetics.

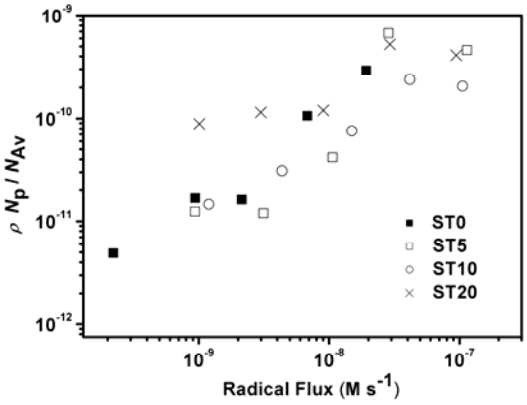

Figure 5.9. Overall entry rate as a function of radical flux for all latexes calculated by the 'slope and intercept method.' Points shown are ST0 (filled squares), ST5 (open squares), ST10 (open circles) and ST20 (crosses).

One hypothesis to explain the observed behavior seen in the electrosterically stabilized latexes in this work is that transfer of radical activity from exited radicals and/or initiator-derived oligomers) to the polyAA hairs on the surface takes place. It is well established that chain transfer to polymer is a significant reaction in the acrylate family (especially the intra-molecular 'backbiting' mechanism in *n*-butyl acrylate[15-17]) and any transfer event to a polyAA hair on the particle surface would lead to a tertiary radical that would be slow to propagate and thus would eventually terminate – essentially a 'radical loss' event. If an exited monomeric radical either undergoes this postulated transfer reaction either while exiting a particle, or attempting to re-enter another particle, this would make the radical loss a first-order loss process.

5.3.3. Testing the 'First-Order' Hypothesis

While the kinetic data collected in this work suggests that electrosterically stabilized systems obey first-order loss kinetics (with no effect on the entry rate coefficient when making this assumption), there is no direct evidence to prove that the system is first order or that the reason for this effect is chain transfer to the polyAA hairs on the particle surface. To help validate this

postulate, experiments must be performed that have the potential to refute what is believed to be happening.

To obtain 'proof of concept' – that is, to prove that chain transfer to polyAA can take place in a styrene polymerization, samples of styrene were polymerized in bulk in the presence of differing amounts of polyAA, made via the precipitation polymerization procedure of Dougherty *et al*.[18] Measurement of the molecular weight distribution (MWD) was attempted for the formed oligo(AA) using size exclusion chromatography (performed on a Shimadzu SEC system with 2 × PLGel Mixed B columns, THF eluent with a flow rate of 1 mL min^{-1}, 28 polystyrene standards from 160 to 5 × 10^6 g mol^{-1} Da used for calibration). The measured $\bar{M}_w$ was far lower than predicted at 300 Da; however, universal calibration breaks down at extremely low molecular weights and as such the precision in the measured value is questionable. Nonetheless, this indicates that the molecular weight of the polyAA formed is extremely low.

Measurement of the chain transfer constant ($C_{tr,AA} = k_{tr,AA} / k_p$) of styrene with polyAA as the 'chain transfer agent' was achieved by polymerizing bulk styrene in the presence of different amounts of the synthesized polyAA (see Experimental section). It can be seen in Figure 5.10 that there is a substantial decrease in the average molecular weight of the formed polystyrene, even when very small amounts of polyAA are present in the reaction mixture. This would suggest that the polyAA is an extremely efficient transfer agent. The value of $C_{tr,AA}$ was calculated via the Mayo method[7] as well as the 'ln P' approach[19] to examine the consistency between the two approaches. The Mayo and ln P plots are shown in Figure 5.11 (both plots exclude the final point from the linear fit as it would seem the formed polystyrene is already at the lowest achievable molecular weight via this method). The ln P method is considered more reliable as it utilizes the slope of the ln $P(M)$ plot taken at the maximum of the SEC distribution to take band broadening into account;[20] both approaches yield a very high value of C_{tr} (see Table **Error! Reference source not found.**). Thus it would seem that chain transfer to polyAA is both probable and

extremely efficient. This experiment is therefore consistent with the postulated mechanism; had the change in MWD not been seen, it would have refuted the hypothesis.

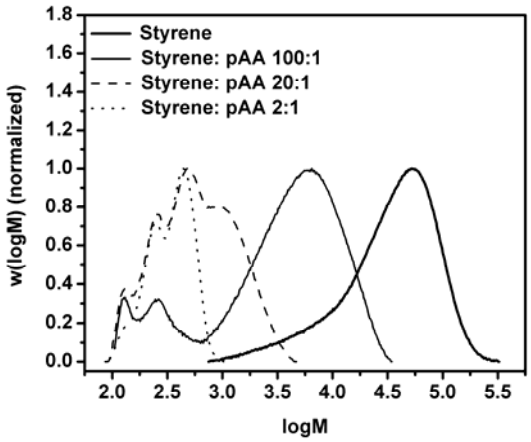

Figure 5.10. Normalized SEC distributions of styrene polymerized in the presence of different amounts of polyAA.

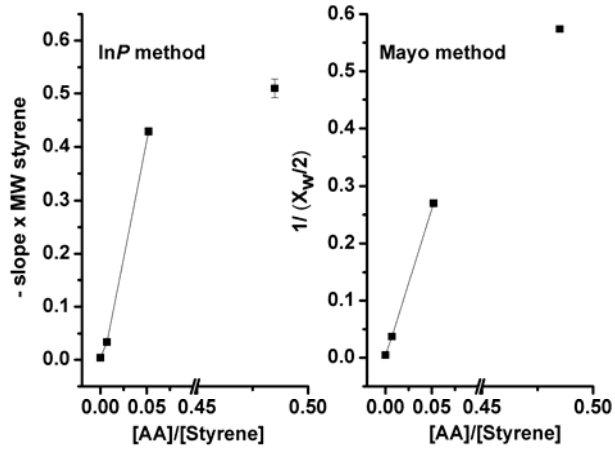

Figure 5.11. Mayo and ln*P* plot comparison to calculate the value of transfer constant $C_{tr,AA}$ for polyAA as a chain transfer agent for styrene polymerizations.

Table 5.2. Values of *C* for polyAA as a chain transfer agent in styrene polymerizations, determined via different methods.

Method	C_{trAA}
ln *P* method	8.4 ± 0.4
Mayo method	5.1 ± 0.1

After proving the concept of polyAA acting as a chain transfer agent in the polymerization of styrene, the experimental samples were re-considered using SEC and nuclear magnetic resonance spectroscopy (NMR) to analyze the resultant polymer to potentially observe any 'branching' off the polyAA, a phenomenon that would result from the termination of a growing polystyrene radical and a mid-chain radical (MCR) on the polyAA backbone. The SEC chromatogram demonstrated that the peak corresponding to the homopolymer of polystyrene was at a much lower molecular weight than expected, indicating that the homopolymer is being formed in the presence of a chain transfer agent. As well as this, the peaks corresponding to the low molecular weight polyAA have increased in intensity, possibly due to the attachment of a short polystyrene oligomer (see Figure 5.12). This attachment can only take place via a termination reaction with a MCR. This provides indirect, qualitative evidence for MCR and branch formation, and the only way such a MCR could be formed is via hydrogen-atom abstraction from the polyAA backbone in a chain transfer reaction.

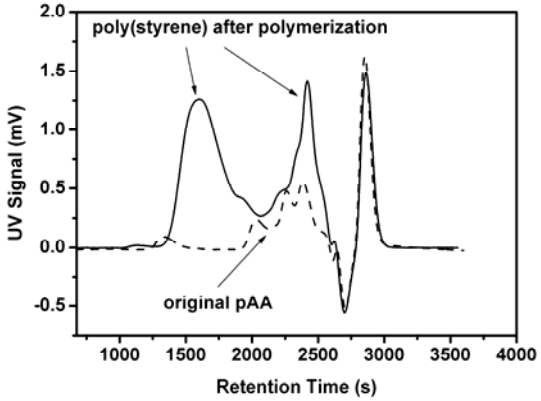

Figure 5.12. SEC Chromatogram of polyAA (dashed line) and the resultant SEC distribution after polymerization of bulk styrene in the presence of this polymer (solid line).

^{13}C solution-state NMR was used aiming at quantifying the amount of quaternary carbons due to grafting of polystyrene onto polyAA. ^{13}C NMR can in principle be used for the direct detection of the quaternary carbon of the branching/grafting point at 49 ppm.[21] Oligo(acrylic acid) produced by radical polymerization is expected to exhibit some branching,[21] even for degrees of polymerization as low as 5. Thus the detection of grafting points of styrene on polyAA could thus only be done by comparing the intensity of the signals at 49 ppm for samples CT1 and CT2, before and after styrene polymerization. The free polyAA CT1 readily dissolved in D_2O at 10 % w/w without the need for any additional base to assist dissolution, and its ^{13}C NMR spectrum of CT1 exhibits a signal at 49 ppm (Figure 5.13). The sample CT2 was added to D_2O at a target of 10% w/w, with the intent that the free polystyrene would not dissolve but the polyAA with any short polystyrene branches would do so; any undissolved polymer was removed by filtration. Unfortunately the ^{13}C signal-to-noise ratio obtained for CT2 in 15 h 30 min was too low to detect a possible signal for any quaternary carbons (Figure 5.13). Indeed, the ^{13}C spectrum of CT2 recorded over 15 h 30 min had a significantly poorer signal-to-noise ratio than that of CT1 recorded over 31 min (Figure 5.13). The ^{1}H spectrum of CT2 also had a poorer signal-to-noise ratio than that of CT1. A simple recovery experiment demonstrated that less than 3% of the

original polymer of CT2 actually dissolved in the D_2O, giving too low a concentration to measure a signal successfully. This recovery experiment however yielded a very powerful result, given that 66% of the polymer sample was composed of AA that should readily dissolve in water. It is therefore postulated that many transfer and termination events take place along each polyAA chain that the polymer becomes essentially water-insoluble, supporting the original hypothesis.

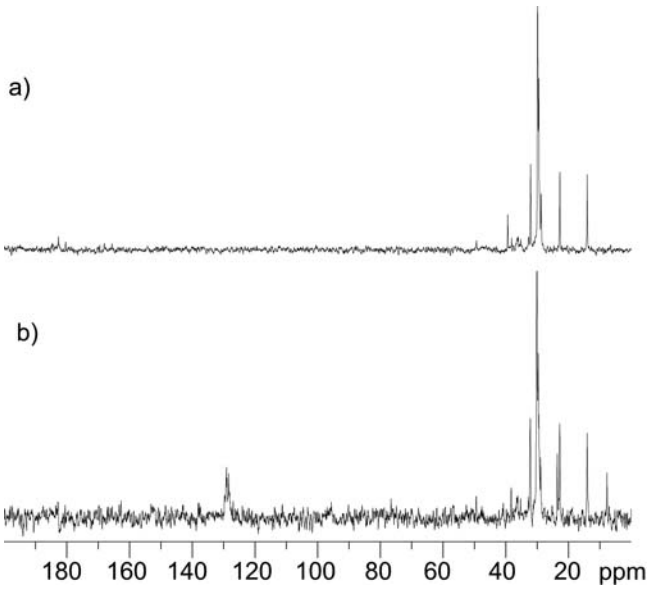

Figure 5.13. ^{13}C solution-state spectra of samples a) CT1 and b) CT2 in D_2O at 333 K.

Both ^{1}H and ^{13}C NMR spectra of CT2 exhibit significant aromatic signals for polystyrene at 6.8 to 7.6 and 125 to 130 ppm respectively (Figures 5.13 and 5.14, and Table 5.3 for chemical shift assignment). These cannot arise from styrene monomer, as no double bond signal at 5.2 to 5.7 and 113 ppm is observed, or from polyAA or dodecanethiol. However, oligomers of styrene without a polar head-group are insoluble in water when their degree of polymerization (DP) exceeds two.[1, 8] Thus the observed polystyrene signals cannot come from dissolved oligostyrene homopolymer, but are expected to come from oligostyrene or polystyrene chains covalently grafted to water-soluble species such as oligo(acrylic acid). Thus the ^{1}H and ^{13}C solution-state

NMR indicate the presence of poly(acrylic acid-*graft*-styrene) via the presence of polystyrene in water at 333 K.

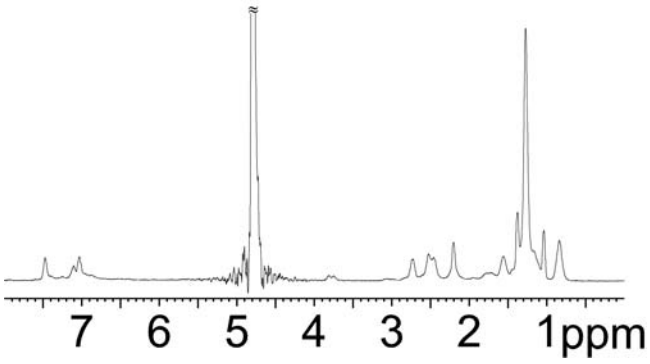

Figure 5.14. ^{1}H solution-state spectrum of sample CT2 in D_2O at 333 K.

Table 5.3. Chemical shift assignment for ^{1}H and ^{13}C NMR spectra of oligoAA,[21] polystyrene,[22] dodecanethiol[23] and AIBN fragment.[23]

^{1}H		^{13}C	
δ (ppm)	Assignment	δ (ppm)	Assignment
0.84	dodecanethiol, CH_3-($\underline{CH_2}$)$_{11}$-S-oligoAA	7.7	???
1.04	oligo AA, CH_2	14.0	dodecanethiol, $\underline{CH_3}$-$(CH_2)_{11}$-S-oligoAA
1.1 to 1.6	dodecanethiol, CH_3-($\underline{CH_2}$)$_{10}$-CH_2-S-oligoAA	22.8	dodecanethiol, CH_3-$\underline{CH_2}$-$(CH_2)_{10}$-S-oligoAA
1.7 to 1.9	polystyrene backbone and AIBN CH_3	23.5	AIBN fragment, CH_3
2.20	oligoAA, CH	25	oligoAA, CH_2
2.4 to 2.8	dodecanethiol, $C_{11}H_{23}$-$\underline{CH_2}$-S-oligoAA	28 to 31	dodecanethiol, CH_3-($\underline{CH_2}$)$_{10}$-CH_2-S-oligoAA
4.79	residual water	32.2	dodecanethiol, CH_3-$(CH_2)_{10}$-$\underline{CH_2}$-S-oligoAA
7.0 to 7.5	polystyrene, aromatic ^{1}H	35 to 40	oligoAA, CH_2, and polystyrene, backbone
		49	oligoAA, quaternary carbon
		128 to 130	PS, aromatic ^{13}C
		183	oligoAA, C=O

As only part of CT2 dissolves in D_2O, a comparison between CT1 and only a part of CT2 with solution-state NMR would be meaningless. Therefore, solid-state NMR spectra of the samples were recorded. ^{13}C CP-MAS and ^{13}C SPE-MAS spectra recorded on sample CT1 exhibited similar resolution. Due to the non-quantitative character of ^{13}C CP-MAS spectra, it was decided to record ^{13}C SPE-MAS spectra of the samples (Figure 5.15). Due to the lower resolution of

these spectra compared to the solution-state ones, the signals of the backbone ^{13}C of polystyrene at 40 to 47 ppm (Table 5.3) overlap with the region in which the quaternary carbon of the grafting point is expected. Thus no easy quantification of a possible grafting signal at 49 ppm could be obtained by ^{13}C solid-state NMR at room temperature. ^{13}C solid-state NMR could be tried on the molten sample, following the method used for successful quantification of branching in poly(alkyl acrylates),[24] as a possible means of further quantification in the future.

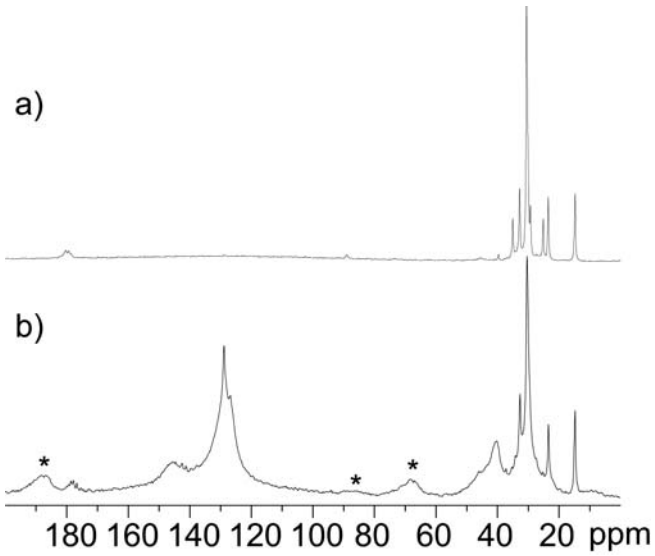

Figure 5.15. ^{13}C solid-state spectra of samples CT2 at 4.5 kHz MAS and room temperature: a) SPE-MAS and b) CP-MAS. The asterisks indicate spinning side bands.

From both the bulk chain transfer experiments and NMR spectral data, there is experimental evidence that polyAA has the ability to act as a chain transfer agent, with the resulting MCR acting as a potential termination site (especially as propagation from a tertiary backbone radical is generally considered to be extremely slow relative to 'linear' propagation). It is anticipated that with respect to the electrosterically stabilized emulsion systems of interest, these reactions affect the overall kinetics and providing another two loss mechanisms (transfer and termination with the resultant MCR formed). The case of the likelihood of these reactions in emulsion as opposed to bulk (and solution) however must also be tested. One simple approach to test this

postulate involved the addition of highly ionized oligoAA to the aqueous phase of an electrostatically stabilized polystyrene latex (a system that displays well understood kinetics), with subsequent seeded dilatometric experiments performed with chemical initiation (persulfate). It was seen that significant inhibition/induction times were observed when the oligoAA was added to the aqueous phase of the conventional styrene emulsion (up to 5 h 30 min at the lowest initiator concentration, see Figure 5.16). This would suggest that the oligoAA is acting as a degradative chain transfer agent,[25] with initiator-derived radicals undergoing chain transfer in the aqueous phase, forming a MCR that does not re-initiate quickly (but may terminate other radicals, providing a rationale for the observed inhibition times).

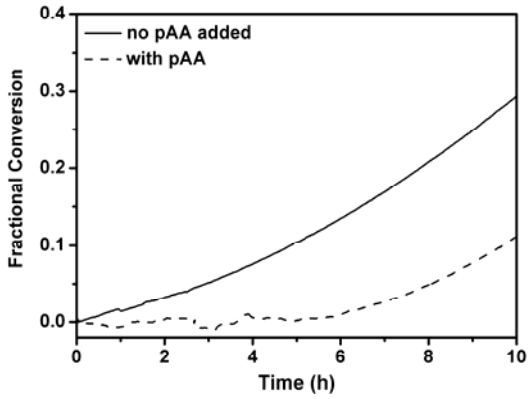

Figure 5.16. Polymerization rate of seeded styrene emulsion polymerization in the presence of added polyAA, showing significant inhibition periods for the polymerization of conventionally stabilized polystyrene latex in the presence of short-chain polyAA in the water phase.

There was also an observed reduction in the steady-state $\overline{n}$ ($\overline{n}_{ss}$) relative to that in the absence of any added oligoAA; however this reduction was not as marked as that seen in the electrosterically stabilized latexes studied previously (most likely because the AA in that case provides a dense layer on the surface of the particle restricting true radical exit, whereas when added to the entire aqueous phase there is no significant 'local' concentration of AA units). Determination of radical entry efficiencies (f_{entry}, the fraction of radicals generated by initiator

that eventually enter a particle) in these experiments only yielded good agreement with the accepted entry mechanism[1] for electrostatically stabilized styrene systems when first-order loss kinetics (Limit 1) were used (see Figure 5.17). This again suggests that exiting monomeric radicals lose radical activity (either by transfer or termination) during an encounter with an AA unit (this time in the aqueous phase rather than on the particle surface).

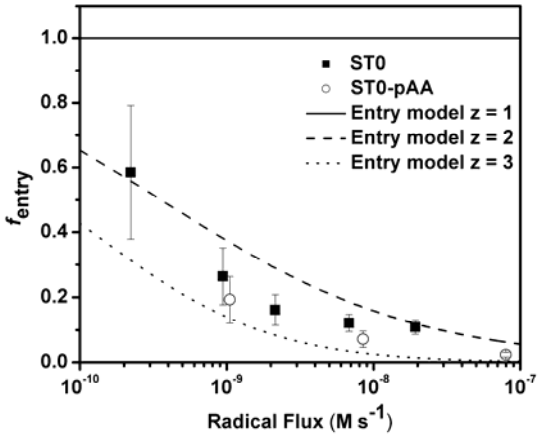

Figure 5.17. Comparison of radical entry efficiencies (f_{entry}) for the conventionally stabilized ST0 latex (treated as 2nd order loss, filled squares) and the same latex with added polyAA (treated as 1st order loss, open circles) for persulfate-initiated experiments; also shown are predicted values for the entry mechanism assuming z = 1 (solid line), z = 2 (dashed line) and z = 3 (dotted line).

5.3.4. Re-Consideration of Previous Data

Similar work in the same area conducted by Coen[13] and Vorwerg[26], albeit with 'uncontrolled' polyAA hairs on the particle surface, revealed a reduction in ρ (assuming Limit 2a kinetics) but nowhere near the reduction in $\bar{n}$ as seen in the work presented here. This is due in part to the much lower particle number and larger particle size of the latexes used in that work (meaning that their calculated $\bar{n}$ should be significantly higher); however it is possible that the data presented in their respective work can be treated assuming first-order loss kinetics. At lower

values of N_p there is only a minor difference between the expected $\overline{n}$ value in electrostatically stabilized systems using Limit 1 and Limit 2a kinetics; re-processing this old data assuming first-order loss gives reasonable agreement with the data collected for the model latexes used (Figure 5.18). It is possible that at such high N_p as used in this work (> 10^{18} L^{-1}), the effect of the polyAA hairs becomes more pronounced in the mathematical treatment of the data; such low $\overline{n}$ values provide a significant difference in the calculation of ρ when different kinetic limits are used.

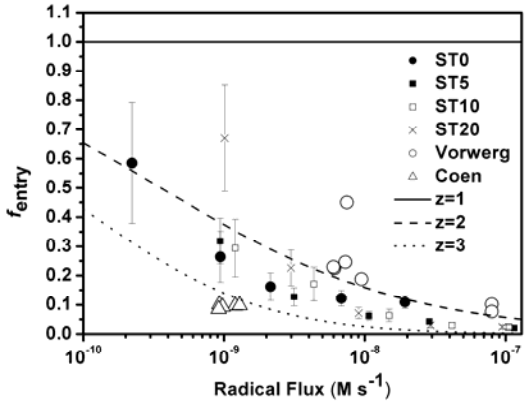

Figure 5.18. Comparison of f_{entry} data for electrosterically stabilized latexes analyzed in this work with re-processed data from Vorwerg *et al.* (large open circles) and Coen *et al.* (large open triangles).

5.3.5. An Apparent Contradiction

While the claim that the polyAA hairy layer acts as an extremely efficient chain transfer agent/termination site is likely with extensive supporting evidence, the treatment of the rate coefficient data for the electrosterically stabilized latexes ST5, ST10 and ST20 in this and the previous chapter is inconsistent. The data for radical exit (Chapter 4) was considered as a 'restricted' diffusion process, but the assumption of re-entry of an exited radical was retained in the data processing. The radical entry results in this chapter however have been explained on the

basis of transfer or termination with a polyAA 'hair' (Limit 1 kinetics) rather than re-entry. Both cannot be correct (or rather, neither can happen to the exclusion of the other), as interaction with the hairy layer will occur in both directions, i.e. a monomeric radical will not desorb in a restricted manner (with a reduced diffusion coefficient) out of the particle and then selectively transfer/terminate on the surface of another particle instead of undergoing re-entry. Similarly the correct order of the radical loss step (either first order or second order with respect to $\overline{n}$) cannot be determined by close inspection of γ-relaxation data from Chapter 4, as the experimental scatter (which is unavoidable due to the nature of dilatometric experiments) yields adequate fits to the data when either limit is used.

As a result, while the data regarding radical entry appears to exhibit first-order kinetics (a phenomenon that can be rationalized through interaction with the polyAA stabilizer on the particle surface), a new approach needs to be taken to explain the overall kinetic picture in these systems that provides a consistent explanation for both radical entry and exit. This requires "limit-free" kinetic modelling, and the development of a new kinetic model is the subject of the next chapter.

5.4. Conclusions

In this chapter, the experimental results from chemically initiated dilatometric experiments were presented with the objective of obtaining radical entry rate coefficients for model electrosterically stabilized latexes. With the rate coefficients for radical exit in these systems obtained in independent experiments (presented in the previous chapter), the entry rate coefficients were determined from steady-state rate data. Using the assumption of re-entry of an exited monomeric radical (a well-accepted phenomenon for electrostatically stabilized polystyrene latexes), which is a second-order radical loss mechanism, unfeasibly small entry rate coefficients are obtained – values that are far lower than typical 'spontaneous' polymerization

entry rate coefficients. This was a particularly unusual result given that the rate of radical entry is governed by aqueous-phase events and little to no departure from the 'control by aqueous phase growth' mechanism was anticipated.

In an attempt to understand the experimental data, the entry rate coefficients of the three model latexes were calculated after re-processing all experimental kinetic data while assuming termination of an exited radical in the aqueous phase (Limit 1 kinetics) as opposed to re-entry. Once this assumption was made, the radical entry rate coefficients and entry efficiencies were in excellent agreement with the Maxwell-Morrison entry model. The length of the stabilizing block on the particle surface was seen to be unimportant – varying the average degree of polymerization of the polyAA block from 5 to 20 units led to little to no variation in the measured rate coefficient. The trend in the experimental data obeying Limit 1 kinetics was evident for three different initiators bearing different charges (positive, negative and neutral).

The apparent first-order loss kinetics was rationalized on the basis of chemical interaction with the polyAA stabilizer on the particle surface, given the well-known ability of poly(alkyl acrylates) to undergo chain transfer reactions. It was postulated that an exited monomeric radical undergoes chain transfer to polyAA, providing another radical loss mechanism. The resultant mid-chain radical (MCR) would also provide a termination site for other monomeric radicals due to the relatively slow propagation from a polymer backbone site. This postulate was supported by separate experiments involving the use of polyAA as a chain transfer agent in the bulk polymerization of styrene, which was validated by SEC experiments. NMR analysis of the resultant samples demonstrated the existence of grafting of poly(styrene) chains onto the polyAA backbone, only possible through termination of a growing poly(styrene) radical with a MCR. Grafting was proven through the extremely poor water-solubility of the resultant polymer. This postulate was further supported through the addition of polyAA to the aqueous phase of a conventionally stabilized latex, a process that resulted in significant inhibition periods and

reduced polymerization rates suggesting that polyAA was acting as a degradative chain transfer agent.

The discovery of the apparent first-order loss mechanism that governs these systems led to the data from prior work (where 'uncontrolled' polyAA-stabilized latexes were used in kinetic experiments) being re-processed assuming Limit 1 kinetics. Agreement with the 'control by aqueous phase growth' entry mechanism was achieved as a result of this re-processing, something that was not considered previously.

While the use of first-order loss kinetics was successful in the treatment of the data from this work, it is accepted that this explanation is at odds with the explanation given to rationalize the data from radical exit experiments presented previously. To provide a consistent explanation of the entire kinetic picture of these systems, a limit-free approach must be adopted where all possible fates (desorption, transfer and termination) are considered simultaneously.

References

1. Maxwell, I. A.; Morrison, B. R.; Napper, D. H.; Gilbert, R. G. *Macromolecules* **1991,** 24, 1629-40.

2. Casey, B. S.; Morrison, B. R.; Maxwell, I. A.; Gilbert, R. G.; Napper, D. H. *Journal of Polymer Science, Part A: Polymer Chemistry* **1994,** 32, 605-630.

3. Morrison, B. R.; Casey, B. S.; Lacik, I.; Leslie, G. L.; Sangster, D. F.; Gilbert, R. G.; Napper, D. H. *Journal of Polymer Science, Part A: Polymer Chemistry* **1994,** 32, 631-49.

4. Lansdowne, S. W.; Gilbert, R. G.; Napper, D. H.; Sangster, D. F. *Journal of the Chemical Society, Faraday Transactions 1: Physical Chemistry in Condensed Phases* **1980,** 76, 1344-55.

5. Gilbert, R. G., *Emulsion Polymerisation: A Mechanistic Approach*. Academic Press: San Diego, 1995.

6. Doherty, W. O. S.; Fellows, C. M.; Gorjian, S.; Senogles, E.; Cheung, W. H. *Journal of Applied Polymer Science* **2004,** 91, 2035-2041.

7. Odian, G., *Principles of Polymerization*. 4th ed.; Wiley Interscience: 2004.

8. van Berkel, K. Y.; Russell, G. T.; Gilbert, R. G. *Macromolecules* **2003,** 36, 3921-3931.

9. Ballard, M. J.; Napper, D. H.; Gilbert, R. G. *Journal of Polymer Science, Polymer Chemistry Edition* **1984,** 22, 3225.

10. Plyasunov, A. V.; Shock, E. L. *Journal of Supercritical Fluids* **2001,** 20, 91-103.

11. Christie, D. I.; Gilbert, R. G.; Congalidis, J. P.; Richards, J. R.; McMinn, J. H. *Macromolecules* **2001,** 34, 5158-5168.

12. Henton, D. E.; Powell, C.; Reim, R. E. *J. Appl. Polym. Sci.* **1997,** 64, (3), 591-600.

13. Coen, E. M.; Lyons, R. A.; Gilbert, R. G. *Macromolecules* **1996,** 29, 5128-5135.

14. Thickett, S. C.; Gilbert, R. G. *Macromolecules* **2006,** 39, (6), 2081-91.

15. Plessis, C.; Arzamendi, G.; Leiza, J. R.; Schoonbrood, H. A. S.; Charmot, D.; Asua, J. M. *Macromolecules* **2000,** 33, 4-7.

16. Ahmad, N. M.; Heatley, F.; Lovell, P. A. *Macromolecules* **1998,** 31, 2822-2827.

17. Beuermann, S.; Buback, M.; Schmaltz, C.; Kuchta, F.-D. *Macromolecular Chemistry and Physics* **1998,** 199, 1209-1216.

18. Doherty, W. O. S.; Fellows, C. M.; Gorjian, S.; Senogles, E.; Cheung, W. H. *J. Appl. Polymer Sci.* **1004,** 91, 2035-41.

19. Clay, P. A.; Gilbert, R. G.; Russell, G. T. *Macromolecules* **1997,** 30, 1935-1946.

20. van Berkel, K. Y.; Russell, G. T.; Gilbert, R. G. *Macromolecules* **2005,** 38, 3214-24.

21. Loiseau, J.; Doërr, N.; Suau, J. M.; Egraz, J. B.; Llauro, M. F.; Ladavière, C. *Macromolecules* **2003,** 36, 3066-77.

22. NMR spectra database of polymers, http://polymer.nims.go.jp/NMR/top_eng.html.

23. Spectral database for organic compounds SDBS, http://www.aist.go.jp/RIODB/SDBS/cgi-bin/cre_index.cgi.

24. Gaborieau, M. Solid-state NMR investigation of spatial and dynamic heterogeneity in acrylic pressure sensitive adhesives (PSAs) compared to model poly(n-alkyl acrylates) and poly(n-alkyl methacrylates). PhD, University Louis Pasteur, Strasbourg, France, 2005.

25. Moad, G.; Solomon, D. H., *The Chemistry of Free Radical Polymerization 2nd Edn.* Elsevier: Amsterdam, 2006.

26. Vorwerg, L.; Gilbert, R. G. *Macromolecules* **2000,** 33, 6693-6703.

6. An Extended Mechanistic Description of Electrosterically Stabilized Systems

Sections of the work presented in this Chapter have previously been published as:

Thickett, S.C., Gaborieau, M. and Gilbert, R.G. *Extended Mechanistic Description of Particle Growth in Electrosterically Stabilized Emulsion Polymerization Systems,* Macromolecules, **2007**, 40, 4710-4720.

"Facts are the air of scientists. Without them you can never fly."

Linus Pauling

6.1. Introduction

The aim of this chapter is to rationalize the hitherto conflicting experimental kinetic data presented for both the radical entry and exit processes in electrosterically stabilized latexes presented thus far. The result from the work on radical exit (Chapter 4) was in agreement with the prior work in the field using uncontrolled latexes[1, 2] – there was a significant reduction in the exit rate coefficient (k) compared to the expected value for particles of that size. This was attributed to a 'restricted diffusion' that was successfully modeled using a modified Smoluchowski equation for diffusion-controlled reactions: it was assumed that a dense polymeric layer on the surface would restrict the ease of an exiting (monomeric) radical to successfully desorb. The results for radical entry (Chapter 5) demonstrated that the polymerization rate (and as a consequence the value of $\overline{n}$, the average number of radicals per particle) was up to an order of magnitude lower than that calculated for an electrostatically stabilized latex at the same initiator concentration, an extremely significant effect. These extremely low $\overline{n}$ values led to values of the entry rate coefficient (ρ) that were unfeasibly low (below what would be the 'thermal' entry rate) when second-order loss kinetics were used in the calculations; second-order loss kinetics were assumed as it is well accepted that radical loss in electrostatically stabilized styrene systems is second-order with respect to $\overline{n}$, a fact verified both experimentally[3] and theoretically.[4] Almost perfect agreement between calculated ρ values and the theoretical values obtained from the 'control by aqueous phase growth' entry mechanism[5] however was seen when first-order loss kinetics were used in the data processing, implying that termination in the aqueous phase rather than re-entry is the dominant fate for an exited species.

The first-order loss claim (a claim highly unusual in styrene systems) was postulated to be due to rapid transfer via hydrogen atom abstraction from a poly(acrylic acid) (polyAA) hair on the surface of the particle once the species exits, a claim supported by separate solution-phase experiments as well several other examples in the literature.[6, 7] The inconsistency presented thus

far, however, is that the exit results are consistent with a 'restricted diffusion' (second-order loss), while the radical entry results are explained via a 'loss by transfer' approach (first-order). Both cannot be happening in exclusivity, and using current thinking, it is difficult to rationalize the experimentally determined radical entry results that suggest a first-order loss mechanism.

Using the well-accepted Smith-Ewart equations[8] as a reference point, an extended kinetic model is given in this chapter that accounts for the observed experimental results for both radical entry and exit in electrosterically stabilized emulsion systems without inconsistency from the choice of data processing. The standard emulsion polymerization kinetic equations for small poly(styrene) particles (the 'zero-one' kinetic limit,[9] a limiting form of the extended Smith-Ewart equations[8]) have been re-written to include additional loss terms unique to systems such as those stabilized by polyAA: namely transfer to a monomer unit within the hairy layer or termination with a resultant mid-chain radical that compete with the standard desorption mechanism. (The inclusion of these mechanisms was supported by SEC and NMR data presented in Chapter 5). This then allows for comparisons with experiment to be made and the behaviour of this kinetic model to be tested. The model presented exists as an extension of the currently accepted emulsion polymerization kinetic equations that, to date, give excellent quantitative agreement with experiment for electrostatically stabilized systems.

6.2. An Extended Kinetic Model

As has been discussed in Chapter 5 as well as the Introduction, the unusual kinetic data seen for electrosterically stabilized latexes has been postulated to be caused by additional reactions taking place between and entering/exiting radical and the polyAA hairy layer. It is well known that the acrylate family of monomers are characterized by extensive intra- and intermolecular chain transfer to polymer;[10-13] synthesis of polyAA is similarly plagued by transfer to polymer at high conversion[7] and under conditions where the monomer concentration is low. It was thus thought

that the polyAA hairy layer is acting as a chain transfer agent on the particle surface, killing radical activity of both entering and exiting radicals. It is also postulated that aqueous-phase radicals, such as those derived from initiator decomposition, can abstract labile hydrogen atoms from the polyAA backbone leading to the formation of a mid-chain radical that can potentially terminate an entering or exiting radical. It has been demonstrated[14] that sulfate ion radicals can rapidly abstract hydrogen atoms from aliphatic hydrocarbons with a variety of side-groups; the rate coefficient for abstraction (detected by ESR spectroscopy) was shown to range from 10^5 – 10^9 M^{-1} s^{-1}. Similarly the relative ease with which graft co-polymers with a polyAA backbone can be made[6, 15] demonstrates how readily polyAA can undergo hydrogen abstraction to form a mid-chain radical site. The likely slow propagation (a relatively stable tertiary radical plus low local monomer concentration) means that these radicals are likely to serve as excellent termination sites for entering and exiting species.

Experimentally all electrosterically stabilized latexes were synthesized at pH = 7, so it is assumed that every acrylic acid (AA) group on the particle surface is fully ionized. Because of this it is assumed that the polyAA chains are fully extended off the particle surface and into the aqueous phase, a phenomenon confirmed by light scattering experiments.[16] Given that the average degree of polymerization of the polyAA block is known from ESI-MS experiments, the width of the hairy layer (denoted δ) is easily determined. Assuming a spherical shell, the volume of the hairy layer can be calculated and combined with the particle number N_p, the volume fraction of the aqueous phase that the hairy layer represents (denoted Φ_{HL}) can be calculated. This volume fraction is a small but not insignificant component of the total aqueous phase – for example the ST10 latex (stabilized by polyAA units of average degree of polymerization = 10) has Φ_{HL} = 5% of the total aqueous phase.

Knowledge of the value of Φ_{HL} is then used assuming perfect partitioning of the total aqueous phase radical concentration. Radicals within the hairy layer are the only ones that can undergo

hydrogen-atom abstraction with the polyAA hairs to form a mid-chain radical (MCR), so if the hairy layer represents 5% of the aqueous phase then it is assumed that 5% of the radicals are in the hairy layer. This assumption may or may not be correct but it serves as a good starting point for modeling purposes. The local acrylic acid concentration ([AA]), which provides a 'concentration' of possible transfer/abstraction sites, is found from the following formula:

$$[\mathrm{AA}] = \frac{\overline{X}_\mathrm{n}(\mathrm{AA})\, n_\mathrm{chains}}{\frac{4}{3}\pi\left((r_\mathrm{s}+\delta)^3 - r_\mathrm{s}^3\right) N_\mathrm{A}} \tag{6.1}$$

where $\overline{X}_\mathrm{n}(\mathrm{AA})$ = number-average degree of polymerization of the AA units per chain, n_chains = number of chains per particle (calculated from the RAFT-in-emulsion synthesis conditions by assuming that every RAFT group when the seed latex is synthesized forms a polyAA chain), N_A = Avogadro's number, r_s = swollen radius of the latex particle and δ = width of the hairy layer. It is assumed that every AA group has one site where transfer/abstraction can take place: it is noted however that pulse radiolysis experiments by von Sonntag *et al*[17] demonstrated that mid-chain radicals form at sites both α and β to the carboxylic acid group in significant amounts – so it is possible that every AA group may yield two active sites for transfer/termination. The rate coefficient for hydrogen-atom abstraction by an aqueous-phase radical (the population of which comprising sulfate ion radicals and oligomers with sulfate end-groups of degree of polymerization less than z) was chosen to be $k_\mathrm{abs} = 8.4 \times 10^5\ \mathrm{M^{-1}\ s^{-1}}$, a lower-bound value taken from the work of Gilbert[14] where the rate coefficient of hydrogen atom abstraction using sulfate ion radicals was measured.

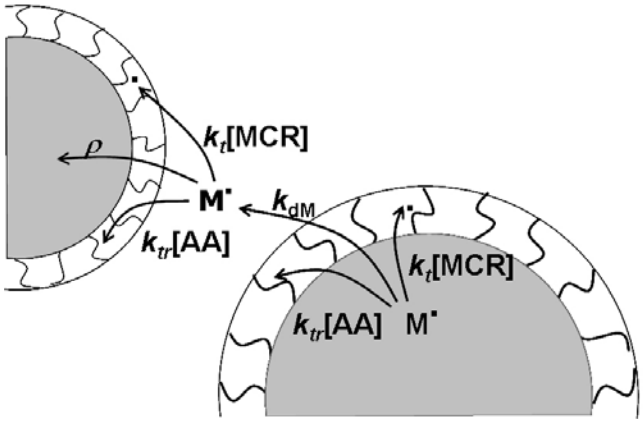

Figure 6.1. The postulated range of chemical fates for a monomeric radical both within the particle interior as well as in the aqueous phase for electrosterically stabilized systems.

The fate for a monomeric radical formed by transfer to polymer within a particle is now complicated by extra reaction pathways: it can propagate within the particle interior, desorb into the hairy layer and undergo a transfer reaction with an AA unit, desorb into the hairy layer and undergo termination with a mid-chain radical (MCR), or completely desorb through the hairy layer and out into the aqueous phase. These various fates are shown in Figure 6.1. Successful desorption into the aqueous phase to form an exited radical ($E^{\bullet}$) allows re-entry kinetics to be considered, where the equivalent reactions can take place – an exited radical can successfully re-enter, or again undergo a transfer or termination event.

The aqueous-phase chemistry is assumed to be identical to that proposed by Maxwell *et al.,*[5] in that an entering radical is a surface-active oligomer of critical degree of polymerization z. However as z-mers do interact with the particle surface in the process of entry, the transfer and termination reactions within the hairy layer are included in the evolution equation for this species. Mid-chain radicals within the polyAA hairy layer are allowed to propagate within this model (they are likely to, albeit slowly as has been seen with acrylates[11]): however the local radical concentration will not be changed by a propagation event. Similarly the monomer concentration is likely to be very low in the hairy layer, making propagation unlikely.

To model kinetic parameters such as the steady-state value of $\bar{n}$ ($\bar{n}_{ss}$) and the entry and exit rate coefficients ρ and k with a view for comparison to experiment, the evolution equations for the zero-one kinetic model (as given by the extended Smith-Ewart equations presented in Chapter 2) were modified to account for the newly considered reactions within the hairy layer on the particle surface. The newly added terms are presented in bold in the following equations:

$$\frac{dN_0}{dt} = \rho\,(N_1^{p} + N_1^{m} - N_0) + k_{dM,HL}N_1^{m} + \boldsymbol{P_{des}(\,k_{trAA}[AA]N_1^{m} + \,2\,k_t[MCR]\,N_1^{m})} \qquad (6.2)$$

$$\frac{dN_1^{m}}{dt} = \rho_{re}N_0 - \rho N_1^{m} - k_{dM}N_1^{m} + k_{tr}C_pN_1^{p} - k_p^{1}C_pN_1^{m} \boldsymbol{- P_{des}\,(k_{trAA}[AA]N_1^{m} + 2\,k_t[MCR]\,N_1^{m}\,)}$$

(6.3)

$$\frac{dN_1^{p}}{dt} = \rho_I N_0 - \rho\,N_1^{p} - k_{tr}C_pN_1^{p} + k_p^{1}C_pN_1^{m} \qquad (6.4)$$

where [AA] = concentration of acrylic acid sites in the hairy layer, [MCR] is the concentration of mid-chain radicals within the hairy layer, k_{trAA} = the rate coefficient for transfer of a styrene radical to a polyAA backbone site (determined in separate chain transfer experiments (see Chapter 5) to be approximately 2100 M^{-1} s^{-1} at 323 K), k_t = the bimolecular rate coefficient for termination between a mid-chain radical and a monomeric styrene radical, $k_{dM,HL}$ = the rate coefficient for complete (restricted) desorption of a monomeric radical through the hairy layer and into the aqueous phase, and P_{des} the probability that a monomeric radical actually makes it from the particle interior to the hairy layer (given by $P_{des} = k_{dM} / (k_{dM} + k_p^{1}C_p)$, where all other symbols are as defined previously). It should be pointed out that in Equation 6.4, the symbol ρ_I refers to the entry rate coefficient for initiator-derived oligomers and thermally generated radicals, as these entering species are generally oligomeric in length. ρ refers to the total entry

rate coefficient, which includes re-entry. The expression used to calculate $k_{dM,HL}$ is given by the formula derived in Chapter 4:

$$k_{dM,HL} = 3D_h \frac{C_w}{C_p} \left(\frac{r_s + \delta}{r_s^2 (\delta + r_s(D_h/D_w))} \right) \tag{6.5}$$

where D_h is the diffusion coefficient of a monomeric radical in the hairy layer (a function of the weight fraction of polymer w_p), D_w the diffusion coefficient of the same species in the aqueous phase, and all other symbols as defined previously.

An important consideration in this model is that it is not assumed that all exited radicals re-enter another particle – the fate of an exited radical is considered explicitly. The re-entry rate coefficient ρ_{re} is given by $k_{re}[E^{\bullet}]$, where k_{re} is the Smoluchowski expression for a diffusion-controlled reaction and $[E^{\bullet}]$ is the exited radical concentration, the evolution equation of which is given by:

$$\frac{d[E^{\bullet}]}{dt} = k_{dM,HL} N_1{}^m \frac{N_p}{N_A} - k_{re}[E^{\bullet}] \frac{N_p}{N_A} - k_t[E^{\bullet}][T^{\bullet}] \mathbf{- k_{trAA}[AA][E^{\bullet}] - 2k_t[MCR][E^{\bullet}]} \tag{6.6}$$

where $[T^{\bullet}]$ is the total aqueous-phase radical concentration, with all other symbols as defined previously. $[T^{\bullet}]$ is considered to be the sum of the concentrations of the initiator-derived oligomers as well as the exited radical concentration.

It is clear that in this model the determination of the mid-chain radical concentration ([MCR]) within the hairy layer is crucial to successful kinetic modelling. The first method used is to apply the steady-state approximation to a (simple) evolution equation whereby MCR's are generated only through abstraction with radicals in the hairy layer and terminated by any other radical (except MCR-MCR termination – even for very small particles the stabilizing chains are sufficient distance apart that MCR's on separate chains should not encounter one another (the

average surface area per chain in the 5AA-stabilized latex is approx 7 nm^2)). This evolution equation is:

$$\frac{d[MCR]}{dt} = k_{abs}[T^{\bullet}]\,\Phi_{HL}[AA] - 2\,k_t\,[T^{\bullet}]\,[MCR] \tag{6.7}$$

whereby application of the steady-state approximation yields:

$$[MCR] = \frac{k_{abs}\,\Phi_{HL}\,[AA]}{2\,k_t} \tag{6.8}$$

The use of the steady-state approximation is at best a starting point, and the full equation (where annihilation of a MCR occurs from a member of the N_1^m population desorbing into the hairy layer and then undergoing termination) can be included in the overall kinetics:

$$\frac{d[MCR]}{dt} = k_{abs}[T^{\bullet}]\,\Phi_{HL}[AA] - 2\,k_t\,P_{des}N_1^m\,[MCR] \tag{6.9}$$

It should be pointed out however that the long-time solution of Equation 6.9 gives a value of [MCR] that is only approximately 20% different from the steady-state approximation value, a difference that does not affect the qualitative results of the model.

Equations 6.2 – 6.4, 6.6 and the modified equations for the Maxwell-Morrison entry mechanism (that is, allowing for transfer and termination events to occur for *z*-mers that can interact with the particle surface) were solved iteratively until numerical convergence for a given initiator concentration to determine the steady-state values of $\bar{n}$ and ρ. Using these two values, first and second-order exit rate coefficients (k_{ct} and k_{cr}) were determined from the two applicable time evolution equations. This provided a collection of model values to allow for direct comparison to experiment.

6.2.1. Comparison With Experimental Results

The values of the various parameters used in the modeling performed in this work are listed in Table 6.1. The experimental $\overline{n}_{ss}$ for the polystyrene latex stabilized by polyAA oligomers of average DP 5 (latex ST5) initiated by persulfate were compared to model values across two orders of magnitude of initiator concentration. The comparison between experimental and model values can be seen in Figure 6.2.

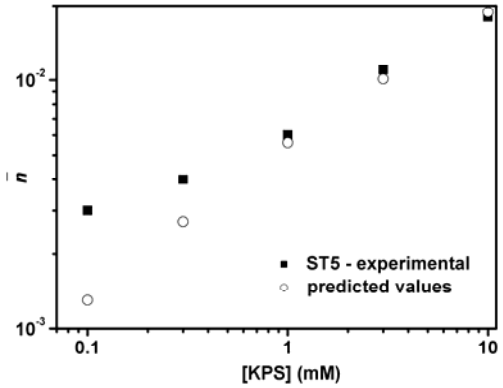

Figure 6.2. Comparison between $\overline{n}_{ss}$ values obtained for the ST5 latex via experiment (black squares) and those obtained from the new kinetic model calculations (open circles).

As is seen, there is good semi-quantitative agreement between the experimental and model $\overline{n}_{ss}$, regarded as satisfactory considering a minimal of model-based assumptions have been made. The lack of accord at the lower [KPS] values can be ascribed to the contribution that thermal ('spontaneous') entry makes to the overall polymerization rate, which becomes more significant when the initiator concentration is low. Most importantly, the general observed trend of extremely low values of $\overline{n}_{ss}$ seen experimentally is replicated by the model results – the expected values of $\overline{n}_{ss}$ for this latex system assuming 'normal' styrene emulsion kinetics[9] are of the order of 0.05 – 0.07, much higher than those calculated here. The reason for this large reduction is that the value of N_1^m is significantly reduced by the addition of the extra loss terms (through transfer

with a polyAA site or termination with a resultant MCR). As the particles synthesized by the 'RAFT-in-Emulsion' method are generally very small (swollen radius = 22 nm), the local concentration of AA units in the hairy layer is high, making transfer/termination much more likely than desorption of a monomeric radical into the aqueous phase (i.e. $P_{des}(k_{trAA}[AA] + k_t[MCR]) >> k_{dM}\,\overline{n}$). This reduces the exited radical concentration $[E^{\bullet}]$ (the ratio $[E^{\bullet}] / [T^{\bullet}]$ is a factor of 10 smaller in the electrosterically stabilized system ST5 when compared to an electrostatically stabilized latex of the same size) indicating a much smaller exited radical population that can potentially re-enter, ensuring that the value of $\overline{n}_{ss}$ remains low.

Table 6.1. Parameters used in the newly developed electrosteric kinetic model.

(Superscript 'a' represents the value used was from this work)

Parameter	Value (units)
k_p	260 M^{-1} s^{-1} [9]
$k_p{}^1$	4 k_p [9]
k_d	4×10^{-6} s^{-1} [18]
k_t	1.75×10^9 M^{-1} s^{-1} [19]
k_{tr}	9.3×10^{-3} M^{-1} s^{-1} [20]
C_w	4.3×10^{-3} M [9]
C_p	7.1 M [a)]
N_p	9.66×10^{18} L^{-1} [a)]
r_s	22.8 nm [a)]
δ	1.25 nm [a)]
D_w	1.3×10^{-9} m^2 s^{-1} [9]
D_h	7.2×10^{-11} m^2 s^{-1} [a)]
k_{abs}	8.4×10^5 M^{-1} s^{-1} [14]
k_{trAA}	2.1×10^3 M^{-1} s^{-1} [a)]
[AA]	0.23 M [a)]
Φ_{HL}	0.02 [a)]

The calculated steady-state values of the entry rate coefficient ρ (and subsequently the entry efficiency f_{entry}) from this model are very close to those found experimentally when assuming first-order loss kinetics, and are in good agreement with the accepted 'control by aqueous phase growth' entry mechanism (see Figures 6.3 and 6.4). This is strong supporting evidence for the use of Limit 1 kinetics during the experimental data processing to calculate experimental entry

rate coefficients in Chapter 5. The 'normal' values of ρ and f_{entry} (i.e. values that are in good agreement with established mechanisms) can be rationalized by considering the likely fates for a surface active *z*-mer, namely entry into a particle or transfer/termination on the particle surface. The likelihood of a *z*-mer undergoing an entry event (given by the pseudo-first-order rate coefficient $k_e N_p/N_A$) is several orders of magnitude more likely than a transfer/termination event on the particle surface prior to entry, making any change to the overall entry rate coefficient ρ essentially insignificant (any significant competition between entry and a loss event on the particle surface only occurs at particle sizes that are extremely small (10 nm swollen radius), and would be difficult to synthesize). The same can be said for the kinetics of re-entry – an exited radical will most likely re-enter, but very few radicals actually escape from a particle into the aqueous phase in the first place.

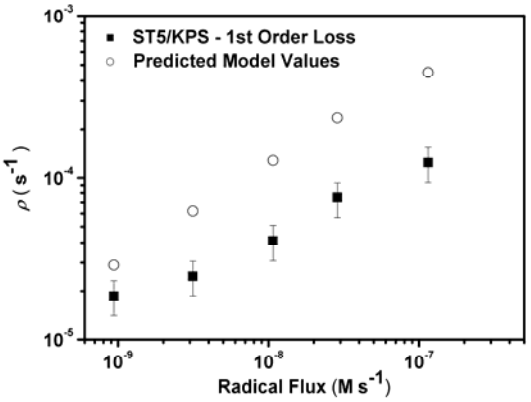

Figure 6.3. Comparison of radical entry rate coefficients obtained for the ST5 latex assuming first order loss (black squares) and those obtained from the new kinetic model (open circles).

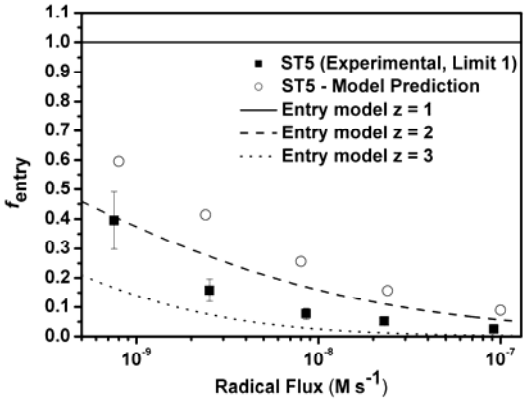

Figure 6.4. Comparison of radical entry efficiencies obtained for the ST5 latex assuming first order loss (black squares) and those obtained from the new kinetic model (open circles).

From the model values of ρ and $\overline{n}_{ss}$, exit rate coefficients assuming both Limit 1 and Limit 2a kinetics were calculated from the appropriate limiting forms of the zero-one equations. As expected, 'sensible' values of k (that were also consistent with experiment) are only found when Limit 1 kinetics are used, due to the linear dependence with respect to $\overline{n}$.

6.2.2. Sensitivity Analysis

It is important to consider the behaviour of the newly developed model, when some of the critical input parameters are varied, to ensure the consistency of the explained results. While the 'best available' parameter values were chosen for this modelling, the model must be robust enough to yield the same conclusion when the parameters are adjusted over a physically reasonable range. Model variables, such as k_{abs} (the abstraction rate coefficient), D_h (the diffusion coefficient within the hairy layer) and k_d (the decomposition rate coefficient of initiator), were tested for parameters that are experimentally measurable: the average number of radicals per particle $\overline{n}$ and the entry efficiency f_{entry}. The model values were adjusted by up to a factor of 10 to see the significance of any changes. The results of the sensitivity analysis are shown in Figures 6.5 and 6.6.

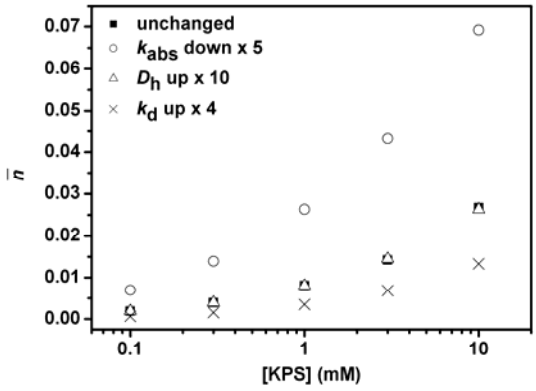

Figure 6.5. Impact of variation of the value of k_{abs} (open circles), D_h (open triangles) and k_d (crosses) on the model $\bar{n}_{ss}$ values (filled squares) from the electrosteric kinetic model.

It was seen that increasing the value of D_h by a factor of 10 (i.e. making the diffusion through the hairy layer faster) had essentially no impact on the model values for both parameters. This is because the 'slow diffusion' is not the dominant fate for very small particles – the dominant fate is instead transfer/termination. Variation of k_d was important only for f_{entry} calculations (Figure 6.6), which makes sense intuitively as k_d dictates the overall rate of initiator-derived radicals and as a consequence how many can actually enter particles. The variation in f_{entry}, when k_d was increased by a factor of four, was approximately a two-fold increase; given the size of the relative error in entry rate coefficient calculations, this does not change the conclusions from the model. A decrease in k_d was modelled because the decomposition rate of persulfate was shown to vary in the presence of polyAA,[18] with the value of k_d quoted to be approximately a factor of four larger than in pure water.

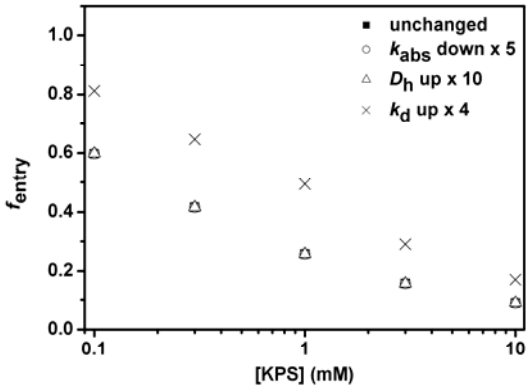

Figure 6.6. Impact of variation of the value of k_{abs} (open circles), D_h (open triangles) and k_d (crosses) on the model f_{entry} values (filled squares) from the electrosteric kinetic model.

The main parameter of interest was k_{abs}, the rate of abstraction of a hydrogen atom along the polyAA chains on the particle surface to form a mid-chain radical. A decrease by a factor of five was modelled; this translated into approximately a three-fold increase in $\overline{n}$ (Figure 6.5). This is because transfer/termination is not as dominant as the value of k_{abs} is reduced; however it should be pointed out that the value of k_{abs} chosen was a lower bound from experimental work involving abstraction of hydrogen atoms via sulfate ion radicals;[14] any modelled increase in k_{abs} makes the model results even more 'first-order'-like. The conclusions drawn from this model do change if the abstraction rate is much slower than assumed – we are in essence reverting back to Limit 2a kinetics (or a hybrid between the two limits) as successful desorption of a monomeric radical becomes more and more likely.

An accurate experimental value for such a rate coefficient in a system such as this (the encounter between a monomeric styrene radical and a polyAA chain) is most likely to be very difficult to measure. Therefore while it is hoped that the value chosen is appropriate, it should be pointed out that a long-chain limit value of k_{trAA} (the transfer rate coefficient in styrene polymerizations while using polyAA as a chain transfer agent) was measured in separate bulk experiments (see Chapter 5); if we consider that the transfer rate coefficient for a monomeric radical scales

analogously to the situation involving propagation of radicals[21-23] then we obtain a value of k_{trAA} that is large enough (2.1×10^4 M^{-1} s^{-1}) to account for observed results (low $\bar{n}$, apparent first-order loss kinetics) without the need to consider mid-chain radicals being formed by abstraction reactions involving radicals with a sulfate end-group. It should be noted that this process is kinetically equivalent to the postulated mechanism put forward in this model and all of the results remain unchanged.

While the model constructed here is sensitive to the size of the transfer/abstraction rate coefficient (essentially the key process in the different mechanism at play in these electrosterically stabilized systems), the use of realistic values for all parameters chosen suggests that the conclusions drawn from this model are indeed valid.

6.2.3. Model Behaviour as a Function of Particle Size

The model was used to make predictions for the behaviour of electrosterically stabilized latexes as a function of size. Despite the ST5, ST10 and ST20 latexes being all the same (small) size (meaning that the parameter of particle size was not originally tested experimentally), it is hoped that the predictive power of this model will provide insight into the behaviour of larger particles stabilized in this manner. It is intuitive that as the size of the polystyrene core becomes larger, the volume fraction of the aqueous phase that exists within the hairy layer (Φ_{HL}) decreases significantly (the total solids content of the latex being held constant). The increased surface area per particle means that each polyAA chain occupies more surface area and the local [AA] concentration within the hairy layer is reduced. This decreases the likelihood of a transfer or abstraction, resulting in a reduction in the steady-state mid-chain radical concentration ([MCR]).

Calculations were performed for a seed latex with a solids content of 10% w/w, stabilized by polyAA chains of average DP = 5. The experimentally determined quantity of 220 stabilizing chains per particle was used in this modelling. The persulfate concentration was held constant at

10^{-3} M, while the swollen particle radius was allowed to vary from 15 to 50 nm. All other parameters used were as reported in Table 6.1. Estimates were made for $D_h(r_s)$, the diffusion coefficient of a monomeric radical within the hairy layer, based on a value determined from the literature[24] (D_h = 7.2 $\times 10^{-11}$ m^2 s^{-1} for particles of swollen radius 22 nm, as used in the experimental work on radical exit (Chapter 4) for these systems) and the known variation of the diffusion coefficient D of a radical in polymer solutions of differing w_p.[25] (The sensitivity analysis performed on this model however demonstrated little variation when the value of D_h was varied by up to a factor of 10, indicating that the precision in this parameter is not critical).

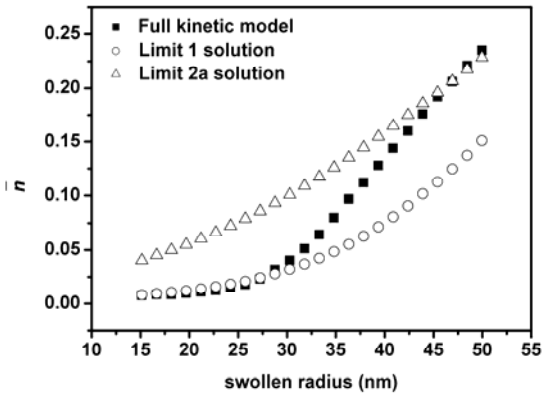

Figure 6.7. Variation of $\bar{n}_{ss}$ ([KPS] = 1 mM) as calculated by the electrosteric kinetic model for a 10% solids latex (filled squares) as a function of particle size, with comparison to the Limit 1 solution (open circles) and Limit 2a solution (open triangles) for such systems.

It was seen from these calculations that the $\bar{n}_{ss}(r_s)$ calculations yielded extremely interesting and informative results. Very small particles gave values of $\bar{n}_{ss}$ that were similar to those predicted by Limit 1 kinetics for an electrostatically stabilized system of identical particle size, but as the particle size increased the value of $\bar{n}_{ss}$ converged towards the Limit 2a value (see Figure 6.7). This suggests a cross-over in the applicable limit in these systems at an intermediate particle size (approximately 35 nm swollen radius) whereby particles larger than this cross-over point

essentially obey 'expected' styrene emulsion kinetics and the effect of the hairy layer is no longer seen.

This observed limit cross-over can be rationalized by comparing the size of the two differing loss mechanisms in these systems – the first-order loss term (transfer or termination) and the second-order loss term (desorption from the particle). For very small particles, the densely packed hairy layer makes rapid abstraction and subsequent termination very likely, while the sparsely covered surface of a larger electrosterically stabilized latex means that successful desorption is more likely than encountering an AA unit or a MCR. The relative sizes of these terms are seen in Figure 6.8.

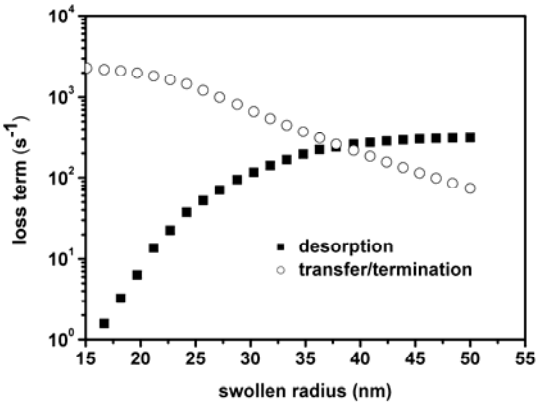

Figure 6.8. Comparison of desorption (filled squares) and transfer/termination (open circles) loss terms as a function of particle size within the electrosteric kinetic model (10% w/w latex).

6.2.4. A Full Model for the Exit Rate Coefficient in Electrosterically Stabilized Systems

The details of the model presented thus far are essentially "limit free" – the sub-limits of the zero-one approximation have not been considered, rather the full solution of the governing kinetic equations. The behaviour of the model has demonstrated that there is a strong changeover between apparent first-order loss kinetics (dominated by termination with (assumed) mid-chain

radicals) and classical desorption and re-entry (second-order loss) as the particle size increases. Ideally an expression for the microscopic rate coefficient for exit (k) as a function of all key parameters should be able to be determined.

If transfer and termination of monomeric styrene radicals with AA units and mid-chain radicals (MCR's) (which has to be preceded by diffusion into the hairy layer from the particle interior) are included in the relevant kinetic equations (see Equation 6.3), then the steady-state expression for $N_1^{\,m}$ (the number of particles with one monomeric species) is given by:

$$N_1^{\,m} = \frac{k_{tr} C_p \pi}{k_{dM} \pi + k_p^{\,1} C_p + P_{des}(k_{trAA}[AA] + k_t[MCR])} \tag{6.10}$$

where all terms are as defined previously. This allows the determination of the (new) full zero-one limit expression for the time evolution of $\bar{n}$, namely:

$$\frac{d\bar{n}}{dt} = \rho(1 - 2\bar{n}) - k_{tr} C_p \left(\frac{k_{dM}\bar{n} + P_{des}(k_{trAA}[AA] + k_t[MCR])}{k_{dM}\bar{n} + k_p^{\,1} C_p + P_{des}(k_{trAA}[AA] + k_t[MCR])} \right) \bar{n} \tag{6.11}$$

The loss term in Equation 6.11 is essentially the microscopic rate coefficient term with both a first-order and a second-order component. The numerator of the above fraction is the key determinant in which limit is most appropriate – the larger of the two terms will dictate the order of the loss mechanism (i.e. if $k_{dM}\bar{n}$ is the larger term, the system is essentially second-order, if $P_{des}(k_{trAA}[AA] + k_t[MCR])$ is larger the system is equivalent to a first-order loss mechanism. From our global model, two limiting expressions for the exit rate coefficient k can be described:

$$\textit{Limit 1: } k_1 = k_{tr} C_p \left(\frac{P_{des}(k_t[MCR] + k_{trAA}[AA])}{k_p^{\,1} C_p + P_{des}(k_t[MCR] + k_{trAA}[AA])} \right) \tag{6.12}$$

$$\textit{Limit 2a: } k_{2a} = \frac{k_{dM\,HL} k_{tr}}{k_p^{\,1}} \tag{6.13}$$

where $k_{dM\ HL}$ is given by Equation 6.5. For the sake of completeness, the transfer/termination term can be included in the Limit 2a expression (Equation 6.13) as it does not become vanishingly small at bigger particle sizes but it is largely insignificant. Using the 'new' Limit 1 expression, a small value of k for a particle of the size used in the corresponding experimental work (22 nm swollen radius) is obtained, compared to that in a particle of the same size without a hairy layer on the surface. This is because 'true escape' rarely happens; a very large percentage of monomeric radicals that actually make it into the hairy layer will be terminated rather than diffuse into the aqueous phase. Mathematically this quantity is similar to the 'restricted diffusion' model developed in Chapter 4. The agreement between this model and experiment is shown in Table 6.2, and it can be seen that the agreement is very good (using the same parameters as given in Table 6.1). The model developed however predicts an increase in k with hair length on the particle surface; however this increase (from 5 to 20 AA units) leads to only a slight increase in k. Within experimental uncertainty, this model fits the values found from first-order fitting of gamma-relaxation experiments. (The slope/intercept results from gamma-relaxation experiments are also very similar in terms of the obtained k values).

Table 6.2. Comparison between experimentally determined Limit 1 exit rate coefficients (k) for electrosterically stabilized latexes made by the RAFT-in-emulsion method and those determined by the electrosteric kinetic model in this work.

Latex	k (Limit 1, experimental) (s^{-1})	k (Limit 1, theoretical model) (s^{-1})
ST5	$6.76\ (\pm 1.32) \times 10^{-3}$	6.99×10^{-3}
ST10	$5.12\ (\pm 1.7) \times 10^{-3}$	7.11×10^{-3}
ST20	$5.05\ (\pm 1.37) \times 10^{-3}$	7.90×10^{-3}

6.2.5. Comparison With Previous Experimental Data

The experimental data collected in this project to understand the kinetics of electrosterically stabilized emulsion systems was through the use of 'model' systems made by the RAFT-in-emulsion process. This has provided a crucial tool for controlling parameters such as the length of the stabilizing block and being able to determine the extent of surface coverage and stabilizer concentration accurately. In turn, this has made comparison with the developed kinetic model to be relatively easy, as traditionally hard-to-measure parameters were well understood.

A crucial component of modeling the kinetics of these systems is to consider those synthesized without the use of a control agent, i.e. free-radically synthesized electrosterically stabilized latexes. The bulk of latexes made on an industrial scale are synthesized in this manner and naturally a deeper understanding of how these systems behave is desirable. Such latexes were used in the kinetic studies of Coen[1] and Vorwerg,[2] where the main complication was that there was no means to characterize or determine the nature of the hairy layer. Using the more accurate experimental work of Vorwerg, an attempt was made to compare the kinetic data from the seed latexes used in that work to the developed model presented in this Chapter (by including the additional loss terms of transfer/termination that had previously not been accounted for).

Using an estimate of the width of the hairy layer at $\delta = 2.5$ nm, parameters such as [AA] and Φ_{HL} were estimated from the recipe for the seed latex syntheses in Vorwerg's work. Both the 'low coverage' latex (5% w/w AA) and 'high coverage' latex (15% w/w AA) were of the order of 35-40 nm swollen radius, placing them in the 'cross-over' region (see Figure 6.7) somewhat between Limit 1 and Limit 2a. It can be seen in Table 6.3 that the general treatment developed within this kinetic model is able to predict the values of $\bar{n}_{ss}$, ρ and the Limit 2a k value of Vorwerg's (Vorwerg treated his data assuming Limit 2a kinetics) to within 20-30 %, an excellent result considering the minimal number of adjustable parameters within the model. It should therefore be possible to predict the overall kinetics (and the appropriate limit to use) for any

electrosterically stabilized latex given a reasonable knowledge of the width and density of the hairy layer on the particle surface, a powerful result for such systems as such analysis has never before been possible.

Table 6.3. Comparison between experimental data collected by Vorwerg for uncontrolled electrosterically stabilized latexes and model values determined in this work.

'Low Coverage' AA Latex (1.94×10^{17} L^{-1})

[KPS] (M)	$\bar{n}$		ρ		k (Limit 2a)	
	Experiment	Model	Experiment	Model	Experiment	Model
6×10^{-4}	0.2	0.259	2.4×10^{-3}	1.9×10^{-3}	5.2×10^{-3}	7.1×10^{-3}

'High Coverage' AA Latex (7.3×10^{16} L^{-1})

[KPS] (M)	$\bar{n}$		ρ		k (Limit 2a)	
	Experiment	Model	Experiment	Model	Experiment	Model
7.5×10^{-4}	0.37	0.26	7×10^{-3}	5.31×10^{-3}	1.2×10^{-2}	1.8×10^{-2}
8×10^{-3}	0.42	0.403	1.34×10^{-2}	1.9×10^{-2}	1.2×10^{-2}	1.3×10^{-2}

6.2.6. Refining the Extended Kinetic Model

As was mentioned in Section 6.2.2, this modelling can be performed by considering that the hydrogen abstraction event from the polyAA backbone is caused by an exiting monomeric radical, without the need to consider MCRs being formed by abstraction reactions involving radicals with a sulfate end-group (such as primary radicals from initiator). Assuming that the transfer rate coefficient for a monomeric radical scales analogously to the situation involving

propagation of radicals[21-23] then we obtain a value of k_{trAA} that is large enough (2.1×10^4 M^{-1} s^{-1}) to account for observed results (low $\bar{n}$, apparent first-order loss kinetics).

This modelling can be refined even further. By considering the stabilizer concentration within the hairy layer as a 'local' concentration, while considering the MCR concentration as a 'bulk' concentration, then the loss terms such as termination of a MCR with an aqueous-phase *z*-mer (when it enters the hairy layer) are easily incorporated. In this case again we assume that it is the exiting species (a member of the N_1^m population) that undergoes chain-transfer to polyAA, as well as termination with a MCR. The result obtained from this modelling is kinetically equivalent to the earlier model described in this Chapter: however it makes more sense intuitively. It is the monomeric radicals that will be crossing the particle/water interface and moving through the hairy layer, while only a small fraction of initiator-derived sulfate radicals will reside in the hairy layer at any given time. One must also consider that the unusual kinetics were observed experimentally for a range of systems where different chemical initiators were used that did not contain sulfate radicals or sulfate groups. Because of this the modelling must be consistent in its approach in explaining these systems. The key equations that now differ from the original derivation of the model are:

$$\frac{dN_1^m}{dt} = \rho_{re}N_0 - \rho N_1^m - k_{dM}N_1^m + k_{tr}C_pN_1^p - k_p^1C_pN_1^m - P_{des}\left(k_{abs}[AA]N_1^m + 2\,k_t[MCR]\,N_1^m\frac{N_p}{N_A}\right) \tag{6.14}$$

$$\frac{d[MCR]}{dt} = P_{des}\,N_1^m\frac{N_p}{N_A}\left(k_{abs}\,\Phi_{HL}\,[AA] - 2\,k_t\,[MCR]\right) - k_{beta}[MCR] - 2\,k_t\,[MCR]\sum_{j\geq z}[IM_j^{\bullet}] \tag{6.15}$$

where k_{beta} is the rate coefficient for beta-scission (as it is well known[17, 26] that acrylates bearing tertiary mid-chain radicals can undergo beta-scission); the value for this rate coefficient was chosen to be 0.18 s^{-1}.[17] The issue of beta-scission will be considered in significantly more detail in the next Chapter. All other parameters in Equations 6.14 and 6.15 are as defined previously. Time dependence of rate coefficients (such as the time dependence of the diffusion-controlled entry rate coefficient k_e) can be included at this stage but is an unnecessary complication. As previously stated, this more robust model yields essentially identical results to the initial work, and the same conclusions are ultimately drawn.

6.3. Supporting Experimental Evidence

One significant result obtained from the extended kinetic model for electrosterically stabilized emulsion polymerization systems is that the apparent first-order loss mechanism is only dominant for small particles (i.e. particles with a swollen radius less than approximately 35 nm for this particular system), while larger particles exhibit the standard second-order loss mechanism (desorption followed by re-entry) for styrene systems.[4, 27] In essence, larger particles experience no effect from the presence of the polymeric stabilizer on their overall kinetics. Experimental validation of this behaviour would be strong supporting evidence of the proposed kinetic model.

6.3.1. Kinetic Experiments Involving Larger Seed Latexes

The 'RAFT-in-Emulsion' method typically results in very small particles when synthesized from an initial pre-formed diblock; the size of the latexes used in this work was well within the region dominated by Limit 1 kinetics according to the kinetic model. To test the behaviour of the model at larger particle sizes, the latex at the end of a seeded dilatometric experiment (one that had been further polymerized, resulting in a large final seed latex) was used as the seed in a new experiment. This method allowed a model parameter (the number of stabilizing groups per

particle) to be held constant, meaning that the surface area per stabilizing chain was significantly increased (and local AA concentration was significantly decreased).

Dilatometric experiments were conducted in accordance with the method outlined in Chapter 5. Latexes were chemically initiated with KPS at three different initiator concentrations spanning two orders of magnitude. The latex was stabilized by polyAA chains of average degree of polymerization = 5 and the swollen radius was 46 nm, much larger than the seed originally used (22 nm). As no γ-relaxation experiments were performed on this latex to determine the exit rate coefficient k, only steady-state values of $\bar{n}$ were calculated. In agreement with the developed kinetic model, much larger values of $\bar{n}_{ss}$ were determined for this latex, in reasonable agreement with the model prediction (see Table 6.4). This again validates the developed model and suggests that the unusual kinetic behavior of electrosterically stabilized latexes is restricted to very small particles.

Table 6.4. Comparison between experimental values of $\bar{n}_{ss}$ for the large ST5 latex and model values obtained by the electrosteric kinetic model for particles of that size.

[KPS] (M)	$\bar{n}$ (Experiment)	$\bar{n}$ (Model)
1.51×10^{-4}	0.069	0.067
1.06×10^{-3}	0.145	0.162
1.34×10^{-2}	0.33	0.269

6.3.2. Competitive Growth Experiments

'Competitive growth' experiments (the seeded polymerization of a bimodal particle size distribution) were originally pioneered by Vanderhoff *et al*.[28] (with subsequent interpretation by Morrison *et al*.[29]) to verify that the entry step (once a radical reaches the critical degree of

polymerization *z*) is diffusion-controlled and as a result has a rate proportional to the radius of the particle that the radical is encountering.

Much information can be obtained by synthesizing two latexes of differing sizes, mixing them together and then polymerizing them on further in seeded experiments. This is because the particles grow at different rates, given that adsorption is proportional to particle size, while radical exit (through transfer then desorption) is proportional to the inverse square of particle size. By monitoring the particle size distribution (PSD) before and after polymerization, the rate coefficient of entry into both particles can be determined. As long as the system remains in Interval II (where the polymerization rate is constant), the value of $\overline{n}_{ss}$ can be found from the following equation:[30]

$$\overline{n}_{ss} = \frac{\frac{4}{3}\pi\,(r_f^3 - r_i^3)\,d_p\,N_A}{k_p\,C_p\,M_0\,t_s} \tag{6.16}$$

where r_i and r_f are the initial and final particle sizes respectively, d_p the density of the polymer, M_0 the molecular weight of the monomer and t_s the time period between the start of the reaction and the time that sampling took place (all other parameters as defined previously).

If we consider two particle populations A and B of differing particle sizes, the rate coefficients for radical entry (denoted ρ_A and ρ_B) can be found from the values of $\overline{n}_{ss}$ for the two latexes. If Limit 1 kinetics are valid (i.e. termination in the aqueous phase, re-entry not significant) then the mathematics is simple – from the steady-state expressions one has:

$$\rho_A = \frac{k_A\,\overline{n}_{ss}^{\,A}}{(1 - 2\,\overline{n}_{ss}^{\,A})} \tag{6.17}$$

where k_A is the exit rate coefficient for latex A (found from independent experiments); an equivalent expression holds for latex B.

If re-entry is significant in a competitive growth experiment, then the kinetic equations are significantly more complicated, as an exited species from latex A can enter a particle from latex B and vice-versa. The extended Smith-Ewart equations need to be considered for both sets of populations; the steady-state approximation is applied to the population of particles from each latex containing one monomeric radical (denoted N_1^{mA} and N_1^{mB} respectively). The exited radical population also is of significance and needs to be considered. The steady-state expressions are:

$$N_1^{mA} = \frac{k_{tr}\, C_p\, N_1^{pA} + k_{reA}[E^\bullet]\, N_0^{A}}{k_p^{1}\, C_p + k_{dM}^{A}} \tag{6.18}$$

$$N_1^{mB} = \frac{k_{tr}\, C_p\, N_1^{pB} + k_{reB}[E^\bullet]\, N_0^{B}}{k_p^{1}\, C_p + k_{dM}^{B}} \tag{6.19}$$

$$[E^\bullet] = \frac{k_{dM}^{A}\, N_1^{mA}\, (N_p^{A} / N_A) + k_{dM}^{B}\, N_1^{mB}\, (N_p^{B} / N_A)}{k_{reA}\, (N_p^{A} / N_A) + k_{reB}\, (N_p^{B} / N_A)} \tag{6.20}$$

where N_p^{A} and N_p^{B} are the particle numbers (units [continuous phase volume]$^{-1}$) of the two latexes, k_{reA} and k_{reB} the re-entry rate coefficients (given by the Smoluchowski equation for diffusion-controlled reactions), N_0^{A} and N_0^{B} the number of particles from both populations containing no radicals, and N_1^{pA} and N_1^{pB} the number of particles containing one polymeric radical. By making the assumption (for both populations A and B) that $N_1^{p} = \overline{n}_{ss}$ and $N_0 = 1 - N_1^{p}$, Equations 6.18 – 6.20 can be solved simultaneously. Once these three populations are known, the rate coefficients ρ_A and ρ_B can then be found through further steady-state approximations (this time for the time evolution of $\overline{n}$):

$$\rho_A = \frac{k_p^{1}\, C_p\, N_1^{mA} - \overline{n}_{ssA}\, (k_{tr}\, C_p + k_{reA}\, [E^\bullet])}{2\, \overline{n}_{ssA} - 1} \tag{6.21}$$

$$\rho_B = \frac{k_p^{1}\, C_p\, N_1^{mB} - \overline{n}_{ssB}\, (k_{tr}\, C_p + k_{reB}\, [E^\bullet])}{2\, \overline{n}_{ssB} - 1} \tag{6.22}$$

In this work, competitive growth experiments were performed using the ST5 and ST10 latexes with their larger equivalent (denoted ST5L and ST10L, formed by growing ST5 and ST10 to a larger size, then cleaning and characterizing those latexes). The particle numbers of average radii of these latexes (measured by HDC as described in Chapter 2) were: ST5L – r_s = 46.4 nm, N_p = 4.9×10^{17} L^{-1}, ST10L – r_s = 39.2 nm, $N_p = 9.1 \times 10^{17}$ L^{-1}. Samples of ST5 and ST5L (as well as ST10 with ST10L) were mixed, with the amount of each latex added chosen such that the number of particles from each population was approximately equal, and the mixed latex was polymerized with styrene (initiation by KPS) at 323 K. Three different initiator concentrations were chosen spanning two orders of magnitude. Samples (2 mL via syringe) were drawn at either 5000 s or 10000 s after commencement of polymerization, the sample inhibited with a hydroquinone solution and the PSD determined by HDC. TEM counts were also performed to ensure the validity of HDC analysis (obtaining the distribution via HDC is significantly quicker and allows for convenient comparison but must be confirmed by a more rigorous method). The evolution of the PSD in a typical experiment is shown in Figure 6.9, while the measured $\bar{n}_{ss}$ data for both latexes is presented in Table 3.2.

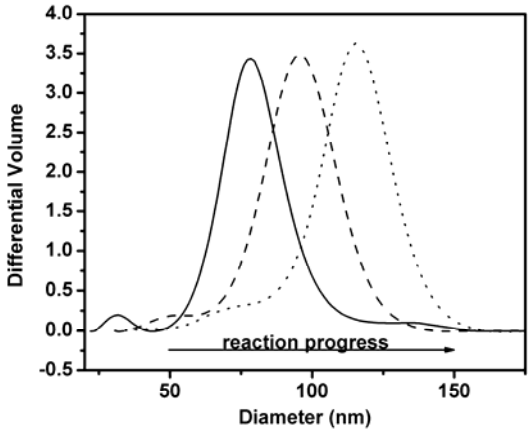

Figure 6.9. Evolution of Particle Size Distribution (PSD, volume distribution) as obtained by HDC for the ST5/ST5L Competitive Growth Experiment ([KPS] = 10 mM). Distributions shown are: Starting Distribution (solid line), Distribution after 5000 s polymerization (dashed line) and Distribution after 10 000 s polymerization (dotted line). The small peak at low particle sizes represents the 'small latex' population, distribution confirmed by TEM.

The choice as to how the data collected in these experiments is processed reveals a great deal into the kinetics governing them. As demonstrated experimentally by Morrison,[29] the ratio of entry rate coefficients of the two latexes is approximately equal to the ratio of the particle radii when re-entry kinetics are assumed. This is not true however for the electrosterically latexes considered here; the ratio of the entry rate coefficients is substantially smaller than the ratio of the radii (Figure 6.10). This is because, as modelling and prior experimental data have shown, the assumption of complete re-entry is an invalid one for small electrosterically stabilized latexes.

Table 6.5. Particle size (from maxima in PSD) and $\bar{n}_{ss}$ data from competitive growth experiments for the ST5 and ST10 latexes (for 5000 s polymerization time). All sizes are diameters (nm).

ST5			
[KPS]	0.1 mM	1 mM	10 mM
Initial size (small)	24.6	24.6	24.6
Final size (small)	30.4	35.1	41.3
$\bar{n}_{ss}$	6.49×10^{-4}	1.91×10^{-3}	3.4×10^{-2}
Initial size (large)	74.9	74.9	74.9
Final size (large)	81.4	85.3	91.2
$\bar{n}_{ss}$	1.41×10^{-3}	5.9×10^{-3}	1.28×10^{-1}
ST10			
Initial size (small)	19	19	19
Final size (small)	27.9	32.4	37.4
$\bar{n}_{ss}$	1.11×10^{-3}	2.2×10^{-3}	$1.58 \times 10^{-2-}$
Initial size (large)	55.8	55.8	55.8
Final size (large)	60.6	66.7	71.5
$\bar{n}_{ss}$	4.27×10^{-3}	1.15×10^{-2}	7.72×10^{-2}

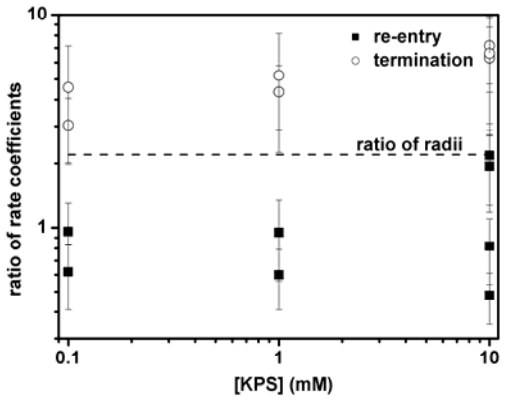

Figure 6.10. Ratio of entry rate coefficients from competitive growth experiments assuming re-entry of exited monomeric radicals (filled squares) and complete aqueous-phase termination (open circles) as a function of initiator concentration. Note the logarithmic y-axis.

The use of 'first-order' loss kinetics in the data processing from these experiments also gives poor results, as the ratio of rate coefficients calculated in this manner is large (note the logarithmic scale in Figure 6.10). The extended kinetic model demonstrated that larger particles (such as the size of the ST5L and ST10L latexes used here) are more likely to exhibit re-entry kinetics due to the reduced stabilizer concentration on the particle surface reducing the likelihood of a transfer/termination event. To allow for the different limits of these two latexes to be considered, a mathematical assumption was made; k_{dMsmall} (the rate coefficient for desorption of a monomeric radical of the latex of smaller particle size) was set to 0 to ensure that the exited radical population was due in entirety to the larger particles. Once this assumption was made, the agreement between the experimental and theoretical ratio was shown to be much improved relative to conventional data treatment (Figure 6.11). This again provides another piece of supporting experimental evidence to suggest that the additional transfer/termination mechanism is real and dominates in systems where the average particle size is small (below 35 nm swollen radius) and the particle surface is densely covered.

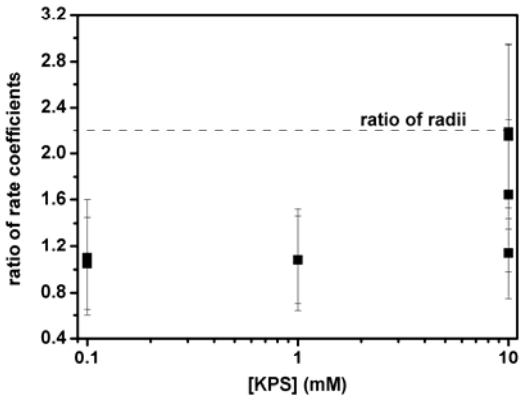

Figure 6.11. Ratio of entry rate coefficients from competitive growth experiments assuming successful exit (desorption) only takes place from large particles.

6.4. Conclusions

In this Chapter, the development of an extended kinetic model to rationalize the apparently inconsistent experimental results for electrosterically stabilized latexes was presented. By considering the apparent first-order loss mechanism that was evident from radical entry experiments and the subsequent explanation (rapid chain transfer to polyAA 'hairs on the particle surface being the dominant loss mechanism) of this phenomenon, these additional mechanistic steps (transfer as well as subsequent termination with the mid-chain radical (MCR)) were included in the kinetic equations that govern particle growth in emulsion systems.

The inclusion of these additional terms (and sensible values of the rate coefficients of these processes) yielded model predictions for $\bar{n}_{ss}$ and f_{entry} that were in good agreement with experiment, interpreted assuming a first-order loss mechanism. This is because the fate of a monomeric radical (capable of exit) is now a competition between different events: successful exit (desorption), as well as the first-order terms of transfer/termination. It was shown that for small, densely covered electrosterically stabilized particles, the likelihood of transfer/termination

is far greater than that of desorption – providing a theoretical validation of the experimental results presented in the previous Chapter. Sensitivity analysis demonstrated only a weak dependence on the key model parameters except for the abstraction rate coefficient k_{abs}: however a experimental lower bound was used in the modelling and it is anticipated that this value is realistic. The conclusions of the model did not change as these parameters were varied.

The particle size dependence of the developed model was tested and it was seen that the relative likelihoods of the various fates of a monomeric radical changed as the particle size increased. As the particles became larger (and the local stabilizer concentration decreased), the rate of successful desorption became much larger than transfer/termination; ultimately the kinetics of these system return to 'normal' Limit 2a kinetics that is well known for styrene-based emulsion systems. The conclusion from this was that the additional loss mechanisms determined in this work are only significant for small electrosterically stabilized particles: however the significant implication from this is that a huge number of industrial emulsion recipes incorporate the use of small, polymerically stabilized seed latexes, making consideration of these terms extremely significant.

Experiments using larger electrosterically stabilized seed latexes were developed to validate the size dependence of the developed model. It was shown that larger latexes (that still fall within the zero-one kinetic region) had much larger values of $\bar{n}_{ss}$ than their smaller counterparts and that these values were very close to the 'expected' Limit 2a (exit then re-entry) result. Similarly 'competitive growth' experiments (where a mixed latex possessing a bimodal particle size distribution was polymerized in seeded experiments) demonstrated that successful exit by desorption is only valid for the larger particles, while the small particles once again demonstrated a first-order loss mechanism. All experiments that were performed for the purpose of model refutation demonstrated agreement with the proposed mechanisms.

References

1. Coen, E. M.; Lyons, R. A.; Gilbert, R. G. *Macromolecules* **1996,** 29, 5128-5135.

2. Vorwerg, L.; Gilbert, R. G. *Macromolecules* **2000,** 33, 6693-6703.

3. Lansdowne, S. W.; Gilbert, R. G.; Napper, D. H.; Sangster, D. F. *Journal of the Chemical Society, Faraday Transactions 1: Physical Chemistry in Condensed Phases* **1980,** 76, 1344-55.

4. Morrison, B. R.; Casey, B. S.; Lacik, I.; Leslie, G. L.; Sangster, D. F.; Gilbert, R. G.; Napper, D. H. *Journal of Polymer Science, Part A: Polymer Chemistry* **1994,** 32, 631-49.

5. Maxwell, I. A.; Morrison, B. R.; Napper, D. H.; Gilbert, R. G. *Macromolecules* **1991,** 24, 1629-40.

6. Guillet, J. E.; Burke, N. A. D. Production of graft copolymers by graft polymerization from the polymer backbone containing attached stable free radicals. 98-2249955

2249955, 19981013., 2000.

7. Loiseau, J.; Doërr, N.; Suau, J. M.; Egraz, J. B.; Llauro, M. F.; Ladavière, C. *Macromolecules* **2003,** 36, 3066-77.

8. Smith, W. V.; Ewart, R. H. *Journal of Chemical Physics* **1948,** 16, 592-9.

9. Gilbert, R. G., *Emulsion Polymerisation: A Mechanistic Approach*. Academic Press: San Diego, 1995.

10. Ahmad, N. M.; Heatley, F.; Lovell, P. A. *Macromolecules* **1998,** 31, 2822-2827.

11. Nikitin, A. N.; Castignolles, P.; Charleux, B.; Vairon, J.-P. *Macromolecular Rapid Communications* **2003,** 24, 778-782.

12. Arzamendi, G.; Plessis, C.; Leiza, J. R.; Asua, J. M. *Macromolecular Theory and Simulations* **2003,** 12, 315-324.

13. Thickett, S. C.; Gilbert, R. G. *Macromolecules* **2005,** 38, 9894-9896.

14. Gilbert, B. C.; Lindsay Smith, J. R.; Taylor, P.; Ward, S.; Whitwood, A. C. *Journal of the Chemical Society, Perkin Transactions 2: Physical Organic Chemistry* **1999**, 1631-1637.

15. Dong, Q.; Liu, Y. *Journal of Applied Polymer Science* **2004,** 92, 2203-2210.

16. Burguiere, C.; Chassenieux, C.; Charleux, B. *Polymer* **2002,** 44, 509-518.

17. von Sonntag, C.; Bothe, E.; Ulanski, P.; Deeble, D. J. *Radiation Physics and Chemistry* **1995,** 46, (4-6, Proceedings of the 9th International Meeting on Radiation Processing, 1994, Pt. 1), 527-32.

18. Henton, D. E.; Powell, C.; Reim, R. E. *Journal of Applied Polymer Science* **1997,** 64, 591-600.

19. van Berkel, K. Y.; Russell, G. T.; Gilbert, R. G. *Macromolecules* **2003,** 36, 3921-3931.

20. Tobolsky, A. V.; Offenbach, J. *Journal of Polymer Science* **1955,** 16, 311-14.

21. Heuts, J. P. A.; Gilbert, R. G.; Radom, L. *Macromolecules* **1995,** 28, 8771-8781.

22. Heuts, J. P. A.; Sudarko; Gilbert, R. G. *Macromolecular Symposia* **1996,** 111, 147-57.

23. Huang, D. M.; Monteiro, M. J.; Gilbert, R. G. *Macromolecules* **1998,** 31, 5175-5187.

24. Yamane, Y.; Ando, I.; Buchholz, F. L.; Reinhardt, A. R.; Schlick, S. *Macromolecules* **2004,** 37, 9841-9849.

25. Strauch, J.; McDonald, J.; Chapman, B. E.; Kuchel, P. W.; Hawkett, B. S.; Roberts, G. E.; Tonge, M. P.; Gilbert, R. G. *Journal of Polymer Science, Part A: Polymer Chemistry* **2003,** 41, 2491-2501.

26. van Herk, A. M. *Macromolecular Rapid Communications* **2001,** 22, 687-689.

27. Casey, B. S.; Morrison, B. R.; Maxwell, I. A.; Gilbert, R. G.; Napper, D. H. *Journal of Polymer Science, Part A: Polymer Chemistry* **1994,** 32, 605-630.

28. Vanderhoff, J. W.; Vitkuske, J. F.; Bradford, E. B.; Alfrey, T. *J. Polym. Sci.* **1956,** 20, 265.

29. Morrison, B. R.; Maxwell, I. A.; Gilbert, R. G.; Napper, D. H. *ACS Symposium Series* **1992,** 492, (Polym. Latexes), 28-44.

30. Morrison, B. The Role of Aqueous-Phase Chemistry in the Kinetics of Emulsion Polymerization. PhD Thesis, The University of Sydney, Sydney, 1994.

7. Secondary Nucleation in Electrosterically Stabilized Systems

Sections of the work presented in this Chapter have previously been published as:

Thickett, S.C., Gaborieau, M. and Gilbert, R.G. *Extended Mechanistic Description of Particle Growth in Electrosterically Stabilized Emulsion Polymerization Systems,* Macromolecules, **2007**, 40, 4710-4720.

"Man is still the most extraordinary computer of all."

John F. Kennedy

7.1. Introduction

This Chapter deals with the issue of secondary nucleation in electrosterically stabilized emulsion polymerization systems. As outlined in Chapter 2, secondary nucleation is the phenomenon where new particles are formed in seeded experiments (i.e. an emulsion polymerization experiment where pre-established polymer particles are used). It is a major issue for the polymer industry as the presence of new (smaller) particles in an emulsion can ruin properties such as the quality of film formation (for latexes used for surface coatings) as well as many other applications. The presence of a bimodal particle size distribution also complicates reaction modelling (which is crucial for polymer reaction engineering, especially on a multi-tonne scale) and in the case of multi-component systems (i.e. the seed polymer and new polymer have different chemical compositions) secondary nucleation leads to 'phase separation' on a sub-micron scale.

For most seeded emulsion formulations, unless extremely unusual reaction conditions are used, (such as abnormally low N_p values – of the order of 10^{12} L^{-1}) secondary nucleation is generally avoided.[1] This avoidance is explained in terms of the surface activity of aqueous-phase oligomer. When an aqueous-phase oligomer becomes surface-active (i.e. the degree of polymerization of the oligomer is z or greater), the likelihood of an entry event into an established particle (with pseudo-first order rate coefficient $k_e N_p / N_A$) is greater than either propagation until degree of polymerization j_{crit} (the particle formation step in the 'homogeneous nucleation' mechanism) or entry into a micelle (the particle formation step in the 'micellar nucleation' mechanism) by several orders of magnitude. This ability to capture aqueous-phase radicals generally ensures no new particle formation; it is usually considered that for particles of 'typical' size (50 nm radius), secondary nucleation need not be considered beyond seed particle numbers of 10^{14} L^{-1}.[1]

The above statement and general mechanistic assumptions presented only apply to electrostatically stabilized emulsion systems. It is well known that significant secondary nucleation has been observed in polymerically stabilized emulsion systems (both sterically and electrosterically stabilized) under conditions where the homogeneous nucleation mechanism predicts that essentially no new particle formation should take place. The micellar nucleation mechanism is unimportant as these systems require no additional surfactant to provide colloisal stability. The work of Vorwerg[2] in measuring exit and entry rate coefficients in polyAA-stabilized latexes was complicated by vast amounts of secondary nucleation and it was shown that the amount of secondary nucleation was a function of pH. Similar issues were met in the work of Hammond[3], who was performing similar experiments but with poly(styrene) latexes stabilized by adsorbed poly(ethylene oxide) (PEO) stabilizing moieties. Figure 7.1 shows the substantial amount of new particles formed in Hammond's work (seed $N_p = 5 \times 10^{16}$ L^{-1}) and the discrepancy between this experimental observation and model predictions. Considering the difference spans several orders of magnitude, the only explanation is that there must be another nucleation mechanism operating in these systems. Attempting to rationalize and understand that mechanism is the focus of this work.

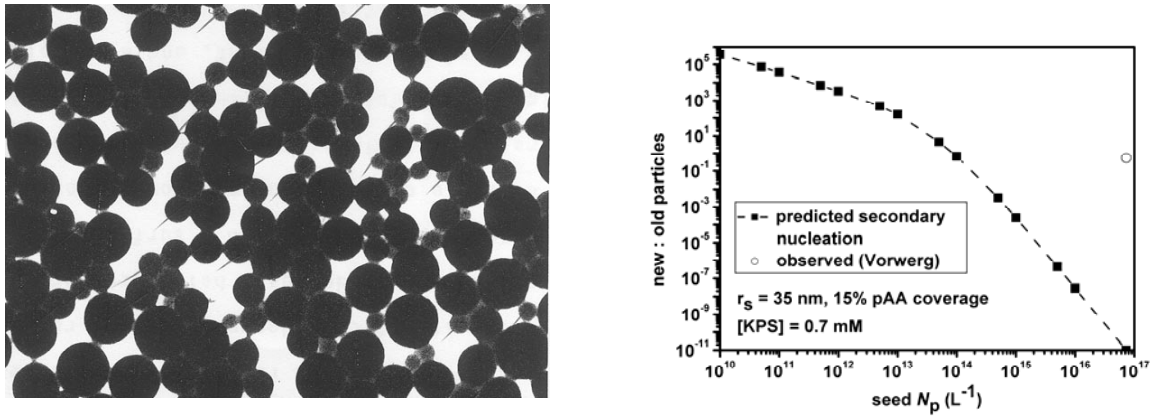

Figure 7.1. TEM Image displaying secondary nucleation in PEO-stabilized emulsion systems (left) and comparison of experimental ratio of new:old particles with theoretical prediction from the homogeneous nucleation model (right). TEM image re-produced from the thesis of Hammond.[3]

7.1.1. The Homogeneous Nucleation Mechanism

The dominant particle formation mechanism in the absence of micelles is homogeneous nucleation[4] (see Figure 7.2). An initiator-derived radical propagates with the small amount of monomer in the aqueous phase, but propagation continues beyond the length z (where surface activity is attained) to a length j_{crit} – the critical chain length before the growing oligomer is no longer soluble in the aqueous phase. This is mechanistically equivalent to the construction of the 'control by aqueous-phase growth' entry mechanism. To be more precise, an oligomer of length j_{crit} undergoes a coil-to-globule transition. This transition excludes water, forming a precursor particle that can become swollen with monomer; these precursor particles either grow via propagation or coagulate with other precursor particles to form a stable particle. This model was first put forward by Fitch and co-workers,[5] with the mathematical quantification of this mechanism known as the 'HUFT' (Hansen, Ugelstad, Fitch and Tsai) model.[6] The value of j_{crit} was estimated on thermodynamic grounds in the work of Maxwell *et al*[7] by considering the Krafft temperature for a series of *n*-alkyl sulfates; for example, it was shown that for styrene that

a pentameric radical should be water-insoluble, i.e. $j_{crit} = 5$. This value was consistent with the work of Goodall,[8] who analyzed the molecular weight distribution of the water-insoluble component of surfactant-free emulsion polymerization experiments and saw that the lowest molecular weight observed corresponded to a degree of polymerization of 10, i.e. the termination product of two pentamers.

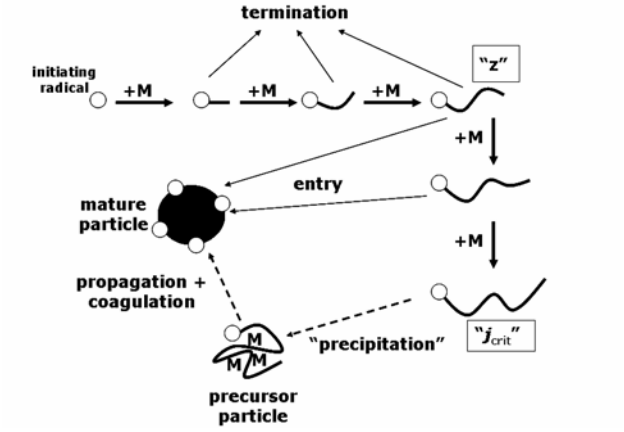

Figure 7.2. Schematic representation of the homogeneous nucleation mechanism.

Quantification of the HUFT model for homogeneous nucleation is an extension of the aqueous-phase kinetics considered for the radical entry mechanism (Chapter 2); propagation beyond the length z is now permitted (with entry occurring at all lengths greater than z in the case of seed particles being present), as well as radical termination of all chain lengths. A new particle is deemed to have formed when a radical attains the degree of polymerization j_{crit}. (Naturally this is a simplification as a precipitated single chain will be highly unstable and prone to coagulation, but provides a starting point for mathematical modelling). These extra terms can be written as:

$$IM_i^{\bullet} + M \xrightarrow{k_{pw}} IM_{i+1}^{\bullet}, \; i \geq z \tag{7.1}$$

$$IM_i^{\bullet} + T^{\bullet} \xrightarrow{k_{tw}} \text{dead product}, \; i \geq z \tag{7.2}$$

$$\mathrm{IM}_i^{\bullet} + \text{old particle} \xrightarrow{\rho_{\mathrm{init}}} \text{entry} \quad i \geq z \tag{7.3}$$

$$\mathrm{IM}_{j\mathrm{crit}-1}^{\bullet} + \mathrm{M} \xrightarrow{k_{\mathrm{pw}}} \text{new particle} \tag{7.4}$$

The resultant evolution equation for these extra terms is given by:

$$\frac{\mathrm{d}[\mathrm{IM}_i^{\bullet}]}{\mathrm{d}t} = k_{\mathrm{p}}C_{\mathrm{w}}([\mathrm{IM}_{i1}^{\bullet}] - [\mathrm{IM}_i^{\bullet}]) - k_{\mathrm{tw}}[\mathrm{IM}_i^{\bullet}][\mathrm{T}^{\bullet}] - k_{\mathrm{e}}^{i}[\mathrm{IM}_i^{\bullet}]\frac{N_{\mathrm{p}}}{N_{\mathrm{A}}}, \; z \leq i \leq (j_{\mathrm{crit}} - 1) \tag{7.5}$$

and the rate of particle formation is given by:

$$\frac{\mathrm{d}N_{\mathrm{p}}/N_{\mathrm{A}}}{\mathrm{d}t} = k_{\mathrm{pw}}C_{\mathrm{w}}[\mathrm{IM}_{j\mathrm{crit}-1}^{\bullet}] \tag{7.6}$$

The evolution equations for these processes are easily solved numerically in the steady state, allowing determination of the rate of particle formation in these systems. The k_{e}^{i} in Equation 7.5 represent the process of entry if an i-mer ($i \geq z$) given by the diffusion-controlled Smoluchowski equation, with the diffusion coefficient being D_i (the diffusion coefficient of an i-meric radical in water) and critical radius being r_{s}. This model does not allow for the coagulation of precursor particles to form a stable moiety, which requires that the kinetics of precursor particles be considered as a function of their volume with knowledge of hetero-coagulation rate coefficients. Inclusion of coagulation terms into the appropriate evolution equations is known as the 'homogeneous-coagulative' treatment,[9, 10] but it is not considered here for simplicity.

Equation 7.5 can be extended to allow for two populations of particles to be present – the seed particles N_{seed} and the newly formed particles N_{new}, allowing for the extent of secondary nucleation by homogeneous nucleation to be considered. Numerical solutions are again rapidly obtained for these systems and comparison with experiment is possible through counting the ratio of new to old particles (through TEM images or a chromatographic technique). This model

has proven extremely successful for the quantification of the amount of secondary nucleation in electrostatically stabilized systems below the CMC[1, 11, 12] and in general it can be considered that secondary nucleation is 'switched off' in most emulsion systems beyond a seed particle concentration of $N_p \approx 10^{14}$ L^{-1}.

7.2. Adsorption Kinetics and Hydrophilic Surfaces

One aspect of electrosterically stabilized latexes that is obviously different to electrostatically stabilized latexes is that particles covered with ionized acid groups possess extremely hydrophilic surfaces. This will change the adsorption isotherm of surface-active species and the likelihood of adsorbing onto the particle surface, which is significant in the case of particle growth (and potential secondary nucleation) as the probability of true entry (i.e. adsorption followed by propagation into the particle interior) is reduced. Reduction of the affinity for the particle surface has the effect of increasing the value of z; if z is increased to the point where $z \approx j_{crit}$ then homogeneous nucleation can occur[1] as opposed to an entry event.

A measure of the adsorption isotherm onto a surface of interest (such as a latex particle surface) can be modeled by the Langmuir adsorption isotherm.[10, 13] The Langmuir isotherm assumes that adsorbing species occupy identical sites (with a maximum packing density) and that only a monolayer is formed; beyond that point the species stay in solution. The Langmuir equation is given by:

$$S_a = a_s + \frac{a_s}{[S_{aq}]b} \tag{7.7}$$

where a_s is the area per surfactant molecule at maximum adsorption, S_a the area occupied per surfactant molecule at aqueous-phase concentration of surfactant $[S_{aq}]$, and b is a constant related to the interface and the surfactant. $[S_{aq}]$ is related to $[S]_{total}$ through simple mass conservation.

Techniques to measure the adsorption isotherm of simple surfactants such as SDS (such as serum replacement[14]) are generally laborious and time consuming (as well as requiring vast amounts of sample). A simpler, faster technique was developed by Morrison[15] where a UV-active surfactant was chosen for study; adsorption of this surfactant was allowed to take place on the latex surface of interest at different surfactant concentrations, the latex samples then centrifuged and the absorption spectra of the aqueous phase then considered. This allows determination of the aqueous-phase surfactant concentration [S_{aq}], which in turn allows one to calculate the amount of surfactant present on the particle surface.

This technique was applied in this work to the electrosterically stabilized latex ST5 (a poly(styrene) latex stabilized with polyAA chains of average degree of polymerization of five units). The surfactant employed was sodium dodecylbenzenesulfonate (SDBS, TCI Chemicals, Figure 7.3) that has an absorbance peak at 261 nm. Stock solutions of SDBS in water were made up at a range of concentrations spanning 5×10^{-5} M to 1×10^{-3} M to construct a calibration curve; absorption spectra were recorded on a Cary-4E UV-Visible Spectrophotometer (Varian). Absorption spectra and calibration curve are shown in Figure 7.4.

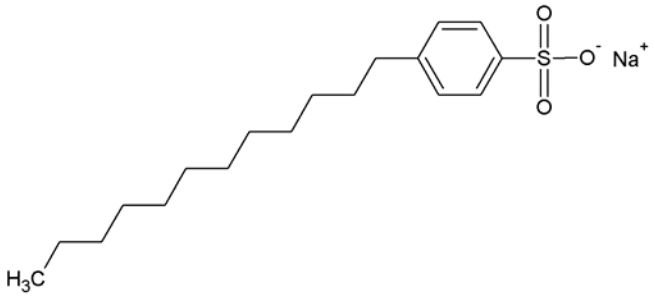

Figure 7.3. Sodium dodecylbenzenesulfonate (SDBS).

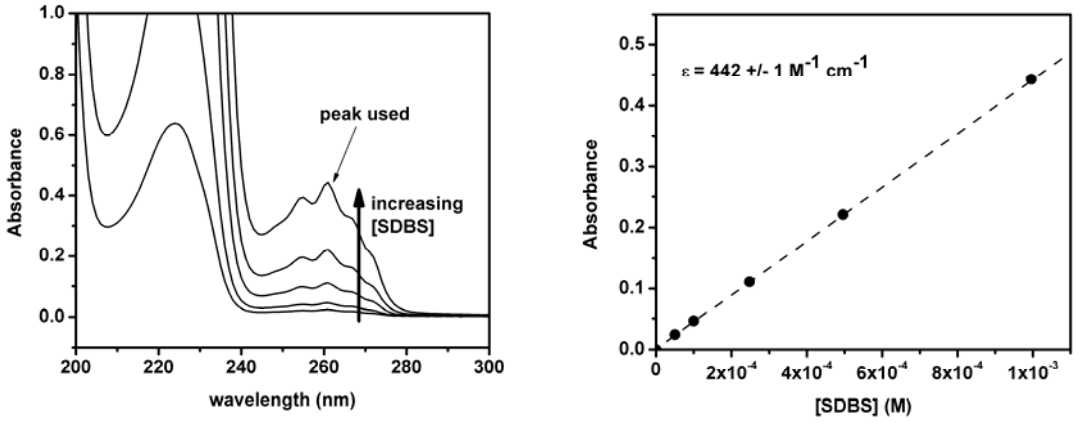

Figure 7.4. Absorption spectra of SDBS in water (left) and Beer-Lambert calibration curve (right).

Samples of ST5 (1 mL) were added to solutions of differing SDBS concentrations (total volume 10 mL) and were stirred magnetically at ambient temperature for three hours. The samples were then placed in thermally sealed polyallomer centrifuge tubes (Beckmann) and centrifuged in an Optima L-100 XP Ultracentrifuge (Beckmann) using a Ti-90 rotor under vacuum. Centrifugation took place at 90 000 rpm for 30 minutes. The aqueous phase was then collected and the UV spectra measured. Identical experiments were performed with dialyzed ST0 latex (electrostatically stabilized) for comparative purposes.

The spectra of the aqueous-phase were not as 'clean' as the stock solutions (see Figure 7.5), and this was most likely due to the extreme difficulty of obtaining pure aqueous phase. Even at very high centrifuge speeds, the act of removing the sample tube from the centrifuge is enough to disturb some of the particle phase back into the aqueous (top) phase, giving the solution a faintly cloudy appearance. This naturally affects the quality of the UV spectra, however the region of interest is largely unaffected. The determined aqueous-phase surfactant concentrations are given in Table 7.1.

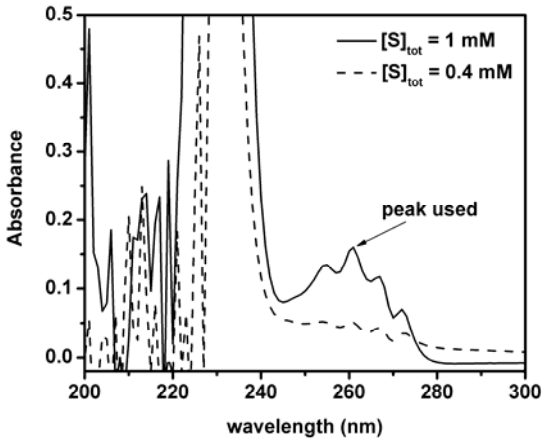

Figure 7.5. UV Absorption spectra from the aqueous phase of latex ST5 at two different SDBS concentrations.

With a knowledge of N_p (the concentration of particles in the latex) and the average particle size (and hence surface area), values of S_a were determined and Langmuir plots (S_a as a function of $[S_{aq}]^{-1}$) were constructed. If the Langmuir isotherm is obeyed, these plots will be linear and the intercept yields a_s, the surface area per surfactant molecule at maximum packing density. It was seen (Figure 7.6) that adsorption onto latex ST0 follows Langmuirian behaviour, with a_s = 53 Å^2; this value is close to literature values for similar surfactants such as SDS (a_s = 43 Å^2 [1, 14, 16]) as one would expect given the similar molecular geometries. The results for latex ST5 however give a very poor linear fit to the Langmuir equation, and a negative intercept which is physically impossible. The experimental points appear to fit an exponential curve, which was discussed by Ahmed[14] as being typical behaviour for adsorption onto porous surfaces. Calculation of the particle surface area occupied by each RAFT-capped chain gives a number of the order of 7 nm^2, so there is (supposedly) ample space on the particle surface for successful surfactant adsorption, unless the polyAA chains adopt an unusual conformation and 'lie down' on the particle surface. Given that the system is at pH 7, this is unlikely as it has been shown[17, 18] that ionized polyAA chains adopt a fully stretched conformation.

Table 7.1. Aqueous-phase surfactant concentration as a function of total surfactant concentration for ST0 and ST5 latexes.

ST0		ST5	
$[S]_{total}$ (M)	$[S]_{aq}$ (M)	$[S]_{total}$ (M)	$[S]_{aq}$ (M)
4.57×10^{-5}	3.39×10^{-5}	4.48×10^{-5}	2.49×10^{-5}
8.98×10^{-5}	6.79×10^{-5}	9.00×10^{-5}	4.98×10^{-5}
2.22×10^{-4}	1.81×10^{-4}	2.13×10^{-4}	8.85×10^{-5}
4.47×10^{-4}	3.35×10^{-4}	3.36×10^{-4}	1.15×10^{-4}
8.9×10^{-4}	6.18×10^{-4}	8.92×10^{-4}	3.62×10^{-4}

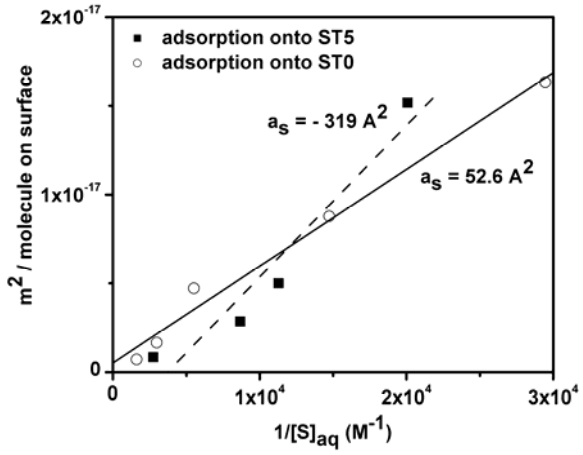

Figure 7.6. Langmuir plots for ST0 (open circles) and ST5 (filled squares) latexes. Note the poor quality of the linear fit to the ST5 data and the physically meaningless negative intercept.

The interpretation of these results is difficult, but it can be definitely said that the surface chemistry of these electrosterically stabilized latexes is different to typical latex particle surfaces. This difference in the adsorption isotherm ultimately affects the likelihood of a successful entry event for a surface-active oligomer; as discussed by Morrison[15] the second-order entry rate coefficient for radical entry is not simply the diffusion-controlled k_e (as is seen in Equation 7.5 as k_e^i), but the product of k_e and the probability of successful entry P_e:

$$k_{entry} = P_e \, k_e \tag{7.8}$$

Here k_e represents the rate coefficient for adsorption only; this is considered to be an equilibrium process with the reverse reaction (desorption) which has the first-order rate coefficient k_{des}. A successful entry event occurs when an adsorbed radical undergoes a propagation step (to prevent further desorption), so the expression for P_e is given by:

$$P_e = \frac{k_p C_p}{k_p C_p + k_{dea}} \tag{7.9}$$

where C_p is the monomer concentration in the particle phase. The ratio k_e / k_{dea} can be related to the Langmuir adsorption isotherm,[15] yielding the following expressions:

$$\frac{k_e}{k_{des}} = \frac{A_{part} \, b}{a_s} \tag{7.10}$$

$$k_{entry} = \frac{k_e \, k_p \, C_p \, A_{part} \, b}{k_e \, a_s + A_{part} \, b \, k_p \, C_p} \tag{7.11}$$

where A_{part} is the surface area of the latex particle in question, and all other terms are as defined previously. It can be seen from Equation 7.11 that different values of a_s and b from the Langmuir Isotherm will affect k_{entry}, and ultimately the likelihood of an entry event as opposed to

propagation until length j_{crit} is attained. The expression k_{entry} can be used instead of k_e^i in Equation 7.5 to account for the reversibility of adsorption and desorption.

The behaviour of k_{entry} as a function of a_s and b was studied to test the impact on the maximum nucleation rate according to the homogeneous nucleation mechanism. The maximum rate of creation of new particles can be found by applying the steady-state approximation to Equation 7.5 and the evolution equations for oligomers of degree of polymerization less than z (see Chapter 2), followed by substitution into Equation 7.6. The following expression is then obtained:[15]

$$\frac{dN_{new}}{dt}(max) = \frac{2\,k_d\,[I]\,(k_p\,C_w)^{j^{crit}}}{(k_p\,C_w + 2k_t\,[T^\bullet])^{z-1}\,(k_p\,C_w + k_{entry}\,\frac{N_{seed}}{N_A} + 2k_t\,[T^\bullet])^{j^{crit}-z+1}} \tag{7.12}$$

where all terms are as defined previously. Using the parameters associated with the ST5 latex (such as the average particle size), Equation 7.12 was solved for [I] = [KPS] = 1 mM as a function of N_{seed}. The sensitivity of the expression with respect to a_s and b (through k_{entry}) was then examined. Model parameters used (such as rate coefficients k_d, k_p etc.) are identical to those used in Chapter 6.

Given the experimental difficulty in measuring values of a_s and b for electrosterically stabilized latexes such as ST5, values were chosen that would ultimately lead to an increase in the nucleation rate (i.e. decreasing b and increasing a_s). The 'SDS values[14, 15]' of $a_s = 0.43$ nm^2 and $b = 7000$ M^{-1} were used as reference points, and the results are shown in Figure 7.7. It can be seen that even significant variation of a_s and b have only a small impact on the maximum nucleation rate, and when model parameters to replicate the work of Vorwerg[2] were used, the increase is not large enough to explain the vast amounts of secondary nucleation observed (see Table 7.2). Therefore any effects that the 'hairy layer' has on adsorption/desorption kinetics is not significant enough to explain the secondary nucleation phenomena in systems such as these.

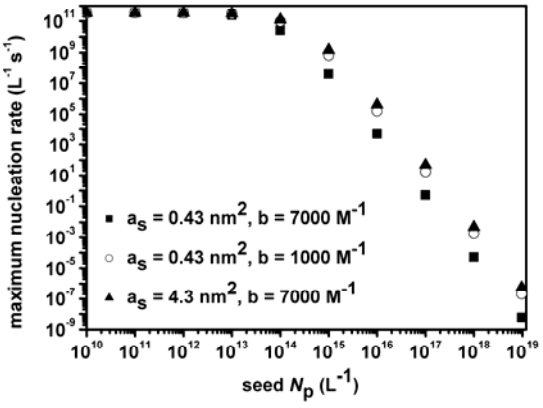

Figure 7.7. Maximum predicted nucleation rate as a function of seed N_p ([I] = 1 mM) and as a function of Langmuir parameters a_s and b.

Table 7.2. Maximum predicted nucleation rate for polyAA-stabilized latexes as synthesized by Vorwerg according to the homogeneous nucleation model.

	a_s = 0.43 nm^2, b = 7000 M^{-1}	a_s = 0.43 nm^2, b = 1000 M^{-1}	a_s = 4.3 nm^2, b = 7000 M^{-1}
$\frac{dN}{dt}$ (L^{-1} s^{-1})	0.154	2.85	7.14

7.3. The 'Fragmentation Nucleation' Postulate

As was discussed extensively in both Chapter 5 and Chapter 6, the dominant loss mechanism in small, electrosterically stabilized particles such as those used in this project was shown to be rapid chain transfer (via hydrogen atom abstraction) involving the polyAA stabilizer, as well as potential subsequent termination of the resultant mid-chain radical (MCR). It should be appreciated that termination is not the only fate for a MCR; a backbone radical such as this can

undergo beta-scission, forming two species – a new secondary radical and a polymer chain with an unsaturated end-group (Figure 7.8). Pulse-radiolysis experiments of aqueous solutions of polyAA have shown[19] that beta-scission occurs at a non-negligible rate (k_{beta} = 0.18 s^{-1}), even at ambient temperatures. Similarly it is predicted that beta-scission is the source of experimental failure in PLP-SEC experiments of acrylates at elevated temperatures,[20] due to the failure to consider chain fragmentation in these systems.

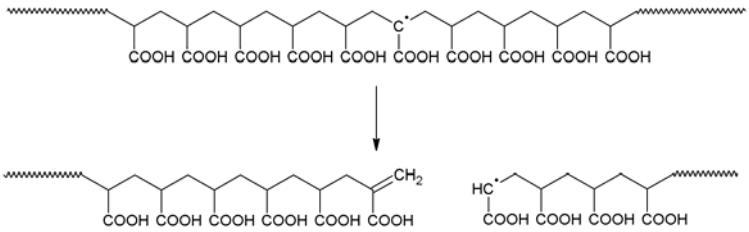

Figure 7.8. Beta-scission in poly(acrylic acid).

In the case of an electrosterically stabilized emulsion, the beta-scission of a MCR would lead to a polyAA species (either bearing a radical or an unsaturated end-group) fragmenting off the particle surface and moving into the aqueous phase. This will have a two-fold effect; the long-term stability of the emulsion will be reduced (as the length of the stabilizing block has been shortened) and a new species capable of chemical reaction is now present in the aqueous phase. Given the orders-of-magnitude discrepancy between the amount of observed secondary nucleation in such systems and the predicted amount from the homogeneous nucleation mechanism, it was postulated that the beta-scission of a MCR is mechanistically important in the creation of new particles. This is shown schematically in Figure 7.9 and was dubbed the 'fragmentation nucleation' mechanism.

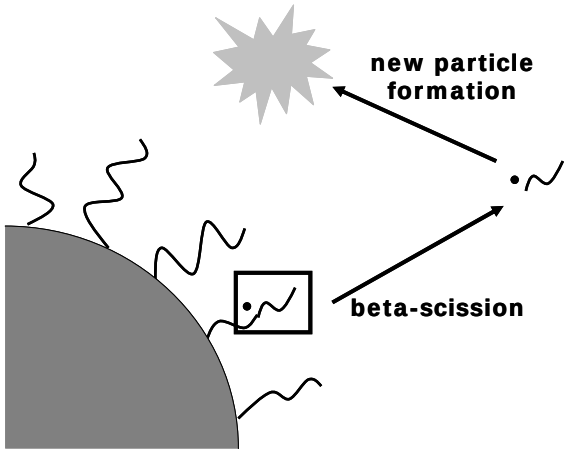

Figure 7.9. Schematic representation of the 'fragmentation nucleation' mechanism.

The fragmented polyAA species can undergo a variety of different chemical reactions in the aqueous phase. These include termination with an aqueous-phase oligomer (if the fragmented species is a polyAA radical), propagation of the macro-monomer (if the fragmented species bears a vinylic end-group), propagation of styrene (if a radical is fragmented) and chain transfer via hydrogen-atom abstraction. It is decidedly unclear as to what chemical steps would ultimately lead to nucleation of a new particle. In this postulate, however, that is irrelevant. By working at the upper bound where every beta-scission event leads to particle nucleation, a model can be constructed that allows the determination of the importance of this process. This model easily follows from the mathematics developed in Chapter 6. One can envisage that the most likely reaction to lead to particle nucleation is an encounter between a poly(styrene) radical and a polyAA chain, leading to the creation of a surface-active species that could 'collapse' down in the aqueous phase and form a species akin to a precursor particle.

As has been mentioned, the modelling presented here works under the assumption that every beta-scission event will lead to particle nucleation. This is clearly an over-simplification but provides an excellent starting point for modelling. Further complications can then be introduced (e.g. nucleation takes place only after fragmentation then termination.) However, if the inclusion of the 'fragmentation nucleation' mechanism does not lead to a substantial increase in the

predicted amount of new particles in these systems then the concept can be dismissed as unimportant at this point.

7.3.1. Steady-State Kinetics

As a first approach to this modelling, the steady-state kinetics developed in Chapter 6 were used and extended to include both the homogeneous nucleation and fragmentation nucleation mechanisms. A seed population N_{seed} is considered, stabilized by a polyAA corona of known thickness (δ) and local stabilizer concentration ([AA]). 'Zero-one' kinetics[1] are assumed, and as a result the population balance of N_0, N_1^m and N_1^p are all considered (as defined previously) at a given initiator concentration [I]. The chemistry of aqueous-phase oligomers are assumed to be identical to the 'Maxwell-Morrison[21]' mechanism where propagation and termination takes place until surface activity is attained. Oligomers of lengths z to ($j_{crit} - 1$) are able to undergo entry into the seed latex population, as well as new particles (N_{new}) when they are formed.

The additional transfer/termination terms involving the polyAA stabilizer are included in the evolution equation for N_1^m, as was seen in Chapter 6. It is repeated here for clarity:

$$\frac{dN_1^m}{dt} = \rho_{re}N_0 - \rho N_1^m - k_{dM}N_1^m + k_{tr}C_pN_1^p - k_p^1C_pN_1^m - P_{des}\left(k_{abs}[AA]N_1^m + 2\,k_t[MCR]\,N_1^m\frac{N_{seed}}{N_A}\right)$$

(7.13)

where all terms are as defined previously. The evolution equation for the MCR population is also required, and is given by:

$$\frac{d[MCR]}{dt} = P_{des}\,N_1^m\frac{N_{seed}}{N_A}\left(k_{abs}\,\Phi_{HL}\,[AA] - 2\,k_t\,[MCR]\right) - k_{beta}[MCR] - 2\,k_t\,[MCR]\sum_{j\geq z}[IM_j^{\bullet}]$$

(7.14)

where beta-scission of the MCR is included. For these purposes the nature of the fragmented species is unimportant (either a radical or an unsaturated moiety), but discrimination of this would have to be included for more detailed mechanistic modelling.

The steady-state approximation is used to determine the population balance of all aqueous-phase oligomers, N_1^{m}, N_1^{p} and [MCR]. However a time dependency is introduced into the model to determine the evolution of N_{new} as a function of time. At $t = 0$, $N_{new} = 0$ (as there are no new particles present in the system). The various steady-state expressions are solved until convergence at any given time and the rate of new particle generation is then found through the following expression:

$$\frac{\mathrm{d}(N_{new}/N_A)}{\mathrm{dt}} = k_p C_W[IM_{jcrit-1}] + k_{beta}[MCR] \tag{7.15}$$

where the first term in Equation 7.15 represents the contribution to new particle formation via the homogeneous nucleation mechanism (propagation to the point of insolubility), while the second term represents the fragmentation nucleation term. The number of new particles (N_{new}) formed in this (sufficiently small) time step is then determined and these population balances are then used as starting values for the next time increment. This time dependency is introduced through the second-order entry rate coefficients $k_e^{\,i}$ (where i is the length of the entering oligomer) which are now allowed to vary as the particles in the system grow, and is given by:

$$k_e^{\,i} = 4\,\pi\,\frac{D_w}{i}\,N_A\left(\frac{3\,k_p\,M_0\,C_p\,d_M}{4\,\pi\,N_A\,d_P(d_M - C_pM_0)}\,\overline{n}\,t\right)^{1/3} \tag{7.16}$$

where M_0 is the mass of the monomer, d_M the density of the monomer, d_P the density of the polymer and D_w the diffusion coefficient of a monomeric radical in water. The time step considered in this work was 0.1 s, and the population balance equations were solved for 1000 s.

From this, final values of N_{new} (and as a result the ratio of new:old particles) were found as a function of the seed N_{seed} value.

In this modelling, the conditions used in the work of Vorwerg[2] were employed as model parameters In Vorwerg's studies extensive secondary nucleation was seen. However, none was seen in the kinetic experiments performed in this work, most likely due to the extremely high value of N_p – over two orders of magnitude larger than that used in Vorwerg's work. The ratio of new to old particles seen by Vorwerg under the conditions used was approximately 0.4, a very large amount (the same order of magnitude as the seed particle number). The various model parameters used are given in Table 7.3.

Table 7.3. Kinetic parameters used in the 'Fragmentation Nucleation' mechanistic model.

Parameter	Value (units)
N_p	7.3×10^{16} L^{-1}
r_s	35.8 (nm)
k_{abs}	8.4×10^5 M^{-1} s^{-1}
[AA]	0.2 M
δ	2 nm
Φ_{HL}	0.025
k_{beta}	0.18 s^{-1}
[KPS]	7.5×10^{-4} M

All other parameters used as defined in Chapter 6.

The results of this modelling are shown in Figure 7.10, with the results from the homogeneous nucleation model also presented for comparative purposes. It can be seen that inclusion of beta-scission of a MCR as a potential nucleation step has the effect of substantially increasing the amount of new particles formed at high values of N_{seed}; this increase relative to the homogeneous nucleation model is over many orders of magnitude. Indeed the obtained result brings the predicted model result into reasonable agreement with the experimental work of Vorwerg, which offers a potential explanation and insight into those results.

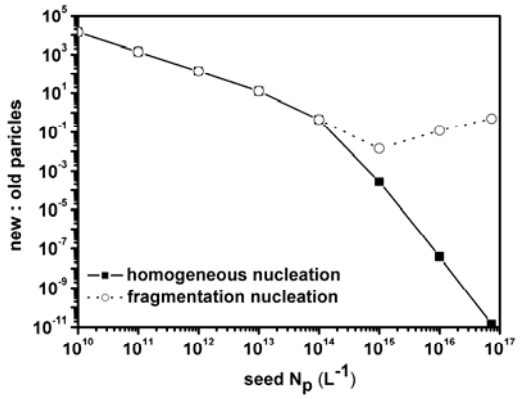

Figure 7.10. Ratio of new to old particles as a function of seed N_p for both the homogeneous (black squares, solid line) and fragmentation nucleation (open circles, dotted line) mechanisms.

It is also clear from Figure 7.10 that for seed N_p values less than approximately 10^{15} L^{-1}, the results converge to the homogeneous nucleation limit. This result (and the decrease in the ratio of new to old particles as N_{seed} is decreased in the region where the fragmentation nucleation limit is dominant) is due to the fact that there are simply not enough MCRs present in the system to provide a substantial concentration for this extra mechanism to be significant. While the local [AA] concentration within the hairy layer remains constant for the same particle morphology, the total volume fraction Φ_{HL} that the hairy layer represents scales with N_p, and so the bulk AA (and hence MCR) concentration decreases very quickly.

7.3.2. Sensitivity Analysis

One of the key parameters in this nucleation model is k_{beta} – the rate coefficient for beta-scission. There is very little published data involving attempts to measure this rate coefficient and the value used (0.18 s^{-1}) was taken from pulse-radiolysis work[19] at room temperature, which represent entirely different reaction conditions to the ones being modeled. It is naturally highly undesirable to have a nucleation model that yields different conclusions when one parameter is varied, so the developed model was re-considered with values of k_{beta} spanning eleven orders of magnitude. The results are presented in Figure 7.11.

The reason for such a wide range of values in this sensitivity analysis is because there is little consistency in the literature regarding the rate coefficients for β-scission in acrylate systems. Peck[22] observed no β-scission for butyl acrylate (BA) systems at 75 °C, while Junkers[23] observed MCR formation in BA systems (which could potentially undergo β-scission) at temperatures as 'low' as 80 °C. Four orders of magnitude exist between the values obtained by Busch[24] and Rantow[25] for high temperature BA polymerization systems where the resultant molecular weight distribution was used to infer information regarding k_{beta}. Data for polyAA itself was found using pulse radiolysis[19] and ESR[26] at room temperature and pressure, and the values of k_{beta} varied between 10^{-1} – 10^{2} s^{-1}. Recent ESR work by Sato and co-workers[27] on the monomer ethyl hexyl acrylate has yielded a value of $k_{beta} \sim 4 \times 10^{-2}$ s^{-1} at room temperature. This substantial variation is most likely due to the fact that these rate coefficients have to be indirectly inferred from other data; however it would seem that β-scission occurs to a greater extent in polyAA than poly(*n*-butyl acrylate).

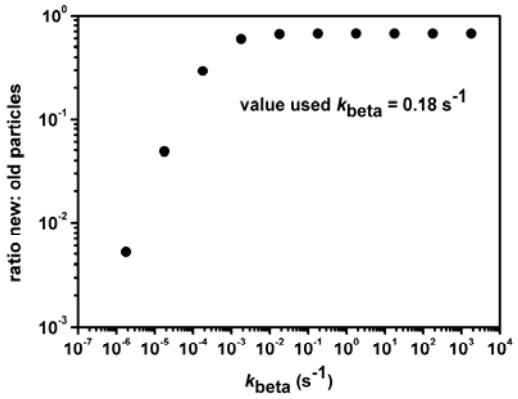

Figure 7.11. Sensitivity analysis with respect to k_{beta} for the fragmentation nucleation model.

It is clear that considering how much the value of k_{beta} is changed, the nucleation model is fairly insensitive to these changes. At large values of k_{beta} the predicted ratio of new to old particles reaches a plateau, while for very low values of k_{beta} the amount of new particles naturally decreases. This decrease however still gives a result that yields far more newly formed particles than predicted by homogeneous nucleation; overall the dependence on k_{beta} is extremely weak. This can be rationalized by the fact that as k_{beta} is reduced, the value of [MCR] will increase (as a term that involves the destruction of a MCR has been reduced). The product k_{beta}[MCR] however remains largely constant, ensuring that the predicted amount of secondary nucleation does not vary substantially as k_{beta} is changed.

7.3.3. Interpreting Model Results

It was seen that adding the fragmentation nucleation mechanism to the homogeneous nucleation mechanism to explain particle formation in these systems significantly increased the likelihood of secondary nucleation at high particle numbers. This can be rationalized by considering the steady-state [MCR] expression; [MCR] is essentially linear in N_p. The population of oligomers that can lead to homogeneous nucleation, (j_{crit} −1)-mers, however, is linked to the population of

all species of lower degrees of polymerization in the aqueous phase – combining all the steady-state solutions of these populations and it can be seen that:

$$[\mathrm{IM}_{j\mathrm{crit}\text{-}1}] \propto \frac{1}{\left(\frac{N_\mathrm{p}}{N_\mathrm{A}}\right)^{j\mathrm{crit}\text{-}z\text{-}1}} \tag{7.17}$$

Therefore, while $z = 2$ and $j_{\mathrm{crit}} = 5$, (standard values for styrene emulsion polymerizations[1, 21]) the population of $(j_{\mathrm{crit}} - 1)$-mers has an inverse square dependence on N_p. Mathematical constants aside, it can be seen that at high N_p values the magnitude of [MCR] (and as a result secondary nucleation) will dominate the homogeneous nucleation mechanism. Similarly at lower values of N_p, the standard homogeneous mechanism will be the dominant particle formation process, as seen in the data presented here. This result is easily implemented as an addition to the transfer/termination loss terms included to explain the particle growth kinetics of emulsion polymerization systems; this nucleation mechanism does not alter the results obtained and presented in Chapter 6.

The results represent somewhat of a conundrum for the chemist attempting to optimize reaction conditions by minimizing secondary nucleation. Small electrosterically stabilized particles (with corresponding high N_p values) will help minimize secondary nucleation, however densely packed 'hairy layers' ensure that transfer/termination (if the stabilizer is able to undergo hydrogen-atom abstraction) will be the dominant loss mechanism and a reduced reaction rate will be seen. Larger particles (with more sparsely covered surfaces) give faster reaction rates (due to higher values of $\bar{n}$ however secondary nucleation due to a reduced N_p is more likely. Ideally a balance should be found – small particles with a minimum amount of employed stabilizer, or stabilizers that are unable to undergo abstraction would be recommended.

7.3.4. Time-Dependent and Distribution-Dependent Modeling

In all of the modelling performed in the work presented in this thesis, a minimum number of model-based assumptions have been used and accurate values of rate coefficients for fundamental reactions (such as propagation, transfer, termination etc.) determined by separate techniques have been used. However all the work conducted has been carried out in the steady-state and assuming a perfectly monodisperse particle size distribution (PSD). This is not a true reflection of reality; while significant effort is put into synthesis of seed latexes with very narrow PSD's (low polydispersity), the distribution is not polydisperse. In modelling particle growth and particle formation kinetics, there is a desire to observe how the distribution changes as a function of time.

The successful modelling of PSD behaviour as a function of time in electrostatically stabilized emulsion systems was successfully performed by Coen *et al*.[11] This modelling is not trivial; the evolution equations for N_0, N_1^m and N_1^p are now partial differential equations with respect to both particle volume and time (e.g. $N_1^p(V,t)$). Particles in the N_1^p population can grow by propagation, leading to an increase in volume; this requires a loss term to be included in the governing differential equation that has not needed to be considered previously. Similarly coagulation terms need to be considered (as two particles with differing volumes combine to form one new particle, again with a different volume). The coding procedure used to solve these equations is as follows:

- An input PSD is chosen, with average radius and known standard deviation. It is assumed to be Gaussian in shape. This distribution is then split into *n* 'bins' with each bin representing the fraction of particles of that particular volume.

- A vector y is created of length $2n$; the first n entries represent the N_0 population (and the division of this distribution into n volume bins) while the second n entries represent the $N_1^{\,p}$ population (and its subsequent division).

- The differential equation governing $N_1^{\,m}$ is again solved using the steady-state approximation, as $N_1^{\,m}$ is typically small and approximately constant.

- The aqueous-phase chemistry is assumed identical to the Maxwell-Morrison 'control by aqueous-phase growth' mechanism[21] with oligomers of length z and greater able to undergo entry. Oligomers of length j_{crit} form new particles via homogeneous nucleation.[1] In the case of this modelling, this means that the value of vector entry $y[n+1]$ is increased as homogeneous nucleation produces a particle of smallest possible volume that is bearing a radical.

- All kinetic equations are solved numerically as a function of time using the Gear algorithm.[28] At time $t = 0$, no particles present contain a radical. Entry events move a particle of volume V' from the N_0 population to the $N_1^{\,p}$ population at the same volume. Propagational growth allows for particles to move 'down' the vector, i.e. to move from volume bin V' to volume bin V''. Every mechanistic event previously considered is accounted for (transfer, diffusion, re-entry etc.)

- After a set period of time, the new volume distribution (and hence PSD) is considered. At any given time quantities such as $\overline{n}$ and ρ can be determined. N_p can also be calculated; if N_p (final) is different to N_p (initial) then it can be said that secondary nucleation has taken place.

This modelling has proven very successful to account for the kinetics of particle growth and secondary nucleation in electrostatically stabilized systems. However to adapt this model for

electrosterically stabilized systems, additional layers of complexity have to be introduced. These are:

- Particles are now coated with a uniform 'hairy layer' of fixed width (δ) with known local stabilizer concentration ([AA]).
- The rate coefficients for desorption of a monomeric radical (k_{dM}) have to be altered to account for restricted diffusion through a polymeric layer (as discussed in Chapter 4.)
- Transfer to polyAA and termination with a MCR have to be included into the relevant kinetic equations.
- An additional differential equation (to account for the gain and loss of MCRs) has to be included.
- A new particle formation term has to be included (the 'fragmentation nucleation' term) – the beta-scission of a MCR leads to creation of a particle of smallest possible volume bearing an active radical (i.e. a member of the $y[n+1]$ population).

These additional requirements were put into the FORTRAN code developed to map the evolution of the PSD of these systems as a function of time. Model input parameters were again chosen to replicate the conditions of Vorwerg,[2] who observed substantial secondary nucleation in these systems. These parameters are provided as a sample input file in Appendix A6. The code was allowed to run for 1000 s (at time increments of 0.1 s). The original code was also run using the same input conditions to determine the variation in the obtained PSDs.

The obtained PSD from running the original code and the modified 'fragmentation nucleation' code for 1000 s is shown in Figure 7.12. As can be seen, at the same N_p the seed latex subjected to the new kinetic scheme grows more slowly (the average particle size is 2.5 nm smaller, a substantial difference after only 1000 s polymerization time). This difference is most likely due

to the fact that the additional loss terms of transfer/termination are included in this kinetic scheme; these events suppress re-entry of monomeric radicals occurring which reduces the overall polymerization rate.

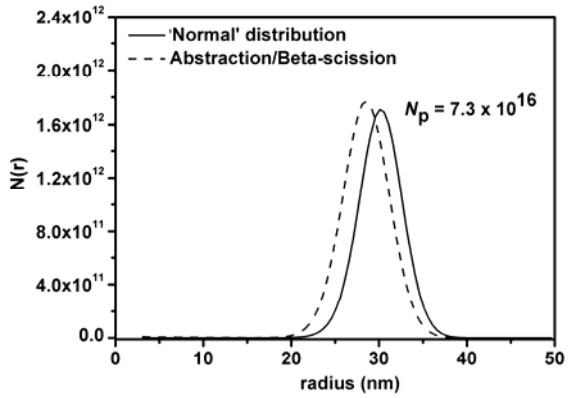

Figure 7.12. PSD after 1000 s polymerization time using sample input parameters. Shown are 'normal' kinetics (solid line) and 'fragmentation nucleation' kinetics (dashed line).

When the resultant PSD is magnified it becomes evident that as well as the seed latex growing more slowly when these additional loss terms are put in place, secondary nucleation is also present under the new kinetic scheme (through beta-scission of a MCR). The new distribution (plotted on a logarithmic scale, Figure 7.13) contains a pronounced 'hump' at small particle sizes while the normal distribution tails off rapidly. The difference in these distributions, represented by this significant tail, is the crop of new particles formed via secondary nucleation. As was discussed, the code was constructed to nucleate a particle into the smallest volume 'bin' for every beta-scission event; these new particles are then able to grow and participate in the overall kinetic scheme. After 1000 s, the particle concentration was $N_p = 7.31 \times 10^{16}$ L^{-1}, an increase of 1×10^{14} L^{-1} relative to the seed particle number. While this increase does not sound overly large (an increase in the particle concentration of approximately 0.15 %), this is substantially more than predicted by the homogeneous nucleation model which predicts an increase of only 10^5 L^{-1}.

The fragmentation nucleation step thus has the effect of increasing the value of N_{new} by nine orders of magnitude.

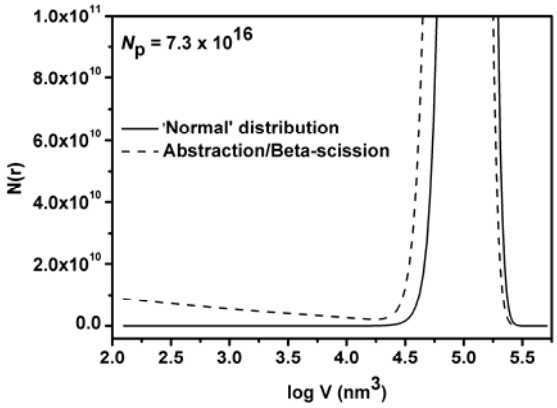

Figure 7.13. PSD after 1000 s polymerization time, plotted on logarithmic scale. Shown are 'normal' kinetics (solid line) and 'fragmentation nucleation' kinetics (dashed line).

Using the same conditions of initiator concentration and other key rate coefficients, the model behaviour as a function of N_{seed} was tested. When N_{seed} was reduced below 10^{14} L^{-1}, the homogeneous nucleation mechanism was once again dominant, as was seen in the steady-state model presented earlier. The obtained distributions (see Figure 7.14) show the 'tail' due to the additional nucleation mechanism becomes less and less important as the seed particle number is reduced, which is to be expected. The ratio of new to old particles was also considered (Figure 7.15) and was shown in general to be in good agreement with the results obtained from the steady-state model. Once again, substantially more secondary nucleation is observed in these systems when this additional mechanism is present.

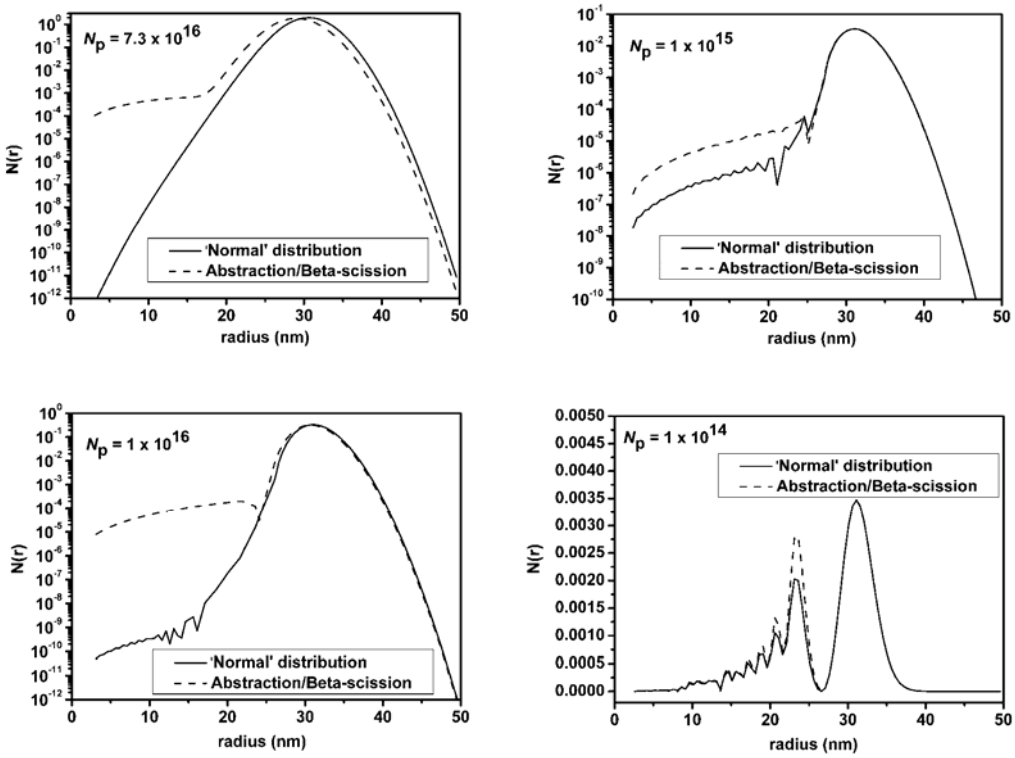

Figure 7.14. Evolution of PSD after 1000 s polymerization time as a function of N_{seed} for both 'normal' kinetics (solid line) and 'fragmentation nucleation' (dashed line) kinetics

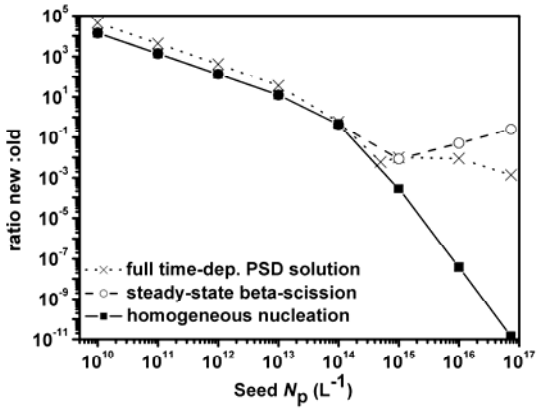

Figure 7.15. Ratio of new to old particles as a function of N_{seed}. Model results shown are for homogeneous nucleation (filled squares), fragmentation nucleation (steady-state, open circles) and fragmentation nucleation (time-dependent, crosses).

7.4. Experimental Evidence

While the reaction of beta-scission of a MCR on a stabilizing 'hair' on the surface of an electrosterically stabilized latex is plausible in theory (given what is known about acrylates), it must be determined if it is experimentally likely under the conditions used in seeded kinetic experiments at 323 K. Similarly the behaviour of the developed kinetic model must be compared to experiment in order to determine that (at the very least) qualitative trends between experiment and theory are in agreement.

7.6.1. Fragmentation of poly(acrylic acid)

To determine if beta-scission occurs at a significant rate under the conditions used in seeded emulsion experiments, a simple experiment was devised using polyAA synthesized by precipitation polymerization (experimental presented in Chapter 5). The polyAA was neutralized in water, and potassium persulfate (KPS) was added to a concentration of 1 mM, a typical concentration used in kinetic experiments. The solution was then stirred and heated at 323 K in a

oxygen-free environment for 24 h. Sulfate ion radicals generated by KPS decomposition are very effective at hydrogen atom abstraction, and in such a system polyAA MCRs would be formed that could potentially fall apart via beta-scission.

The polyAA was analyzed by size exclusion chromatography (SEC) before and after treatment with KPS to determine any changes in the molecular weight distribution (MWD). The obtained chromatograms are shown in Figure 7.16. As can be seen, the distribution of the polymer and the oligomeric moieties are shifted to longer elution times after KPS treatment. Given the manner in which SEC separation works, this means that the polymer has decreased in size (hydrodynamic volume); the only way that this can happen in the absence of any monomer is that the polymer has fragmented (via beta-scission) into smaller component chains. This supports the postulate that beta-scission can take place at the reaction temperature in question, and proves the existence of MCRs forming along the polyAA backbone.

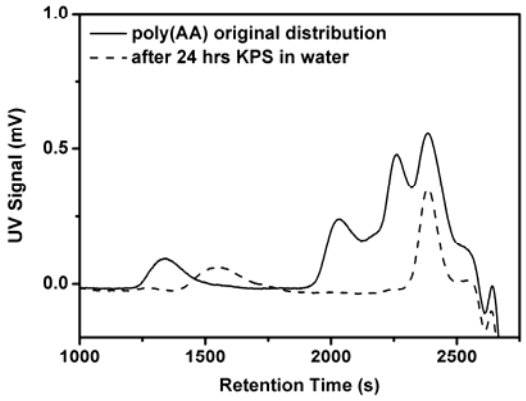

Figure 7.16. SEC chromatogram of polyAA before (solid line) and after (dashed line) treatment with potassium persulfate in water for 24 h, 323 K.

7.6.2. Secondary Nucleation as a Function of Seed Particle Number

In the work of Vorwerg[2] the kinetics of electrosterically stabilized systems was not considered as a function of seed particle number (all experiments were done at the same N_p value). One of the most useful tools in validating or refuting nucleation models however is to determine the amount of new particles formed as a function of N_{seed}, as different mechanistic models give different behaviour. In the 'fragmentation nucleation' model presented in this Chapter, it has been shown that the predicted ratio of new to old particles is very high at large values of N_{seed}, and that this value is approximately constant (i.e. within the same order of magnitude) over the entire region where the fragmentation mechanism dominates the homogeneous nucleation mechanism.

In order to compare this to experimental results, an electrosterically stabilized latex prepared by conventional free-radical emulsion polymerization was prepared and diluted to four different final N_p concentrations spanning an order of magnitude. The synthetic procedure for the seed latex was equivalent to that used for the 'high coverage' latex synthesized by Vorwerg (where the polyAA represents 15 % w/w of the total polymer present); this was chosen as the seed latex as the final value of N_p (5.4×10^{17} L^{-1}, unswollen average radius = 31.2 nm) was much lower than that for latexes made by the 'RAFT-in-Emulsion' method[29] ensuring that secondary nucleation would be more likely. Seeded experiments were performed with styrene at 323 K, using an initiator concentration of [KPS] = 1 mM. The four latexes were then analyzed by hydrodynamic chromatography (HDC) in order to determine the final PSD and the ratio of new to old particles.

A typical PSD is shown in Figure 7.17. As can be seen, a new population at small particle sizes has formed (i.e. secondary nucleation has occurred). Normalization of the obtained signal and consideration of the relative peak areas allows for the ratio of new:old particles to be determined (it is important, however, to realize that the number distribution (not the volume distribution) must be used). Comparison of this ratio as a function of N_{seed} with theoretically predicted results,

which is shown in Figure 7.18. It is clear that the fragmentation nucleation model provides a much better fit to the experimental data compared to the homogeneous nucleation model, which is too small by many orders of magnitude. The quantitative disagreement is most likely due to the various model assumptions present in the work, however the agreement (within an order of magnitude) between experiment and theory is now correct for the first time on a semi-quantitative level. The theoretically obtained PSD however agrees poorly with experiment with respect to the population of newly formed particles, due to the assumptions made within the modelling as to the size of a newly nucleated particle. This disagreement with respect to small particle sizes is shown in Figure 7.17.

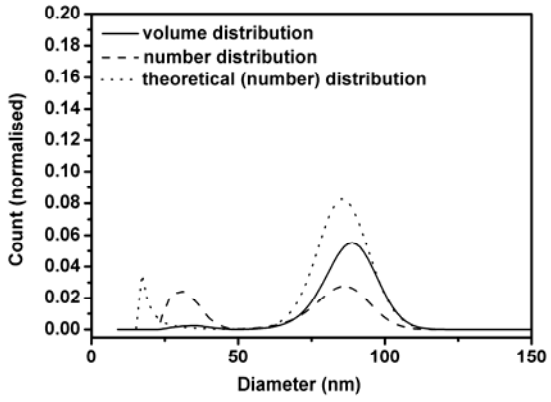

Figure 7.17. PSD of electrosterically stabilized latex (measured by HDC which provides volume distribution) after further polymerization with styrene, [KPS] = 1 mM. New particles are shown by the new population at small particle sizes $N_{seed} = 2.5 \times 10^{17}$ L^{-1}. Theoretical distribution is also shown for comparative purposes.

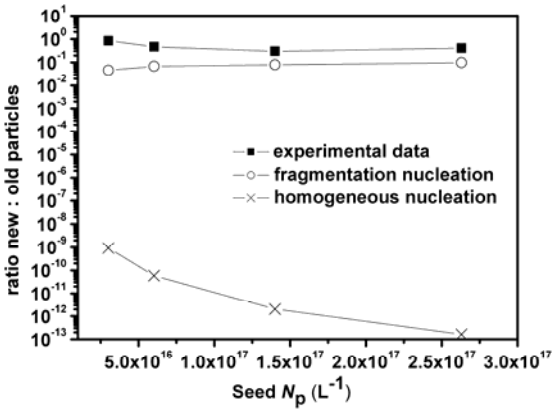

Figure 7.18. Ratio of new to old particles as a function of N_{seed}; points shown here represent experimental data (filled squares, fragmentation nucleation model results (open circles) and homogeneous nucleation results (crosses).

7.6.3. Examination of the Beta-Scission Postulate

While the inclusion of beta-scission of a MCR as a reaction that is involved in particle formation in electrosterically stabilized emulsion systems leads to a kinetic model that gives very good agreement with experiment, this postulate is by no means the definitive answer as to what is actually happening in these systems. Several points of conjecture remain.

The first issue is whether or not there is simply enough material 'fragmented' into the aqueous phase that would lead to particle formation. Beta-scission of a MCR relies first upon the formation of a MCR, which (in our model) is assumed to take place via hydrogen abstraction with an exiting monomeric radical. An exiting radical can only be formed by transfer to monomer; all of these events occur on different timescales and rely on one another to take place. This ultimately yields a concentration of fragmented species (either radicals or unsaturated chains) that is very low.

Secondly, the issue as to what happens to the fragmented species must be addressed. The model presented here has worked at the upper bound assumption that every fragmentation event leads to particle nucleation. However in reality a hydrophilic polymer chain residing in the aqueous phase is highly unlikely to participate in particle formation at all. If encounter with an aqueous-phase oligomer was to take place (such as propagation or termination), the species formed would possibly be a surface-active species composed of polyAA and poly(styrene). Considering that there is considerable particle surface area present for adsorption, it is difficult to picture that this molecule would nucleate a new particle.

One piece of supporting evidence for the fragmentation nucleation model is that beta-scission is pH-dependent. The work of von Sonntag[19] demonstrated that beta-scission is common at neutral and high pH, while the reaction is suppressed at pH = 4 and below. Interestingly, at low pH Vorwerg did not observe any secondary nucleation in seeded experiments.[2] If beta-scission is a key step in particle nucleation in these systems, then these results correlate perfectly (and with respect to kinetic modelling, this is the same as setting $k_{beta} = 0$ for low pH simulations). No work was done in this project with regards to variation of pH of latexes synthesized by controlled-radical techniques due to colloidal stability issues (and the very low degree of polymerization of the stabilizing chains). However this remains an important, and poorly understood area of research in emulsion polymerization. The proposed mechanism can also be applied to any sterically or electrosterically stabilized emulsion system where the stabilizer has labile hydrogen atoms that are susceptible to chain transfer to polymer, not solely polyAA systems as have been studied here. One system that this mechanism is also applicable to is poly(ethylene oxide) (PEO) stabilized systems, that have been shown in previous work[3] to exhibit extensive secondary nucleation As PEO can be crosslinked[30] and be used as a polymer graft[31] under appropriate conditions, it is clear that H-atom abstraction can potentially take place in systems stabilized in this manner. This provides an explanation to the unusual kinetic behaviour also exhibited in these systems.

7.5. Conclusions

In this chapter, the area of secondary nucleation in electrosterically stabilized emulsion polymerization systems has been discussed. Given the extreme disparity between the experimentally observed amount of new particle formation in polyAA-stabilized latexes and that predicted by the 'homogeneous nucleation' mechanistic model, there must be other particle formation mechanisms occurring in these systems.

One area of difference between electrostatically and electrosterically stabilized latexes is that the surface of an electrosterically stabilized latex is considerably more hydrophilic due to the presence of grafted water-soluble (and ionized) polymer. This is likely to affect the adsorption isotherm of surface active species, and adsorption of a model compound (a UV-active surfactant) was tested for the ST5 latex (a poly(styrene) latex stabilized by polyAA chains of average degree of polymerization = 5). It was shown that this latex did not exhibit Langmuirian behaviour; the results were similar to the predicted behaviour for adsorption onto a porous surface. Allowing for the equilibrium between adsorption and desorption prior to a successful entry event did not significantly change the predicted amount of new particle formation through the homogeneous nucleation model. It is expected, however, that adsorption kinetics of these systems are significantly different and are likely to be a function of surface charge, stabilizer conformation and pH.

A postulate was put forward to develop a new particle formation mechanism based on the kinetic model developed to explain radical entry and exit kinetics in electrosterically stabilized systems. It is known that rapid chain transfer (via hydrogen atom abstraction) to polyAA is a dominant radical loss mechanism that influences particle growth kinetics and results in the formation of a mid-chain radical (MCR). It was postulated that the beta-scission of such a MCR (that would lead to fragmentation of a polyAA species into the aqueous phase) is an important mechanistic step in the nucleation of new particles. By assuming that every beta-scission event forms a new

particle, a steady-state kinetic model was developed with 'best estimate' values of rate coefficients for reactions such as beta-scission. It was shown that at very high seed particle numbers, the ratio of new to old particles was significantly increased in the presence of this mechanism – several orders of magnitude larger than that predicted by homogeneous nucleation. The obtained results were also in good agreement to what had been observed experimentally by other researchers.

A full time-dependent kinetic model was also developed to model this postulated procedure, which allowed the monitoring of the full particle size distribution (PSD) as a function of time. It was seen that in the presence of the additional particle nucleation mechanism (dubbed 'fragmentation nucleation'), the obtained PSD exhibited clear secondary nucleation. Variation of N_{seed} again demonstrated the dominance of this new mechanism at high particle numbers, due to the increased amount of polyAA (and MCRs) present in the system.

To support this postulate, experiments were performed where a polyAA-stabilized latex was grown further in seeded experiments using different N_{seed} values under identical conditions of temperature and initiator concentration. Secondary nucleation was evident after analysis of the final PSD; the experimental ratio of new to old particles was in very good agreement (within the same order of magnitude) with the newly developed kinetic model. Further experiments where aqueous solutions of polyAA were treated with potassium persulfate (KPS) at 323 K demonstrated that beta-scission occurs at appreciable rates (verified by considering the MWD of the polyAA before and after KPS treatment, which demonstrated significant chain fragmentation had taken place), supporting the developed postulate.

While very little is known about beta-scission of poly(acrylates), and no accurate measures of the relevant rate coefficients have been performed, the developed model gives good semi-quantitative prediction of the amount of secondary nucleation in electrosterically stabilized latexes for the first time. The model is also applicable to other sterically stabilized systems (such

as poly(ethylene oxide)-stabilized systems) where hydrogen abstraction from the stabilizing moiety can take place.

References

1. Gilbert, R. G., *Emulsion Polymerisation: A Mechanistic Approach*. Academic Press: San Diego, 1995.

2. Vorwerg, L.; Gilbert, R. G. *Macromolecules* **2000,** 33, 6693-6703.

3. Hammond, M. Sterically Stabilized Emulsion Systems. Honours Thesis, Honours Thesis,The University of Sydney, Sydney, 1983.

4. Priest, W. J. *J. Phys. Chem.* **1952,** 56, 1077-82.

5. Fitch, R. M.; Tsai, C. H., Particle formation in polymer colloids. III. Prediction of the number of particles by a homogeneous nucleation theory. In *Polymer Colloids*, Fitch, R. M., Ed. Plenum: New York, 1971; pp 73-102.

6. Ugelstad, J.; Hansen, F. K. *Rubber Chem. Technol.* **1976,** 49, 536-609.

7. Maxwell, I. A.; Morrison, B. R.; Napper, D. H.; Gilbert, R. G. *Macromolecules* **1991,** 24, 1629-40.

8. Goodall, A. R.; Wilkinson, W. C.; Hearn, J. *Journal of Polymer Science, Polymer Chemistry Edition* **1977,** 15, 2193.

9. Feeney, P. J.; Napper, D. H.; Gilbert, R. G. *Macromolecules* **1984,** 17, 2520.

10. Feeney, P. J.; Napper, D. H.; Gilbert, R. G. *Macromolecules* **1987,** 20, 2922.

11. Coen, E. M.; Gilbert, R. G.; Morrison, B. R.; Leube, H.; Peach, S. *Polymer* **1998,** 39, 7099-7112.

12. Morrison, B. R.; Gilbert, R. G. *Macromolecular Symposia* **1995,** 92, 13-30.

13. Gardon, J. L. *Journal of Polymer Science, Polymer Chemistry Edition* **1968,** 6, 623-41.

14. Ahmed, S. M.; El-Aasser, M. S.; Micale, F. J.; Poehlein, G. W.; Vanderhoff, J. W. *Polym. Colloids 2 [Two], [Proc. Symp. Phys. Chem. Prop. Colloidal Part.]* **1980**, 265-87.

15. Morrison, B. The Role of Aqueous-Phase Chemistry in the Kinetics of Emulsion Polymerization. PhD Thesis, The University of Sydney, Sydney, 1994.

16. Morrison, B. R.; Casey, B. S.; Lacik, I.; Leslie, G. L.; Sangster, D. F.; Gilbert, R. G.; Napper, D. H. *Journal of Polymer Science, Part A: Polymer Chemistry* **1994,** 32, 631-49.

17. Burguiere, C.; Chassenieux, C.; Charleux, B. *Polymer* **2002,** 44, 509-518.

18. Burguiere, C.; Pascual, S.; Bui, C.; Vairon, J.-P.; Charleux, B.; Davis, K. A.; Matyjaszewski, K.; Betremieux, I. *Macromolecules* **2001,** 34, 4439-4450.

19. von Sonntag, C.; Bothe, E.; Ulanski, P.; Deeble, D. J. *Radiation Physics and Chemistry* **1995,** 46, (4-6, Proceedings of the 9th International Meeting on Radiation Processing, 1994, Pt. 1), 527-32.

20. van Herk, A. M. *Macromolecular Rapid Communications* **2001,** 22, 687-689.

21. Maxwell, I. A.; Morrison, B. R.; Napper, D. H.; Gilbert, R. G. *Macromolecules* **1991,** 24, 1629-40.

22. Peck, A. N. F.; Hutchinson, R. A. *Macromolecules* **2004,** 37, 5944-5951.

23. Junkers, T.; Koo, S. P. S.; Davis, T. P.; Stenzel, M. H.; Barner-Kowollik, C. *Macromolecules* **2007,** 40, (25), 8906-8912.

24. Busch, M.; Mueller, M. *Macromolecular Symposia* **2004,** 206, (Polymer Reaction Engineering V), 399-418.

25. Rantow, F. S.; Soroush, M.; Grady, M. C.; Kalfas, G. A. *Polymer* **2006,** 47, 1423-1435.

26. Florin, R. E.; Sicilio, F.; Wall, L. A. *Journal of Research of the National Bureau of Standards, Section A: Physics and Chemistry* **1968,** 72, 49-73.

27. Sato, E.; Emoto, T.; Zetterlund, P. B.; Yamada, B. *Macromolecular Chemistry and Physics* **2004,** 205, (14), 1829-1839.

28. Gear, C. W., *Numerical Initial Boundary Value Problems in Ordinary Differential Equations*. Prentice-Hall: New York, 1971.

29. Ferguson, C. J.; Hughes, R. J.; Nguyen, D.; Pham, B. T. T.; Gilbert, R. G.; Serelis, A. K.; Such, C. H.; Hawkett, B. S. *Macromolecules* **2005,** 38, 2191-2204.

30. Emami, S. H.; Salovey, R.; Hogen-Esch, T. E. *Journal of Polymer Science, Part A: Polymer Chemistry* **2002,** 40, 3021-3026.

31. Guillet, J. E.; Burke, N. A. D. Production of graft copolymers by graft polymerization from the polymer backbone containing attached stable free radicals. 98-2249955

2249955, 19981013., 2000.

8. Conclusions and Outcomes

"It is the tension between creativity and scepticism that has created the stunning, unexpected findings of science."

Carl Sagan

8.1. Outcomes From This Project

In this project, the kinetics of both particle growth and particle formation in electrosterically stabilized has been extensively studied. Prior to this work, the kinetics of such systems had been both poorly understood and improperly characterized, due to a number of synthetic limitations[1-3] – an unsatisfactory situation for such a large component of the field of emulsion polymerization. The discoveries made in this project have revealed a number of hitherto unsuspected mechanisms present in systems where poly(acrylic acid) (polyAA) stabilization is employed, and are most likely applicable to any system where the polymeric stabilizer contains labile hydrogen atoms along the polymer backbone. As a result, the overall kinetic picture and genuine chemical understanding of electrosterically stabilized emulsion polymerization systems has been substantially improved.

The major outcomes and conclusions from this work can be summarized as follows:

- A successful methodology was developed to synthesize "model" electrosterically stabilized latexes using the 'RAFT-in-Emulsion' method.[4] This was followed by treatment of the latex with *tert*-butylhydroperoxide (TBHP) at elevated temperature to remove the RAFT functionality. Subsequent dialysis to remove the moderately water-soluble TBHP was carried out to clean the resultant latex. This technique proved very successful, with minimal coagulation of the latex, no substantial changes in particle size and complete loss of living character upon further polymerization. Three latexes were synthesized with differing length of the polyAA stabilizing block (5, 10 and 20 monomer units).

- Model latexes were synthesized with a poly(styrene) core as opposed to a poly(*n*-butyl acrylate) (poly(*n*-BA)) core as it was shown that systems where a poly(*n*-BA) latex was further polymerized with styrene, significant rate retardation was seen. This pronounced

decrease was a result of an elevated exit rate coefficient measured in systems of this nature by γ-relaxation dilatometry. This phenomenon was attributed to extensive chain transfer to the poly(*n*-BA) seed polymer by growing poly(styrene) radicals, leading to a tertiary backbone radical that is slow to propagate but quick to terminate. This was supported by SEC data that showed the poly(styrene) MWD shifted to much lower molecular weights than predicted from the absence of any additional chain transfer agent.

- The exit rate coefficients for the three electrosterically stabilized latexes in question were measured by γ-relaxation dilatometry, a method which provides a means to monitor radical loss mechanisms in emulsion systems essentially independent of other radical processes (entry etc.). The experimental results demonstrated a significant decrease in the exit rate coefficient k for these systems (up to a factor of 10) compared to model predictions for electrostatically stabilized latexes of the same size. This decrease was also a function of the length of the stabilizing moiety on the particle surface. This result was consistent with a 'restricted diffusion' effect, whereby the exiting species (a monomeric radical formed by chain transfer to monomer) has to pass through a dense layer of polymer on the particle surface. As a result, the diffusion coefficient is reduced. Mathematical modeling (where the Smoluchowski equation for diffusion-controlled encounter reactions was modified to account for such a two-phase system) yielded results that gave excellent semi-quantitative agreement with experiment. However, subsequent experiments showed that this model was insufficient in itself to explain all radical loss events in the presence of pAA hairs.

- Using three different chemical initiators (yielding a positively charged, a negatively charged and a neutral radical), seeded kinetic experiments involving these latexes demonstrated significantly reduced polymerization rates and very small values of $\overline{n}_{ss}$ (the steady-state average number of radicals per particle) compared to predicted values from

well-established theoretical models.[5, 6] Using the calculated values of $\bar{n}_{ss}$ and k from separate experiments, values of the entry rate coefficient ρ and the entry efficiency f_{entry} were determined. Assuming 'Limit 2a' kinetics (where an exited radical undergoes re-entry, the dominant fate for styrene-based systems[6, 7]), values of f_{entry} were unfeasibly small – much lower than any anticipated background ('thermal') polymerization rate. However upon processing the obtained kinetic data assuming Limit 1 kinetics (termination of an exited radical), the entry efficiency data gave almost perfect agreement with the well-accepted 'control by aqueous phase growth' entry mechanism.[8] This agreement was seen for all three latexes (with different length stabilizing blocks) and all three different chemical initiators.

- The apparent first-order loss mechanism was postulated to be due to reaction with the polyAA stabilizers on the particle surface. As acrylates are well known to undergo inter- and intra-molecular chain transfer to polymer,[9-11] it was proposed that the exited radical undergoes transfer (via hydrogen-atom abstraction) to the polyAA, leading to the loss of a radical that can re-enter and continue polymerization within the particle interior. The resulting mid-chain radical (MCR) on the particle surface can also terminate an exited radical and serves as an additional loss mechanism. These postulates were supported by separate experiments that proved that polyAA can act as a chain transfer agent in the polymerization of styrene, and that the addition of polyAA to the aqueous phase of an electrostatically stabilized latex gave a similar reduction in polymerization rate. NMR measurements also detected the presence of polyAA with poly(styrene) grafted onto the backbone, a species that could only be formed through the termination of a MCR, further supporting the proposed hypothesis.

- To rationalize the different approaches to explain the experimental kinetic data, an extended kinetic model was developed that was based on the original Smith-Ewart

equations that govern emulsion polymerization kinetics. The fate of a monomeric radical was considered to be a competition between the following events: successful desorption, transfer and termination. Radicals that successfully exited a given particle are then subjected to the same competition between the possible fates when considering re-entry. The addition of these two extra terms yielded a kinetic model that was in outstanding agreement with experimentally obtained values of both $\overline{n}_{ss}$ and f_{entry}. The apparent first-order loss mechanism seen experimentally was rationalized on the basis that transfer or termination are far more likely than successful desorption for small particles covered by a dense layer of polymeric stabilizer.

- In an attempt to explain the highly unusual amounts of secondary nucleation seen in seeded experiments involving electrosterically stabilized latexes,[3, 12] the fate of a MCR formed in the radical loss mechanism previously outlined was considered. Acrylates bearing a tertiary backbone radical can undergo beta-scission[13, 14] and it was postulated that beta-scission may be an important reaction to consider with respect to the particle nucleation mechanisms governing these systems. A kinetic model was constructed where every beta-scission event led to formation of a new particle and it was seen that the model results gave good agreement with experimental data. Supporting evidence (such as the fragmentation of polyAA in aqueous solution when exposed to a radical source in the absence of any monomer) of this proposed mechanism was presented.

The various new (and previously unsuspected) mechanisms present in emulsion systems stabilized by polyAA have been a major outcome from this project, as it provides the research scientist (or industrial chemist) wishing to model, or qualitatively understand, such a process a more complete picture as to what takes place at a molecular level. One of the most significant results from the kinetic model developed here (and supported with experimental results) is that the new loss mechanisms (chain transfer to polymer and subsequent termination) only dominate

the kinetics of these systems when the particle size is very small and the polymeric 'hairy layer' is very densely packed. In the modeling presented in this thesis, this dominance was only for particles smaller than 35 nm swollen radius. While many latexes used and synthesized are much larger than this, many industrial formulations (e.g. for the synthesis of paints, adhesives and surface coatings) often employ small, polymerically stabilized latexes as a seed in their synthetic processes. As a result, the understanding gained in this project for the behaviour of these small latexes is unquestionably important.

8.2. Scope for Future Work

While considerable advances have been made in this project with respect to the understanding of the kinetics of electrosterically stabilized emulsion polymerization systems, there are significant areas of research in this area that remain a challenge for the polymer scientist.

One of the main areas of research is the investigation of the pH dependence of the kinetics of these systems. This was not investigated in the current project due to the difficulties in varying the pH of the latexes synthesized while preserving colloidal stability. Ideally the kinetic behaviour of these systems should be analyzed when the stabilizing 'hairs' are fully protonated, that is, at low pH. The conformation of the polyAA chains will be altered by the removal of the electrostatic repulsion effect generated by the ionized carboxylic acid groups, which may affect the ability for radicals to diffuse through the hairy layer. Similarly the hydrogen-atom abstraction reaction (which was shown to be so important for the mechanisms of radical loss in these systems) may be more or less significant under different pH conditions. It was previously shown by Vorwerg[3] that secondary nucleation in electrosterically stabilized systems is strongly dependent on pH. Particle growth kinetics are also likely to be different and should be a significant area of research in these systems.

The results presented in this work relate to polyAA-stabilized emulsion systems. They are also applicable to any emulsion where the stabilizing moiety possesses labile hydrogen atoms along the polymer backbone. A corollary of this result is that stabilizers that do not possess the ability to undergo chain transfer to polymer (e.g. poly(methacrylic acid)) should exhibit kinetics that are similar to those predicted by the various theories of particle growth for electrostatically stabilized latexes. The study of systems such as these should be a focus of research in this area, as this would provide further information on the role of the stabilizing group in the kinetics of electrosterically stabilized emulsion systems. Furthermore, this may be an option considered by those involved in the manufacture of polymers on a large scale, as moving away from stabilizers with labile hydrogen atoms avoids the complicated kinetics presented in this work.

The area of secondary nucleation, which was addressed in Chapter 7 of this thesis, is still a poorly addressed area of research in this field. The modelling presented in Chapter 7 gave semi-quantitative agreement with experiment, but experiments need to be performed to either support of refute the postulated 'fragmentation nucleation' mechanism. The issue of beta-scission of polyAA is poorly understood in general and is further complicated in heterogeneous media such as in the emulsion systems being studied. Further work to understand and accurately measure the rate coefficient of beta-scission in polyAA would improve the accuracy of the constructed kinetic model. Similarly experiments to measure the amount of fragmented polymer in the aqueous phase in these emulsion systems would be ideal to help quantify the importance of the beta-scission reaction. This could be done by 'tagging' the polyAA with a UV chromophore or a fluorescent marker that would assist in the detection of (what is likely to be) very small amounts of polymer in the aqueous phase. Further insights into other potential mechanisms that may be significant in particle nucleation in these systems would also be welcome.

In conclusion, while there is more to be done from both a technologically driven and research standpoint, the work presented within this thesis goes a significant way to help understand the kinetic behaviour of electrosterically stabilized emulsion polymerization systems.

References

1. Coen, E. M.; Lyons, R. A.; Gilbert, R. G. *Macromolecules* **1996,** 29, 5128-5135.

2. De Bruyn, H.; Gilbert, R. G.; White, J. W.; Schulz, J. C. *Polymer* **2003,** 44, 4411-4420.

3. Vorwerg, L.; Gilbert, R. G. *Macromolecules* **2000,** 33, 6693-6703.

4. Ferguson, C. J.; Hughes, R. J.; Nguyen, D.; Pham, B. T. T.; Gilbert, R. G.; Serelis, A. K.; Such, C. H.; Hawkett, B. S. *Macromolecules* **2005,** 38, 2191-2204.

5. Gilbert, R. G., *Emulsion Polymerisation: A Mechanistic Approach*. Academic Press: San Diego, 1995.

6. Morrison, B. R.; Casey, B. S.; Lacik, I.; Leslie, G. L.; Sangster, D. F.; Gilbert, R. G.; Napper, D. H. *Journal of Polymer Science, Part A: Polymer Chemistry* **1994,** 32, 631-49.

7. Casey, B. S.; Morrison, B. R.; Maxwell, I. A.; Gilbert, R. G.; Napper, D. H. *Journal of Polymer Science, Part A: Polymer Chemistry* **1994,** 32, 605-630.

8. Maxwell, I. A.; Morrison, B. R.; Napper, D. H.; Gilbert, R. G. *Macromolecules* **1991,** 24, 1629-40.

9. Ahmad, N. M.; Heatley, F.; Lovell, P. A. *Macromolecules* **1998,** 31, 2822-2827.

10. Nikitin, A. N.; Castignolles, P.; Charleux, B.; Vairon, J.-P. *Macromolecular Rapid Communications* **2003,** 24, 778-782.

11. Couvreur, L.; Piteau, G.; Castignolles, P.; Tonge, M.; Coutin, B.; Charleux, B.; Vairon, J.-P. *Macromolecular Symposia* **2001,** 174, (Polymerization Processes and Polymer Materials I), 197-207.

12. Hammond, M. Sterically Stabilized Emulsion Systems. Honours Thesis, Honours Thesis,The University of Sydney, Sydney, 1983.

13. van Herk, A. M. *Macromolecular Rapid Communications* **2001,** 22, 687-689.

14. von Sonntag, C.; Bothe, E.; Ulanski, P.; Deeble, D. J. *Radiation Physics and Chemistry* **1995,** 46, (4-6, Proceedings of the 9th International Meeting on Radiation Processing, 1994, Pt. 1), 527-32.

Appendices

A1. Kinetic Data from Poly(*n*-BA) Experiments

Table A1. Steady-State Average Number of Radicals per Particle (Persulfate Initiation)

[KPS] (M)	$\bar{n}_{ss}$
1.58×10^{-04}	3.56×10^{-03}
9.49×10^{-05}	1.38×10^{-02}
3.34×10^{-04}	9.56×10^{-03}
2.87×10^{-04}	8.96×10^{-03}
1.12×10^{-03}	2.43×10^{-02}
1.00×10^{-03}	2.25×10^{-02}
3.11×10^{-03}	5.95×10^{-02}
9.70×10^{-03}	8.67×10^{-02}

Table A2. Entry Rate Coefficient Data (Limit 1 and Limit 2a Processing):

[KPS] (average) (M)	ρ (Limit 2a) (s^{-1})	f_{entry} (Limit 2a) (s^{-1})	ρ (Limit 1) (s^{-1})	f_{entry} (Limit 1) (s^{-1})
1.26×10^{-04}	4.99×10^{-06}	3.52×10^{-02}	1.23×10^{-04}	8.68×10^{-01}
3.11×10^{-04}	6.75×10^{-06}	1.59×10^{-02}	1.50×10^{-04}	3.52×10^{-01}
1.06×10^{-03}	4.59×10^{-05}	3.24×10^{-02}	4.65×10^{-04}	3.28×10^{-01}
3.11×10^{-03}	3.36×10^{-04}	7.91×10^{-02}	1.35×10^{-03}	3.17×10^{-01}
9.70×10^{-03}	7.61×10^{-04}	5.36×10^{-02}	2.05×10^{-03}	1.44×10^{-01}

A2. Exit Rate Coefficients for Electrosterically Stabilized Poly(styrene) Latexes

Exit Rate Coefficient Data from Gamma-Relaxation Experiments:

Table A3. Data from the ST0 latex.

$\overline{n}_{ss}$ (in-source)	$\overline{n}_{ss}$ (out-of-source)	k (s^{-1})	ρ_{spont} (s^{-1})
0.118	0.0216	4.09×10^{-02}	5.38×10^{-05}
0.113	0.0232	4.15×10^{-02}	3.17×10^{-05}
0.105	0.0201	4.52×10^{-02}	1.77×10^{-05}
0.0691	0.0229	3.03×10^{-02}	5.83×10^{-06}
0.0745	0.0184	3.60×10^{-02}	2.00×10^{-05}
0.068	0.0137	3.82×10^{-02}	2.81×10^{-06}

Table A4. Data from the ST5 latex (Limit 2a data processing).

$\overline{n}_{ss}$ (in-source)	$\overline{n}_{ss}$ (out-of-source)	k (s^{-1})	ρ_{spont} (s^{-1})
9.27×10^{-03}	0.002	7.60×10^{-03}	n/a
1.00×10^{-02}	0.0019	6.93×10^{-03}	n/a
9.28×10^{-03}	0.00184	1.50×10^{-02}	n/a
8.43×10^{-03}	0.00202	1.31×10^{-02}	n/a
8.35×10^{-03}	0.0008	1.74×10^{-02}	n/a
3.66×10^{-03}	3.00×10^{-04}	1.77×10^{-02}	n/a
4.13×10^{-03}	1.50×10^{-04}	1.89×10^{-02}	n/a
3.99×10^{-03}	2.10×10^{-04}	3.56×10^{-02}	n/a
5.43×10^{-03}	2.60×10^{-04}	2.43×10^{-02}	n/a
9.27×10^{-03}	0.002	7.60×10^{-03}	n/a

Table A5. Data from the ST5 latex (Limit 1 data processing).

$\overline{n}_{ss}$ (in-source)	$\overline{n}_{ss}$ (out-of-source)	k (s^{-1})	ρ_{spont} (s^{-1})
9.27×10^{-03}	0.002	7.01×10^{-03}	n/a
1.00×10^{-02}	0.0019	5.24×10^{-03}	n/a
9.28×10^{-03}	0.00184	5.13×10^{-03}	n/a
8.43×10^{-03}	0.00202	9.00×10^{-03}	n/a
8.35×10^{-03}	0.0008	7.41×10^{-03}	n/a
9.27×10^{-03}	0.002	7.01×10^{-03}	n/a

Table A6. Data from the ST10 latex (Limit 2a data processing).

$\overline{n}_{ss}$ (in-source)	$\overline{n}_{ss}$ (out-of-source)	k (s^{-1})	ρ_{spont} (s^{-1})
0.013	-	4.54×10^{-03}	n/a
0.0141	-	4.40×10^{-03}	n/a
0.02	-	3.27×10^{-03}	n/a
0.016	-	4.74×10^{-03}	n/a
0.011	-	6.12×10^{-03}	n/a
0.008	-	5.20×10^{-03}	n/a
0.0067	-	6.90×10^{-03}	n/a
5.96×10^{-03}	-	2.42×10^{-03}	n/a
3.80×10^{-03}	-	8.71×10^{-03}	n/a
0.013	-	4.54×10^{-03}	n/a
0.0141	-	4.40×10^{-03}	n/a

Table A7. Data from the ST10 latex (Limit 1 data processing).

$\overline{n}_{ss}$ (in-source)	$\overline{n}_{ss}$ (out-of-source)	k (s^{-1})	ρ_{spont} (s^{-1})
0.013	-	4.22×10^{-03}	n/a
0.0141	-	4.58×10^{-03}	n/a
0.02	-	2.76×10^{-03}	n/a
0.016	-	4.72×10^{-03}	n/a
0.011	-	8.20×10^{-03}	n/a
0.008	-	6.14×10^{-03}	n/a
0.0067	-	5.22×10^{-03}	n/a

Table A8. Data from the ST20 latex (Limit 2a data processing).

$\overline{n}_{ss}$ (in-source)	$\overline{n}_{ss}$ (out-of-source)	k (s^{-1})	ρ_{spont} (s^{-1})
0.006	-	6.30×10^{-03}	n/a
0.0075	-	2.28×10^{-03}	n/a
0.0067	-	3.77×10^{-03}	n/a
0.0071	-	3.67×10^{-03}	n/a
0.0085	-	4.92×10^{-03}	n/a
0.0107	-	7.51×10^{-03}	n/a
4.20×10^{-03}	-	1.81×10^{-03}	n/a

Table A9. Data from the ST20 latex (Limit 1 data processing).

$\overline{n}_{ss}$ (in-source)	$\overline{n}_{ss}$ (out-of-source)	k (s^{-1})	ρ_{spont} (s^{-1})
0.006	-	5.02×10^{-03}	n/a
0.0075	-	2.88×10^{-03}	n/a
0.0067	-	4.26×10^{-03}	n/a
0.0071	-	6.75×10^{-03}	n/a
0.0085	-	6.66×10^{-03}	n/a
0.0107	-	4.43×10^{-03}	n/a
4.20×10^{-03}	-	5.32×10^{-03}	n/a

Exit Rate Coefficient Data from Gamma-Re-insertion Experiments:

Table A10. Data for ST0 Latex.

$\bar{n}_0$	Slope	Intercept	A (s^{-1})	k (Lim 2a) (s^{-1})	k (Lim 1) (s^{-1})
0.0278	6.96×10^{-05}	-0.00367	6.23×10^{-04}	3.38×10^{-02}	1.11×10^{-02}
0.0263	6.52×10^{-05}	-0.00492	6.23×10^{-04}	3.56×10^{-02}	1.02×10^{-02}
0.0168	3.79×10^{-05}	-0.00335	6.32×10^{-04}	3.88×10^{-02}	7.17×10^{-03}
0.0304	4.22×10^{-05}	-0.00295	6.32×10^{-04}	3.12×10^{-02}	6.75×10^{-03}

Table A11. Data for ST10 Latex.

$\bar{n}_0$	Slope	Intercept	A (s^{-1})	k (Lim 2a) (s^{-1})	k (Lim 1) (s^{-1})
4.61×10^{-04}	7.11 × -05	-0.0066	6.36×10^{-03}	1.55×10^{-02}	1.01×10^{-02}
2.90×10^{-03}	7.68×10^{-05}	-0.00824	6.36×10^{-03}	1.82×10^{-02}	6.91×10^{-03}
1.68×10^{-03}	5.98×10^{-05}	-0.01033	6.40×10^{-03}	8.05×10^{-03}	4.66×10^{-03}
5.43×10^{-03}	7.24×10^{-05}	-0.0079	6.40×10^{-03}	1.20×10^{-02}	4.66×10^{-03}
4.92×10^{-03}	1.03×10^{-04}	-0.00341	6.40×10^{-03}	1.86×10^{-02}	1.23×10^{-02}

Table A12. Data for ST20 Latex.

$\bar{n}_0$	Slope	Intercept	A (s^{-1})	k (Lim 2a) (s^{-1})	k (Lim 1) (s^{-1})
2.63×10^{-03}	9.86×10^{-05}	-0.0016	9×10^{-03}	6.20×10^{-02}	4.58×10^{-02}
1.33×10^{-03}	9.68×10^{-05}	-0.00486	9×10^{-03}	2.63×10^{-02}	1.71×10^{-02}
2.87×10^{-03}	6.16×10^{-05}	-0.00361	4.56×10^{-03}	1.56×10^{-02}	1.31×10^{-02}
3.63×10^{-03}	5.85×10^{-05}	-0.00188	4.56×10^{-03}	2.65×10^{-02}	2.17×10^{-02}

Slope-Intercept Method *k* Values (Persulfate Initiation, Limit 1 processing):

[KPS] (mM)	slope	intercept	A (s^{-1})	ρ (s^{-1})	k (s^{-1})
		ST0			
0.1	2.18×10^{-05}	-0.2772	6.58×10^{-04}	2.61×10^{-06}	7.30×10^{-05}
0.3	2.73×10^{-05}	-0.1312	6.39×10^{-04}	8.89×10^{-06}	1.90×10^{-04}
1	3.08×10^{-05}	-0.172	6.27×10^{-04}	8.63×10^{-06}	1.60×10^{-04}
10	7.05×10^{-05}	-0.049	6.54×10^{-04}	1.55×10^{-04}	1.13×10^{-03}
		ST5			
0.1	1.84×10^{-05}	-0.065	6.71×10^{-03}	7.76×10^{-07}	2.82×10^{-04}
0.3	2.37×10^{-05}	-0.1162	6.52×10^{-03}	7.41×10^{-07}	2.02×10^{-04}
1	3.86×10^{-05}	-0.089	6.45×10^{-03}	2.60×10^{-06}	4.30×10^{-04}
3	6.97×10^{-05}	-0.0179	6.42×10^{-03}	4.20×10^{-05}	3.80×10^{-03}
10	1.15×10^{-04}	-0.071	6.48×10^{-03}	2.87×10^{-05}	1.56×10^{-03}
		ST10			
0.1	2.69×10^{-05}	-0.125	6.31×10^{-03}	9.17×10^{-07}	2.13×10^{-04}
0.3	5.50×10^{-05}	-0.247	6.16×10^{-03}	1.94×10^{-06}	2.19×10^{-04}
1	6.89×10^{-05}	-0.159	6.11×10^{-03}	4.73×10^{-06}	4.24×10^{-04}
3	9.24×10^{-05}	-0.09	6.31×10^{-03}	1.50×10^{-05}	9.97×10^{-04}
10	1.79×10^{-04}	-0.04	6.19×10^{-03}	1.29×10^{-05}	4.22×10^{-03}
		ST20			
0.1	4.58×10^{-05}	-0.06	4.72×10^{-03}	7.41×10^{-06}	7.49×10^{-04}
0.3	5.60×10^{-05}	-0.07	4.70×10^{-03}	9.63×10^{-06}	7.85×10^{-04}
1	6.23×10^{-05}	-0.08	4.85×10^{-03}	1.00×10^{-05}	7.59×10^{-04}
3	7.23×10^{-05}	-0.025	4.76×10^{-03}	4.39×10^{-05}	2.80×10^{-03}
10	1.41×10^{-04}	-0.122	4.73×10^{-03}	3.45×10^{-05}	1.09×10^{-03}

A3. Derivation of the 'Restricted Diffusion' Exit Model

By modifying the Smoluchowski equation for a radical adsorbing onto the particle by including diffusion through both the aqueous phase and then a hairy layer of fixed width, a mathematical expression for k_{dM} (the rate coefficient for radical desorption) can be found.

Fick's 2nd Law states:

$$\frac{\partial c}{\partial t} = D\nabla^2 c \tag{A.1}$$

where D is the diffusion coefficient of the medium and c is the concentration of radicals. There are two regions of interest – inside the hairy layer (c_h) and in the aqueous phase (c_w). Assuming steady state conditions for both regions, the problem reduces to solving $\nabla^2 c = 0$.

Assuming spherically symmetric co-ordinates we obtain at the second order differential equation

$$\frac{\mathrm{d}^2 c}{\mathrm{d}r^2} + \frac{2}{r}\frac{\mathrm{d}c}{\mathrm{d}r} = 0 \tag{A.2}$$

where r is the radial displacement from the origin of the system (the centre of the spherical particle). Using a simple reduction-of-order method the general solution of these equations is

$$c = a + \frac{b}{r} \tag{A.3}$$

where a and b are constants. It can be assumed that this equation holds in both regions, with the constants a and b controlled by the boundary conditions in this system. The swollen radius of the particle is r_s, and the width of the hairy layer is δ. For an interface-boundary problem, at the interface of the water and the hairy layer, the concentration of the radicals must be continuous

(approach the same limit from either side of the interface) and the flux across this surface must be identical for both equations, i.e.

$$-D_{\mathrm{h}} \left.\frac{\mathrm{d}c_{\mathrm{h}}}{\mathrm{d}r}\right|_{r=r_{\mathrm{s}}+\delta} = -D_{\mathrm{w}} \left.\frac{\mathrm{d}c_{\mathrm{w}}}{\mathrm{d}r}\right|_{r=r_{\mathrm{s}}+\delta} \tag{A.4}$$

These restrictions dictate what values the constants will take.

Let

$$c_{\mathrm{h}} = a_{\mathrm{h}} + \frac{b_{\mathrm{h}}}{r} \tag{A.5}$$

When $r = r_{\mathrm{s}}$, $c_{\mathrm{h}} = 0$. Therefore

$$a_{\mathrm{h}} = -\frac{b_{\mathrm{h}}}{r_{\mathrm{s}}} \tag{A.6}$$

and

$$c_{\mathrm{h}} = b_{\mathrm{h}}\left(\frac{1}{r} - \frac{1}{r_{\mathrm{s}}}\right). \tag{A.7}$$

When $r = \infty$, $c_{\mathrm{w}} = c_{\mathrm{inf}}$ (to be defined later).

Hence

$$a_{\mathrm{w}} = c_{\mathrm{inf}} \tag{A.8}$$

and

$$c_w = c_{inf} + \frac{b_w}{r} \quad . \tag{A.9}$$

Using the conditions mentioned above, when $r = r_s + \delta$, $c_w = c_h$. Therefore

$$c_{inf} + \frac{b_w}{r_s + \delta} = -b_h \left(\frac{\delta}{r_s(r_s + \delta)} \right) \tag{A.10}$$

Similarly the condition from the requirement that the radical fluxes must be equivalent yields

$$D_w \left(\frac{b_w}{(r_s+\delta)^2} \right) = D_h \left(\frac{b_h}{(r_s+\delta)^2} \right) \tag{A.11}$$

or simply $D_w\, b_w = D_h\, b_h$.

Re-arranging Equation A.11 we have

$$b_w = \frac{D_h}{D_w} b_h \tag{A.12}$$

and so

$$c_{inf} + \frac{D_h}{D_w} \frac{b_h}{(r_s + \delta)} = - b_h \left(\frac{\delta}{r_s(r_s + \delta)} \right) \tag{A.13}$$

which upon rearrangement gives us the expression

$$b_h = - c_{inf} \left(\frac{r_s(r_s+\delta)}{\delta + r_s(D_h/D_w)} \right) \tag{A.14}$$

Therefore the concentration of monomeric radicals inside the hairy layer is

$$c_h = c_{inf} \left(\frac{r_s(r_s+\delta)}{\delta + r_s(D_h/D_w)} \right) \left(\frac{1}{r_s} - \frac{1}{r} \right) \tag{A.15}$$

The flux at the surface of the particle is therefore

$$-D_{\mathrm{h}}\left.\frac{\mathrm{d}c_{\mathrm{h}}}{\mathrm{d}r}\right|_{r=r_{\mathrm{s}}} = -D_{\mathrm{h}}\frac{b_{\mathrm{h}}}{r_{\mathrm{s}}^{2}} \tag{A.16}$$

and so the rate of reaction at the surface is equal to

$$4\pi r_{\mathrm{s}}^{2} \times (\text{radical flux}) = 4\pi c_{\mathrm{inf}}\left(\frac{r_{\mathrm{s}}(r_{\mathrm{s}}+\delta)}{\delta + r_{\mathrm{s}}(D_{\mathrm{h}}/D_{\mathrm{w}})}\right)D_{\mathrm{h}} \tag{A.17}$$

As the rate of entry can also be written as $k_{\mathrm{ads}}[\mathrm{M}](N_{\mathrm{p}}/N_{\mathrm{Av}}) = k_{\mathrm{ads}}[\mathrm{M}][\mathrm{P}]$ where [P] is the concentration of particles, then the number of particles $P = N_{\mathrm{Av}}[\mathrm{P}]V$ where V is the volume of the system.

Hence the global flow of radicals equals

$$4\pi c_{\mathrm{inf}}\left(\frac{r_{\mathrm{s}}(r_{\mathrm{s}}+\delta)}{\delta + r_{\mathrm{s}}(D_{\mathrm{h}}/D_{\mathrm{w}})}\right)D_{\mathrm{h}}N_{\mathrm{Av}}[\mathrm{P}]V \tag{A.18}$$

Re-arranging Equation A.18 allows us to say that the 'modified' expression for k_{ads} is

$$k_{\mathrm{ads}} = 4\pi\left(\frac{r_{\mathrm{s}}(r_{\mathrm{s}}+\delta)}{\delta + r_{\mathrm{s}}(D_{\mathrm{h}}/D_{\mathrm{w}})}\right)D_{\mathrm{h}}N_{\mathrm{Av}} \tag{A.19}$$

From this expression and the principle of microscopic reversibility, we can formulate an expression for the desorption of a monomeric radical in this system.

$$\mathrm{M}^{\cdot} + \text{particle} \underset{k_{\mathrm{dM}}}{\overset{k_{\mathrm{ads}}}{\rightleftharpoons}} (\text{particle-M}) \tag{A.20}$$

The rate of monomer molecules being captured by a given particle is $k_{ads}C_w$, while the total rate of escaping per unit time is given by $k_{dM}V_sC_pN_{Av}$. Equating these two (when at equilibrium) gives allows one to rearrange and solve for k_{dM}, namely:

$$k_{dM} = 3D_h\frac{C_w}{C_p}\left(\frac{r_s+\delta}{r_s^2\,(\delta+r_s(D_h/D_w))}\right) \tag{A.21}$$

A4. Kinetic Data from Chemically Initiated Experiments

Entry Rate Coefficient and Entry Efficiency Values. Presented below are the experimentally determined values for the initiator-derived entry rate coefficient (ρ_{init}) and the entry efficiency (f_{entry}) for all latexes analyzed in this work.

Table A13. Data for ST0 latex, assuming Limit 2a kinetics.

[initiator] (M)	ρ_{init} (s-1)	error (s-1)	f_{entry}	error
Initiator: Potassium persulfate				
1.11×10^{-04}	6.86×10^{-05}	2.43×10^{-05}	5.85×10^{-01}	2.07×10^{-01}
4.71×10^{-04}	1.32×10^{-04}	1.82×10^{-05}	2.64×10^{-01}	8.70×10^{-02}
1.07×10^{-03}	1.84×10^{-04}	2.21×10^{-05}	1.62×10^{-01}	4.65×10^{-02}
3.41×10^{-03}	4.42×10^{-04}	4.02×10^{-05}	1.22×10^{-01}	2.65×10^{-02}
9.67×10^{-03}	1.12×10^{-03}	9.08×10^{-05}	1.09×10^{-01}	2.12×10^{-02}
Initiator: VA-086				
1.61×10^{-04}	5.11×10^{-05}	2.28×10^{-05}	4.19×10^{-01}	1.87×10^{-01}
4.73×10^{-04}	7.23×10^{-05}	2.96×10^{-05}	2.01×10^{-01}	8.23×10^{-02}
1.28×10^{-03}	1.03×10^{-04}	2.78×10^{-05}	1.06×10^{-01}	2.85×10^{-02}
4.04×10^{-03}	9.67×10^{-05}	5.6×10^{-05}	3.15×10^{-02}	1.83×10^{-02}
1.20×10^{-02}	3.98×10^{-04}	6.78×10^{-05}	4.36×10^{-02}	7.42×10^{-03}

Table A14. Data for ST5 latex, assuming Limit 1 and Limit 2a kinetics.

[initiator] (M)	ρ_{init} (s^{-1}) (Limit 2a)	f_{entry} (Limit 2a)	ρ_{init} (s^{-1}) (Limit 1)	f_{entry} (Limit 1)
Initiator: Potassium Persulfate				
9.43×10^{-05}	2.28×10^{-07}	1.94×10^{-02}	1.86×10^{-05}	3.18×10^{-01}
3.15×10^{-04}	4.01×10^{-07}	1.02×10^{-02}	2.47×10^{-05}	1.27×10^{-01}
1.07×10^{-03}	1.09×10^{-06}	8.22×10^{-03}	4.09×10^{-05}	6.18×10^{-02}
2.88×10^{-03}	3.64×10^{-06}	1.01×10^{-02}	7.50×10^{-05}	4.20×10^{-02}
1.15×10^{-02}	9.86×10^{-06}	7.89×10^{-03}	1.24×10^{-04}	2.00×10^{-02}
Initiator: VA-086				
1.96×10^{-04}	6.59×10^{-09}	3.78×10^{-04}	3.16×10^{-06}	1.81×10^{-01}
5.45×10^{-04}	1.79×10^{-08}	3.69×10^{-04}	5.20×10^{-06}	1.07×10^{-01}
1.33×10^{-03}	6.19×10^{-09}	5.25×10^{-05}	3.06×10^{-06}	2.59×10^{-02}
3.60×10^{-03}	6.52×10^{-08}	2.04×10^{-04}	9.94×10^{-06}	3.11×10^{-02}
1.28×10^{-02}	3.90×10^{-08}	3.42×10^{-05}	7.69×10^{-06}	6.75×10^{-03}
Initiator: V-50				
2.69×10^{-05}	6.00×10^{-10}	3.73×10^{-05}	9.53×10^{-07}	5.92×10^{-02}
6.49×10^{-05}	1.68×10^{-09}	4.32×10^{-05}	1.59×10^{-06}	4.11×10^{-02}
2.43×10^{-04}	2.69×10^{-08}	1.85×10^{-04}	6.38×10^{-06}	4.40×10^{-02}
7.01×10^{-04}	1.78×10^{-07}	4.24×10^{-04}	1.65×10^{-05}	3.92×10^{-02}
1.87×10^{-03}	4.27×10^{-07}	3.82×10^{-04}	2.55×10^{-05}	2.28×10^{-02}

Table A15. Data for ST10 latex, assuming Limit 1 and Limit 2a kinetics.

[initiator] (M)	ρ_{init} (s^{-1}) (Limit 2a)	f_{entry} (Limit 2a)	ρ_{init} (s^{-1}) (Limit 1)	f_{entry} (Limit 1)
Initiator: Potassium Persulfate				
1.20×10^{-04}	1.84×10^{-07}	1.23×10^{-02}	2.20×10^{-05}	2.94×10^{-01}
4.37×10^{-04}	8.15×10^{-07}	1.49×10^{-02}	4.66×10^{-05}	1.71×10^{-01}
1.50×10^{-03}	1.31×10^{-06}	6.98×10^{-03}	5.92×10^{-05}	6.32×10^{-02}
4.18×10^{-03}	2.20×10^{-06}	4.18×10^{-03}	7.70×10^{-05}	2.93×10^{-02}
$1.06\times10\text{-}^{02}$	8.90×10^{-06}	6.69×10^{-03}	1.57×10^{-04}	2.37×10^{-02}
Initiator: VA-086				
1.76×10^{-04}	4.47×10^{-09}	2.85×10^{-04}	3.42×10^{-06}	2.18×10^{-01}
4.87×10^{-04}	1.88×10^{-08}	4.31×10^{-04}	7.01×10^{-06}	1.61×10^{-01}
1.37×10^{-03}	3.91×10^{-08}	3.18×10^{-04}	1.01×10^{-05}	8.23×10^{-02}
4.00×10^{-03}	5.91×10^{-08}	1.65×10^{-04}	1.25×10^{-05}	3.48×10^{-02}
1.36×10^{-02}	7.52×10^{-08}	6.17×10^{-05}	1.41×10^{-05}	1.15×10^{-02}
Initiator: V-50				
6.87×10^{-05}	5.98×10^{-09}	1.37×10^{-04}	3.95×10^{-06}	9.22×10^{-02}
1.93×10^{-04}	7.10×10^{-08}	5.78×10^{-04}	1.37×10^{-05}	1.14×10^{-01}
5.87×10^{-04}	2.85×10^{-07}	7.96×10^{-04}	2.74×10^{-05}	7.49×10^{-02}
1.77×10^{-03}	5.84×10^{-07}	4.79×10^{-04}	3.94×10^{-05}	3.58×10^{-02}

Table A16. Data for ST20 latex, assuming Limit 1 and Limit 2a kinetics.

[initiator] (M)	ρ_{init} (s^{-1}) (Limit 2a)	f_{entry} (Limit 2a)	ρ_{init} (s^{-1}) (Limit 1)	f_{entry} (Limit 1)
Initiator: Potassium Persulfate				
1.01×10^{-04}	9.14×10^{-07}	6.10×10^{-02}	5.01×10^{-05}	6.70×10^{-01}
3.00×10^{-04}	1.38×10^{-06}	2.52×10^{-02}	6.16×10^{-05}	2.26×10^{-01}
9.08×10^{-04}	1.61×10^{-06}	8.54×10^{-03}	6.66×10^{-05}	7.11×10^{-02}
2.94×10^{-03}	2.26×10^{-06}	4.27×10^{-03}	7.91×10^{-05}	3.01×10^{-02}
9.50×10^{-03}	8.96×10^{-06}	6.74×10^{-03}	1.60×10^{-04}	2.42×10^{-02}
Initiator: VA-086				
1.88×10^{-04}	1.43×10^{-09}	6.38×10^{-05}	1.96×10^{-06}	8.75×10^{-02}
4.50×10^{-04}	3.96×10^{-09}	7.36×10^{-05}	3.26×10^{-06}	6.07×10^{-02}
1.34×10^{-03}	4.34×10^{-09}	2.71×10^{-05}	3.42×10^{-06}	2.14×10^{-02}
4.64×10^{-03}	1.09×10^{-08}	1.96×10^{-05}	5.42×10^{-06}	9.77×10^{-03}
1.26×10^{-02}	7.85×10^{-08}	5.22×10^{-05}	1.46×10^{-05}	9.69×10^{-03}
Initiator: V-50				
8.81×10^{-05}	7.91×10^{-08}	1.08×10^{-03}	1.42×10^{-05}	1.93×10^{-01}
1.12×10^{-04}	1.67×10^{-07}	1.80×10^{-03}	2.07×10^{-05}	2.22×10^{-01}
5.47×10^{-04}	9.53×10^{-07}	2.71×10^{-05}	2.09×10^{-03}	1.09×10^{-01}
1.59×10^{-03}	1.62×10^{-06}	1.96×10^{-05}	1.22×10^{-03}	4.98×10^{-02}

A5. Parameters Used for the 'Control By Aqueous Phase Growth' Entry Model

Parameter	Value (units)
z	2 (KPS), 3 (VA-086), 1 (V-50)
k_p	260 M^{-1} s^{-1}
k_p^1	4 k_p
k_d	1×10^{-6} s^{-1} (KPS), 7.14×10^{-7} s^{-1} (VA-086), 4.98×10^{-6} s^{-1} (V-50)
k_t	1.75×10^{9} M^{-1} s^{-1}
k_{tr}	9.3×10^{-3} M^{-1} s^{-1}
C_w	4.3×10^{-3} M
C_p	Sample dependent
N_p	Sample dependent
D_w	1.3×10^{-9} m^2 s^{-1}

A6. Derivation of Maximum Secondary Nucleation Rate Expression by the Homogeneous Nucleation Mechanism

(The expression shown for the determination of the maximum rate of secondary nucleation in a seeded emulsion system was originally presented in the PhD thesis of Bradley Morrison, The University of Sydney, 1994. As this work was never published in a peer-reviewed journal, it is repeated here for the benefit of the reader).

The derivation of the maximum rate of secondary nucleation by the 'homogeneous nucleation' mechanism involves an extension of the aqueous-phase oligomeric chemistry that was developed in the 'control by aqueous phase growth' entry model of Maxwell and co-workers. For oligomers of DP < z (where the radical is now considered to be surface active), the following chemical reactions take place:

$$\text{initiator} \xrightarrow{fk_d} 2\,\text{I}^\bullet \tag{A.22}$$

$$\text{I}^\bullet + \text{M} \xrightarrow{k_{pi}} \text{IM}^\bullet \tag{A.23}$$

$$\text{IM}_{i\text{-}1}^\bullet + \text{M} \xrightarrow{k_{pw}} \text{IM}_i^\bullet\,,\ i < \text{z} \tag{A.24}$$

$$\text{IM}_i^\bullet + \text{T}^\bullet \xrightarrow{k_{tw}} \text{dead product},\ i < \text{z} \tag{A.25}$$

$$\text{IM}_\text{z}^\bullet + \text{particle} \xrightarrow{\rho_{init}} \text{entry} \tag{A.26}$$

That is, once the degree of polymerization z is attained, irreversible and 'instantaneous' entry into a pre-existing particle takes place. However these equations can be extended up to the

degree of polymerization j_{crit}, whereby the oligomer is completely water-insoluble and precipitates out of solution by undergoing a coil-to-globule transition. In the homogeneous nucleation model, it is assumed that a new particle is formed when the length j_{crit} is reached. Between the lengths z and j_{crit}, oligomers can propagate, terminate or undergo an entry event into a pre-existing particle. The relevant equations are:

$$IM_i^{\bullet} + M \xrightarrow{k_{pw}} IM_{i+1}^{\bullet}, \; i \geq z \tag{A.27}$$

$$IM_i^{\bullet} + T^{\bullet} \xrightarrow{k_{tw}} \text{dead product}, \; i \geq z \tag{A.28}$$

$$IM_i^{\bullet} + \text{old particle} \xrightarrow{\rho_{init}} \text{entry} \;\; i \geq z \tag{A.29}$$

$$IM_{j_{crit}-1}^{\bullet} + M \xrightarrow{k_{pw}} \text{new particle} \tag{A.30}$$

By applying the steady-state approximation to the evolution equations for the above two sets of chemical reactions, the following expressions are obtained:

$$[IM_1^{\bullet}] = \frac{2 f k_d [I]}{k_{pw} [M]_w + 2 k_{tw} [T_w^{\bullet}]} \tag{A.31}$$

$$[IM_i^{\bullet}] = \frac{k_{pw} C_w [IM_{i-1}^{\bullet}]}{k_{pw} C_w + 2 k_{tw} [T_w^{\bullet}]}, \; 1 < i < z \tag{A.32}$$

$$[IM_j^{\bullet}] = \frac{k_{pw} C_w [IM_{j-1}^{\bullet}]}{k_{pw} C_w + 2 k_{tw} [T_w^{\bullet}] + k_e \frac{N_{seed}}{N_A}}, \; z \leq j < j_{crit} \tag{A.33}$$

The rate of generation of new particles is given by:

$$\frac{dN_{new}/N_A}{dt} = k_{pw} C_w [IM^{\bullet}_{j_{crit}-1}] \tag{A.34}$$

Through an iterative substitution into Equation A.34, one then arrives at the final expression:

$$\frac{\mathrm{d}N_{\mathrm{new}}/N_{\mathrm{A}}}{\mathrm{dt}} = \frac{2\,k_{\mathrm{d}}\,[\mathrm{I}]\,(k_{\mathrm{p}}\,C_{\mathrm{w}})^{j\mathrm{crit}-1}}{(k_{\mathrm{p}}\,C_{\mathrm{w}} + 2k_{\mathrm{t}}\,[\mathrm{T}^{\bullet}])^{z}\,(k_{\mathrm{p}}\,C_{\mathrm{w}} + k_{\mathrm{e}}\,\frac{N_{\mathrm{seed}}}{N_{\mathrm{A}}} + 2k_{\mathrm{t}}\,[\mathrm{T}^{\bullet}])^{j\mathrm{crit}-z-1}} \tag{A.35}$$

A7. FORTRAN Code for 'Fragmentation Nucleation' Mechanistic Model

For a copy of the source code and a sample input file, please contact the author or download the files from:

http://www.uq.edu.au/gilbertgroup/sec_nuc_electrosteric.f

http://www.uq.edu.au/gilbertgroup/sample_input.dat

Biography

Stuart Thickett was born on the 17th of April, 1982 in Sydney, New South Wales. He attended Peakhurst South Public School and Hurstville Public School before completing his Higher School Certificate at Sydney Technical High School, Bexley in 1999. He represented his school in golf and cricket, as well as playing for his local Peakhurst South Cricket Club for four seasons.

In 2000 he began his undergraduate training at The University of Sydney. In 2002 he graduated with a Bachelor of Science (Advanced) degree with majors in Chemistry and Mathematics (Pure). In 2003 he completed his Honours year under the supervision of Professor Robert (Bob) Gilbert in the Key Centre for Polymer Colloids within the School of Chemistry at The University of Sydney. This work focused on *ab initio* quantum chemical modelling of the propagation step of acrylic acid polymerization. For this work he received First Class Honours and The University Medal.

In 2004 he commenced his Doctor of Philosophy at the same institution, covering the research topic outlined in this thesis. During his studies he was awarded an Australian Postgraduate Award, the Gritton Scholarship, the Surface Coatings Association of Australia Scholarship four times, as well as the RJW Le Fevre Student Lectureship of 2006. In July 2008 he will commence a post-doctoral position within the School of Chemistry at The University of Toronto.

"Now, at that time, there did not exist polyethylene, which would have suited me perfectly since it is light, flexible and splendidly impermeable: but it is also a bit too incorruptible, and not by chance by God Almighty himself, although He is a master of polymerization, He abstained from patenting it: He does not like incorruptible things."

Primo Levi, *The Periodic Table*